

Alma Mater Studiorum – Università di Bologna

DOTTORATO DI RICERCA IN

Ingegneria Civile, Chimica, Ambientale e dei Materiali

Ciclo XXX

**Settore Concorsuale: 08/B2**

**Settore Scientifico Disciplinare: ICAR/08**

HIGHER-ORDER STRONG AND WEAK FORMULATIONS  
FOR ARBITRARILY SHAPED DOUBLY-CURVED SHELLS  
MADE OF ADVANCED MATERIALS

**Presentata da: Michele Bacciocchi**

**Coordinatore Dottorato**

**Prof. Luca Vittuari**

**Supervisore**

**Prof. Erasmo Viola**

**Co-supervisore**

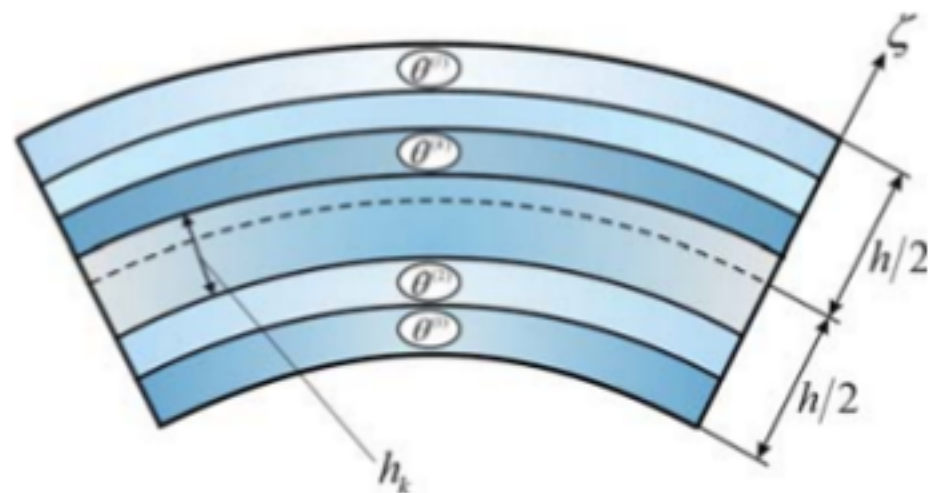
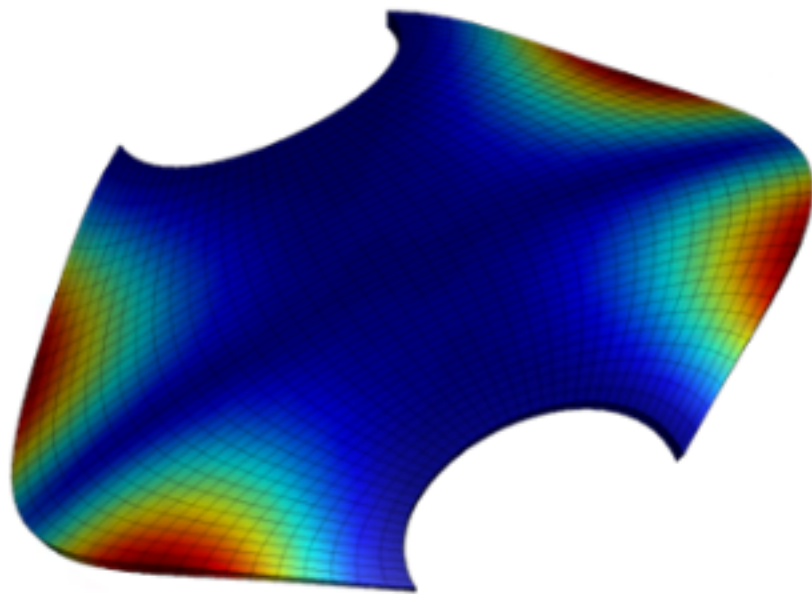
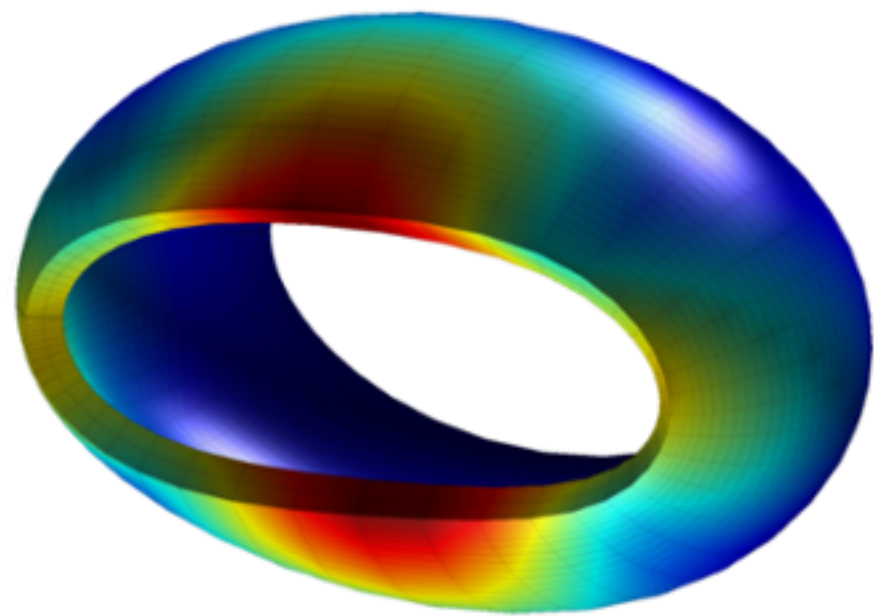
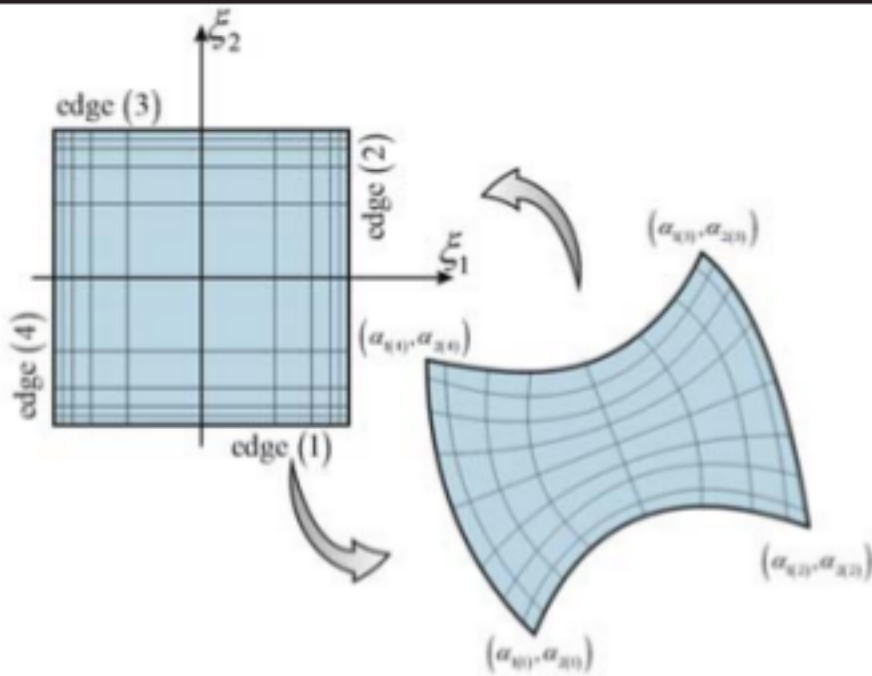
**Prof. Francesco Tornabene**

**Esame finale anno 2018**



# Higher-order Strong and Weak Formulations for Arbitrarily Shaped Doubly-Curved Shells Made of Advanced Materials

PhD Thesis in  
Civil, Chemical, Environmental, and Materials Engineering



Alma Mater Studiorum - University of Bologna

PhD Candidate

**Michele Bacciocchi**

Advisor: Prof. Erasmo Viola

Co-Advisor: Prof. Francesco Tornabene

**XXX Cycle**



*Every path is the right path.  
Everything could've been anything else.  
And it would have just as much meaning.*

(From the movie "Mr. Nobody", 2009)



## *Acknowledgements*

I am extremely grateful to all the members of my research group, Professor Erasmo Viola, Assistant Professor Francesco Tornabene and Junior Assistant Professor Nicholas Fantuzzi, for their steady support, constant encouragement, confidence and friendship.

Their undeniable expertise has allowed to reach challenging and admirable objectives in the last three years. We can be absolutely proud of them. Special thanks must be expressed to my co-advisor for his guidance throughout the research activity we faced together.

I would like to thank also my family for their support to all my challenges and the freedom they granted me to pursue my passions. I would not be writing these words without your directions and the countless opportunities you all have permitted.

These acknowledgements would not be complete without mentioning all my friends that have always believed in me and supported my choices.

*Bologna, May 2018*

*Michele Bacciocchi*



# *Index*

PREFACE.....	XI
--------------	----

## **1 DIFFERENTIAL AND INTEGRAL QUADRATURE METHODS: A GENERAL APPROACH**

<b>1.1 DERIVATIVE APPROXIMATION .....</b>	<b>4</b>
1.1.1 BASIS FUNCTIONS .....	9
1.1.1.1 Lagrange polynomials .....	9
1.1.1.2 Trigonometric Lagrange polynomials .....	11
1.1.1.3 Orthogonal polynomials .....	12
1.1.1.3.1 <i>Jacobi polynomials</i> .....	12
1.1.1.3.2 <i>Hermite polynomials</i> .....	14
1.1.1.3.3 <i>Laguerre polynomials</i> .....	14
1.1.1.4 Power functions.....	15
1.1.1.5 Exponential functions.....	15
1.1.1.6 Boubaker polynomials.....	15
1.1.1.7 Bessel functions.....	16
1.1.1.8 Fourier functions .....	15
1.1.2 GRID POINT DISTRIBUTIONS .....	17
1.1.3 EXTENSION TO TWO-DIMENSIONAL DOMAINS .....	17
<b>1.2 INTEGRAL APPROXIMATION .....</b>	<b>21</b>

## **2 SHELL STRUCTURES: PRINCIPLES OF DIFFERENTIAL GEOMETRY**

<b>2.1 DIFFERENTIAL GEOMETRY .....</b>	<b>27</b>
2.1.1 CURVES IN THREE-DIMENSIONAL SPACE .....	27
2.1.2 SURFACES .....	31
2.1.2.1 Parametric curves and first fundamental form .....	31

---

2.1.2.2 Outward unit normal vector .....	34
2.1.2.3 Second fundamental form .....	34
2.1.2.4 Main curvatures .....	36
2.1.2.5 Fundamental theorem of the theory of surfaces .....	36
2.1.2.6 Gaussian curvature .....	39
2.1.2.7 Classifications of surfaces .....	40
<b>2.2 SHELL STRUCTURES .....</b>	<b>41</b>
<b>2.3 NUMERICAL CONSIDERATIONS .....</b>	<b>44</b>
2.3.1 DISTORTED DOMAINS AND ISOGEOMETRIC MAPPING .....	44
2.3.1.1 Non-Uniform Rational Basis Splines .....	50

### **3 STRONG AND WEAK FORMULATIONS FOR DOUBLY-CURVED SHELLS: HIGHER-ORDER THEORIES**

<b>3.1 SHELL STRUCTURAL MODEL .....</b>	<b>56</b>
3.1.1 BRIEF NOTES ON THREE-DIMENSIONAL ELASTICITY .....	57
3.1.1.1 Anisotropic materials .....	59
3.1.1.2 Orthotropic materials .....	60
3.1.1.3 Isotropic materials .....	61
3.1.2 MAIN ASSUMPTIONS .....	62
3.1.3 DISPLACEMENT FIELD .....	63
3.1.3.1 Higher-order Shear Deformation Theories .....	65
3.1.3.2 Displacement interpolation using Lagrange polynomials .....	66
3.1.4 KINEMATIC EQUATIONS .....	69
3.1.5 CONSTITUTIVE EQUATIONS .....	78
3.1.5.1 Composite materials .....	78
3.1.5.1.1 <i>Fibrous composites</i> .....	79
3.1.5.1.2 <i>Granular composites</i> .....	83
3.1.5.1.3 <i>Laminated composites</i> .....	93
3.1.6 EQUATIONS OF MOTION .....	94
3.1.6.1 Generalized external actions .....	105

3.1.6.1.1	<i>Surface loads</i> .....	105
3.1.6.1.2	<i>Volume loads</i> .....	106
3.1.6.1.3	<i>Winkler-Pasternak elastic foundation</i> .....	107
3.1.7	STRONG FORMULATION.....	110
3.1.7.1	Governing equations for distorted domains .....	117
3.1.7.2	Discrete form of the governing equations .....	119
3.1.8	WEAK FORMULATION .....	120
3.1.8.1	Governing equations for distorted domains .....	130
3.1.8.2	Discrete form of the governing equations .....	133
3.1.8.2.1	<i>Discrete equations for regular domains</i> .....	134
3.1.8.2.2	<i>Discrete equations for distorted domains</i> .....	135
<b>3.2</b>	<b>EXTERNAL RESTRAINTS</b> .....	<b>139</b>
3.2.1	CONTINUITY CONDITIONS .....	142
<b>3.3</b>	<b>REMARKS ON FIRST-ORDER THEORIES</b> .....	<b>143</b>
<b>4</b>	<b>NUMERICAL APPLICATIONS: FREE VIBRATION ANALYSIS</b>	
<b>4.1</b>	<b>MOTION EQUATIONS</b> .....	<b>145</b>
4.1.1	STRONG FORMULATION.....	146
4.1.2	WEAK FORMULATION .....	147
4.1.3	SOLUTION OF THE EIGENVALUE PROBLEM.....	148
<b>4.2</b>	<b>NUMERICAL APPLICATIONS</b> .....	<b>149</b>
4.2.1	CONVERGENCE ANALYSIS .....	150
4.2.2	COMPARISON WITH THE FEM .....	165
4.2.3	HIGHER-ORDER SHEAR DEFORMATION THEORIES.....	172
4.2.4	ARBITRARILY SHAPED DOMAINS .....	178
4.2.4	EFFECT OF CNT AGGLOMERATION .....	190
<b>CONCLUSIONS</b> .....		<b>197</b>
<b>REFERENCES</b> .....		<b>199</b>



# *Preface*

This work aims to present an efficient and accurate higher-order formulation to solve the strong and weak forms of the fundamental equations that govern the mechanical behavior of doubly-curved shell structures made of innovative and advanced materials. In particular, the thesis is focused on the development of a numerical tool which can guarantee high levels of accuracy with a low computational effort in the dynamic analysis of the structural elements under consideration. In order to highlight the validity of the proposed approach, the inadequacy of some commercial tools based on the Finite Element Method (FEM) is also proven. A set of comparison tests is presented for this purpose.

The present thesis is organized in four chapters. In the first one, the Differential Quadrature (DQ) and Integral Quadrature (IQ) methods are discussed according to a general approach. In particular, the fundamental aspects of the two different numerical methods, required respectively for the approximation of derivatives and integrals, are presented. These techniques carry out numerically derivatives and integrals, by means of weighted sums of the values that the function (to differentiate or integrate) assumes in some discrete points placed within the reference domain. Several approaches and basis functions for the polynomial interpolation are presented for the computation of the so-called weighting coefficients.

The second chapter focuses on the main aspects of differential geometry. The analytical description of doubly-curved surfaces that are described in orthogonal and principal coordinates, which are taken as the middle surfaces of shell structures, is presented. This mathematical approach represents an extremely efficient tool to compute easily those geometric quantities that are needed in the governing equations of doubly-curved structures, such as the main radii of curvature and the Lamè parameters. In addition, a final section is added to present an isogeometric mapping based on Non-Uniform Rational Basis Spline (NURBS), which can be used to describe arbitrarily shaped and distorted surfaces.

The shell structural model, instead, is discussed in the third chapter, after some brief notes on three-dimensional elasticity. An Equivalent Single Layer (ESL) approach is employed to this aim. In particular, the theoretical framework is based on a unified formulation that allows to develop and compare several structural theories characterized by different orders of kinematic expansion. Thus, various Higher-order Shear Deformation Theories (HSDTs) can

be obtained. The governing equations are obtained by means of the well-known Hamilton's variational principle. The strong formulation of the fundamental system of governing equations is presented first. Then, the corresponding weak formulation is developed as well.

For this purpose, a higher-order Lagrangian approximation of the degrees of freedom, which consists in the nodal displacements, is adopted. For both formulations, the application of various kinds of external loads and boundary conditions are discussed. In particular, a complete description of the strong and weak formulations is shown. For the latter, two different continuity requirements are discussed, which are the  $C^1$  and  $C^0$ . On the other hand, the strong formulation is always solved by enforcing boundary conditions that satisfy the  $C^1$  hypotheses. It should be noted that the DQ and IQ methods are used respectively to obtain the corresponding discrete form of the governing equations for the strong and weak formulations.

In the same chapter, many sections are focused on constitutive laws for advanced composite materials, which are fibrous composites, granular composites, and laminated composites. In addition, a micromechanical model is presented to take into account the effect of agglomeration in the so-called nanocomposites, which are a particular class of granular composites with a reinforcing phase made of Carbon Nanotubes (CNTs).

A set of numerical analyses is presented and discussed in the last chapter. All the analyses are carried out from the dynamic point of view. In other words, the solutions are presented in terms of natural frequencies. As a preliminary test, the convergence, accuracy, and stability features of the numerical approaches and the theoretical model are discussed. Then, the present methodologies are compared with the well-known Finite Element Method (FEM). For this purpose, a commercial software is used. In conclusion, many applications are shown to prove that the proposed approaches can deal easily with distorted shells made of advanced constituents.

Finally, the main results of the thesis are summarized and discussed briefly in the concluding section, where the advantages of the current methodologies are emphasized.

# *Chapter 1*

## *Differential and Integral Quadrature Methods: A General Approach*

Each physical phenomenon can be modeled by means of a set of differential equations from the mathematical point of view. Several parameters and variables are consequently involved in these governing equations. Depending on to physical event that must be analyzed, these parameters assume a different meaning and relatively complex equations can be carried out [1-5].

As far as the structural mechanics is concerned, these governing equations are developed to link together and evaluate consequently various mechanical quantities, such as the displacement field, the natural frequencies, or the stress and strain distributions, of a three-dimensional medium. For this purpose, the main aim of scientists and engineers who work in this field is to solve the corresponding governing equations, by applying also the proper initial and boundary conditions. Thus, the mathematical model of a physical phenomenon is accomplished once appropriate hypotheses and premises are introduced. This statement is completely general and valid for each mechanical field.

Nevertheless, it should be recalled that a closed-form solution cannot be obtained in general for these mathematical models, unless strong simplifications are taken into account. In other words, the systems of differential equations at issue cannot be solved analytically. For this purpose, a numerical method must be used to get an approximate solution. In the last decades, several numerical approaches have been developed to this aim [6-15].

As highlighted in the papers [11-15], two formulations of the same system of governing equations can be developed, which are the strong and weak (or variational) formulations, respectively. These two approaches require a different numerical method to approximate the unknown fields and obtain the solution. In the following, the basic aspects of these two methodologies are briefly introduced.

Once the governing equations that rule a generic structural problem are obtained, together with the corresponding boundary conditions, a differential system is written. If the strong formulation is solved, a numerical tool able to approximate derivatives is needed, since these equations are directly changed into a discrete system [15].

On the other hand, the differentiability requirement is reduced through a weighted integral statement if the corresponding weak form of the governing equations are developed [14, 15]. In other words, the governing differential system of equations is replaced by an integral one. Thus, an equivalent integral formulation of lower order has to be solved when the weak formulation is considered [15]. As a consequence, a numerical approximation of integrals has to be performed. It should be recalled that the Finite Element Method (FEM), developed in the early 1940s [16-23], is based on the variational (or weak) form of the governing equations.

As it can be easily deduced from these concise definitions, two different numerical approaches can be used to obtain the solution of both the strong and weak formulations, which allow to approximate derivatives and integrals, respectively. In this chapter, the Differential Quadrature (DQ) and Integral Quadrature (IQ) methods are discussed for these purposes. In particular, the former is used to approximate derivatives, whereas the latter provides a numerical solution for the integration procedure.

The DQ method was firstly developed by Bellman and his coworkers in the early 1970s, who proposed a numerical tool able to approximate partial and total derivatives [24-26]. They named their technique as “quadrature” to underline the similarity with the well-known Gaussian quadrature, developed in the previous years [27]. The DQ method, in fact, allowed

to evaluate the numerical derivative of a generic smooth function at a point as a linear weighted summation of the values that the function itself assumes in each point of the domain. The key points of their approach were the evaluation of the weighting coefficients required by the sum in hand and the placement of several discrete points within the domain. Therefore, the method at issue had its roots in the functional approximation [28]. Nevertheless, it should be recalled that this methodology led to numerical errors in terms of accuracy when a large number of discrete nodes was chosen. In particular, these problems could arise if more than thirteen points were used to discretize the domain, since a Vandermonde-like matrix had to be inverted to compute the weighting coefficients.

The previous researches by Bellman and coworkers [24-26] and the works by Civan and Sliepcevich [29-33] were the starting points of an enhanced approach. This methodology was presented by Quan and Chang in the late 1980s, who developed a closed-form solution for the evaluation of the weighting coefficients, when peculiar basis functions were used for the functional approximations [34, 35]. According to their method, a stable and accurate solution could be found even if the number of discrete points in the domain was greater than thirteen.

As highlighted in the review paper by Finlayson and Scriven [28], the DQ technique could be classified as a particular case of the well-known method of weighted residual, likewise the Spectral Methods (SMs), whose features were summarized in the work by Gottlieb and Orszag [36]. Further details concerning these methodologies can be found in the books by Boyd [37], Canuto et al. [38], Quarteroni et al. [39], Shen et al. [40], and Trefethen [41]. The similarity between DQ method and SMs was underlined by Chen in his thesis [42], as well as in the book by Boyd [37].

For the sake of completeness, it should be mentioned that both DQ method and SMs employed global basis functions defined in the whole domain for the functional approximation, which could be chosen as polynomials of high degree. This aspect represented one of the biggest differences with respect to the classical FEM, in which local functions of low degree were assumed as basis functions. These functions, in fact, were linear or quadratic polynomials defined only in specific subintervals in which the whole domain was discretized [13]. In other words, the SMs represented a global approach, whereas the FEM denoted a local one. Due to these properties, SMs were really accurate and characterized by a fast convergence. Nevertheless, the accuracy, stability and reliability features of SMs depended on the number of discrete points and their position as well.

Shu gave the greatest contribution for the development of the DQ method in the early 1990s [43, 44]. He proposed, in fact, a more stable and general approach for computing the weighting coefficients for any derivative order through a set of recursive expressions. The Lagrange polynomials, as well as the trigonometric Lagrange polynomials, were assumed as basis functions and the choice of the discrete grid distribution could be performed arbitrarily. In other words, the definition of the weighting coefficients were independent from the position of the discrete points in the reference domain if the aforementioned basis functions were used for the functional approximation. This approach was termed as Generalized Differential Quadrature (GDQ) to underline its general features, as specified in the papers by Shu and Richards [45, 46]. Further details concerning the DQ method and its development can be found in the review papers by Bert and Malik [47] and by Tornabene et al. [13].

Finally, it should be mentioned that the definition of the weighting coefficients introduced by Bellman and Casti for the approximation of derivatives was used by Civan to develop an integration technique, known as Integral Quadrature (IQ) method [48]. Several numerical tests concerning the IQ method were later presented by Civan and Sliepcevich in their works [29-33]. A more general approach were developed once Shu provided the recursive expressions for the evaluation of the weighting coefficients. Consequently, the Generalized Integral Quadrature (GIQ) method was presented as counterpart of the GDQ method [43, 44].

## 1.1 DERIVATIVE APPROXIMATION

The current section is focused on the approximation of derivatives. The main aspects of the DQ method are presented for this purpose. In particular, a general view on the numerical approach at issue is illustrated.

Let us consider a smooth function  $f(x)$ , which is defined within the one-dimensional closed domain  $[a, b]$ . It is worth noting that  $a, b$  represent the boundary values. Since the derivatives of  $f(x)$  are evaluated in specific nodes of this domain,  $I_N$  discrete points must be placed within the interval  $[a, b]$ . In other words, one gets

$$a = x_1, x_2, \dots, x_k, \dots, x_{I_N-1}, x_{I_N} = b \quad (1.1)$$

where the coordinate of the generic element  $x_k$  is given by

$$x_k = \frac{b-a}{d-c}(z_k - c) + a \quad (1.2)$$

for  $k = 1, 2, \dots, I_N$ . As it can be noted in definition (1.2), the position of  $x_k$  depends on the quantity  $z_k$ , which denotes the placement of the  $k$ -th node of a generic grid distribution defined in the reference interval  $[c, d]$ . To this aim, various discrete distributions can be used and the values of  $z_k$  are assumed as

$$z_k = \frac{r_k - r_1}{r_{I_N} - r_1} \quad (1.3)$$

where the meanings of  $r_k$ , for  $k = 1, 2, \dots, I_N$ , is defined by the grid distribution itself. In fact,  $r_k$  denotes the position of the  $k$ -th discrete point within the domain in which the distribution is defined. Several examples of grid point distributions will be illustrated in the following paragraphs. Finally, the one-dimensional scheme at issue is shown in Figure 1.1 for the sake of completeness. The values that the function  $f(x)$  assumes in these discrete nodes are denoted generally by  $f(x_k)$ , for  $k = 1, 2, \dots, I_N$ .

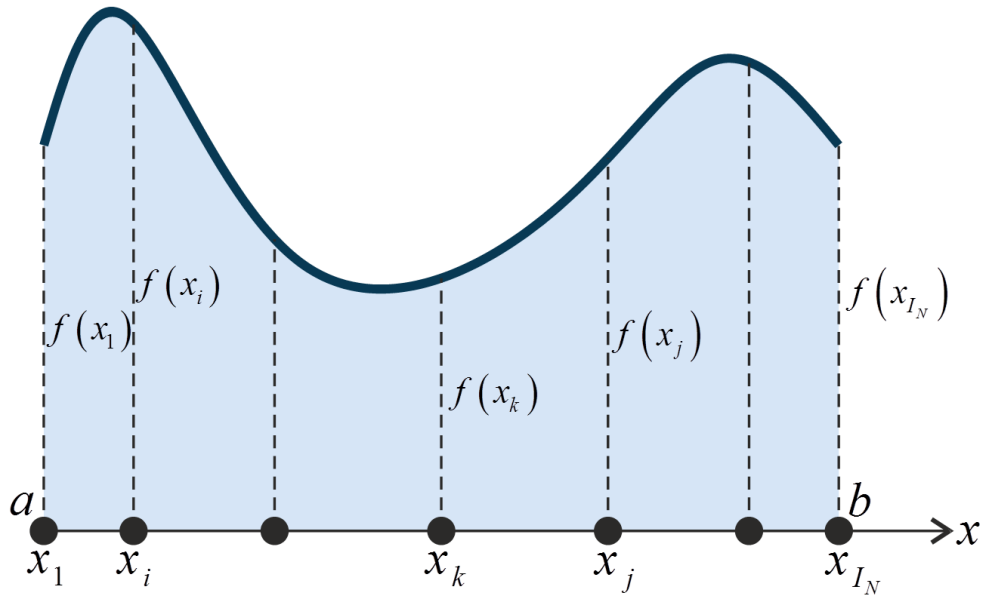


**Figure 1.1** – Discrete points for a one-dimensional scheme.

At this point, a set of polynomial basis functions  $\psi_j(x)$ , for  $j=1,2,\dots,I_N$ , must be introduced to approximate the generic function  $f(x)$  within the reference domain. The following definition is required for this purpose

$$f(x) \cong \sum_{j=1}^{I_N} \lambda_j \psi_j(x) \quad (1.4)$$

in which  $\psi_j(x)$  stands for the  $j$ -th polynomial of the basis functions, whereas  $\lambda_j$  are the unknown coefficients to be computed. As it will be shown in the next sections, different basis functions can be employed. For conciseness purpose, a compact vector notation can be used. It is convenient to collect the functional values  $f(x_k)$  in the corresponding vector  $\mathbf{f}$  defined below

$$\mathbf{f} = \left[ f(x_1) \quad \cdots \quad f(x_k) \quad \cdots \quad f(x_{I_N}) \right]^T \quad (1.5)$$

Analogously, the same nomenclature can be employed to collect the unknown coefficients  $\lambda_j$  in the conforming vector  $\boldsymbol{\lambda}$

$$\boldsymbol{\lambda} = \left[ \lambda_1 \quad \cdots \quad \lambda_k \quad \cdots \quad \lambda_{I_N} \right]^T \quad (1.6)$$

Consequently, the approximation (1.4) takes the following aspect

$$\mathbf{f} \cong \mathbf{A}\boldsymbol{\lambda} \quad (1.7)$$

where  $\mathbf{A}$  is the coefficient matrix. Its generic element  $A_{ij}$  is given by the value that the  $j$ -th basis function assumes in the  $i$ -th discrete point of the domain. In other words, one gets

$$A_{ij} = \psi_j(x_i) \quad (1.8)$$

for  $i, j = 1, 2, \dots, I_N$ . The operator  $\mathbf{A}$  is a square matrix whose size is  $I_N \times I_N$ . By definition, the  $n$ -th order derivative of the considered function  $f(x)$  is given by

$$\frac{d^n f(x)}{dx^n} = \sum_{j=1}^{I_N} \lambda_j \frac{d^n \psi_j(x)}{dx^n} \quad (1.9)$$

for  $n = 1, 2, \dots, I_N - 1$ . Expression (1.9) is valid since the coefficients  $\lambda_j$  do not depend on  $x$ . Thus, the derivative is moved directly to the basis functions due to the linearity. If  $\mathbf{f}^{(n)}$  denotes the vector that collects the  $n$ -th order derivatives of the function  $f(x)$  in each discrete point of the domain as specified below

$$\mathbf{f}^{(n)} = \left[ \left. \frac{d^n f(x)}{dx^n} \right|_{x_1} \quad \dots \quad \left. \frac{d^n f(x)}{dx^n} \right|_{x_k} \quad \dots \quad \left. \frac{d^n f(x)}{dx^n} \right|_{x_{I_N}} \right]^T \quad (1.10)$$

relation (1.9) becomes

$$\mathbf{f}^{(n)} = \mathbf{A}^{(n)} \boldsymbol{\lambda} \quad (1.11)$$

Recalling equation (1.9), it is easy to deduct that the generic element  $A_{ij}^{(n)}$  of the corresponding matrix  $\mathbf{A}^{(n)}$  is given by

$$A_{ij}^{(n)} = \left. \frac{d^n \psi_j(x)}{dx^n} \right|_{x_i} \quad (1.12)$$

The definition of  $\boldsymbol{\lambda}$  can be obtained from equation (1.7) if the matrix  $\mathbf{A}$  is inverted. This property depends on the choice of both the basis functions and the discrete grid distributions. One gets

$$\boldsymbol{\lambda} = \mathbf{A}^{-1} \mathbf{f} \quad (1.13)$$

By inserting expression (1.13) into the definition (1.11), the vector  $\mathbf{f}^{(n)}$  assumes the following aspect

$$\mathbf{f}^{(n)} = \mathbf{A}^{(n)} \mathbf{A}^{-1} \mathbf{f} \quad (1.14)$$

At this point, the differential operator  $\mathbf{D}^{(n)}$ , whose size is  $I_N \times I_N$ , can be introduced

$$\mathbf{D}^{(n)} = \mathbf{A}^{(n)} \mathbf{A}^{-1} \quad (1.15)$$

Thus, relation (1.14) becomes

$$\mathbf{f}^{(n)} = \mathbf{D}^{(n)} \mathbf{f} \quad (1.16)$$

For the sake of completeness, it should be noted that the differential operator  $\mathbf{D}^{(n)}$  is computable as the product of the coefficient matrix and its inverse one. This procedure could turn out to be inaccurate if the matrix  $\mathbf{A}$  is ill-conditioned. In general, this happens when the domain is discretized by using a high number of sampling points and the coefficient matrix  $\mathbf{A}$  becomes similar to the well-known Vandermonde matrix. This issue is negligible for particular choice of the basis functions, as it will be explained in the following paragraphs. Finally, relation (1.9) can be written also as follows

$$\left. \frac{d^n f(x)}{dx^n} \right|_{x_i} = \sum_{j=1}^{I_N} D_{ij}^{(n)} f(x_j) \quad (1.17)$$

where  $D_{ij}^{(n)}$  is the generic element of  $\mathbf{D}^{(n)}$ , which assumes the aspect shown below

$$D_{ij}^{(n)} = \left( \mathbf{A}^{(n)} \mathbf{A}^{-1} \right)_{ij} \quad (1.18)$$

It should be pointed out that  $D_{ij}^{(n)}$  stands for the weighting coefficients required for the  $n$ -th order derivative. In general, this procedure is valid for each combination of basis functions and discrete grid distributions, without any restriction. Nevertheless, closed-form expressions are available in the literature for the evaluation of these coefficients. Such relations do not require the inversion of the coefficient matrix even if the definition of the numerical derivatives is equivalent. In these circumstances, the weighting coefficients will be denoted by the symbol  $\zeta_{ij}^{(n)}$ .

At this point, it should be recalled that the reference domain, which could be named also physical domain, could be defined in an interval different from the one of the chosen basis functions. Thus, the following coordinate change is required to move from the definition interval to the physical domain

$$\frac{d^n f(x)}{dx^n} = \left( \frac{r_{I_N} - r_1}{x_{I_N} - x_1} \right)^n \frac{d^n f(x(r))}{dr^n} \quad (1.19)$$

for  $n = 1, 2, \dots, I_N - 1$ . The physical domain  $x$ , whose length is given by  $x_{I_N} - x_1$ , can be related to the domain  $r$  of the basis polynomials by means of the following relation

$$x(r) = \frac{x_{I_N} - x_1}{r_{I_N} - r_1} (r - r_1) + x_1 \quad (1.20)$$

It is clear that  $r_{I_N} - r_1$  specifies the length of the domain in which the basis functions are defined. The following linear transformation allows to compute the weighting coefficients  $\zeta_{ij}^{(n)}$  (or  $D_{ij}^{(n)}$ ) in the physical domain, as a function of the weighting coefficients  $\tilde{\zeta}_{ij}^{(n)}$  (or  $\tilde{D}_{ij}^{(n)}$ ) related to the basis function domain

$$\zeta_{ij}^{(n)} = \left( \frac{r_N - r_1}{x_N - x_1} \right)^n \tilde{\zeta}_{ij}^{(n)} \quad (1.21)$$

with  $i, j = 1, 2, \dots, I_N$  and  $n = 1, 2, \dots, I_N - 1$ .

At this point, it should be mentioned that a matrix multiplication approach can be also used to compute the weighting coefficient matrix for the  $n$ -th order derivatives  $\mathbf{D}^{(n)}$ , once the

operator which includes the weighting coefficients for the first-order derivatives  $\mathbf{D}^{(1)}$  is obtained. The recursive approach in hand assume the following aspect

$$\mathbf{D}^{(n)} = \mathbf{D}^{(n-1)}\mathbf{D}^{(1)} \quad (1.22)$$

in which  $\mathbf{D}^{(n-1)}$  is the coefficient matrix related to the  $(n-1)$ -th order derivatives.

### 1.1.1 BASIS FUNCTIONS

In this section, several sets of basis functions that can be used to approximate a generic smooth function  $f(x)$  are illustrated. In general, the weighting coefficients for the derivative can be evaluated by inverting the matrix  $\mathbf{A}$ . The closed form solutions are also presented when available in the literature.

#### 1.1.1.1 Lagrange polynomials

The Lagrange polynomials  $l_j(r)$ , for  $j=1,2,\dots,I_N$ , are defined in the reference domain  $r \in ]-\infty, +\infty[$  and assume the following definitions

$$l_j(r) = \frac{\mathcal{L}(r)}{(r-r_j)\mathcal{L}^{(1)}(r)} \quad (1.23)$$

where

$$\begin{aligned} \mathcal{L}(r) &= \prod_{k=1}^{I_N} (r-r_k) \\ \mathcal{L}^{(1)}(r_j) &= \prod_{k=1, j \neq k}^{I_N} (r_j-r_k) \end{aligned} \quad (1.24)$$

It should be noted that the polynomial basis has  $I_N$  functions of degree  $I_N-1$ . In other words, each polynomial identifies  $I_N-1$  roots. If the Lagrange polynomials are taken as basis functions, the coefficient matrix  $\mathbf{A}$  turns out to be equal to the identity matrix  $\mathbf{I}$ , since the following property is valid

$$l_j(r_i) = \begin{cases} 0 & \text{for } i \neq j \\ 1 & \text{for } i = j \end{cases} \quad (1.25)$$

Relations (1.25) specify that the  $j$ -th polynomial assumes a unitary value only in the corresponding root ( $r_i = r_j$ ). Consequently, the matrix  $\mathbf{A}$  is not ill-conditioned and it is always invertible, even for a higher number of discrete points. Thus, the weighting coefficients (1.18) can be written as follows

$$D_{ij}^{(n)} = \left( \mathbf{A}^{(n)} \mathbf{A}^{-1} \right)_{ij} = \left( \mathbf{A}^{(n)} \mathbf{I} \right)_{ij} = A_{ij}^{(n)} \quad (1.26)$$

In other words, one gets  $A_{ij}^{(n)} = l_j^{(n)}(r_i)$ , where  $l_j^{(n)}(r_i)$  stands for the  $n$ -th order derivative of the polynomial (1.23) evaluated at  $r_i$ . Typically, when the coefficient matrix is inverted and the Lagrange polynomials are used, the numerical approach is known as Lagrange Spectral Collocation Method. Nevertheless, the same interpolating functions are used by Shu [44] to derive a recursive formulation for the evaluation of the weighting coefficients  $\tilde{\zeta}_{ij}^{(n)}$ . Without presenting the whole treatise proposed by Shu, in the following the recursive formulae for the weighting coefficients are shown for the  $n$ -th order derivatives, with  $i, j = 1, 2, \dots, I_N$  and  $n = 1, 2, \dots, I_N - 1$

$$\tilde{\zeta}_{ij}^{(n)} = n \left( \tilde{\zeta}_{ij}^{(1)} \tilde{\zeta}_{ii}^{(n-1)} - \frac{\tilde{\zeta}_{ij}^{(n-1)}}{r_i - r_j} \right) \quad (1.27)$$

for  $i \neq j$ , and

$$\tilde{\zeta}_{ij}^{(n)} = - \sum_{j=1, j \neq i}^{I_N} \tilde{\zeta}_{ij}^{(n)} \quad (1.28)$$

for  $i = j$ . The symbol  $\tilde{\zeta}_{ij}^{(1)}$  denotes the weighting coefficients for the first-order derivatives, which can be evaluated as shown below

$$\tilde{\zeta}_{ij}^{(1)} = \frac{\mathcal{L}^{(1)}(r_i)}{(r_i - r_j) \mathcal{L}^{(1)}(r_j)} \quad (1.29)$$

This approach, which considers the recursive formulation proposed by Shu, is known as GDQ method, as specified in the introduction.

### 1.1.1.2 Trigonometric Lagrange polynomials

The trigonometric Lagrange polynomials are denoted by  $g_j(r)$ , for  $j = 1, 2, \dots, I_N$ , and can be defined in the reference domains  $r \in [0, \pi]$ ,  $r \in [0, 2\pi]$  or  $r \in [-\pi/4, \pi/4]$ . They assume the following aspect

$$g_j(r) = \frac{\mathcal{G}(r)}{\sin\left(\frac{r-r_j}{2}\right)\mathcal{G}^{(1)}(r_j)} \quad (1.30)$$

where

$$\begin{aligned} \mathcal{G}(r) &= \prod_{k=1}^N \sin\left(\frac{r-r_k}{2}\right) \\ \mathcal{G}^{(1)}(r_j) &= \prod_{k=1, k \neq j}^N \sin\left(\frac{r_j-r_k}{2}\right) \end{aligned} \quad (1.31)$$

These polynomials have the same features of the previous ones  $l_j(r)$ . In particular, property (1.25) is valid even in this circumstance

$$g_j(r_i) = \begin{cases} 0 & \text{for } i \neq j \\ 1 & \text{for } i = j \end{cases} \quad (1.32)$$

Thus, the weighting coefficients for the derivatives can be computed by means of the general approach presented above, since the coefficient matrix is not ill-conditioned. As in the previous case, one gets  $A_{ij}^{(n)} = g_j^{(n)}(r_i)$ , in which  $g_j^{(n)}(r_i)$  represents the  $n$ -th order derivative of the polynomial (1.30) evaluated at  $r_i$ .

A recursive formulation for the evaluation of the weighting coefficients up to the fourth-order derivatives have been presented by Shu [44], with  $i, j = 1, 2, \dots, I_N$

$$\tilde{\zeta}_{ij}^{(1)} = \frac{\mathcal{G}^{(1)}(r_i)}{2 \sin\left(\frac{r_i-r_j}{2}\right)\mathcal{G}^{(1)}(r_j)} \quad (1.33)$$

$$\tilde{\zeta}_{ij}^{(2)} = \tilde{\zeta}_{ij}^{(1)} \left( 2\tilde{\zeta}_{ii}^{(1)} - \cot\left(\frac{r_i-r_j}{2}\right) \right) \quad (1.34)$$

$$\tilde{\zeta}_{ij}^{(3)} = \tilde{\zeta}_{ij}^{(1)} \left( 3\tilde{\zeta}_{ii}^{(2)} + \frac{1}{2} \right) - \frac{3}{2} \tilde{\zeta}_{ij}^{(2)} \cot \left( \frac{r_i - r_j}{2} \right) \quad (1.35)$$

$$\tilde{\zeta}_{ij}^{(4)} = \tilde{\zeta}_{ij}^{(1)} \left( 4\tilde{\zeta}_{ii}^{(3)} - \tilde{\zeta}_{ii}^{(1)} \right) + \frac{3}{2} \tilde{\zeta}_{ij}^{(2)} + \left( \frac{\tilde{\zeta}_{ij}^{(1)}}{2} - 2\tilde{\zeta}_{ij}^{(3)} \right) \cot \left( \frac{r_i - r_j}{2} \right) \quad (1.36)$$

for  $i \neq j$ . Expression (1.28) is still valid in this case for  $i = j$ , with  $n = 1, 2, 3, 4$ . The current approach is known as Harmonic Differential Quadrature (HDQ) method.

### 1.1.1.3 Orthogonal polynomials

Another class of basis functions that can be used for the functional approximation is the one of orthogonal polynomials. They are characterized by the fact that two different polynomials of the basis are orthogonal to each other with respect to their inner product. Among them, the classical orthogonal polynomials are the most used, such as the Jacobi polynomials and its subcategories, the Hermite polynomials, and Laguerre polynomials.

#### 1.1.1.3.1 Jacobi polynomials

The Jacobi polynomials, also known as hypergeometric polynomials, represent the solution to the so-called Jacobi differential equation and include the Gegenbauer polynomials, the Legendre polynomials, the Lobatto polynomials, and the Chebyshev polynomials as special cases. The Jacobi polynomials  $J_j^{(\gamma, \delta)}(r)$  are defined in the domain  $r \in [-1, 1]$  and can be obtained by means of the following differential expression

$$J_j^{(\gamma, \delta)}(r) = \frac{(-1)^{j-1}}{2^{j-1} (j-1)! (1-r)^\gamma (1+r)^\delta} \frac{d^{j-1}}{dr^{j-1}} \left( (1-r)^{j-1+\gamma} (1+r)^{j-1+\delta} \right) \quad (1.37)$$

for  $j = 1, 2, \dots, I_N$ . Alternatively, a recursive formula can be used

$$J_j^{(\gamma, \delta)}(r) = \frac{(2j + \gamma + \delta - 3) \left( (2j + \gamma + \delta - 2)(2j + \gamma + \delta - 4)r + \gamma^2 - \delta^2 \right) J_{j-1}^{(\gamma, \delta)}(r)}{2(j-1)(j + \gamma + \delta - 1)(2j + \gamma + \delta - 4)} + \frac{(j + \gamma - 2)(j + \delta - 2)(2j + \gamma + \delta - 2) J_{j-2}^{(\gamma, \delta)}(r)}{(j-1)(j + \gamma + \delta - 1)(2j + \gamma + \delta - 4)} \quad (1.38)$$

for  $j = 3, 4, \dots, I_N$ , with  $J_1^{(\gamma, \delta)}(r) = 1$  and  $J_2^{(\gamma, \delta)}(r) = (2(\gamma + 1) + (\gamma + \delta + 2)(r - 1))/2$ . A closed form solution for the evaluation of the weighting coefficients for the derivatives up to the second-order was proposed by Quan and Chang [34, 35], by using the corresponding distribution only as discrete grid. Without losing generality, in the present work the weighting coefficients are evaluated by inverting the coefficient matrix  $\mathbf{A}$ . It should be noted that the Jacobi polynomials are written as a function of the two parameters  $\gamma$  and  $\delta$ , assuming  $\gamma, \delta > -1$ . For a particular choice of these parameters, other polynomial sets can be derived as Gegenbauer polynomials  $C_j^{(\lambda)}(r)$ :  $\lambda = \gamma + 1/2 = \delta + 1/2$ , with  $\lambda > -1/2$ ;

- Legendre polynomials  $L_j(r)$ :  $\gamma = \delta = 0$ ;
- Lobatto polynomials  $A_j(r)$ :  $\gamma = \delta = 1$ ;
- Chebyshev polynomials (first kind)  $T_j(r)$ :  $\gamma = \delta = -1/2$ ;
- Chebyshev polynomials (second kind)  $U_j(r)$ :  $\gamma = \delta = 1/2$ ;
- Chebyshev polynomials (third kind)  $V_j(r)$ :  $\gamma = -\delta = -1/2$ ;
- Chebyshev polynomials (fourth kind)  $W_j(r)$ :  $\gamma = -\delta = 1/2$ ;

It should be recalled that recursive formulations for the definitions of such polynomials are available in the literature, as illustrated in the book by Tornabene et al. [5]. For the sake of completeness, those expressions are listed also in Table 1.1.

**Table 1.1** – Recursive formulations for the orthogonal polynomials descending from the Jacobi ones.

Gegenbauer polynomials	
$C_j^{(\lambda)}(r) = \frac{2r}{j-1}(j+\lambda-2)C_{j-1}^{(\lambda)}(r) - \frac{1}{j-1}(j+2\lambda-3)C_{j-2}^{(\lambda)}(r)$ for $j = 2, \dots, I_N$ , with $C_1^{(\lambda)}(r) = 1$ , $C_2^{(\lambda)}(r) = 2\lambda r$	
Legendre polynomials	Lobatto polynomials
$L_j(r) = \frac{(2j-3)rL_{j-1}(r) - (j-2)L_{j-2}(r)}{j-1}$ for $j = 3, \dots, I_N$ , with $L_1(r) = 1$ , $L_2(r) = r$	$A_j(r) = \frac{d}{dr}(L_{j+1}(r))$ for $j = 1, \dots, I_N$
Chebyshev polynomials (I kind)	Chebyshev polynomials (II kind)
$T_j(r) = 2rT_{j-1}(r) - T_{j-2}(r)$ for $j = 3, \dots, I_N$ , with $T_1(r) = 1$ , $T_2(r) = r$	$U_j(r) = 2rU_{j-1}(r) - U_{j-2}(r)$ for $j = 3, \dots, I_N$ , with $U_1(r) = 1$ , $U_2(r) = 2r$
Chebyshev polynomials (III kind)	Chebyshev polynomials (IV kind)
$V_j(r) = 2rV_{j-1}(r) - V_{j-2}(r)$ for $j = 3, \dots, I_N$ , with $V_1(r) = 1$ , $V_2(r) = 2r - 1$	$W_j(r) = 2rW_{j-1}(r) - W_{j-2}(r)$ for $j = 3, \dots, I_N$ , with $W_1(r) = 1$ , $W_2(r) = 2r + 1$

### 1.1.1.3.2 Hermite polynomials

The Hermite polynomials  $H_j(r)$  are defined within the whole real domain  $r \in ]-\infty, +\infty[$ . They can be evaluated by means of the so-called Rodrigues' formula

$$H_j(r) = (-1)^{j-1} e^{r^2} \frac{d^{j-1}}{dr^{j-1}} (e^{-r^2}) \quad (1.39)$$

for  $j = 1, 2, \dots, I_N$ . It is clear that the index  $j$  defines the polynomial degree, which depends on the total number of discrete points  $I_N$  in the reference domain. Alternatively, the following recursive expression can be used

$$H_j(r) = 2rH_{j-1}(r) - 2(j-2)H_{j-2}(r) \quad (1.40)$$

for  $j = 3, 4, \dots, I_N$ , with  $H_1(r) = 1$  and  $H_2(r) = 2r$ . The inverse matrix of  $\mathbf{A}$  is required to evaluate the weighting coefficients, since a closed form solution does not exist for this purpose.

### 1.1.1.3.3 Laguerre polynomials

Differently from the previous polynomials, the Laguerre ones  $G_j(r)$  are defined only in the positive part of the real domain  $r \in [0, +\infty[$ . The Rodrigues' formula is used to compute these polynomials

$$G_j(r) = \frac{1}{(j-1)! e^{-r}} \frac{d^{j-1}}{dr^{j-1}} (r^{j-1} e^{-r}) \quad (1.41)$$

for  $j = 1, 2, \dots, I_N$ . Similarly, a recursive approach can be employed

$$G_j(r) = \frac{(2j-3-r)G_{j-1}(r) - (j-2)G_{j-2}(r)}{j-1} \quad (1.42)$$

for  $j = 3, 4, \dots, I_N$ , with  $G_1(r) = 1$  and  $G_2(r) = 1 - r$ . The weighting coefficients can be evaluated only through the inversion of the coefficient matrix  $\mathbf{A}$ .

### 1.1.1.4 Power functions

The power functions  $Z_j(r)$  (or monomial functions) represent the simplest choice for the basis functions. Nevertheless, the coefficient matrix becomes similar to the Vandermonde one, when the number of discrete point is high (in general, for  $I_N > 13$ ). These polynomials are defined in the whole real domain  $r \in ]-\infty, +\infty[$ , for  $j = 1, 2, \dots, I_N$

$$Z_j(r) = r^{j-1} \quad (1.43)$$

The weighting coefficients can be only computed by means of the inversion of the coefficient matrix  $\mathbf{A}$ , since a closed form expression is not available in the literature.

### 1.1.1.5 Exponential functions

As the previous ones, the exponential basis functions  $E_j(r)$  are defined in the whole real domain  $r \in ]-\infty, +\infty[$ . The following expression is used to define these functions

$$E_j(r) = e^{(j-1)r} \quad (1.44)$$

for  $j = 1, 2, \dots, I_N$ . The exponential functions show the same behavior of the previous function set. Even in this case, the coefficient matrix  $\mathbf{A}$  must be inverted to obtain the weighting coefficients for the derivatives.

### 1.1.1.6 Boubaker polynomials

Boubaker polynomials  $Q_j(r)$  are evaluated in the whole real domain  $r \in ]-\infty, +\infty[$  through the following expression

$$Q_j(r) = \sum_{k=0}^{\phi(j-1)} (-1)^k \binom{j-1-k}{k} \frac{j-1-4k}{j-1-k} r^{j-1-2k} \quad (1.45)$$

for  $j = 2, 3, \dots, I_N$  and  $Q_1(r) = 1$ . Function  $\phi(j-1)$  in (1.45) is defined as follows

$$\phi(j-1) = \frac{2(j-1) + \left( (-1)^{j-1} - 1 \right)}{4} \quad (1.46)$$

Alternatively, a recursive relation can be employed

$$Q_j(r) = rQ_{j-1}(r) - Q_{j-2}(r) \quad (1.47)$$

for  $j = 4, 5, \dots, I_N$ , with  $Q_1(r) = 1$ ,  $Q_2(r) = r$  and  $Q_3(r) = r^2 + 2$ . A closed form solution for the weighting coefficients does not exist, thus the coefficient matrix  $\mathbf{A}$  must be inverted.

### 1.1.1.7 Bessel functions

Bessel polynomials  $P_j(r)$  are defined in the whole real domain  $r \in ]-\infty, +\infty[$ . The following explicit expression allows to obtain the polynomials at issue

$$P_j(r) = \sum_{k=0}^{j-1} \frac{(j-1+k)!}{(j-1-k)!k!} \left(\frac{r}{2}\right)^k \quad (1.48)$$

for  $j = 2, 3, \dots, I_N$  and  $P_1(r) = 1$ . Alternatively, they can be computed through a recursive approach

$$P_j(r) = (2j-3)rP_{j-1}(r) + P_{j-2}(r) \quad (1.49)$$

for  $j = 3, 4, \dots, I_N$ , with  $P_1(r) = 1$  and  $P_2(r) = 1 + r$ . Even in this circumstance, a closed form solution for the weighting coefficients is not available.

### 1.1.1.8 Fourier functions

The Fourier basis functions  $F_j(r)$  can be used for the functional approximation. For this purpose, sine and cosine functions are employed. The following expressions are required to compute the basis function at issue in the reference domain  $r \in [0, 2\pi]$

$$\begin{cases} F_j(r) = \cos\left(\frac{j}{2}r\right) & \text{for } j \text{ even} \\ F_j(r) = \sin\left(\frac{j-1}{2}r\right) & \text{for } j \text{ odd} \end{cases} \quad (1.50)$$

for  $j = 2, 3, \dots, I_N$  and  $F_1(r) = 1$ . The weighting coefficients are evaluated through the inversion of the matrix  $\mathbf{A}$ .

### 1.1.2 GRID POINT DISTRIBUTIONS

The numerical approach at issue requires the introduction of  $I_N$  discrete points within the reference domain. Mathematically speaking, this aspect is given by relation (1.2). In this paragraph, the values of  $z_k$  are specified for several grid distributions available in the literature. For this purpose, the definition of  $z_k$  shown in (1.3) should be recalled, too. For the sake of conciseness, various grid point distributions are listed in Table 1.2.

### 1.1.3 EXTENSION TO TWO-DIMENSIONAL DOMAINS

The treatise just presented can be easily extended to two-dimensional domain. For this purpose, a two-dimensional smooth function  $f(x, y)$  must be introduced. The domain in hand is defined by the boundary values  $x \in [a, b]$  and  $y \in [c, d]$ . As in the previous simpler case, the domain must be discretized by placing  $I_N$  and  $I_M$  sampling point along  $x$  and  $y$  directions, respectively. The same distributions presented in Table 1.2 can be used for this purpose. For the sake of clarity, a two-dimensional domain and the corresponding discrete points are shown in Figure 1.2.

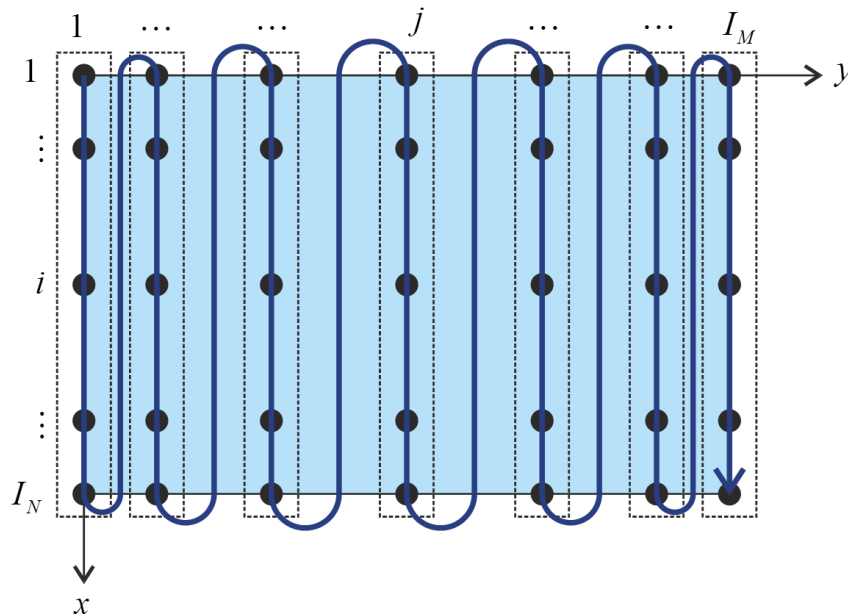


**Figure 1.2** – Discretization of a two-dimensional domain.

**Table 1.2** - Examples of discrete grid distributions.

Uniform (Unif)	Chebyshev-Gauss-Lobatto (Cheb-Gau-Lob)
$z_k = \frac{k-1}{I_N-1}, k = 1, 2, \dots, I_N$	$r_k = \cos\left(\frac{I_N-k}{I_N-1}\pi\right), k = 1, 2, \dots, I_N, r \in [-1, 1]$
Quadratic (Quad)	Chebyshev I kind (Cheb I)
$\begin{cases} z_k = 2\left(\frac{k-1}{I_N-1}\right)^2, k = 1, 2, \dots, \frac{I_N+1}{2} \\ z_k = -2\left(\frac{k-1}{I_N-1}\right)^2 + 4\left(\frac{k-1}{I_N-1}\right) - 1, k = \frac{I_N+1}{2} + 1, \dots, I_N - 1, I_N \end{cases}$	$r_k = \cos\left(\frac{2(I_N-k)+1}{2I_N}\pi\right), k = 1, 2, \dots, I_N, r \in [-1, 1]$
Chebyshev II kind (Cheb II)	Approximate Legendre (App Leg)
$r_k = \cos\left(\frac{I_N-k+1}{I_N+1}\pi\right), k = 1, 2, \dots, I_N, r \in [-1, 1]$	$r_k = \left(1 - \frac{1}{8I_N^2} + \frac{1}{8I_N^3}\right) \cos\left(\frac{4(I_N-k)+3}{4I_N+2}\pi\right),$ $k = 1, 2, \dots, I_N, r \in [-1, 1]$
Legendre-Gauss (Leg-Gau)	Radau I kind (Rad I)
$r_k = \text{roots of } (1-r^2)L_{I_N-1}(r), k = 1, 2, \dots, I_N, r \in [-1, 1]$	$r_k = \text{roots of } (1-r)(L_{I_N}(-r) + L_{I_N-1}(-r)),$ $k = 1, 2, \dots, I_N, r \in [-1, 1]$
Chebyshev-Gauss (Cheb-Gau)	Legendre-Gauss-Lobatto (Leg-Gau-Lob)
$r_1 = -1, r_{I_N} = 1, r_k = \cos\left(\frac{2(I_N-k)-1}{2(I_N-2)}\pi\right),$ $k = 2, 3, \dots, I_N - 1, r \in [-1, 1]$	$r_k = \text{roots of } (1-r^2)A_{I_N-1}(r), k = 1, 2, \dots, I_N, r \in [-1, 1]$
Hermite (Her)	Laguerre (Lag)
$r_k = \text{roots of } H_{I_N+1}(r), k = 1, 2, \dots, I_N, r \in ]-\infty, +\infty[$	$r_k = \text{roots of } G_{I_N+1}(r), k = 1, 2, \dots, I_N, r \in [0, +\infty[$
Chebyshev-Gauss-Radau (Cheb-Gau-Rad)	Non-uniform Ding (Ding)
$r_k = \cos\left(\frac{2(I_N-k)}{2I_N-1}\pi\right), k = 1, 2, \dots, I_N, r \in [-1, 1]$	$z_k = \frac{1}{2}\left(1 - \sqrt{2} \cos\left(\frac{\pi}{4} + \frac{\pi}{2} \frac{k-1}{I_N-1}\right)\right), k = 1, 2, \dots, I_N$
Legendre (Leg)	Chebyshev III kind (Cheb III)
$r_k = \text{roots of } L_{I_N+1}(r), k = 1, 2, \dots, I_N, r \in [-1, 1]$	$r_k = \cos\left(\frac{2(I_N-k)+1}{2I_N+1}\pi\right), k = 1, 2, \dots, I_N, r \in [-1, 1]$
Chebyshev IV kind (Cheb IV)	Lobatto (Lob)
$r_k = \cos\left(\frac{2(I_N-k+1)}{2I_N+1}\pi\right), k = 1, 2, \dots, I_N, r \in [-1, 1]$	$r_k = \text{roots of } A_{I_N+1}(r), k = 1, 2, \dots, I_N, r \in [-1, 1]$
Legendre-Gauss-Radau (Leg-Gau-Rad)	Radau II kind (Rad II)
$r_k = \text{roots of } L_{I_N+1}(r) + L_{I_N}(r), k = 1, 2, \dots, I_N, r \in [-1, 1]$	$r_k = \text{roots of } (1-r)(L_{I_N}(r) + L_{I_N-1}(r)),$ $k = 1, 2, \dots, I_N, r \in [-1, 1]$
Jacobi (Jac)	Jacobi-Gauss (Jac-Gau)
$r_k = \text{roots of } J_{I_N-1}^{(\gamma, \delta)}(r), k = 1, 2, \dots, I_N, r \in [-1, 1]$	$r_k = \text{roots of } (1-r^2)J_{I_N-1}^{(\gamma, \delta)}(r), k = 1, 2, \dots, I_N, r \in [-1, 1]$

In order to facilitate the computer implementation, it is convenient to collect the discrete points following the order given by the arrow depicted in Figure 1.2. In other words, the points are collected “by column” (the dotted boxes in Figure 1.2). Therefore, the points can be listed as follows

$$(x_1, y_1), (x_2, y_1), \dots, (x_{I_N}, y_1), (x_1, y_2), \dots, (x_{I_N}, y_2), \dots, (x_1, y_{I_M}), (x_{I_N}, y_{I_M}) \quad (1.51)$$

For the sake of simplicity, these points can be also collected in the corresponding vector  $\boldsymbol{\pi}$ , whose  $k$ -th element  $\pi_k$  is given by

$$\pi_k = (x_i, y_j)_k \quad (1.52)$$

for  $i = 1, 2, \dots, I_N$ ,  $j = 1, 2, \dots, I_M$ , and  $k = i + (j-1)I_N$ . In extended notation, one gets

$$\boldsymbol{\pi} = \left[ \begin{array}{c} \underbrace{(x_1, y_1)_1 \quad (x_2, y_1)_2 \quad \dots \quad (x_{I_N}, y_1)_{I_N}}_{\text{first column}} \\ \underbrace{(x_1, y_2)_{I_N+1} \quad \dots \quad (x_{I_N}, y_2)_{2I_N}}_{\text{second column}} \\ \dots \dots \underbrace{(x_1, y_{I_M})_{I_N I_M - I_N + 1} \quad \dots \quad (x_{I_N}, y_{I_M})_{I_N I_M}}_{\text{last column}} \end{array} \right]^T \quad (1.53)$$

The same order is chosen also to list the values that the function  $f(x, y)$  assumes in each point of the domain

$$\begin{aligned} f(x_1, y_1), f(x_2, y_1), \dots, f(x_{I_N}, y_1), f(x_1, y_2), \dots \\ \dots, f(x_{I_N}, y_2), \dots, f(x_1, y_{I_M}), f(x_{I_N}, y_{I_M}) \end{aligned} \quad (1.54)$$

The corresponding vector  $\mathbf{f}$  can be introduced as well. Its generic element  $f_k$  is given by

$$f_k = f(x_i, y_j)_k \quad (1.55)$$

for  $i = 1, 2, \dots, I_N$ ,  $j = 1, 2, \dots, I_M$ , and  $k = i + (j-1)I_N$ . In extended notation, one gets

$$\mathbf{f} = \left[ \begin{array}{c} \underbrace{f(x_1, y_1)_1 \quad f(x_2, y_1)_2 \quad \dots \quad f(x_{I_N}, y_1)_{I_N}}_{\text{first column}} \\ \underbrace{f(x_1, y_2)_{I_N+1} \quad \dots \quad f(x_{I_N}, y_2)_{2I_N}}_{\text{second column}} \\ \dots \dots \underbrace{f(x_1, y_{I_M})_{I_N I_M - I_N + 1} \quad \dots \quad f(x_{I_N}, y_{I_M})_{I_N I_M}}_{\text{last column}} \end{array} \right]^T \quad (1.56)$$

It is clear that the size of both  $\boldsymbol{\pi}$  and  $\mathbf{f}$  is  $I_N I_M \times 1$ . At this point, the weighting coefficients for the two-dimensional derivatives must be illustrated. For this purpose, it is convenient to introduce the Kronecker product “ $\otimes_k$ ”. Let us consider two generic matrices  $\mathbf{A}$  and  $\mathbf{B}$ , whose sizes are  $f \times g$  and  $p \times q$  respectively. The Kronecker product of  $\mathbf{A}$  and  $\mathbf{B}$  is explained below

$$\mathbf{A} \otimes_k \mathbf{B} = \begin{bmatrix} a_{11} \mathbf{B} & \cdots & a_{1g} \mathbf{B} \\ \vdots & \ddots & \vdots \\ a_{f1} \mathbf{B} & \cdots & a_{fg} \mathbf{B} \end{bmatrix} \quad (1.57)$$

in which  $a_{ij}$  denotes the generic element of  $\mathbf{A}$ , for  $i=1, \dots, f$  and  $j=1, \dots, g$ . In extended notation, the product (1.57) becomes

$$\mathbf{A} \otimes \mathbf{B} = \begin{bmatrix} a_{11}b_{11} & a_{11}b_{12} & \cdots & a_{11}b_{1q} & \cdots & \cdots & a_{1g}b_{11} & a_{1g}b_{12} & \cdots & a_{1g}b_{1q} \\ a_{11}b_{21} & a_{11}b_{22} & \cdots & a_{11}b_{2q} & \cdots & \cdots & a_{1g}b_{21} & a_{1g}b_{22} & \cdots & a_{1g}b_{2q} \\ \vdots & \vdots & \ddots & \vdots & \cdots & \cdots & \vdots & \vdots & \ddots & \vdots \\ a_{11}b_{p1} & a_{11}b_{p2} & \cdots & a_{11}b_{pq} & \cdots & \cdots & a_{1g}b_{p1} & a_{1g}b_{p2} & \cdots & a_{1g}b_{pq} \\ \vdots & \vdots & \cdots & \vdots & \ddots & \cdots & \vdots & \vdots & \cdots & \vdots \\ \vdots & \vdots & \cdots & \vdots & \ddots & \cdots & \vdots & \vdots & \cdots & \vdots \\ a_{f1}b_{11} & a_{f1}b_{12} & \cdots & a_{f1}b_{1q} & \cdots & \cdots & a_{fg}b_{11} & a_{fg}b_{12} & \cdots & a_{fg}b_{1q} \\ a_{f1}b_{21} & a_{f1}b_{22} & \cdots & a_{f1}b_{2q} & \cdots & \cdots & a_{fg}b_{21} & a_{fg}b_{22} & \cdots & a_{fg}b_{2q} \\ \vdots & \vdots & \ddots & \vdots & \cdots & \cdots & \vdots & \vdots & \ddots & \vdots \\ a_{f1}b_{p1} & a_{f1}b_{p2} & \cdots & a_{f1}b_{pq} & \cdots & \cdots & a_{fg}b_{p1} & a_{fg}b_{p2} & \cdots & a_{fg}b_{pq} \end{bmatrix} \quad (1.58)$$

where  $b_{kl}$  is the generic element of  $\mathbf{B}$ , for  $k=1, \dots, p$  and  $l=1, \dots, q$ . The size of the resultant matrix is  $fp \times gq$ .

For the sake of conciseness, the differentiation procedure is presented only in matrix form. Let us introduce the operators  $\mathbf{D}_x^{(n)}$  and  $\mathbf{D}_y^{(m)}$ , which collect the weighting coefficients for the derivatives along  $x$  and  $y$ , respectively. These matrices can be easily computed as shown in (1.15). The symbols  $n$  and  $m$  represent the derivative orders. The weighting coefficients for the two-dimensional case under consideration are computed as follows

$$\mathbf{C}_x^{(n)} = \mathbf{I}_{I_M \times I_M} \otimes_k \mathbf{D}_x^{(n)} \quad (1.59)$$

$$\mathbf{C}_y^{(m)} = \mathbf{D}_y^{(m)} \otimes_k \mathbf{I}_{I_N \times I_N} \quad (1.60)$$



$$I = \int_{x_i}^{x_j} f(x) dx \cong \sum_{k=1}^{I_N} w_k^{ij} f(x_k) \quad (1.65)$$

in which  $w_k^{ij}$  represents the weighting coefficients for the integration at issue. It is important to underline that the summation in the definition (1.65) takes into account all the grid points, even if the integration is limited in the interval  $[x_i, x_j]$ . In other words, the functional values related to the points outside from the reference sub-interval are involved. Differently from the well-known Gaussian approaches, this integration scheme allows to compute the weighting coefficients without any limitation on the choice of the grid point distributions.

In order to evaluate the weighing coefficients for the integration, the coefficients for the first-order derivatives collected in the corresponding matrix  $\mathbf{D}^{(1)}$  are required. If  $D_{ij}^{(1)}$  represents the generic element of  $\mathbf{D}^{(1)}$ , for  $i=1,2,\dots,I_N$  and  $j=1,2,\dots,I_M$ , the following quantities must be computed

$$\bar{D}_{ij}^{(1)} = \frac{x_i - \tilde{c}}{x_j - \tilde{c}} D_{ij}^{(1)} \quad (1.66)$$

for  $i \neq j$ , and

$$\bar{D}_{ij}^{(1)} = D_{ij}^{(1)} + \frac{1}{x_i - \tilde{c}} \quad (1.67)$$

for  $i = j$ . The arbitrary constant  $\tilde{c}$  should be set equal to  $\tilde{c} = b + 10^{-10}$  to guarantee the accuracy of the solution and the stability of the procedure [15]. As illustrated in the book by Shu [44], this assumption comes from the definition of the numerical integration. In fact, integrals are always defined up to an additive constant.

The coefficients  $\bar{D}_{ij}^{(1)}$  can be conveniently collected in the corresponding operator  $\bar{\mathbf{D}}^{(1)}$ , whose size is evidently  $I_N \times I_N$ . Without addressing the complete procedure, the weighting coefficients for the integration, which can be collected in the corresponding matrix  $\mathbf{W}$ , are related to the matrix  $\bar{\mathbf{D}}^{(1)}$  as shown below

$$\mathbf{W} = (\bar{\mathbf{D}}^{(1)})^{-1} \quad (1.68)$$

The elements of  $\mathbf{W}$  are specified by  $w_{ij}$ , for  $i, j = 1, 2, \dots, I_N$ . At this point, the weighting coefficients  $w_k^{ij}$  introduced in (1.65) can be related to the coefficients  $w_{ij}$  collected in  $\mathbf{W}$

according to the following expression

$$w_k^{jj} = w_{jk} - w_{ik} \quad (1.69)$$

for  $k = 1, 2, \dots, I_N$ . It is clear that  $I_N$  coefficients are evaluated. For the sake of conciseness, these quantities can be included in the corresponding vector  $\mathbf{W}_x$  of size  $1 \times I_N$ . Consequently, definition (1.65) can be written also in compact matrix form

$$I = \mathbf{W}_x \mathbf{f} \quad (1.70)$$

where  $\mathbf{f}$  is the vector of the functional values defined in (1.5).

A conventional integral is achieved when the integration limits coincide with the boundary values of the domain  $[a, b]$ . In other words, this condition is obtained when  $x_i = x_1 = a$  and  $x_j = x_{I_N} = b$ . The integral assume the following aspect

$$I = \int_a^b f(x) dx \cong \sum_{k=1}^{I_N} w_k^{I_N} f(x_k) \quad (1.71)$$

where  $w_k^{I_N}$  represents the weighting coefficients that can be evaluated as shown below

$$w_k^{I_N} = w_{I_N k} - w_{1k} \quad (1.72)$$

for  $k = 1, 2, \dots, I_N$ . Finally, a coordinate transformation must be performed if the physical domain  $[a, b]$  is different from the one in which the basis functions are defined, denoted by  $[\alpha, \beta]$ . One gets

$$w_k^{I_N} = \frac{b-a}{\beta-\alpha} \tilde{w}_k^{I_N} \quad (1.73)$$

in which  $w_k^{I_N}$  stands for the weighting coefficients in the physical domain, whereas  $\tilde{w}_k^{I_N}$  represents the coefficients in the reference domain bounded as  $[\alpha, \beta]$ .

Following the same ideas shown in the previous section, this procedure can be easily extended to a two-dimensional case. Let us consider a proper domain, defined by the boundary values  $x \in [a, b]$  and  $y \in [c, d]$ . If  $f(x, y)$  represents a generic two-dimensional function, its integral in the sub-intervals  $[x_i, x_j]$  and  $[y_m, y_n]$ , with  $x_i, x_j \in [a, b]$  and  $y_m, y_n \in [c, d]$ , for  $x_i > a$ ,  $x_j < b$  and  $y_m > c$ ,  $y_n < d$ , is given by



# *Chapter 2*

## *Shell Structures: Principles of Differential Geometry*

Shell structures are widely used in several engineering fields, such as civil, mechanical, aerospace, naval, automotive, and even biomedical. Cooling towers of nuclear reactors, boat hulls, tanks for liquid containment, bodies of cars, fuselages and wing panels of airplanes, space vehicles, artificial body parts, mechanical components, architectural designs, are some examples of shells and curved structures that everybody knows. Thus, this concise list should let us understand that shell structures are normally used for common applications, which can be easily encountered in everyday life [49-57].

Their extensive use is fomented by several advantages, which are mainly induced by their curved geometries. In particular, shell structures are characterized by an extraordinary stiffness, a high level of resistance, and a noticeably strength-to-weight ratio. Furthermore, these structures are extremely efficient when they have to bear external loads, due to their curvature. Their peculiar shape, in fact, has a great influence on the structural response. Therefore, vibrational characteristics, stress and strain distributions, critical rotation speed, as well as buckling load, are all affected by the shell curvature.

Each shell can be described as an elastic body defined by two curved surfaces. The distance between the two surfaces, which denotes the thickness of the structure, is small if compared to the other two dimensions. A generic shell element of thickness  $h$  is shown for the sake of clarity in Figure 2.1.

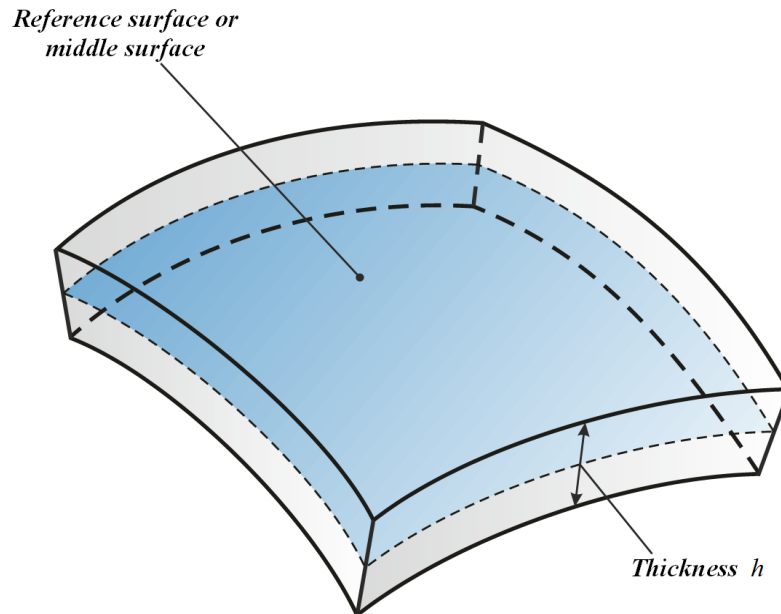


**Figure 2.1** – Generic shell element of thickness  $h$  [57].

The shape of any shell structure is completely defined once its middle surface is accurately specified. The description of these shapes represents one of the biggest issues that should be faced when a shell structure is studied. These difficulties are even greater if the shell is defined by two different radii of curvature. Similar structures are known as doubly-curved shells. On the other hand, if the geometry depends only on a sole radius of curvature, the structure is named singly-curved shell. Finally, if both the radii of curvature assume infinite values and the two external surfaces degenerate into two planes, the shell is called plate. These definitions can be used to classify in a preliminary manner a generic shell structure.

As mentioned above, the modeling of curved surfaces could be difficult. To the best of the author's knowledge, the differential geometry provides the analytical tools to describe accurately and in a complete manner a doubly-curved surface, as illustrated in the book by Kraus [50]. Thus, this chapter is focused on the description of the shell geometries through the principles of differential geometry.

## 2.1 DIFFERENTIAL GEOMETRY

The most important geometric feature of a generic shell structure is its middle surface, which represents the reference domain of the differential equations that govern its mechanical behavior. Thus, it is evident that an efficient analytical tool is required to describe completely the surface at issue. The main aim of this chapter is to provide a general theoretical framework for the description of a shell structures. For this purpose, the differential geometry is employed. For the sake of completeness, it should be recalled that the differential geometry is that part of geometry which aims to study planar and spatial curves, by means of differential calculus. Its fundamental aspects are presented first for a space curve, and then the treatise is extended also to three-dimensional surfaces. In fact, the theory of surfaces is needed for the geometric characterization of the structures under consideration. In the present section, only the main aspects are presented. A more complete treatise can be found in the books by Kraus [50] and by Tornabene et al. [56, 57].

### 2.1.1 CURVES IN THREE-DIMENSIONAL SPACE

As mentioned above, the theory of space curves is a prerequisite to understand the theory of surfaces in space, needed for the description of the shell middle surface.

Let us consider first a global reference system  $Ox_1x_2x_3$ . Each principal direction is identified by the corresponding unit vector, denoted respectively by  $\mathbf{e}_1, \mathbf{e}_2, \mathbf{e}_3$ . A curve  $\mathcal{C}$  in this three-dimensional space can be defined through the position vector  $\mathbf{x}$ , specified below

$$\mathbf{x} = x_1(\xi)\mathbf{e}_1 + x_2(\xi)\mathbf{e}_2 + x_3(\xi)\mathbf{e}_3 \quad (2.1)$$

for any value of the parameter  $\xi$ , defined in the closed interval  $[\xi_1, \xi_2]$ . These elements are presented also in graphical form in Figure 2.2.

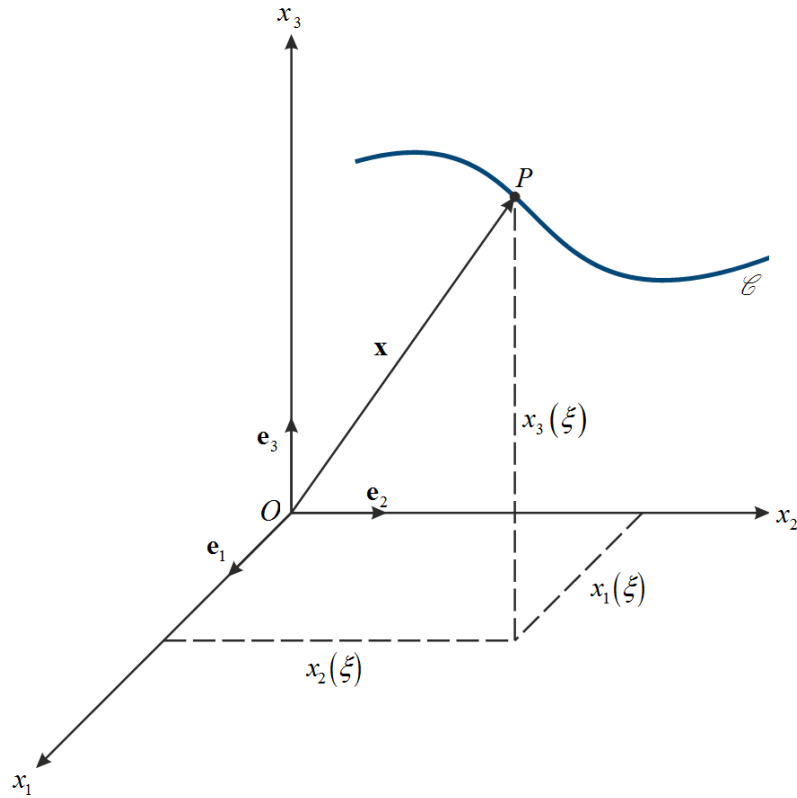


**Figure 2.2** – Generic curve in the three-dimensional space [57].

At this point, it is convenient to introduce the curvilinear abscissa  $s$  along the curve path. The derivative with respect to the coordinate  $s$  of the position vector  $\mathbf{x}$  can be evaluated as follows

$$\frac{d\mathbf{x}}{ds} = \frac{dx_1}{ds} \mathbf{e}_1 + \frac{dx_2}{ds} \mathbf{e}_2 + \frac{dx_3}{ds} \mathbf{e}_3 \quad (2.2)$$

The scalar product of the quantity in (2.2) by itself leads to the following relation

$$\frac{d\mathbf{x}}{ds} \cdot \frac{d\mathbf{x}}{ds} = \left(\frac{dx_1}{ds}\right)^2 + \left(\frac{dx_2}{ds}\right)^2 + \left(\frac{dx_3}{ds}\right)^2 = \frac{(dx_1)^2 + (dx_2)^2 + (dx_3)^2}{(ds)^2} \quad (2.3)$$

From the differential calculus, it is known that

$$(ds)^2 = (dx_1)^2 + (dx_2)^2 + (dx_3)^2 \quad (2.4)$$

Thus, by comparing relations (2.4) and (2.3), one gets

$$\frac{d\mathbf{x}}{ds} \cdot \frac{d\mathbf{x}}{ds} = 1 \quad (2.5)$$

Consequently, the vector  $d\mathbf{x}/ds$  represents a unit vector, whose geometric meaning is depicted graphically in Figure 2.3.

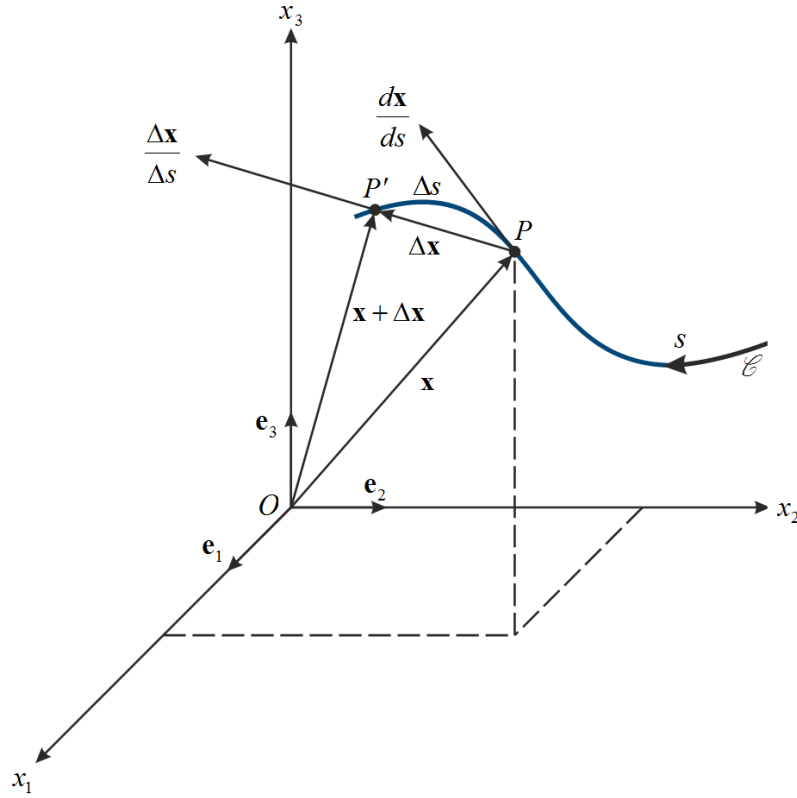


**Figure 2.3** – Geometric interpretation of the unit vector  $d\mathbf{x}/ds$  [57].

With reference to Figure 2.3, the arc length included between the points  $P$  and  $P'$  on the curve  $\mathcal{C}$  is denoted by  $\Delta s$ . These two points are linked by the vector  $\Delta \mathbf{x}$ . It is possible to note that the vector  $\Delta \mathbf{x}/\Delta s$  has the same direction of  $\Delta \mathbf{x}$ . The tangent unit vector  $\mathbf{t}$  can be defined as follows

$$\mathbf{t} = \frac{d\mathbf{x}}{ds} = \lim_{\Delta s \rightarrow 0} \frac{\Delta \mathbf{x}}{\Delta s} \quad (2.6)$$

In other words, the tangent unit vector  $\mathbf{t}$  is obtained assuming  $\Delta s \rightarrow 0$ . Since the curvilinear abscissa is a time dependent variable  $s(t)$ , the derivative with respect to  $t$  of the position vector  $\mathbf{x}$  can be computed, too

$$\dot{\mathbf{x}} = \frac{d\mathbf{x}}{dt} = \frac{d\mathbf{x}}{ds} \cdot \frac{ds}{dt} = \frac{ds}{dt} \mathbf{t} = \dot{s} \mathbf{t} \quad (2.7)$$

This last quantity is also a tangent vector, but its length could be different from unity. The vector  $\dot{\mathbf{x}}$  in (2.7) represent a velocity.

At this point, the definition of the osculating plane naturally arises. Let us consider a plane passing through three consecutive and distinct points laying on a generic curve  $\mathcal{C}$ . As a limit

case, two of these points tend to the third one. This plane is known as osculating plane. If  $\mathbf{X}$  is a vector that denotes a generic point upon this plane, the vector  $(\mathbf{X} - \mathbf{x})$  is located on the same plane of the tangent vector  $\dot{\mathbf{x}}$  and of the vector  $\ddot{\mathbf{x}}$ . This last quantity defines the velocity of variation of the vector  $\dot{\mathbf{x}}$ . Analytically speaking, one gets

$$(\mathbf{X} - \mathbf{x}) \cdot (\dot{\mathbf{x}} \wedge \ddot{\mathbf{x}}) = 0 \quad (2.8)$$

since the mixed product of three coplanar vectors is equal to zero. The principal normal to the curve at the point  $P$ , which is identified by the vector  $\mathbf{x}$ , is defined as that vector within the osculating plane which is orthogonal to the tangent  $\mathbf{t}$  of the curve at the same point.

Having in mind relation (2.5), it is possible to deduce that the scalar product of the unit vector  $\mathbf{t}$  by itself is equal to one. If the derivative with respect to the arc length  $s$  of this scalar product is performed, one gets

$$\frac{d}{ds}(\mathbf{t} \cdot \mathbf{t}) = 2\mathbf{t} \cdot \mathbf{t}' = 0 \quad (2.9)$$

It is clear that the vector  $\mathbf{t}'$  is perpendicular to  $\mathbf{t}$ . Recalling also the definition of the unit vector  $\mathbf{t}$ , the following expression can be obtained

$$\mathbf{t} = \frac{d\mathbf{x}}{ds} = \frac{d\mathbf{x}}{dt} \cdot \frac{dt}{ds} = \dot{\mathbf{x}}t' \quad (2.10)$$

Thus, the tangential and normal vectors to the curve in the considered point allow to define the osculating plane.

On the other hand, the following expression is achieved by deriving relation (2.10) with respect to the arc length  $s$

$$\begin{aligned} \mathbf{t}' &= \frac{d}{ds} \left( \frac{d\mathbf{x}}{dt} \frac{dt}{ds} \right) = \frac{d\mathbf{x}}{dt} \frac{d^2t}{ds^2} + \frac{d}{ds} \left( \frac{d\mathbf{x}}{dt} \right) \frac{dt}{ds} = \dot{\mathbf{x}}t'' + \frac{d}{dt} \left( \frac{d\mathbf{x}}{ds} \right) t' = \dot{\mathbf{x}}t'' + \frac{d}{dt} \left( \frac{d\mathbf{x}}{dt} \frac{dt}{ds} \right) t' = \\ &= \dot{\mathbf{x}}t'' + \frac{d(\dot{\mathbf{x}}t')}{dt} t' = \dot{\mathbf{x}}t'' + \frac{d\dot{\mathbf{x}}}{dt} (t')^2 + \dot{\mathbf{x}}t' \frac{d(t')}{dt} = \dot{\mathbf{x}}t'' + \ddot{\mathbf{x}}(t')^2 + \dot{\mathbf{x}}t' \frac{d(t')}{dt} = \\ &= \dot{\mathbf{x}}t'' + \ddot{\mathbf{x}}(t')^2 + \dot{\mathbf{x}}t' \frac{d}{ds} \left( \frac{dt}{dt} \right) = \dot{\mathbf{x}}t'' + \ddot{\mathbf{x}}(t')^2 + \dot{\mathbf{x}}t' \frac{d(1)}{ds} = \dot{\mathbf{x}}t'' + \ddot{\mathbf{x}}(t')^2 \end{aligned} \quad (2.11)$$

It can be noted that the vector  $\mathbf{t}'$  is defined in the same plane on which  $\dot{\mathbf{x}}$  and  $\ddot{\mathbf{x}}$  are lying. In other words, it is located within the osculating plane too. Since it has been proven that  $\mathbf{t}'$  is perpendicular to  $\mathbf{t}$ , it is possible to state that it shares the same direction of the main normal. Therefore, it is proportional to the unit normal vector  $\mathbf{n}$

$$\mathbf{t}' = \mathbf{k} = k \mathbf{n} \quad (2.12)$$

where  $\mathbf{k}$  stands for the curvature vector, which defines the variability rate of the direction of the tangent vector of a moving point along the curve. The proportionality factor  $k$  represents the curvature, whereas the radius of curvature  $R$  is given by its reciprocal ( $R = k^{-1}$ ). It should be pointed out that the direction of the main normal  $\mathbf{n}$  is arbitrary. Thus, the sign of the curvature  $k$  depends on the direction chosen for  $\mathbf{n}$ . By definition, the normal vector  $\mathbf{n}$  is assumed to be oriented from the center of curvature towards the exterior. Consequently, the curvature is positive ( $k > 0$ ) if the direction of  $\mathbf{n}$  and  $\mathbf{k}$  is the same; on the other hand, its sign is negative ( $k < 0$ ) if the direction of  $\mathbf{n}$  is opposite to the one of  $\mathbf{k}$ .

## 2.1.2 SURFACES

The theory of surfaces can be developed once the preliminary results presented in the previous section are introduced. The theoretical framework shown in the following paragraphs represents a key point for the description of the shell middle surface, taken as reference domain for various kinds of structural problems. As specified above, these aspects are presented in a more complete manner by Kraus [50] and by Tornabene et al. [56, 57].

### 2.1.2.1 Parametric curves and first fundamental form

Let us consider the same three-dimensional space introduced in the previous section. The global reference system is denoted by  $Ox_1x_2x_3$ . A generic surface  $\mathcal{S}$  can be described as a function of two parameters  $\alpha_1$  and  $\alpha_2$ . The parameters at issue are the curvilinear coordinates of the surface. It should be noted that the so-called parametric curves or coordinate lines of the surface can be obtained by fixing a coordinate and increasing the other at the same time. These parametric curves are depicted graphically in Figure 2.4.

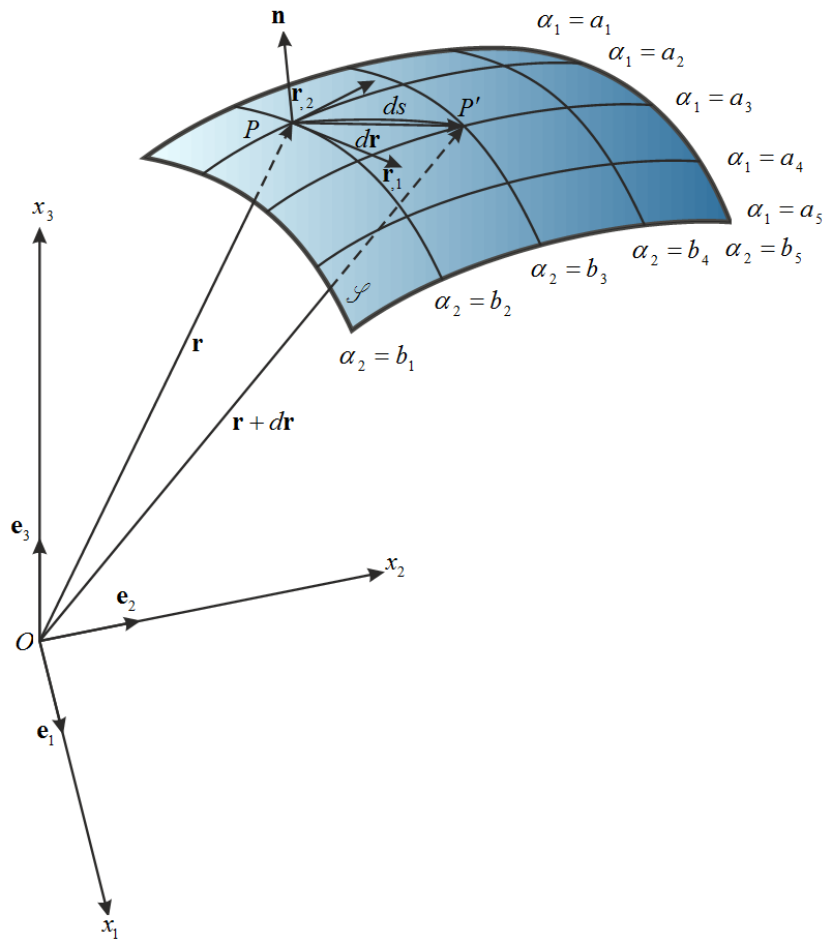


**Figure 2.4** – Surface in a three-dimensional space.

A generic point  $P$  of the surface  $\mathcal{S}$  in the three-dimensional space can be defined through the position vector  $\mathbf{r}(\alpha_1, \alpha_2)$  shown below

$$\mathbf{r}(\alpha_1, \alpha_2) = f_1(\alpha_1, \alpha_2)\mathbf{e}_1 + f_2(\alpha_1, \alpha_2)\mathbf{e}_2 + f_3(\alpha_1, \alpha_2)\mathbf{e}_3 \quad (2.13)$$

where  $f_1, f_2, f_3$  are continuous functions that provide a single value for each couple of coordinates  $\alpha_1, \alpha_2$ . As specified in Figure 2.4, the infinitesimal variation  $d\mathbf{r}$  represents the distance between the points  $P$  and  $P'$ , which is infinitely close to the first one. It assumes the following aspect

$$d\mathbf{r} = \mathbf{r}_1 d\alpha_1 + \mathbf{r}_2 d\alpha_2 \quad (2.14)$$

in which  $\mathbf{r}_i = \partial\mathbf{r}/\partial\alpha_i$ , for  $i = 1, 2$ . It should be noted that the differential quantity (2.14) is a vector. The scalar product of  $d\mathbf{r}$  by itself can be evaluated too

$$d\mathbf{r} \cdot d\mathbf{r} = (ds)^2 = E(d\alpha_1)^2 + 2Fd\alpha_1 d\alpha_2 + G(d\alpha_2)^2 \quad (2.15)$$

where the first fundamental coefficients of the surface  $E, F, G$  are introduced. These quantities are defined as follows

$$E = \mathbf{r}_{,1} \cdot \mathbf{r}_{,1}, \quad F = \mathbf{r}_{,1} \cdot \mathbf{r}_{,2}, \quad G = \mathbf{r}_{,2} \cdot \mathbf{r}_{,2} \quad (2.16)$$

These coefficients are employed to evaluate the infinitesimal arch length along the parametric curve. For this purpose, one gets

$$ds_1 = \sqrt{E} d\alpha_1, \quad ds_2 = \sqrt{G} d\alpha_2 \quad (2.17)$$

in which  $ds_1$  is the infinitesimal length along a curve with  $\alpha_2$  constant, whereas  $ds_2$  is the same quantity along a curve with  $\alpha_1$  constant. It should be noted that the coefficient  $F$  is equal to zero if the an orthogonal mesh grid is described by the parametric curves, since  $\mathbf{r}_{,1}$  and  $\mathbf{r}_{,2}$  represent the tangent vectors to the lines defined by constant values of  $\alpha_2$  and  $\alpha_1$ , respectively. If this condition is verified, the first fundamental form (2.15) becomes

$$(ds)^2 = A_1^2 (d\alpha_1)^2 + A_2^2 (d\alpha_2)^2 \quad (2.18)$$

where the *Lamè parameters* of the surface  $A_1, A_2$  are introduced. Their definitions can be easily deduced

$$A_1 = \sqrt{E}, \quad A_2 = \sqrt{G} \quad (2.19)$$

By means of the first fundamental form just presented, it is possible to evaluate the length of a generic arch on the surface  $\mathcal{S}$  as follows

$$s = \int_{\xi_0}^{\xi_1} \sqrt{E \left( \frac{d\alpha_1}{d\xi} \right)^2 + 2F \frac{d\alpha_1}{d\xi} \frac{d\alpha_2}{d\xi} + G \left( \frac{d\alpha_2}{d\xi} \right)^2} d\xi \quad (2.20)$$

Having in mind definitions (2.19) and assuming that the coordinates  $\alpha_1, \alpha_2$  describe an orthogonal mesh grid, expression (2.20) becomes

$$s = \int_{\xi_0}^{\xi_1} \sqrt{A_1^2 \left( \frac{d\alpha_1}{d\xi} \right)^2 + A_2^2 \left( \frac{d\alpha_2}{d\xi} \right)^2} d\xi \quad (2.21)$$

### 2.1.2.2 Outward unit normal vector

A unit normal vector  $\mathbf{n}(\alpha_1, \alpha_2)$  can be defined in each point  $P$  within the surface. This vector is orthogonal to the plane identified by the vectors  $\mathbf{r}_{,1}$ ,  $\mathbf{r}_{,2}$ . In other words, the unit vector  $\mathbf{n}$  has the direction of the cross product of  $\mathbf{r}_{,1}$  and  $\mathbf{r}_{,2}$ . Mathematically speaking, it assumes the following definition

$$\mathbf{n}(\alpha_1, \alpha_2) = \frac{\mathbf{r}_{,1} \times \mathbf{r}_{,2}}{|\mathbf{r}_{,1} \times \mathbf{r}_{,2}|} \quad (2.22)$$

where “ $\times$ ” stand for the cross product. Since the direction of the normal vector  $\mathbf{n}$  is arbitrary, by definition it is assumed that its conventional direction is taken from the concave side towards the convex one.

### 2.1.2.3 Second fundamental form

The curvature vector  $\mathbf{k}$  of a generic surface in the three-dimensional space can be written as follows

$$\mathbf{k} = \mathbf{t}' = \frac{d\mathbf{t}}{ds} = \mathbf{k}_n + \mathbf{k}_t \quad (2.23)$$

where  $\mathbf{k}_n$  and  $\mathbf{k}_t$  represent the normal and tangential components, respectively. They can be named as normal curvature vector and tangential curvature vector. The normal curvature  $\mathbf{k}_n$  can be defined as a function of the outward normal vector  $\mathbf{n}$  as shown below

$$\mathbf{k}_n = -k_n \mathbf{n} \quad (2.24)$$

in which  $k_n$  is known as normal curvature. Since it is assumed by definition that the direction of  $\mathbf{k}$  is opposite to the positive direction of  $\mathbf{n}$ , the minus sign is introduced in (2.24). At this point, it should be recalled that the normal unit vector  $\mathbf{n}$  is orthogonal to the tangential one  $\mathbf{t}$ . Thus, the following relation is satisfied

$$\mathbf{n} \cdot \mathbf{t} = 0 \quad (2.25)$$

The derivative of the dot product (2.25) with respect to the arc length  $s$  can be computed as well

$$\frac{d\mathbf{n}}{ds} \cdot \mathbf{t} + \mathbf{n} \cdot \frac{d\mathbf{t}}{ds} = 0 \quad \rightarrow \quad \frac{d\mathbf{n}}{ds} \cdot \mathbf{t} = -\mathbf{n} \cdot \frac{d\mathbf{t}}{ds} \quad (2.26)$$

Recalling definition (2.23) and having in mind that  $\mathbf{t} = d\mathbf{r}/ds$ , equation (2.26) takes the following aspect

$$\frac{d\mathbf{n} \cdot d\mathbf{r}}{d\mathbf{r} \cdot d\mathbf{r}} = k_n \quad (2.27)$$

where the infinitesimal variation  $d\mathbf{n}$  is given by

$$d\mathbf{n} = \mathbf{n}_{,1}d\alpha_1 + \mathbf{n}_{,2}d\alpha_2 \quad (2.28)$$

in which  $\mathbf{n}_{,i} = \partial\mathbf{n}/\partial\alpha_i$ , for  $i=1,2$ . The dot product at the numerator in (2.27) represents the second fundamental form, which can be computed as follows

$$d\mathbf{n} \cdot d\mathbf{r} = L(d\alpha_1)^2 + 2Md\alpha_1d\alpha_2 + N(d\alpha_2)^2 \quad (2.29)$$

where  $L, M, N$  are the second fundamental coefficients. They can be computed as shown below

$$L = \mathbf{r}_{,1} \cdot \mathbf{n}_{,1}, \quad 2M = (\mathbf{r}_{,1} \cdot \mathbf{n}_{,2} + \mathbf{r}_{,2} \cdot \mathbf{n}_{,1}), \quad N = \mathbf{r}_{,2} \cdot \mathbf{n}_{,2} \quad (2.30)$$

At this point, relation (2.27) can be written in general as follows

$$k_n = \frac{L(d\alpha_1)^2 + 2Md\alpha_1d\alpha_2 + N(d\alpha_2)^2}{E(d\alpha_1)^2 + 2Fd\alpha_1d\alpha_2 + G(d\alpha_2)^2} \quad (2.31)$$

The following alternative expressions for the second fundamental magnitudes can be obtained if the relations  $\mathbf{r}_{,1} \cdot \mathbf{n} = 0$  and  $\mathbf{r}_{,2} \cdot \mathbf{n} = 0$  are differentiated

$$L = -\mathbf{r}_{,11} \cdot \mathbf{n}, \quad M = -\mathbf{r}_{,12} \cdot \mathbf{n}, \quad N = -\mathbf{r}_{,22} \cdot \mathbf{n} \quad (2.32)$$

with  $\mathbf{r}_{,ij} = \partial^2\mathbf{r}/\partial\alpha_i\partial\alpha_j$ , for  $i=1,2$ . Finally, it should be noted that all the fundamental quantities can be written as a function of the curvilinear coordinates  $\alpha_1$  and  $\alpha_2$ . In addition, the normal curvature depends only on the quantity  $d\alpha_2/d\alpha_1$ , which denotes a direction. It is possible to prove that each curve that is tangent to the same direction and passes through that point is characterized by the same value of  $k_n$ .

### 2.1.2.4 Main curvatures

Relation (2.31) provide those directions for which the normal curvature presents maximum or minimum values. By introducing the position  $\lambda = d\alpha_2/d\alpha_1$  and performing the proper manipulations, one gets

$$k_n(\lambda) = \frac{L + 2M\lambda + N\lambda^2}{E + 2F\lambda + G\lambda^2} \quad (2.33)$$

In order to find those extreme values, the following derivative with respect to  $\lambda$  must be set equal to zero

$$\frac{dk_n(\lambda)}{d\lambda} = 0 \quad (2.34)$$

In the previous paragraphs, it has been highlighted that the parametric lines are orthogonal and coincide with the main curvature directions. Consequently, one gets  $F = 0$ . In addition, it is possible to prove that even the coefficient  $M$  is equal to zero if those parametric lines coincide with the main curvature directions. Mathematically speaking, one gets

$$F = M = 0 \quad (2.35)$$

Without addressing the complete treatise, it can be proven that the *principal curvatures*  $k_{n1}$  and  $k_{n2}$  of the surface assume the following aspect

$$k_{n1} = \frac{1}{R_1} = \frac{L}{E}, \quad k_{n2} = \frac{1}{R_2} = \frac{N}{G} \quad (2.36)$$

if relation (2.35) is satisfied, where  $R_1, R_2$  are principal radii of curvature.

### 2.1.2.5 Fundamental theorem of the theory of surfaces

The derivatives of the unit vectors along the parametric lines are required to develop the fundamental theorem of the theory of surfaces. These unit vectors are specified by  $\mathbf{t}_1, \mathbf{t}_2, \mathbf{n}$ . In particular,  $\mathbf{t}_1, \mathbf{t}_2$  are directed along the tangents to the principal directions  $\alpha_1$  and  $\alpha_2$ . On the other hand,  $\mathbf{n}$  is the outward normal unit vector. It should be specified that these unit vectors are always orthogonal two by two. By definition, the unit vectors at issue can be defined as follows

$$\mathbf{t}_1 = \frac{\mathbf{r}_{,1}}{|\mathbf{r}_{,1}|} = \frac{\mathbf{r}_{,1}}{A_1}, \quad \mathbf{t}_2 = \frac{\mathbf{r}_{,2}}{|\mathbf{r}_{,2}|} = \frac{\mathbf{r}_{,2}}{A_2}, \quad \mathbf{n} = \mathbf{t}_1 \times \mathbf{t}_2 = \frac{\mathbf{r}_{,1} \times \mathbf{r}_{,2}}{A_1 A_2} \quad (2.37)$$

At this point, the derivatives of the unit vectors in (2.37) are required. In particular, the six quantities  $\mathbf{n}_{,1}, \mathbf{n}_{,2}, \mathbf{t}_{1,1}, \mathbf{t}_{1,2}, \mathbf{t}_{2,1}, \mathbf{t}_{2,2}$  must be evaluated. It should be specified that the subscript after the comma identifies the principal direction  $\alpha_1$  or  $\alpha_2$  along which the derivatives are performed. For this purpose, it can be noted that  $\mathbf{n}_{,1}, \mathbf{n}_{,2}$  are both orthogonal to  $\mathbf{n}$  and lie on the plane defined by the unit vectors  $\mathbf{t}_1, \mathbf{t}_2$ . For the sake of clarity, the quantity  $\mathbf{n}_{,1}$  can be written as follows to satisfy the properties just mentioned

$$\mathbf{n}_{,1} = a\mathbf{t}_1 + b\mathbf{t}_2 \quad (2.38)$$

where  $a, b$  denotes the projections of  $\mathbf{n}_{,1}$  along  $\mathbf{t}_1, \mathbf{t}_2$ , respectively. Analogously, the vectors  $\mathbf{t}_{1,1}, \mathbf{t}_{1,2}$  are orthogonal to  $\mathbf{t}_1$  itself. For instance, the vector  $\mathbf{t}_{1,1}$  can be expressed as follows

$$\mathbf{t}_{1,1} = c\mathbf{n} + d\mathbf{t}_2 \quad (2.39)$$

in which  $c, d$  represent its projections along  $\mathbf{n}, \mathbf{t}_2$ , respectively. The same considerations are valid for the other required quantities. Without addressing the complete mathematical proof, one gets

$$\mathbf{t}_{1,1} = -\frac{A_{1,2}}{A_2}\mathbf{t}_2 - \frac{A_1}{R_1}\mathbf{n}, \quad \mathbf{t}_{1,2} = \frac{A_{2,1}}{A_1}\mathbf{t}_2 \quad (2.40)$$

$$\mathbf{t}_{2,1} = \frac{A_{1,2}}{A_2}\mathbf{t}_1, \quad \mathbf{t}_{2,2} = -\frac{A_{2,1}}{A_1}\mathbf{t}_1 - \frac{A_2}{R_2}\mathbf{n} \quad (2.41)$$

$$\mathbf{n}_{,1} = \frac{A_1}{R_1}\mathbf{t}_1, \quad \mathbf{n}_{,2} = \frac{A_2}{R_2}\mathbf{t}_2 \quad (2.42)$$

where  $A_{1,i} = \partial A_1 / \partial \alpha_i$  and  $A_{2,i} = \partial A_2 / \partial \alpha_i$ , for  $i = 1, 2$ . Finally, it should be noted that the derivatives in (2.40)-(2.42) can be written as a function of the unit vectors  $\mathbf{t}_1, \mathbf{t}_2, \mathbf{n}$ . The complete treatise is omitted for conciseness purpose, but it is presented exhaustively in the book by Kraus [50].

At this point, the so-called Gauss-Codazzi conditions can be shown to define, three differential equations that represent the mathematical relationships between the Lamè parameters  $A_1, A_2$  and the principal radii of curvature  $R_1, R_2$ . Such relations are needed to

verify if an arbitrary choice of  $A_1, A_2, R_1, R_2$  defines an admissible surface. The following relations are valid only if the second-order derivatives of the unit vectors (2.37) are continuous. In this circumstance and recalling that  $\mathbf{n}_{,12} = \mathbf{n}_{,21}$ , one gets

$$\left( \frac{A_1}{R_1} \mathbf{t}_1 \right)_{,2} - \left( \frac{A_2}{R_2} \mathbf{t}_2 \right)_{,1} = 0 \quad (2.43)$$

in which the notation  $_{,i} = \partial/\partial\alpha_i$ , for  $i=1,2$ , is employed. By performing the derivatives in (2.43) and having in mind the definitions of  $\mathbf{t}_1, \mathbf{t}_2$  introduced above, the following result is carried out

$$\mathbf{t}_1 \left( -\frac{A_{1,2}}{R_2} + \left( \frac{A_1}{R_1} \right)_{,2} \right) + \mathbf{t}_2 \left( \frac{A_{2,1}}{R_1} - \left( \frac{A_2}{R_2} \right)_{,1} \right) = 0 \quad (2.44)$$

Equation (2.44) is verified only if the following relations, known as Codazzi conditions, are satisfied

$$\frac{A_{1,2}}{R_2} = \left( \frac{A_1}{R_1} \right)_{,2}, \quad \frac{A_{2,1}}{R_1} = \left( \frac{A_2}{R_2} \right)_{,1} \quad (2.45)$$

In the same manner, recalling that  $\mathbf{t}_{,12} = \mathbf{t}_{,21}$  and  $\mathbf{t}_{2,12} = \mathbf{t}_{2,21}$ , a third differential equation, known as Gauss condition, is achieved

$$\left( \frac{A_{2,1}}{A_1} \right)_{,1} + \left( \frac{A_{1,2}}{A_2} \right)_{,2} = -\frac{A_1 A_2}{R_1 R_2} \quad (2.46)$$

The Gauss-Codazzi conditions are required to state the so-called *fundamental theorem of the theory of surfaces*, which can be expressed as follows: “If the fundamental quantities  $E, G, L, N$  (with  $E > 0$  and  $G > 0$ ) are written in terms of the principal curvilinear coordinates  $\alpha_1$  and  $\alpha_2$ , are sufficiently differentiable and verify the Gauss-Codazzi conditions, then a real surface is uniquely identified, whose first I and second fundamental forms II are given by

$$\begin{aligned} \text{I} &= E(d\alpha_1)^2 + G(d\alpha_2)^2 \\ \text{II} &= L(d\alpha_1)^2 + N(d\alpha_2)^2 \end{aligned} \quad (2.47)$$

*The surface in hand is completely defined, except for its location*”. It should be specified that this theorem is limited to those surfaces described by principal and orthogonal curvilinear

coordinates, since  $F = M = 0$ . More general conditions could be developed to include the case of surfaces with generic parametric lines.

### 2.1.2.6 Gaussian curvature

With reference to the Gauss condition (2.46), it is possible to note that it includes the so-called Gaussian curvature  $\Gamma_G$ , as shown below

$$\Gamma_G = \frac{1}{R_1 R_2} \quad (2.48)$$

In other words, the Gaussian curvature is defined as the reciprocal of the product of the two main radii of curvature of the surface. This quantity can be used to classify a generic surface, according to its sign. In fact, the Gaussian curvature can be positive, negative, or even null. In particular, the Gaussian curvature is positive if both the centers of curvature ( $C_1$  and  $C_2$ ), related to normal sections corresponding to the main directions of the surface, are located on the same side with respect to the surface itself. On the other hand, the Gaussian curvature is negative if the centers of curvatures lie on two opposite sides with respect to the surface. Finally, the Gaussian curvature is null if one of the two radii of curvature is equal to infinity. For the sake of completeness, a plate is obtained if the two radii of curvature are both equal to infinity (the Gaussian curvature is also null). A graphical representation of the Gaussian curvature is depicted in Figure 2.5.

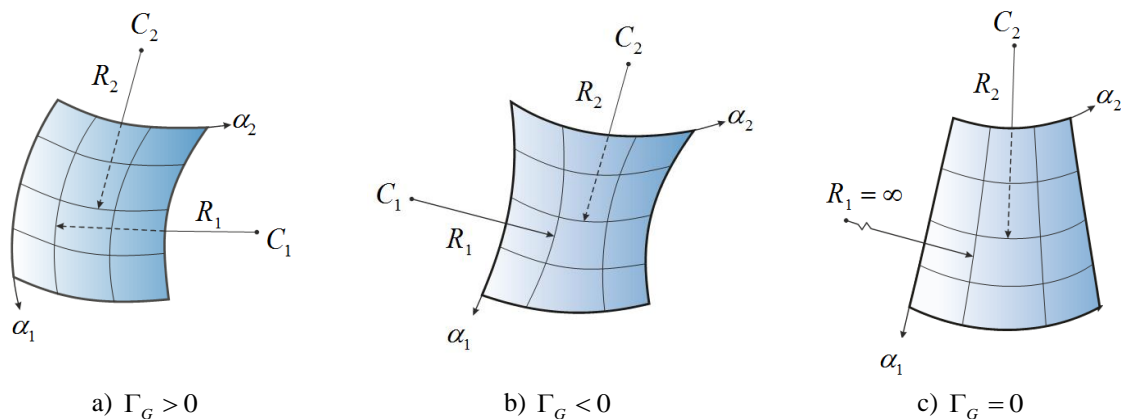


**Figure 2.5** –Gaussian curvature.

It should be specified that Gaussian curvature is a scalar punctual function. Thus, a generic curved surface can be characterized by several areas with positive, negative or zero values of Gaussian curvature. However, in practical applications these surfaces are characterized by the Gaussian curvature with a prevalent sign, or even unique.

### 2.1.2.7 Classifications of surfaces

Several ways to categorize a surface are possible. In particular, a classification can be performed according to the shape, to the Gaussian curvature, or to the developability of the surfaces. If the shape is the classifying parameter, the following surfaces can be defined:

- *Surfaces of revolution*: These surfaces are generated by the rotation of a plane curve, known as meridian, about an axis that not necessarily intersects the meridian.
- *Surfaces of translation*: These surfaces are originated by the translation of a plane curve parallel to the plane in which the curve itself is defined, along another plane curve or a straight line. Doubly-curved and singly-curved translational surfaces are originated, respectively.
- *Ruled surfaces*: These surfaces are achieved by translating a straight line along two curves, placed at the edge of the line itself. The generating lines are not necessarily orthogonal to the planes containing these curves.

On the other hand, the following surfaces can be obtained if the classifying parameter is the Gaussian curvature:

- *Singly-curved surfaces*: These surfaces are characterized by a null value of Gaussian curvature. The surfaces at issue can be revolution surfaces, translational surfaces, or ruled surface.
- *Doubly-curved surfaces with positive Gaussian curvature*: These doubly-curved surfaces are characterized by a positive value of Gaussian curvature. Some surfaces of revolution, certain surfaces of translation and also ruled surfaces are included in this group.
- *Doubly-curved surfaces with negative Gaussian curvature*: These doubly-curved surfaces are characterized by a negative value of Gaussian curvature. This group includes some revolution, translational and ruled surfaces.

- *Degenerate surfaces*: These surfaces are characterized by both the radii of curvature equal to infinite and the Gaussian curvature is equal to zero, consequently.

Finally, the following classification can be performed if the surfaces are developable or not:

- *Developable surfaces*: These surfaces can be developed into a plane without making cuts and deformations. In general, singly-curved surfaces are developable.
- *Non-developable surfaces*: These surfaces must be cut or deformed to develop them on a plane. In general, doubly-curved surfaces are typically non-developable.

## 2.2 SHELL STRUCTURES

As clearly specified in the introduction, the theory of surfaces just presented in the previous section is required to describe the middle surface of a generic shell structure, which is taken as the reference domain for the governing equations. Thus, it is necessary to compute the corresponding geometric quantities, such as the Lamè parameters and the radii of curvature, for a complete characterization of the surface at issue. Some surfaces that can be described through this approach are illustrated in the books by Tornabene et al. [56, 57].

In the general case of doubly-curved shells, these coefficients are defined in a curvilinear orthogonal coordinate reference system and all the geometric quantities depend on  $\alpha_1, \alpha_2$ . In particular, the position vector of the middle surface is given by  $\mathbf{r} \equiv \mathbf{r}(\alpha_1, \alpha_2)$ . The Enneper surface, the ellipsoid and the so-called degenerate plates (parabolic, elliptic and bipolar) are example of doubly-curved shells that require this description. The same kind of description is needed for the reference surface of doubly-curved translational shells, which are obtained translating a planar curve upon another curve, keeping the plane containing the translating curve (generatrix) orthogonal to the fixed curve (directrix). Elliptic and hyperbolic paraboloid and curved cylinders with circular and elliptic cross-sections are examples of the doubly-curved shells of translation in hand. The doubly-curved shells of revolution come from the previous ones. The curvilinear coordinate can be taken as  $\alpha_1 \equiv \varphi, \alpha_2 \equiv \vartheta$  and the position vector assumes the following aspect  $\mathbf{r} \equiv \mathbf{r}(\varphi, \vartheta)$ . The parameters  $\varphi, \vartheta$  represent the spherical

coordinates of the surface. It is well-known that the reference surface of revolution shells is given by the rotation of a plane curve (called meridian) about the revolution axis, which belongs to the plane of the meridian itself. Thus, it should be clear that the shape of these structures is well-defined only if the Cartesian equation of the meridian curve is given. For this purpose, hyperbolic, catenary shaped, elliptic, cycloidal, parabolic, tractrix shaped, and free-form meridian can be introduced. Revolution surfaces can be defined as particular cases of surface of translation, too. In this circumstance, the meridian curve (generatrix) slides on a circular curve, which represents the directrix. If the meridian curve is a straight line, singly-curved shells are obtained. This is the case of conical and circular cylindrical shells. The circular plates are the degenerate case of this group. In this circumstance, the curvilinear coordinates become  $\alpha_1 \equiv x$ ,  $\alpha_2 \equiv \vartheta$ , and the position vector assumes the following form  $\mathbf{r} \equiv \mathbf{r}(x, \vartheta)$ . On the other hand, singly-curved shells of translation, also known as straight cylinders, are obtained by straightening the parallel of a doubly-curved shell of revolution. As in the previous family, these structures are defined by the shape of the curved profile. In this circumstance, the position vector is given in the form  $\mathbf{r} \equiv \mathbf{r}(\varphi, y)$ , since the principal coordinates are assumed equal to  $\alpha_1 \equiv \varphi$ ,  $\alpha_2 \equiv y$ .

Finally, rectangular plates can be obtained by straightening the parallel and the meridian of a doubly-curved shell of revolution at the same time. In other words, one gets  $\alpha_1 \equiv x$ ,  $\alpha_2 \equiv y$ . The position vector takes the following aspect  $\mathbf{r} \equiv \mathbf{r}(x, y)$ . Rectangular plates are clearly degenerate shells, since they have zero curvatures and both the main radii of curvature are equal to zero. The interested reader can find the explicit expressions of the position vector of these reference surfaces in the books by Tornabene et al. [56, 57].

Once the position vector  $\mathbf{r} \equiv \mathbf{r}(\alpha_1, \alpha_2)$  is introduced to identify a generic point  $P'$  upon the middle surface of the shell, it is possible to define also the position of a point  $P$  within the three-dimensional shell structure of overall thickness  $h$  through the general position vector  $\mathbf{R} \equiv \mathbf{R}(\alpha_1, \alpha_2, \zeta)$  defined below

$$\mathbf{R}(\alpha_1, \alpha_2, \zeta) = \mathbf{r}(\alpha_1, \alpha_2) + \zeta \mathbf{n}(\alpha_1, \alpha_2) \quad (2.49)$$

where  $\zeta$  stands for the coordinate along the outward unit normal vector  $\mathbf{n}$ , as depicted in Figure 2.6.

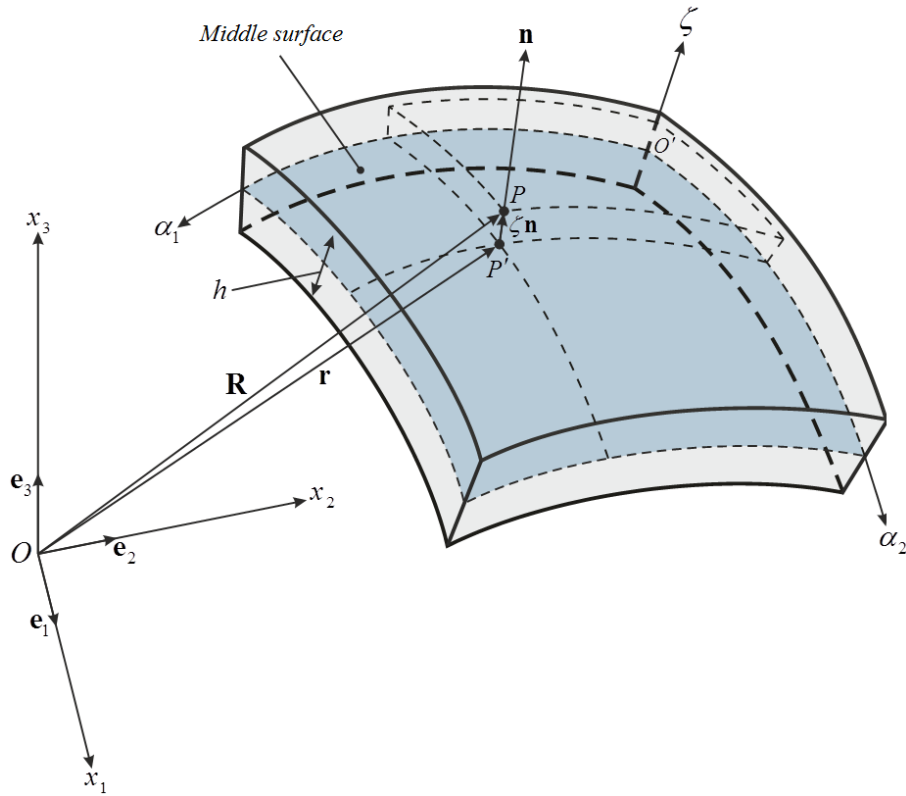


Figure 2.6 – Generic three-dimensional shell element.

As specified above, the coordinates  $\alpha_1, \alpha_2$  assume a different meaning according to the kind of surface employed as middle surface. It should be also specified that the surface at issue is univocally defined if a closed domain is specified. In other words, the following limitations must be imposed

$$\alpha_1 \in [\alpha_1^0, \alpha_1^1], \quad \alpha_2 \in [\alpha_2^0, \alpha_2^1] \quad (2.50)$$

where  $\alpha_1^0, \alpha_1^1$  and  $\alpha_2^0, \alpha_2^1$  denote the minimum and maximum boundary values of the reference domain. Analogously, the coordinate  $\zeta$  assumes all the values included within the shell thickness, as specified below

$$\zeta \in \left[ -\frac{h}{2}, \frac{h}{2} \right] \quad (2.51)$$

Finally, it should be noted that  $O'\alpha_1\alpha_2\zeta$  represents the local reference system of a generic shell element.

## 2.3 NUMERICAL CONSIDERATIONS

From the numerical point of view, the DQ method presented previously is used to evaluate all the derivatives with respect to the principal coordinates  $\alpha_1, \alpha_2$  of the geometric quantities introduced in the current chapter. For this purpose, the shell middle surface must be discretized by placing  $I_N, I_M$  discrete points along  $\alpha_1, \alpha_2$ , respectively. In other words, one gets

$$\begin{aligned}\alpha_1^0 &= \alpha_{11}, \alpha_{12}, \dots, \alpha_{1f}, \dots, \alpha_{1I_N} = \alpha_1^1 \\ \alpha_2^0 &= \alpha_{21}, \alpha_{22}, \dots, \alpha_{2g}, \dots, \alpha_{2I_M} = \alpha_2^1\end{aligned}\quad (2.52)$$

where  $\alpha_1^0, \alpha_2^0$  and  $\alpha_1^1, \alpha_2^1$  have the same meaning illustrated above. According to the general approach presented in the previous chapter, there is no limitation on the choice of the grid point distributions. Thus, the following expressions can be used to define the generic coordinates  $\alpha_{1f}, \alpha_{2g}$  of a discrete point within the two-dimensional domain at issue

$$\alpha_{1f} = \frac{\alpha_1^1 - \alpha_1^0}{r_{I_N} - r_1} (r_f - r_1) + \alpha_1^0 \quad (2.53)$$

$$\alpha_{2g} = \frac{\alpha_2^1 - \alpha_2^0}{r_{I_M} - r_1} (r_g - r_1) + \alpha_2^0 \quad (2.54)$$

for  $f = 1, 2, \dots, I_N$  and  $g = 1, 2, \dots, I_M$ , in which the meaning of  $r_f, r_g$  can be found in Table 1.2. For the sake of clarity, the procedure of discretizing a generic shell middle surface is depicted in Figure 2.7. From the computational point of view, the discrete domain denoted by (2.53)-(2.54) represents a rectangular regular domain.

### 2.3.1 DISTORTED DOMAINS AND ISOGEOMETRIC MAPPING

A proper coordinate transformation, known as mapping procedure, can be introduced at this point and applied to the regular domains described in the previous section to define arbitrarily shaped curved surfaces, as the one depicted in Figure 2.8.

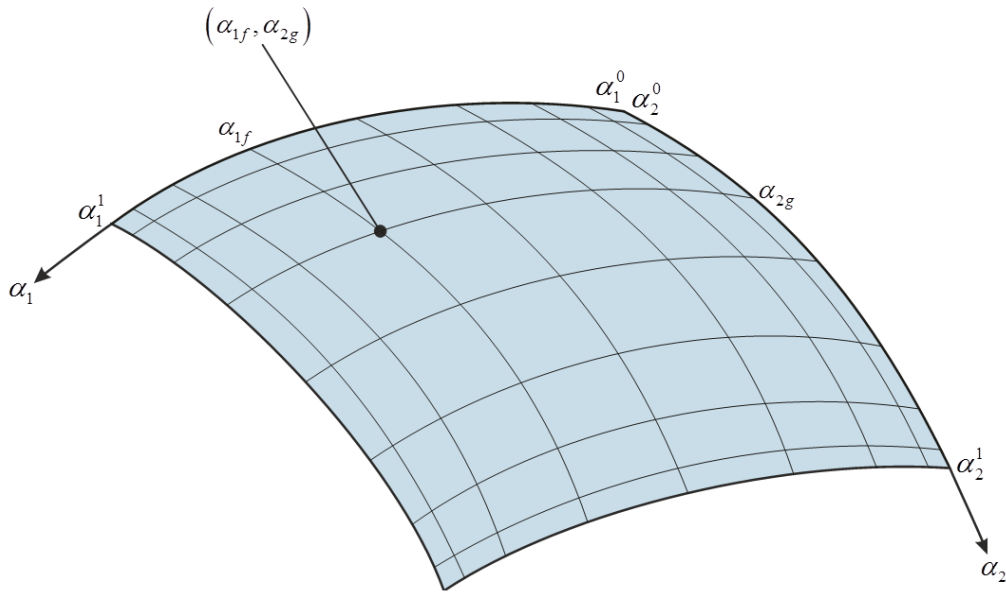


**Figure 2.7** – Discretization of a two-dimensional domain.

The main aspect of this procedure is to convert a regular domain, described by the principal coordinate  $\alpha_1, \alpha_2$ , into a distorted element. In other words, the original problem is moved into the computational domain, also known as parent space, which is described by the natural coordinates  $\xi_1, \xi_2$ .

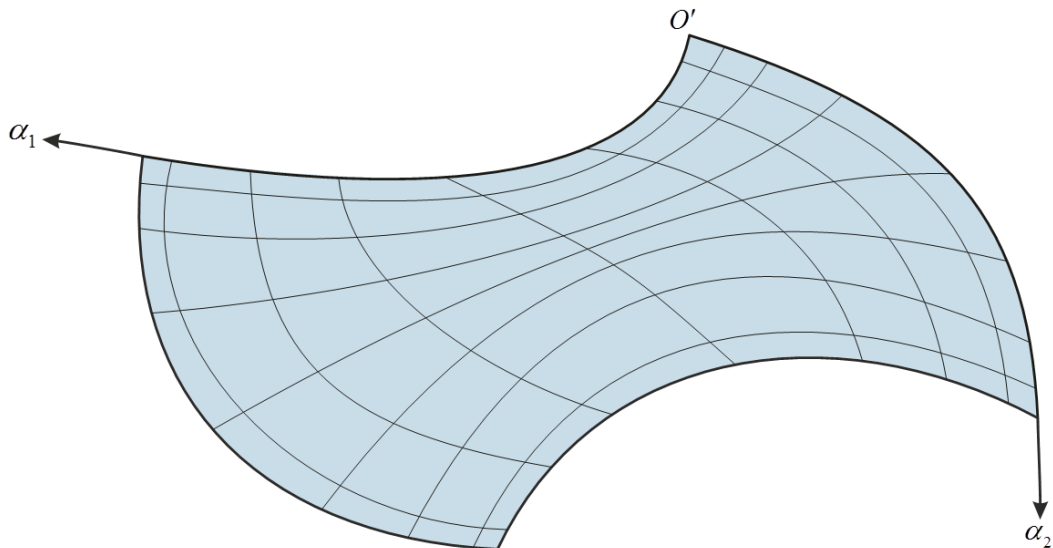


**Figure 2.8** – Distorted domain.

These coordinates are defined in the following intervals

$$\xi_1 \in [-1, +1], \quad \xi_2 \in [-1, +1] \quad (2.55)$$

For the sake of completeness, the parent space at issue is shown in Figure 2.9.

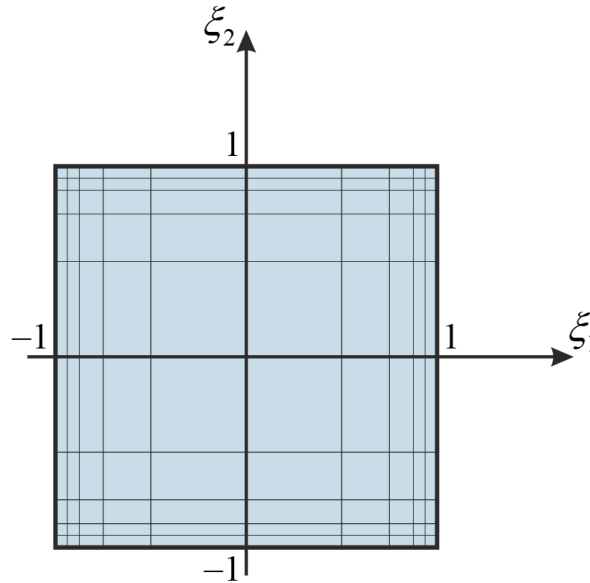


**Figure 2.9** – Parent space (or computational element).

Mathematically speaking, the mapping procedure is obtained once the following expressions are introduced

$$\alpha_1 = \alpha_1(\xi_1, \xi_2), \quad \alpha_2 = \alpha_2(\xi_1, \xi_2) \quad (2.56)$$

It should be recalled that this methodology is the same used in the well-known Finite Element Method (FEM) to describe any kind of distorted element. In general, the mapping procedure for a single element is carried out through the classic shape function. Nevertheless, a more general and versatile approach is presented here. In fact, the coordinate transformation (2.56) is achieved by means of the so-called blending functions, which are extremely effective functions to describe distorted domains. For the sake of completeness, it should be highlighted that these functions are extremely useful to represent arbitrarily shaped domains, by taking advantage of the versatility of Computer-Aided Design (CAD) software. The nonlinear coordinate transformation at issue is achieved by the following relations

$$\begin{aligned}
 \alpha_1(\xi_1, \xi_2) = & \frac{1}{2} \left( (1-\xi_2)\bar{\alpha}_{1(1)}(\xi_1) + (1+\xi_1)\bar{\alpha}_{1(2)}(\xi_2) + \right. \\
 & \left. + (1+\xi_2)\bar{\alpha}_{1(3)}(\xi_1) + (1-\xi_1)\bar{\alpha}_{1(4)}(\xi_2) \right) + \\
 & -\frac{1}{4} \left( (1-\xi_1)(1-\xi_2)\alpha_{1(1)} + (1+\xi_1)(1-\xi_2)\alpha_{1(2)} + \right. \\
 & \left. + (1+\xi_1)(1+\xi_2)\alpha_{1(3)} + (1-\xi_1)(1+\xi_2)\alpha_{1(4)} \right)
 \end{aligned} \tag{2.57}$$

$$\begin{aligned}
 \alpha_2(\xi_1, \xi_2) = & \frac{1}{2} \left( (1-\xi_2)\bar{\alpha}_{2(1)}(\xi_1) + (1+\xi_1)\bar{\alpha}_{2(2)}(\xi_2) + \right. \\
 & \left. + (1+\xi_2)\bar{\alpha}_{2(3)}(\xi_1) + (1-\xi_1)\bar{\alpha}_{2(4)}(\xi_2) \right) + \\
 & -\frac{1}{4} \left( (1-\xi_1)(1-\xi_2)\alpha_{2(1)} + (1+\xi_1)(1-\xi_2)\alpha_{2(2)} + \right. \\
 & \left. + (1+\xi_1)(1+\xi_2)\alpha_{2(3)} + (1-\xi_1)(1+\xi_2)\alpha_{2(4)} \right)
 \end{aligned} \tag{2.58}$$

where  $\bar{\alpha}_{1(1)}, \bar{\alpha}_{1(2)}, \bar{\alpha}_{1(3)}, \bar{\alpha}_{1(4)}$  and  $\bar{\alpha}_{2(1)}, \bar{\alpha}_{2(2)}, \bar{\alpha}_{2(3)}, \bar{\alpha}_{2(4)}$  stand for those parametric curves, linked to each principal coordinate, which allow to describe the arbitrary shape of each edge of the distorted domain. These curves are effectively obtained by the Non-Uniform Rational Basis Splines (NURBS). On the other hand, the symbols  $\alpha_{1(1)}, \alpha_{2(1)}, \alpha_{1(2)}, \alpha_{2(2)}, \alpha_{1(3)}, \alpha_{2(3)}$  and  $\alpha_{1(4)}, \alpha_{2(4)}$  in (2.57)-(2.58) represent the coordinates of each corner of the quadrilateral domain at issue. For the sake of clarity, the mapping just shown is depicted in Figure 2.10.

In general, the mapping procedure requires that all the spatial derivatives of a generic problem are written in the new coordinate system  $\xi_1, \xi_2$ . In other words, each variable and its derivatives with respect to the coordinates  $\alpha_1, \alpha_2$  have to be mapped into the computational space. First of all, the first-order derivatives of any generic function with respect to the natural coordinates must be evaluated. The well-known chain rule of differentiation provides the following result

$$\begin{bmatrix} \frac{\partial}{\partial \xi_1} \\ \frac{\partial}{\partial \xi_2} \end{bmatrix} = \begin{bmatrix} \frac{\partial \alpha_1}{\partial \xi_1} & \frac{\partial \alpha_2}{\partial \xi_1} \\ \frac{\partial \alpha_1}{\partial \xi_2} & \frac{\partial \alpha_2}{\partial \xi_2} \end{bmatrix} \begin{bmatrix} \frac{\partial}{\partial \alpha_1} \\ \frac{\partial}{\partial \alpha_2} \end{bmatrix} = \mathbf{J} \begin{bmatrix} \frac{\partial}{\partial \alpha_1} \\ \frac{\partial}{\partial \alpha_2} \end{bmatrix} \tag{2.59}$$

in which  $\mathbf{J}$  is the Jacobian matrix linked to the coordinate transformation in hand.

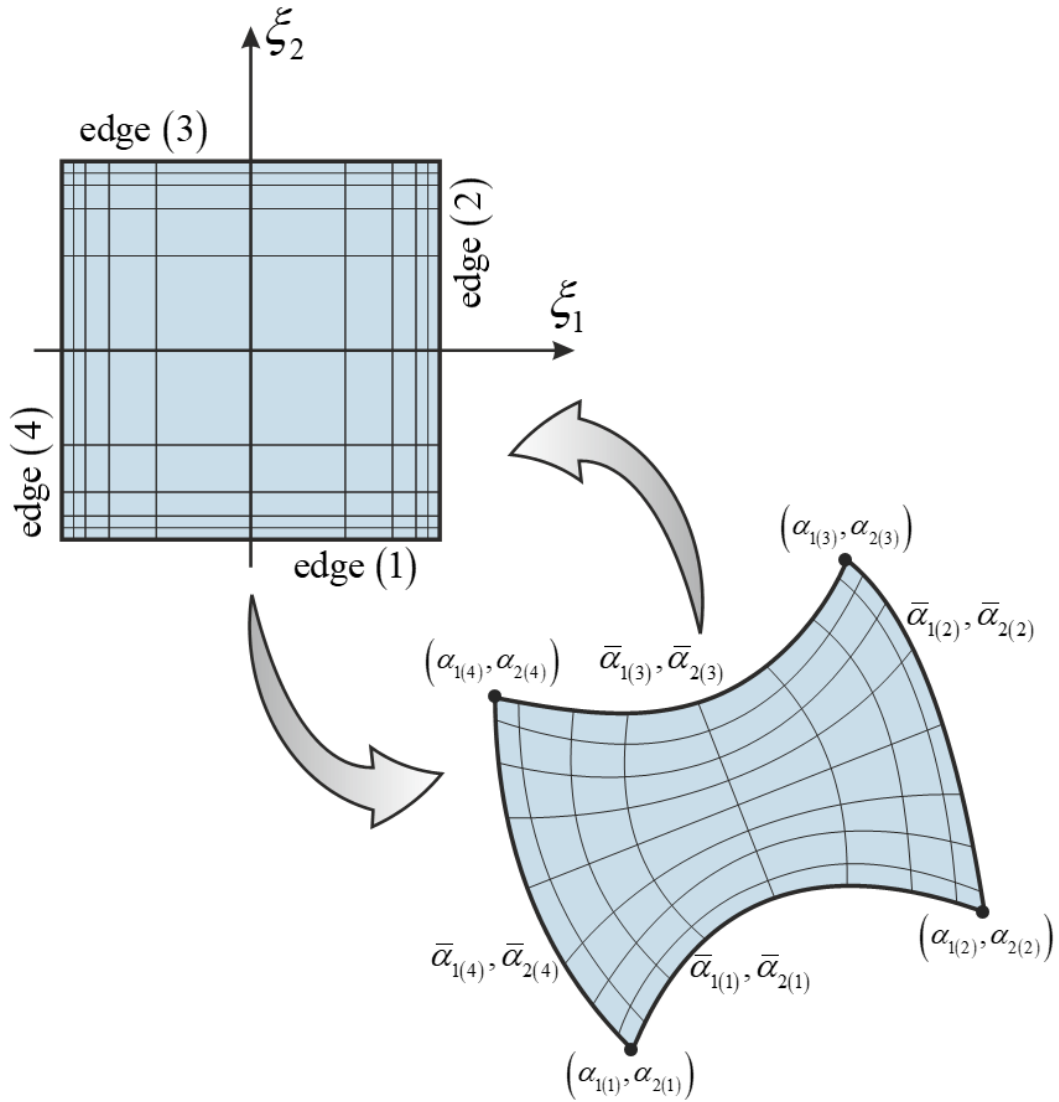


Figure 2.10 – Isogeometric mapping.

The determinant of the Jacobian matrix ( $\det \mathbf{J}$ ) is given by

$$\det \mathbf{J} = \frac{\partial \alpha_1}{\partial \xi_1} \frac{\partial \alpha_2}{\partial \xi_2} - \frac{\partial \alpha_2}{\partial \xi_1} \frac{\partial \alpha_1}{\partial \xi_2} \quad (2.60)$$

Since expressions (2.56) represent a one-to-one mapping, the inverse relations of (2.59) can be evaluated. One gets

$$\begin{bmatrix} \frac{\partial}{\partial \alpha_1} \\ \frac{\partial}{\partial \alpha_2} \end{bmatrix} = \begin{bmatrix} \frac{\partial \xi_1}{\partial \alpha_1} & \frac{\partial \xi_2}{\partial \alpha_1} \\ \frac{\partial \xi_1}{\partial \alpha_2} & \frac{\partial \xi_2}{\partial \alpha_2} \end{bmatrix} \begin{bmatrix} \frac{\partial}{\partial \xi_1} \\ \frac{\partial}{\partial \xi_2} \end{bmatrix} = \mathbf{J}^{-1} \begin{bmatrix} \frac{\partial}{\partial \xi_1} \\ \frac{\partial}{\partial \xi_2} \end{bmatrix} \quad (2.61)$$

where the inverse of Jacobian matrix  $\mathbf{J}^{-1}$ , which can be written as follows

$$\mathbf{J}^{-1} = \frac{1}{\det \mathbf{J}} \begin{bmatrix} \frac{\partial \alpha_2}{\partial \xi_2} & -\frac{\partial \alpha_2}{\partial \xi_1} \\ -\frac{\partial \alpha_1}{\partial \xi_2} & \frac{\partial \alpha_1}{\partial \xi_1} \end{bmatrix} \quad (2.62)$$

It should be noted that the coordinate change is admissible only if  $\det \mathbf{J} \neq 0$ . This condition is verified since the mapping in (2.56) denotes a one-to-one transformation. The following notations can be defined by comparing expressions (2.61) and (2.62)

$$\begin{aligned} \xi_{1,\alpha_1} &= \frac{\partial \xi_1}{\partial \alpha_1} = \frac{1}{\det \mathbf{J}} \frac{\partial \alpha_2}{\partial \xi_2}, & \xi_{1,\alpha_2} &= \frac{\partial \xi_1}{\partial \alpha_2} = -\frac{1}{\det \mathbf{J}} \frac{\partial \alpha_1}{\partial \xi_2} \\ \xi_{2,\alpha_1} &= \frac{\partial \xi_2}{\partial \alpha_1} = -\frac{1}{\det \mathbf{J}} \frac{\partial \alpha_2}{\partial \xi_1}, & \xi_{2,\alpha_2} &= \frac{\partial \xi_2}{\partial \alpha_2} = \frac{1}{\det \mathbf{J}} \frac{\partial \alpha_1}{\partial \xi_1} \end{aligned} \quad (2.63)$$

At this point, the second-order operators can be obtained as well

$$\frac{\partial^2}{\partial \alpha_1^2} = \xi_{1,\alpha_1}^2 \frac{\partial^2}{\partial \xi_1^2} + \xi_{2,\alpha_1}^2 \frac{\partial^2}{\partial \xi_2^2} + 2\xi_{1,\alpha_1}\xi_{2,\alpha_1} \frac{\partial^2}{\partial \xi_1 \partial \xi_2} + \xi_{1,\alpha_1\alpha_1} \frac{\partial}{\partial \xi_1} + \xi_{2,\alpha_1\alpha_1} \frac{\partial}{\partial \xi_2} \quad (2.64)$$

$$\frac{\partial^2}{\partial \alpha_2^2} = \xi_{1,\alpha_2}^2 \frac{\partial^2}{\partial \xi_1^2} + \xi_{2,\alpha_2}^2 \frac{\partial^2}{\partial \xi_2^2} + 2\xi_{1,\alpha_2}\xi_{2,\alpha_2} \frac{\partial^2}{\partial \xi_1 \partial \xi_2} + \xi_{1,\alpha_2\alpha_2} \frac{\partial}{\partial \xi_1} + \xi_{2,\alpha_2\alpha_2} \frac{\partial}{\partial \xi_2} \quad (2.65)$$

$$\begin{aligned} \frac{\partial^2}{\partial \alpha_1 \partial \alpha_2} &= \xi_{1,\alpha_1}\xi_{1,\alpha_2} \frac{\partial^2}{\partial \xi_1^2} + \xi_{2,\alpha_1}\xi_{2,\alpha_2} \frac{\partial^2}{\partial \xi_2^2} + \\ &+ \left( \xi_{1,\alpha_1}\xi_{2,\alpha_2} + \xi_{1,\alpha_2}\xi_{2,\alpha_1} \right) \frac{\partial^2}{\partial \xi_1 \partial \xi_2} + \xi_{1,\alpha_1\alpha_2} \frac{\partial}{\partial \xi_1} + \xi_{2,\alpha_1\alpha_2} \frac{\partial}{\partial \xi_2} \end{aligned} \quad (2.66)$$

where the following notation is employed for conciseness purposes

$$\xi_{1,\alpha_1\alpha_1} = \frac{1}{\det \mathbf{J}^2} \left( \frac{\partial \alpha_2}{\partial \xi_2} \frac{\partial^2 \alpha_2}{\partial \xi_1 \partial \xi_2} - \left( \frac{\partial \alpha_2}{\partial \xi_2} \right)^2 \frac{\det \mathbf{J}_{\xi_1}}{\det \mathbf{J}} - \frac{\partial \alpha_2}{\partial \xi_1} \frac{\partial^2 \alpha_2}{\partial \xi_2^2} + \frac{\partial \alpha_2}{\partial \xi_1} \frac{\partial \alpha_2}{\partial \xi_2} \frac{\det \mathbf{J}_{\xi_2}}{\det \mathbf{J}} \right) \quad (2.67)$$

$$\xi_{1,\alpha_2\alpha_2} = \frac{1}{\det \mathbf{J}^2} \left( \frac{\partial \alpha_1}{\partial \xi_2} \frac{\partial^2 \alpha_1}{\partial \xi_1 \partial \xi_2} - \left( \frac{\partial \alpha_1}{\partial \xi_2} \right)^2 \frac{\det \mathbf{J}_{\xi_1}}{\det \mathbf{J}} - \frac{\partial \alpha_1}{\partial \xi_1} \frac{\partial^2 \alpha_1}{\partial \xi_2^2} + \frac{\partial \alpha_1}{\partial \xi_1} \frac{\partial \alpha_1}{\partial \xi_2} \frac{\det \mathbf{J}_{\xi_2}}{\det \mathbf{J}} \right) \quad (2.68)$$

$$\xi_{1,\alpha_1\alpha_2} = \frac{1}{\det \mathbf{J}^2} \left( -\frac{\partial \alpha_2}{\partial \xi_2} \frac{\partial^2 \alpha_1}{\partial \xi_1 \partial \xi_2} + \frac{\partial \alpha_2}{\partial \xi_2} \frac{\partial \alpha_1}{\partial \xi_2} \frac{\det \mathbf{J}_{\xi_1}}{\det \mathbf{J}} + \frac{\partial \alpha_2}{\partial \xi_1} \frac{\partial^2 \alpha_1}{\partial \xi_2^2} - \frac{\partial \alpha_2}{\partial \xi_1} \frac{\partial \alpha_1}{\partial \xi_2} \frac{\det \mathbf{J}_{\xi_2}}{\det \mathbf{J}} \right) \quad (2.69)$$

$$\xi_{2,\alpha_1\alpha_1} = \frac{1}{\det \mathbf{J}^2} \left( -\frac{\partial \alpha_2}{\partial \xi_2} \frac{\partial^2 \alpha_2}{\partial \xi_1^2} + \frac{\partial \alpha_2}{\partial \xi_2} \frac{\partial \alpha_2}{\partial \xi_1} \frac{\det \mathbf{J}_{\xi_1}}{\det \mathbf{J}} + \frac{\partial \alpha_2}{\partial \xi_1} \frac{\partial^2 \alpha_2}{\partial \xi_1 \partial \xi_2} - \left( \frac{\partial \alpha_2}{\partial \xi_1} \right)^2 \frac{\det \mathbf{J}_{\xi_2}}{\det \mathbf{J}} \right) \quad (2.70)$$

$$\xi_{2,\alpha_2\alpha_2} = \frac{1}{\det \mathbf{J}^2} \left( -\frac{\partial \alpha_1}{\partial \xi_2} \frac{\partial^2 \alpha_1}{\partial \xi_1^2} + \frac{\partial \alpha_1}{\partial \xi_2} \frac{\partial \alpha_1}{\partial \xi_1} \frac{\det \mathbf{J}_{\xi_1}}{\det \mathbf{J}} + \frac{\partial \alpha_1}{\partial \xi_1} \frac{\partial^2 \alpha_1}{\partial \xi_1 \partial \xi_2} - \left( \frac{\partial \alpha_1}{\partial \xi_1} \right)^2 \frac{\det \mathbf{J}_{\xi_2}}{\det \mathbf{J}} \right) \quad (2.71)$$

$$\xi_{2,\alpha_1\alpha_2} = \frac{1}{\det \mathbf{J}^2} \left( -\frac{\partial \alpha_2}{\partial \xi_1} \frac{\partial^2 \alpha_1}{\partial \xi_1 \partial \xi_2} + \frac{\partial \alpha_1}{\partial \xi_2} \frac{\partial \alpha_1}{\partial \xi_1} \frac{\det \mathbf{J}_{\xi_1}}{\det \mathbf{J}} + \frac{\partial \alpha_2}{\partial \xi_2} \frac{\partial^2 \alpha_1}{\partial \xi_1^2} - \frac{\partial \alpha_2}{\partial \xi_1} \frac{\partial \alpha_1}{\partial \xi_1} \frac{\det \mathbf{J}_{\xi_2}}{\det \mathbf{J}} \right) \quad (2.72)$$

The first-order derivatives with respect to the natural coordinates  $\xi_1, \xi_2$  of the determinant of the Jacobian matrix (2.63) are required, too. These definitions are shown below

$$\det \mathbf{J}_{\xi_1} = \frac{\partial \alpha_1}{\partial \xi_1} \frac{\partial^2 \alpha_2}{\partial \xi_1 \partial \xi_2} - \frac{\partial \alpha_2}{\partial \xi_1} \frac{\partial^2 \alpha_1}{\partial \xi_1 \partial \xi_2} + \frac{\partial \alpha_2}{\partial \xi_2} \frac{\partial^2 \alpha_1}{\partial \xi_1^2} - \frac{\partial \alpha_1}{\partial \xi_2} \frac{\partial^2 \alpha_2}{\partial \xi_1^2} \quad (2.73)$$

$$\det \mathbf{J}_{\xi_2} = -\frac{\partial \alpha_1}{\partial \xi_2} \frac{\partial^2 \alpha_2}{\partial \xi_1 \partial \xi_2} + \frac{\partial \alpha_2}{\partial \xi_2} \frac{\partial^2 \alpha_1}{\partial \xi_1 \partial \xi_2} - \frac{\partial \alpha_2}{\partial \xi_1} \frac{\partial^2 \alpha_1}{\partial \xi_2^2} + \frac{\partial \alpha_1}{\partial \xi_1} \frac{\partial^2 \alpha_2}{\partial \xi_2^2} \quad (2.74)$$

The mapping procedure just presented must be used to study those structural problems of plates and shells in which the reference domains are not regular but characterized by arbitrary shapes [58-62].

### 2.3.1.1 Non-Uniform Rational Basis Splines

The coordinate transformation presented in the previous paragraph is based on the use of NURBS. For the sake of completeness, the main features of these curves are briefly presented in the following. A more complete treatise can be found in the book by Piegl and Tiller [63]. By definition, the  $p$ -th degree NURBS curve takes the following aspect

$$\mathbf{C}(u) = \frac{\sum_{i=0}^n N_{i,p}(u) w_i \mathbf{P}_i}{\sum_{i=0}^n N_{i,p}(u) w_i} \quad (2.75)$$

for  $a \leq u \leq b$ , where  $\mathbf{P}_i$  is the vector of the control points which define the control polygon,  $w_i > 0$  stands for the weighting coefficients of the curves, whereas  $N_{i,p}(u)$  represents the  $i$ -th basis spline function of  $p$ -th degree (or order  $p+1$ ) defined on the following non-uniform knot vector

$$\mathbf{U} = \left[ \underbrace{a, \dots, a}_{p+1}, u_{p+1}, \dots, u_{m-p-1}, \underbrace{b, \dots, b}_{p+1} \right] \quad (2.76)$$

In other words, the knot vector just mentioned represents a sequence of parameters that define where and how the control points affect the curve.  $a, b$  denote the limits of the domain in which the curve is described.

It should be recalled that the control points are included into a list of points which describe the NURBS shape. Each point of the curve, in fact, can be represented as a weighted sum of some control points, in which the weights change according to the polynomial function.

The basis spline functions (or B-spline) of  $p$ -th degree can be defined through a recursive approach. In particular, the  $i$ -th B-spline is given by

$$N_{i,0}(u) = \begin{cases} 1 & \text{if } u_i \leq u < u_{i+1} \\ 0 & \text{otherwise} \end{cases} \quad (2.77)$$

$$N_{i,p}(u) = \frac{u - u_i}{u_{i+p} - u_i} N_{i,p-1}(u) + \frac{u_{i+p+1} - u}{u_{i+p+1} - u_{i+1}} N_{i+1,p-1}(u) \quad (2.78)$$

Having in mind these relations, it should be noted that the first order functions represent step functions that have a value different from zero only in the following interval  $[u_i, u_{i+1})$ , which is known as the  $i$ -th knot span. The  $i$ -th knot span could be characterized by zero length, due to the fact that not all the knots have to be distinct. Assuming  $p > 1$ , the B-spline basis functions  $N_{i,p}(u)$  can be obtained as a linear combination of other two bases, whose order is  $p-1$ . It should be also noted that the B-spline basis functions are piecewise polynomials that can be defined within the real line. The properties of these curves are exhaustively analyzed in the book by Piegl and Tiller [63].



# *Chapter 3*

## *Strong and Weak Formulations for Doubly-Curved Shells: Higher-order Theories*

The classic three-dimensional elasticity theory represents the most complete approach to investigate the mechanical behavior of doubly-curved shell structures [64-74]. Nevertheless, this methodology is extremely onerous in terms of calculus requirements. Thus, two-dimensional theories are developed to reduce the computations needed to get the solution. For this purpose, some assumptions and hypotheses have to be introduced, without losing the accuracy of three-dimensional approaches. In other words, the main simplification of these theories is the decrease of the number of computations by considering the shell middle surface as the reference domain of the problem.

Several models characterized by different assumptions have been developed in the last century, starting from the Kirchhoff-Love theory for thin plates and shells [75]. Due to the small value of thickness, the shear strains can be neglected according to this model. The names Classical Plate Theory (CPT) and Classical Shell Theory (CST) are currently used to denote such theories, if thin plates and shells have to be studied, respectively. For the sake of

completeness, the researches presented by Sanders [76], Timoshenko and Woinowsky-Krieger [77], Flügge [78], Gol'Denveizer [79], Novozhilov [80], Vlasov [81], Ambartsumyan [49], Kraus [50], Lekhnitskii et al. [82], Leissa [83, 84], Slizard [85], Dowell [86], Donnel [87], Calladine [88], Niordson [89], Markuš [90], Vorovich [91], Ventsel and Krauthammer [92], can be mentioned due to their contribution given to the development of these models. Nevertheless, these theories are inadequate to model the mechanical behavior of moderately thick and thick structures, since shear strains, as well as rotary inertias, cannot be neglected due to higher value of thickness. These effects have been included for the first time in the well-known First-order Shear Deformation Theory (FSDT), developed by Reissner and Mindlin [93, 94]. Thereafter, several authors employed this model for their researches related to plates and shells. For instance, the works by Libai and Simmonds [95], Liew et al. [96], Gould [97], Reddy [98], Wang et al. [99], Soedel [100], Wang et al. [101], Mindlin [102], Awrejcewicz et al. [103], Voyiadjis and Woelke [104], and Chakraverty [105], can be cited for this purpose. Further examples of plates and shells analyzed in the theoretical framework of this model can be found in the papers [106-119].

However, the increasing use of advanced materials has proven the inadequacy of classical and first-order theories to model the effective mechanical behavior of plates and shells made of innovative constituents. Among them, composite materials should be recalled due to their enhanced mechanical properties with respect to conventional materials [120-143]. In particular, the most exploited classes of composite materials are the ones of laminated and sandwich composites [144-146], as well as Functionally Graded Materials (FGMs) [147-172]. The recent advancements in the technologies for the manufacturing process have also increased the development of the so-called smart composites [173-175] and materials reinforced by curvilinear fibers based on the Variable Angle Tow (VAT) concept [176-191]. Analogously, the improvement of nanotechnologies has allowed to apply a reinforcement phase at the nano-scale. For instance, the outstanding mechanical behavior of the so-called nanocomposites reinforced by Carbon Nanotubes (CNTs) has been investigated in several papers [192-209].

When innovative and advanced constituents are employed in plate and shell structures, the inadequacy of lower-order models, such as classical and first-order ones, could be particularly evident, since some effects caused by peculiar mechanical configurations are not well-captured by the structural theory. As clearly explained in the papers by Librescu and Reddy

[210], Whitney and Pagano [211], Whitney and Sun [212], Reddy [213-215], and Reddy and Liu [216], more refined approaches are needed to obtain a structural behavior that is closer to the three-dimensional one. This is the main reason that has led to the development of Higher-order Structural Theories (HSDTs), as highlighted also in the works [217-222]. In general, these approaches are characterized by enriched kinematic models able to describe more complex displacement fields. Consequently, a better approximation of the effective structural response can be reached.

The turning point in the development of HSDTs has been provided by Carrera [223-227], who defined the bases of a Unified Formulation, known as Carrera Unified Formulation (CUF). By means of this approach, several enriched kinematic models and higher-order theory can be easily obtained and compared, by choosing the order of kinematic expansion. Analogously, the kinematic expansion can assume several forms, since a free choice of the so-called thickness functions can be performed. In addition, this formulation includes also the class of kinematic based zig-zag theories, since the Murakami's function can be added to the kinematic model [226-227]. This choice is extremely useful when the mechanical behavior of soft-core sandwich structures has to be investigated. For completeness purpose, it should be mentioned that more general versions of the CUF have been developed. For this purpose, the Generalized Unified Formulation (GUF) presented by Demasi [228] and the Sublaminated Generalized Unified Formulation (S-GUF) proposed by D'Ottavio [229] can be cited.

At this point, it should be mentioned that HSDTs are commonly categorized in two different groups, which are the Equivalent Single Layer (ESL) and Layer-wise (LW) approaches. In general, an ESL approach can analyze a composite structure considering its middle surface as the reference domain, in which all the geometric and mechanical parameters, as well as the degrees of freedom of the problem, are defined [230-245]. On the other hand, a LW approach is employed to investigate the mechanical behavior of laminated composite structures made of several plies (or layers), by defining the kinematic expansion, and consequently the degrees of freedom, along the thickness of each layer. In general, this approach can describe continuous displacement fields, characterized by discontinuities of their derivatives at the interfaces of the various layers [246-249]. A similar behavior can be obtained through an ESL model embedded with the Murakami's function. Finally, an hybrid approach with intermediate features between the ESL and LW methodologies, known as Equivalent Layer-wise (ELW) can be obtained too, as shown in [250].

### 3.1 SHELL STRUCTURAL MODEL

Once the shell middle surface is described through the differential geometry presented in the previous chapter, it is possible to obtain those governing equations which rule its mechanical behavior. The following structural model is two-dimensional and defined in the reference domain, which coincides with the shell middle surface itself. The degrees of freedom, as well as the mechanical properties, are all computed on that surface. Thus, the current approach is clearly an Equivalent Single Layer (ESL) model. The main assumptions presented below are valid only if the coordinates of the local reference system  $O'\alpha_1\alpha_2\zeta$  are orthogonal and principal. Therefore, the fundamental equations of a generic shell element of thickness  $h$  are written in the local reference system  $O'\alpha_1\alpha_2\zeta$ , as depicted in Figure 3.1.

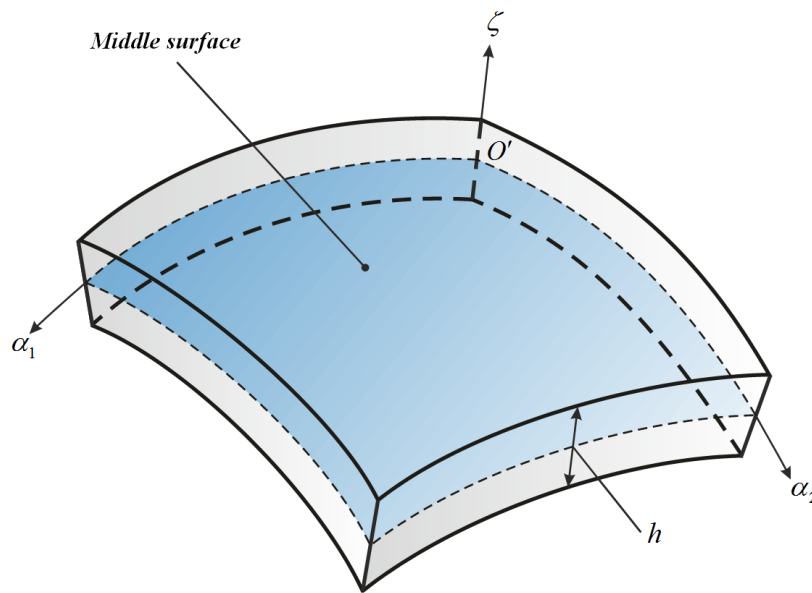


**Figure 3.1** – Local reference system  $O'\alpha_1\alpha_2\zeta$  of a generic shell element.

The displacement field of an arbitrary point within the three-dimensional shell is described by three displacement components  $U_1, U_2, U_3$  defined along each principal coordinate. In other words, these quantities represent the three-dimensional displacements along the coordinate lines  $\alpha_1, \alpha_2, \zeta$ , respectively. It should be recalled that  $U_1, U_2, U_3$  depend on both the position within the medium and on the time variable  $t$ . For the sake of conciseness, the

corresponding vector  $\mathbf{U} = \mathbf{U}(\alpha_1, \alpha_2, \zeta, t)$  can be introduced

$$\mathbf{U} = [U_1(\alpha_1, \alpha_2, \zeta, t) \quad U_2(\alpha_1, \alpha_2, \zeta, t) \quad U_3(\alpha_1, \alpha_2, \zeta, t)]^T \quad (3.1)$$

A Unified Formulation (UF) will be presented in the next sections to describe several displacement fields characterized by an arbitrary order of kinematic expansion [223-227].

Finally, it should be mentioned that the present approach is valid to analyze the mechanical behavior of thick and moderately thick shells. This category is defined by the following relation

$$\frac{1}{100} \leq \max\left(\frac{h}{R_{\min}}, \frac{h}{L_{\min}}\right) \leq \frac{1}{5} \quad (3.2)$$

where  $R_{\min}, L_{\min}$  denote respectively the minor radius of curvature and the smaller length of the shell structure under consideration.

### 3.1.1 BRIEF NOTES ON THREE-DIMENSIONAL ELASTICITY

Before introducing the shell structural model, some brief notes on the three-dimensional elasticity theory are presented. It is well-known that the stress state in each point  $P$  of a three-dimensional medium is defined by the following  $3 \times 3$  stress tensor

$$\begin{bmatrix} \sigma_1 & \tau_{12} & \tau_{13} \\ \tau_{21} & \sigma_2 & \tau_{23} \\ \tau_{31} & \tau_{32} & \sigma_3 \end{bmatrix} \quad (3.3)$$

By considering the local reference system  $O'\alpha_1\alpha_2\zeta$  and recalling that  $\alpha_1, \alpha_2$  are orthogonal and principal coordinates, it should be noted that  $\sigma_1, \sigma_2, \sigma_3$  represents the normal stresses that act along the three mutually orthogonal directions  $\alpha_1, \alpha_2, \zeta$ , respectively. On the other hand, the shear stresses  $\tau_{12}, \tau_{13}, \tau_{23}, \tau_{21}, \tau_{31}, \tau_{32}$  act on three mutually orthogonal planes. If the symmetry of the stress tensor is introduced, the number of independent stress components is reduced to six, since the following relation is valid

$$\tau_{12} = \tau_{21}, \quad \tau_{13} = \tau_{31}, \quad \tau_{23} = \tau_{32} \quad (3.4)$$

For the sake of conciseness, these six independent components can be collected in the corresponding vector  $\boldsymbol{\sigma} = \boldsymbol{\sigma}(\alpha_1, \alpha_2, \zeta, t)$

$$\boldsymbol{\sigma} = [\sigma_1 \quad \sigma_2 \quad \tau_{12} \quad \tau_{13} \quad \tau_{23} \quad \sigma_3]^T \quad (3.5)$$

In order to understand the meaning of these quantities, the stress components included in  $\boldsymbol{\sigma}$  are graphically depicted in Figure 3.2 for a generic three-dimensional medium extracted from a shell structure.

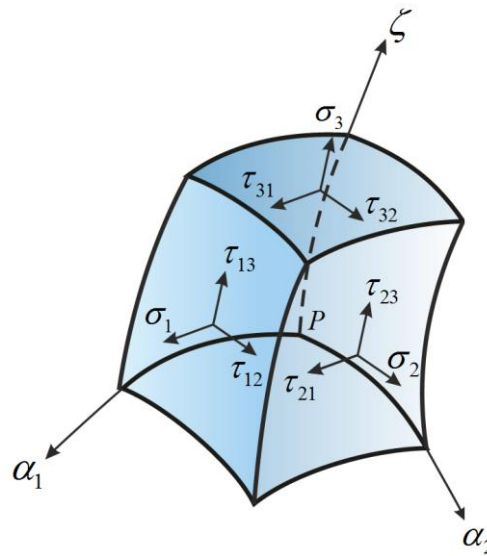


**Figure 3.2** – Stress components acting on an infinitesimal three-dimensional element.

The deformed configuration is described by means of the strain components. The complete set of these components is collected into the corresponding  $3 \times 3$  strain tensor

$$\begin{bmatrix} \varepsilon_1 & \gamma_{12} & \gamma_{13} \\ \gamma_{12} & \varepsilon_2 & \gamma_{23} \\ \gamma_{13} & \gamma_{23} & \varepsilon_3 \end{bmatrix} \quad (3.6)$$

Due to the symmetry properties of this tensor, it is clear that only six independent strains are required to describe the deformation process. For conciseness purposes, these six independent components are collected in the corresponding vector  $\boldsymbol{\varepsilon} = \boldsymbol{\varepsilon}(\alpha_1, \alpha_2, \zeta, t)$

$$\boldsymbol{\varepsilon} = [\varepsilon_1 \quad \varepsilon_2 \quad \gamma_{12} \quad \gamma_{13} \quad \gamma_{23} \quad \varepsilon_3]^T \quad (3.7)$$

The equations that relate the strain and stress components just introduced are known as constitutive laws. If the constitutive relations are linear and the material is elastic, which

means that the constitutive behavior is function only of the deformations, the medium is called *hyperelastic*. By definition, an elastic body is a solid made of a continuous constituent able of undergoing deformations that disappear when the applied loads are removed. Mathematically speaking, a linear elastic medium is characterized by the linear relation between stress and strain components shown below

$$\boldsymbol{\sigma} = \mathbf{C}\boldsymbol{\varepsilon} \quad (3.8)$$

where  $\mathbf{C}$  is the  $6 \times 6$  constitutive matrix which collects the so-called elastic constants of the material denoted by  $C_{ij}$ , for  $i, j = 1, 2, \dots, 6$ . Equations (3.8) are known as generalized Hooke laws. In extended matrix notation, relation (3.8) assumes the following aspect for an elastic medium

$$\begin{bmatrix} \sigma_1 \\ \sigma_2 \\ \tau_{12} \\ \tau_{13} \\ \tau_{23} \\ \sigma_3 \end{bmatrix} = \begin{bmatrix} C_{11} & C_{12} & C_{16} & C_{14} & C_{15} & C_{13} \\ C_{21} & C_{22} & C_{26} & C_{24} & C_{25} & C_{23} \\ C_{61} & C_{62} & C_{66} & C_{64} & C_{65} & C_{63} \\ C_{41} & C_{42} & C_{46} & C_{44} & C_{45} & C_{43} \\ C_{51} & C_{52} & C_{56} & C_{54} & C_{55} & C_{53} \\ C_{31} & C_{32} & C_{36} & C_{34} & C_{35} & C_{33} \end{bmatrix} \begin{bmatrix} \varepsilon_1 \\ \varepsilon_2 \\ \gamma_{12} \\ \gamma_{13} \\ \gamma_{23} \\ \varepsilon_3 \end{bmatrix} \quad (3.9)$$

In general, 36 elastic constants  $C_{ij}$  are required for a complete mechanical characterization of the elastic medium. Nevertheless, this number is reduced if particular material configurations are investigated. In the following, the Hooke laws are specialized only for anisotropic, orthotropic, and isotropic medium. Further details concerning the three-dimensional elasticity theory in principal curvilinear coordinates can be found in the books by Tornabene et al. [56, 57].

### 3.1.1.1 Anisotropic materials

If the medium is anisotropic, the independent elastic constants are reduced to 21 since the matrix  $\mathbf{C}$  turns out to be symmetric. In other words, one gets  $C_{ij} = C_{ji}$  and the stress-strain relation (3.9) becomes

$$\begin{bmatrix} \sigma_1 \\ \sigma_2 \\ \tau_{12} \\ \tau_{13} \\ \tau_{23} \\ \sigma_3 \end{bmatrix} = \begin{bmatrix} C_{11} & C_{12} & C_{16} & C_{14} & C_{15} & C_{13} \\ C_{12} & C_{22} & C_{26} & C_{24} & C_{25} & C_{23} \\ C_{16} & C_{26} & C_{66} & C_{64} & C_{65} & C_{63} \\ C_{14} & C_{24} & C_{64} & C_{44} & C_{45} & C_{43} \\ C_{15} & C_{25} & C_{65} & C_{45} & C_{55} & C_{53} \\ C_{13} & C_{23} & C_{63} & C_{43} & C_{53} & C_{33} \end{bmatrix} \begin{bmatrix} \varepsilon_1 \\ \varepsilon_2 \\ \gamma_{12} \\ \gamma_{13} \\ \gamma_{23} \\ \varepsilon_3 \end{bmatrix} \quad (3.10)$$

The constitutive operator  $\mathbf{C}$  can be also named stiffness matrix.

### 3.1.1.2 Orthotropic materials

The number of elastic coefficients is reduced to 9 if the elastic medium has three orthogonal planes of material symmetry. In this circumstance, the material is orthotropic and the relation (3.9) assumes the following aspect

$$\begin{bmatrix} \sigma_1 \\ \sigma_2 \\ \tau_{12} \\ \tau_{13} \\ \tau_{23} \\ \sigma_3 \end{bmatrix} = \begin{bmatrix} C_{11} & C_{12} & 0 & 0 & 0 & C_{13} \\ C_{12} & C_{22} & 0 & 0 & 0 & C_{23} \\ 0 & 0 & C_{66} & 0 & 0 & 0 \\ 0 & 0 & 0 & C_{44} & 0 & 0 \\ 0 & 0 & 0 & 0 & C_{55} & 0 \\ C_{13} & C_{23} & 0 & 0 & 0 & C_{33} \end{bmatrix} \begin{bmatrix} \varepsilon_1 \\ \varepsilon_2 \\ \gamma_{12} \\ \gamma_{13} \\ \gamma_{23} \\ \varepsilon_3 \end{bmatrix} \quad (3.11)$$

The mechanical characterization of an orthotropic medium can be performed also in terms of engineering constants, which are the Young's moduli  $E_1, E_2, E_3$ , the shear moduli  $G_{12}, G_{13}, G_{23}$ , and the Poisson's ratios  $\nu_{12}, \nu_{13}, \nu_{23}$ . For this purpose, the following relations must be recalled too

$$\frac{\nu_{ij}}{E_i} = \frac{\nu_{ji}}{E_j}, \quad G_{ij} = G_{ji} \quad (3.12)$$

for  $i, j = 1, 2, 3$ . The nine independent elastic coefficients can be related to these engineering constants as follows

$$\begin{aligned} C_{11} &= \frac{1 - \nu_{23}\nu_{32}}{E_2 E_3 \Delta}, & C_{12} &= \frac{\nu_{21} + \nu_{31}\nu_{23}}{E_2 E_3 \Delta}, & C_{13} &= \frac{\nu_{31} + \nu_{21}\nu_{32}}{E_2 E_3 \Delta} \\ C_{22} &= \frac{1 - \nu_{13}\nu_{31}}{E_1 E_3 \Delta}, & C_{23} &= \frac{\nu_{32} + \nu_{12}\nu_{31}}{E_1 E_3 \Delta}, & C_{33} &= \frac{1 - \nu_{12}\nu_{21}}{E_1 E_2 \Delta} \\ C_{44} &= G_{13}, & C_{55} &= G_{23}, & C_{66} &= G_{12} \end{aligned} \quad (3.13)$$

where

$$\Delta = \frac{1 - \nu_{12}\nu_{21} - \nu_{23}\nu_{32} - \nu_{31}\nu_{13} - 2\nu_{21}\nu_{32}\nu_{13}}{E_1 E_2 E_3} \quad (3.14)$$

### 3.1.1.2 Isotropic materials

When an elastic medium is characterized by the same properties in all the directions outgoing from each point, the independent elastic coefficients are reduced to 2. This material is called isotropic and the constitutive relation (3.8) becomes

$$\begin{bmatrix} \sigma_1 \\ \sigma_2 \\ \tau_{12} \\ \tau_{13} \\ \tau_{23} \\ \sigma_3 \end{bmatrix} = \begin{bmatrix} C_{11} & C_{12} & 0 & 0 & 0 & C_{12} \\ C_{12} & C_{11} & 0 & 0 & 0 & C_{12} \\ 0 & 0 & \frac{C_{11}-C_{12}}{2} & 0 & 0 & 0 \\ 0 & 0 & 0 & \frac{C_{11}-C_{12}}{2} & 0 & 0 \\ 0 & 0 & 0 & 0 & \frac{C_{11}-C_{12}}{2} & 0 \\ C_{12} & C_{12} & 0 & 0 & 0 & C_{11} \end{bmatrix} \begin{bmatrix} \varepsilon_1 \\ \varepsilon_2 \\ \gamma_{12} \\ \gamma_{13} \\ \gamma_{23} \\ \varepsilon_3 \end{bmatrix} \quad (3.15)$$

As shown above, the mechanical characterization can be performed in terms of engineering constants, recalling that for an isotropic medium one gets

$$E_1 = E_2 = E_3 = E, \quad G_{13} = G_{23} = G_{12} = G, \quad \nu_{12} = \nu_{13} = \nu_{23} = \nu \quad (3.16)$$

Only two independent constants are required, since the following relation can be introduced

$$G = \frac{E}{2(1+\nu)} \quad (3.17)$$

Thus, the elastic parameters  $C_{11}, C_{12}$  can be related to the engineering constants as follows

$$C_{11} = \frac{E(1-\nu)}{(1+\nu)(1-2\nu)}, \quad C_{12} = \frac{\nu E}{(1+\nu)(1-2\nu)} \quad (3.18)$$

### 3.1.2 MAIN ASSUMPTIONS

As just mentioned, the key aspect of this UF is that the order of kinematic expansion which defines the displacement field is a free parameter that can be chosen arbitrarily. Thus, several Higher-order Shear Deformation Theories (HSDTs) can be developed. The following hypotheses must be introduced:

- Differently from first-order models, the three-dimensional normal strain  $\varepsilon_3$  is not equal to zero. In other words, the stretching effect is admissible. Mathematically speaking, one gets

$$\varepsilon_3 = \varepsilon_3(\alpha_1, \alpha_2, \zeta, t) \neq 0 \quad (3.19)$$

- Analogously, the transverse shear strains are included in the model. Thus, each line that is orthogonal to the reference surface of the shell before its deformation could be not straight, nor necessarily normal to the middle surface, once the deformation process is over.
- The small displacements hypothesis is required to refer each calculation to the undeformed configuration. In other words, the shell deflections are small and the strains are infinitesimal. In particular, the displacement component  $U_3$  is negligible if compared to the shell thickness. One gets

$$U_3 = U_3(\alpha_1, \alpha_2, \zeta, t) \ll h \quad (3.20)$$

- Contrarily from first-order model, the normal stress  $\sigma_3$  can assume values different from zero. Mathematically speaking, one gets

$$\sigma_3 = \sigma_3(\alpha_1, \alpha_2, \zeta, t) \neq 0 \quad (3.21)$$

- A linear elastic constitutive relation is introduced to describe the mechanical behavior of the constituents.
- The rotary inertia terms and the initial curvatures are included in the model.

It should be recalled that the shell middle surface is described by the principal curvilinear coordinates  $\alpha_1, \alpha_2, \zeta$ . The third coordinate  $\zeta$  can be denoted also by  $\alpha_3$ , so that the notation  $\alpha_i$ , for  $i = 1, 2, 3$ , can be conveniently used.

### 3.1.3 DISPLACEMENT FIELD

The three-dimensional displacement components  $U_1, U_2, U_3$  can be defined through the following relations

$$\begin{aligned} U_1 &= \sum_{\tau=0}^{N+1} F_{\tau}^{\alpha_1} u_1^{(\tau)} \\ U_2 &= \sum_{\tau=0}^{N+1} F_{\tau}^{\alpha_2} u_2^{(\tau)} \\ U_3 &= \sum_{\tau=0}^{N+1} F_{\tau}^{\alpha_3} u_3^{(\tau)} \end{aligned} \quad (3.22)$$

where  $F_{\tau}^{\alpha_1} = F_{\tau}^{\alpha_1}(\zeta)$ ,  $F_{\tau}^{\alpha_2} = F_{\tau}^{\alpha_2}(\zeta)$ ,  $F_{\tau}^{\alpha_3} = F_{\tau}^{\alpha_3}(\zeta)$  denote the shear functions (or thickness functions), whereas  $u_1^{(\tau)} = u_1^{(\tau)}(\alpha_1, \alpha_2, t)$ ,  $u_2^{(\tau)} = u_2^{(\tau)}(\alpha_1, \alpha_2, t)$ ,  $u_3^{(\tau)} = u_3^{(\tau)}(\alpha_1, \alpha_2, t)$  are the generalized displacement components evaluated on the shell middle surface. The parameter  $\tau$  stands for the order of kinematic expansion and can be chosen arbitrarily as  $\tau = 0, 1, 2, \dots, N+1$ . On the other hand,  $N$  represents the maximum order of kinematic expansion. For the sake of clarity, definition (3.22) can be written by using the following extended notation

$$\begin{aligned} U_1 &= F_0^{\alpha_1} u_1^{(0)} + F_1^{\alpha_1} u_1^{(1)} + F_2^{\alpha_1} u_1^{(2)} + F_3^{\alpha_1} u_1^{(3)} + \dots + F_N^{\alpha_1} u_1^{(N)} + F_{N+1}^{\alpha_1} u_1^{(N+1)} \\ U_2 &= F_0^{\alpha_2} u_2^{(0)} + F_1^{\alpha_2} u_2^{(1)} + F_2^{\alpha_2} u_2^{(2)} + F_3^{\alpha_2} u_2^{(3)} + \dots + F_N^{\alpha_2} u_2^{(N)} + F_{N+1}^{\alpha_2} u_2^{(N+1)} \\ U_3 &= F_0^{\alpha_3} u_3^{(0)} + F_1^{\alpha_3} u_3^{(1)} + F_2^{\alpha_3} u_3^{(2)} + F_3^{\alpha_3} u_3^{(3)} + \dots + F_N^{\alpha_3} u_3^{(N)} + F_{N+1}^{\alpha_3} u_3^{(N+1)} \end{aligned} \quad (3.23)$$

As highlighted in the book by Tornabene et al. [57], the thickness functions can assume different meanings to describe several higher-order displacement fields. One of the simplest choices is to employ  $F_{\tau}^{\alpha_i} = \zeta^{\tau}$ , for  $\tau = 0, 1, 2, \dots, N$  and  $i = 1, 2, 3$ , as shear functions, in which  $\zeta^{\tau}$  is a power-law function.

The  $(N+1)$ -th order of kinematic expansion, instead, is always related to the so-called Murakami's function [226, 227], denoted by  $Z = Z(\zeta)$ . Therefore, one gets  $F_{N+1}^{\alpha_i} = Z$ , for  $i = 1, 2, 3$ . The function at issue allows to model the zig-zag effect along the shell thickness. In other word, it is possible to describe a continuous displacement field, but characterized by a different slope between two adjacent layers, if a laminated structure is analyzed. This effect is usually caused by the different transverse stiffness of the constituents. For instance, this is the

case of sandwich structures, in which a highly deformable core is inserted in the lamination scheme. Let us consider a laminated composite structure made of  $l$  plies (or layer), as shown in the scheme of Figure 3.3. Further details and comments concerning laminated composite structures will be presented for completeness purposes in the next sections.

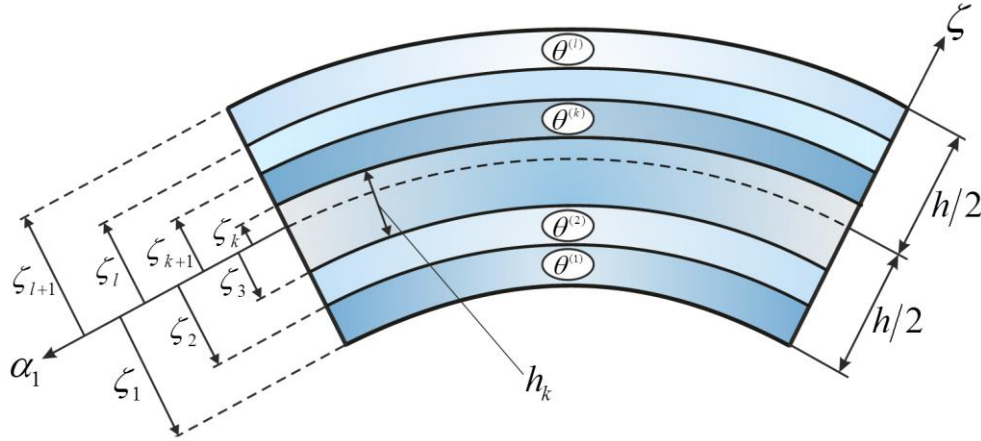


**Figure 3.3** – Layer identification for a laminated composite structure.

If the  $k$ -th layer is identified by the coordinates  $\zeta_k$  and  $\zeta_{k+1}$  measured along the thickness, which denote also its thickness itself  $h_k = \zeta_{k+1} - \zeta_k$ , the Murakami's function can be written as follows

$$Z = (-1)^k \left( \frac{2}{\zeta_{k+1} - \zeta_k} \zeta - \frac{\zeta_{k+1} + \zeta_k}{\zeta_{k+1} - \zeta_k} \right) \quad (3.24)$$

At this point, it is convenient to collect the three generalized displacement components for each order of kinematic expansion in the corresponding vector  $\mathbf{u}^{(\tau)} = \mathbf{u}^{(\tau)}(\alpha_1, \alpha_2, t)$  defined below

$$\mathbf{u}^{(\tau)} = \left[ u_1^{(\tau)}(\alpha_1, \alpha_2, t) \quad u_2^{(\tau)}(\alpha_1, \alpha_2, t) \quad u_3^{(\tau)}(\alpha_1, \alpha_2, t) \right]^T \quad (3.25)$$

It should be specified that the quantities in (3.25) represent the degrees of freedom of the current model. For the sake of conciseness, the following compact notation can be introduced to describe the displacement field (3.22) in matrix form

$$\mathbf{U} = \sum_{\tau=0}^{N+1} \mathbf{F}_{\tau} \mathbf{u}^{(\tau)} \quad (3.26)$$

in which  $\mathbf{F}_{\tau}$  is a  $3 \times 3$  diagonal matrix that collects the thickness function

$$\mathbf{F}_\tau = \begin{bmatrix} F_\tau^{\alpha_1} & 0 & 0 \\ 0 & F_\tau^{\alpha_2} & 0 \\ 0 & 0 & F_\tau^{\alpha_3} \end{bmatrix} \quad (3.27)$$

for  $\tau = 0, 1, 2, \dots, N+1$ .

### 3.1.3.1 Higher-order Shear Deformation Theories

The kinematic model (3.26) allows to define several HDTS by choosing the order of expansion and the thickness functions. According to this general approach, the kinematic expansion can be different along each principal direction, since  $F_\tau^{\alpha_i}$ , for  $i=1,2,3$  are arbitrary functions. Nevertheless, it is possible also to assume the following relation to simplify the treatise

$$F_\tau^{\alpha_1} = F_\tau^{\alpha_2} = F_\tau^{\alpha_3} = \zeta^\tau \quad (3.28)$$

for  $\tau = 0, 1, 2, \dots, N$ . Consequently, a set of HSDTs based on a power-law expansion is established. At this point, the various theories depends only on the maximum order of kinematic expansion  $N$ . In these hypotheses, the displacement field (3.23) becomes

$$\begin{aligned} U_1 &= u_1^{(0)} + \zeta u_1^{(1)} + \zeta^2 u_1^{(2)} + \zeta^3 u_1^{(3)} + \dots + \zeta^N u_1^{(N)} + Z u_1^{(N+1)} \\ U_2 &= u_2^{(0)} + \zeta u_2^{(1)} + \zeta^2 u_2^{(2)} + \zeta^3 u_2^{(3)} + \dots + \zeta^N u_2^{(N)} + Z u_2^{(N+1)} \\ U_3 &= u_3^{(0)} + \zeta u_3^{(1)} + \zeta^2 u_3^{(2)} + \zeta^3 u_3^{(3)} + \dots + \zeta^N u_3^{(N)} + Z u_3^{(N+1)} \end{aligned} \quad (3.29)$$

if the Murakami's function is embedded in the model. Alternatively, the last terms are omitted. The acronyms EDN and EDZN are introduced to classify and specify univocally these HSDTs with and without the Murakami's function, respectively. In particular, the letter "E" means that the theory is based on an ESL approach, whereas "D" states that the generalized displacements represent the unknown of the problem at issue. Letter "Z", instead, stands for the zig-zag effect, when embedded. For instance, the following theories are developed assuming a maximum order expansion  $N$  up to the fourth order

$$\begin{aligned} N=1 & \rightarrow \begin{cases} \text{ED1} \\ \text{EDZ1} \end{cases} & N=2 & \rightarrow \begin{cases} \text{ED2} \\ \text{EDZ2} \end{cases} \\ N=3 & \rightarrow \begin{cases} \text{ED3} \\ \text{EDZ3} \end{cases} & N=4 & \rightarrow \begin{cases} \text{ED4} \\ \text{EDZ4} \end{cases} \end{aligned} \quad (3.30)$$

For the sake of clarity, the qualitative through-the-thickness displacement tendency for some HSDTs illustrated in (3.30) is depicted in Figure 3.4. The kinematic field of the well-known Reissner-Mindlin theory (FSDT) is also shown for completeness purposes.

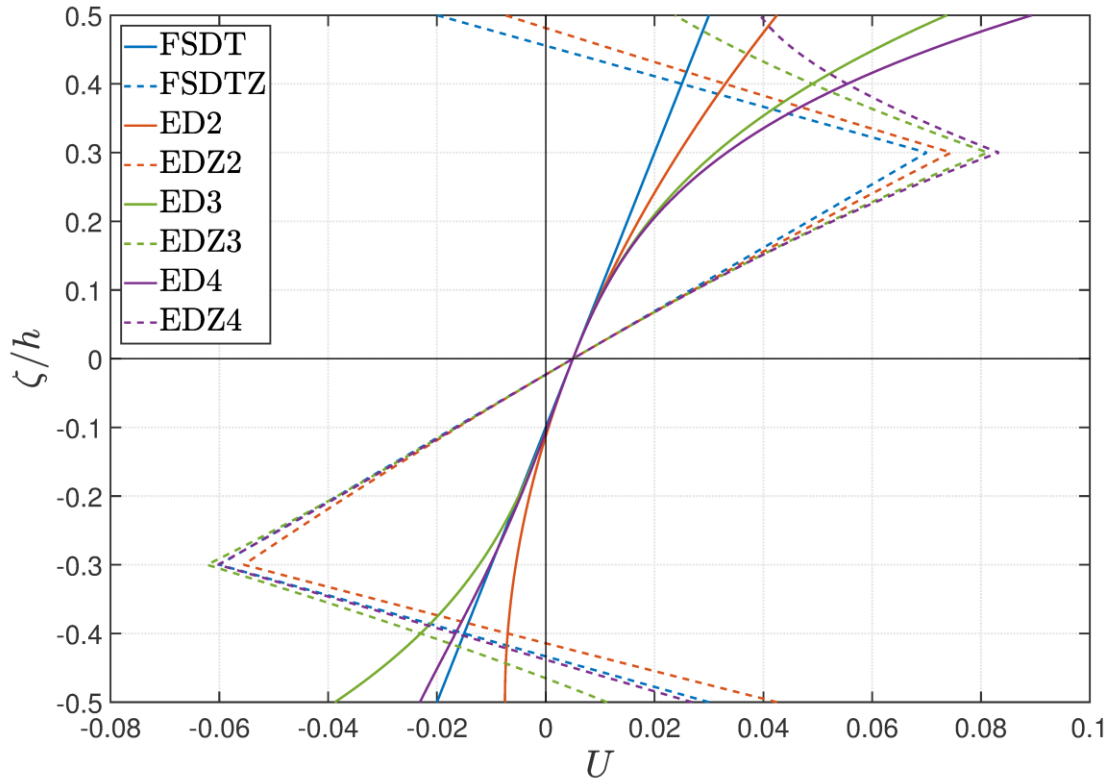


**Figure 3.4** – Qualitative through-the-thickness displacement tendency for several HSDTs, with and without the Murakami’s function.

### 3.1.3.2 Displacement interpolation using Lagrange polynomials

In order to develop the weak formulation of the governing equations, the generalized displacements collected in  $\mathbf{u}^{(\tau)}$ , which denote the degrees of freedom of the model, must be approximated and written as a function of some nodal quantities. The key aspect of the weak form, in fact, is the assumption of a kinematic model in terms of nodal displacements, which are the unknown parameters of the problem. In particular, the present approach is based on a polynomial interpolation of higher-order obtained through the use of the Lagrange polynomials.

The two dimensional domain under consideration must be discretized in a preliminary phase as specified in the previous chapter. If the shell middle surface is described by means of the principal coordinates  $\alpha_1, \alpha_2$ , the following expressions are employed to define the generic coordinates  $\alpha_{1f}, \alpha_{2g}$  of a discrete point within the reference domain

$$\alpha_{1f} = \frac{\alpha_1^1 - \alpha_1^0}{r_{I_N} - r_1} (r_f - r_1) + \alpha_1^0 \quad (3.31)$$

$$\alpha_{2g} = \frac{\alpha_2^1 - \alpha_2^0}{r_{I_M} - r_1} (r_g - r_1) + \alpha_2^0 \quad (3.32)$$

for  $f = 1, 2, \dots, I_N$  and  $g = 1, 2, \dots, I_M$ , according to what has been shown previously. Thus, the grid distribution is made of  $I_N \times I_M$  nodes. The generalized displacements can be computed in each discrete point as  $u_{1(fg)}^{(\tau)} = u_1^{(\tau)}(\alpha_{1f}, \alpha_{2g}, t)$ ,  $u_{2(fg)}^{(\tau)} = u_2^{(\tau)}(\alpha_{1f}, \alpha_{2g}, t)$ , and  $u_{3(fg)}^{(\tau)} = u_3^{(\tau)}(\alpha_{1f}, \alpha_{2g}, t)$ . The generalized displacements (3.25) for each order  $\tau$  of kinematic expansion can be written as a function of these nodal displacements as follows

$$\begin{bmatrix} u_1^{(\tau)} \\ u_2^{(\tau)} \\ u_3^{(\tau)} \end{bmatrix} = \sum_{f=1}^{I_N} \sum_{g=1}^{I_M} \begin{bmatrix} l_f(\alpha_1) l_g(\alpha_2) & 0 & 0 \\ 0 & l_f(\alpha_1) l_g(\alpha_2) & 0 \\ 0 & 0 & l_f(\alpha_1) l_g(\alpha_2) \end{bmatrix} \begin{bmatrix} u_{1(fg)}^{(\tau)} \\ u_{2(fg)}^{(\tau)} \\ u_{3(fg)}^{(\tau)} \end{bmatrix} \quad (3.33)$$

where  $l_f(\alpha_1), l_g(\alpha_2)$  are the  $f$ -th and  $g$ -th Lagrange interpolating polynomials of degree  $I_N - 1$  and  $I_M - 1$ , respectively. They are defined along the principal lines of curvature and assume the following aspect

$$l_f(\alpha_1) = \frac{\prod_{i=1}^{I_N} (\alpha_1 - \alpha_{1i})}{(\alpha_1 - \alpha_{1f}) \prod_{i=1, i \neq f}^{I_N} (\alpha_{1f} - \alpha_{1i})} \quad (3.34)$$

$$l_g(\alpha_2) = \frac{\prod_{j=1}^{I_M} (\alpha_2 - \alpha_{2j})}{(\alpha_2 - \alpha_{2g}) \prod_{j=1, j \neq g}^{I_M} (\alpha_{2g} - \alpha_{2j})} \quad (3.35)$$

For the sake of conciseness, the nodal displacements can be collected in the corresponding

vector  $\bar{\mathbf{u}}^{(\tau)} = \bar{\mathbf{u}}^{(\tau)}(\alpha_{1f}, \alpha_{2g}, t)$ . For this purpose, these quantities can be included in this vector by following the same order of the scheme depicted in Figure 1.2 to facilitate the implementation. Consequently, the vector  $\bar{\mathbf{u}}^{(\tau)}$  is given by

$$\begin{aligned} \bar{\mathbf{u}}^{(\tau)} &= \left[ \bar{\mathbf{u}}_1^{(\tau)} \quad \bar{\mathbf{u}}_2^{(\tau)} \quad \bar{\mathbf{u}}_3^{(\tau)} \right]^T = \\ &= \left[ \left[ \begin{array}{ccc|ccc} u_{1(11)}^{(\tau)} & \cdots & u_{1(I_N1)}^{(\tau)} & u_{1(12)}^{(\tau)} & \cdots & u_{1(I_N2)}^{(\tau)} & \cdots & u_{1(I_M)}^{(\tau)} & \cdots & u_{1(I_N I_M)}^{(\tau)} \\ \cdots & & & \cdots & & & \cdots & & & \cdots \\ \cdots & & & u_{2(11)}^{(\tau)} & \cdots & u_{2(I_N1)}^{(\tau)} & u_{2(12)}^{(\tau)} & \cdots & u_{2(I_N2)}^{(\tau)} & \cdots & u_{2(I_M)}^{(\tau)} & \cdots & u_{2(I_N I_M)}^{(\tau)} \\ \cdots & & & & & & & & & & & & \cdots \\ \cdots & & & u_{3(11)}^{(\tau)} & \cdots & u_{3(I_N1)}^{(\tau)} & u_{3(12)}^{(\tau)} & \cdots & u_{3(I_N2)}^{(\tau)} & \cdots & u_{3(I_M)}^{(\tau)} & \cdots & u_{3(I_N I_M)}^{(\tau)} \end{array} \right] \right]^T \end{aligned} \quad (3.36)$$

for  $\tau = 0, 1, 2, \dots, N, N+1$ . It is clear that  $\bar{\mathbf{u}}_1^{(\tau)}, \bar{\mathbf{u}}_2^{(\tau)}, \bar{\mathbf{u}}_3^{(\tau)}$  are the vectors that collect the nodal displacements along  $\alpha_1, \alpha_2, \zeta$ , respectively. Quantities in (3.36) are the unknown of the problems. The size of  $\bar{\mathbf{u}}^{(\tau)}$  is given by  $(3I_N I_M) \times 1$  for each order of the kinematic expansion of the UF. Definition (3.33) can be conveniently written as follows in matrix form

$$\mathbf{u}^{(\tau)} = \mathbf{N}^T \bar{\mathbf{u}}^{(\tau)} \quad (3.37)$$

in which  $\mathbf{N}^T$  is the matrix of the Lagrange interpolating polynomials defined below

$$\mathbf{N}^T = \begin{bmatrix} \bar{\mathbf{N}}^T & \mathbf{0} & \mathbf{0} \\ \mathbf{0} & \bar{\mathbf{N}}^T & \mathbf{0} \\ \mathbf{0} & \mathbf{0} & \bar{\mathbf{N}}^T \end{bmatrix} \quad (3.38)$$

Its size is clearly given by  $3 \times (3I_N I_M)$ . On the other hand, the sub-matrices  $\bar{\mathbf{N}}^T$ , whose size is  $1 \times (I_N I_M)$ , include the Lagrange polynomials for the approximation. The Lagrange polynomials (3.34)-(3.35) should be collected in the corresponding vectors  $\mathbf{l}_{\alpha_1}, \mathbf{l}_{\alpha_2}$

$$\mathbf{l}_{\alpha_1} = \left[ l_1(\alpha_1) \quad \cdots \quad l_f(\alpha_1) \quad \cdots \quad l_{I_N}(\alpha_1) \right] \quad (3.39)$$

$$\mathbf{l}_{\alpha_2} = \left[ l_1(\alpha_2) \quad \cdots \quad l_g(\alpha_2) \quad \cdots \quad l_{I_M}(\alpha_2) \right] \quad (3.40)$$

in which the size of  $\mathbf{l}_{\alpha_1}, \mathbf{l}_{\alpha_2}$  is  $1 \times I_N$  and  $1 \times I_M$ , respectively. Once the vectors (3.39)-(3.40) are introduced, the matrices  $\bar{\mathbf{N}}^T$  can be obtained by means of the Kronecker product “ $\otimes_k$ ” as follows

$$\begin{aligned}
 \bar{\mathbf{N}}^T &= \mathbf{l}_{\alpha_2} \otimes_k \mathbf{l}_{\alpha_1} \\
 &= \left[ l_1(\alpha_2) \left[ l_1(\alpha_1) \ \cdots \ l_{I_N}(\alpha_1) \right] \ \cdots \right. \\
 &\quad \cdots \ l_g(\alpha_2) \left[ l_1(\alpha_1) \ \cdots \ l_{I_N}(\alpha_1) \right] \ \cdots \\
 &\quad \left. \cdots \ l_{I_M}(\alpha_2) \left[ l_1(\alpha_1) \ \cdots \ l_{I_N}(\alpha_1) \right] \right]
 \end{aligned} \tag{3.41}$$

Once the kinematic model is introduced, it is possible to establish the kinematic equations that relate the three-dimensional strain components (3.7) to the displacements (3.22).

### 3.1.4 KINEMATIC EQUATIONS

Without addressing the whole procedure to obtain the kinematic equations for a generic doubly-curved shell structure, which can be found in the book by Tornabene et al. [57], the relations between the three-dimensional strain components and the three-dimensional displacements are shown below

$$\varepsilon_1 = \frac{1}{H_1} \left( \frac{1}{A_1} \frac{\partial U_1}{\partial \alpha_1} + \frac{U_2}{A_1 A_2} \frac{\partial A_1}{\partial \alpha_2} + \frac{U_3}{R_1} \right) \tag{3.42}$$

$$\varepsilon_2 = \frac{1}{H_2} \left( \frac{1}{A_2} \frac{\partial U_2}{\partial \alpha_2} + \frac{U_1}{A_1 A_2} \frac{\partial A_2}{\partial \alpha_1} + \frac{U_3}{R_2} \right) \tag{3.43}$$

$$\gamma_{12} = \frac{1}{H_1} \left( \frac{1}{A_1} \frac{\partial U_2}{\partial \alpha_1} - \frac{U_1}{A_1 A_2} \frac{\partial A_1}{\partial \alpha_2} \right) + \frac{1}{H_2} \left( \frac{1}{A_2} \frac{\partial U_1}{\partial \alpha_2} - \frac{U_2}{A_1 A_2} \frac{\partial A_2}{\partial \alpha_1} \right) \tag{3.44}$$

$$\gamma_{13} = \frac{1}{H_1} \left( \frac{1}{A_1} \frac{\partial U_3}{\partial \alpha_1} - \frac{U_1}{R_1} \right) + \frac{\partial U_1}{\partial \zeta} \tag{3.45}$$

$$\gamma_{23} = \frac{1}{H_2} \left( \frac{1}{A_2} \frac{\partial U_3}{\partial \alpha_2} - \frac{U_2}{R_2} \right) + \frac{\partial U_2}{\partial \zeta} \tag{3.46}$$

$$\varepsilon_3 = \frac{\partial U_3}{\partial \zeta} \tag{3.47}$$

For the sake of conciseness, equations (3.42)-(3.47) can be conveniently written in matrix form as follows

$$\begin{bmatrix} \varepsilon_1 \\ \varepsilon_2 \\ \gamma_{12} \\ \gamma_{13} \\ \gamma_{23} \\ \varepsilon_3 \end{bmatrix} = \begin{bmatrix} \frac{1}{H_1 A_1} \frac{\partial}{\partial \alpha_1} & \frac{1}{H_1 A_1 A_2} \frac{\partial A_1}{\partial \alpha_2} & \frac{1}{H_1 R_1} \\ \frac{1}{H_2 A_1 A_2} \frac{\partial A_2}{\partial \alpha_1} & \frac{1}{H_2 A_2} \frac{\partial}{\partial \alpha_2} & \frac{1}{H_2 R_2} \\ \frac{1}{H_2 A_2} \frac{\partial}{\partial \alpha_2} - \frac{1}{H_1 A_1 A_2} \frac{\partial A_1}{\partial \alpha_2} & \frac{1}{H_1 A_1} \frac{\partial}{\partial \alpha_1} - \frac{1}{H_2 A_1 A_2} \frac{\partial A_2}{\partial \alpha_1} & 0 \\ \frac{\partial}{\partial \zeta} - \frac{1}{H_1 R_1} & 0 & \frac{1}{H_1 A_1} \frac{\partial}{\partial \alpha_1} \\ 0 & \frac{\partial}{\partial \zeta} - \frac{1}{H_2 R_2} & \frac{1}{H_2 A_2} \frac{\partial}{\partial \alpha_2} \\ 0 & 0 & \frac{\partial}{\partial \zeta} \end{bmatrix} \begin{bmatrix} U_1 \\ U_2 \\ U_3 \end{bmatrix} \quad (3.48)$$

where  $A_1, A_2$  are the Lamè parameters of the shell middle surface, whereas  $R_1, R_2$  are the corresponding main radii of curvature. On the other hand, quantities  $H_1, H_2$  are defined below

$$H_1 = 1 + \frac{\zeta}{R_1}, \quad H_2 = 1 + \frac{\zeta}{R_2} \quad (3.49)$$

A compact vector notation can be also used to represent equation (3.48)

$$\boldsymbol{\varepsilon} = \mathbf{D}\mathbf{U} \quad (3.50)$$

in which the meaning of the kinematic operator  $\mathbf{D}$  can be easily deduced from the corresponding extended relation (3.48). At this point, it is convenient to assume that the matrix  $\mathbf{D}$  is given by the product of two additional operators

$$\mathbf{D} = \mathbf{D}_\zeta \mathbf{D}_\Omega \quad (3.51)$$

where  $\mathbf{D}_\zeta$  collects all the terms depending on the coordinate  $\zeta$  and the derivatives with respect to  $\zeta$  itself. It assumes the following aspect

$$\mathbf{D}_\zeta = \begin{bmatrix} \frac{1}{H_1} & 0 & 0 & 0 & 0 & 0 & 0 & 0 & 0 \\ 0 & \frac{1}{H_2} & 0 & 0 & 0 & 0 & 0 & 0 & 0 \\ 0 & 0 & \frac{1}{H_1} & \frac{1}{H_2} & 0 & 0 & 0 & 0 & 0 \\ 0 & 0 & 0 & 0 & \frac{1}{H_1} & 0 & \frac{\partial}{\partial \zeta} & 0 & 0 \\ 0 & 0 & 0 & 0 & 0 & \frac{1}{H_2} & 0 & \frac{\partial}{\partial \zeta} & 0 \\ 0 & 0 & 0 & 0 & 0 & 0 & 0 & 0 & \frac{\partial}{\partial \zeta} \end{bmatrix} \quad (3.52)$$

The derivatives with respect to the principal coordinates  $\alpha_1, \alpha_2$ , as well as the terms related to the main curvatures, are included in the second matrix  $\mathbf{D}_\Omega$ , which can be obtained as the summation of three additional operators

$$\mathbf{D}_\Omega = \mathbf{D}_\Omega^{\alpha_1} + \mathbf{D}_\Omega^{\alpha_2} + \mathbf{D}_\Omega^{\alpha_3} \quad (3.53)$$

where the kinematic operators  $\mathbf{D}_\Omega^{\alpha_1}, \mathbf{D}_\Omega^{\alpha_2}, \mathbf{D}_\Omega^{\alpha_3}$  are defined below

$$\mathbf{D}_\Omega^{\alpha_1} = \begin{bmatrix} \frac{1}{A_1} \frac{\partial}{\partial \alpha_1} & \frac{1}{A_1 A_2} \frac{\partial A_2}{\partial \alpha_1} & -\frac{1}{A_1 A_2} \frac{\partial A_1}{\partial \alpha_2} & \frac{1}{A_2} \frac{\partial}{\partial \alpha_2} & -\frac{1}{R_1} & 0 & 1 & 0 & 0 \\ 0 & 0 & 0 & 0 & 0 & 0 & 0 & 0 & 0 \\ 0 & 0 & 0 & 0 & 0 & 0 & 0 & 0 & 0 \end{bmatrix}^T \quad (3.54)$$

$$\mathbf{D}_\Omega^{\alpha_2} = \begin{bmatrix} 0 & 0 & 0 & 0 & 0 & 0 & 0 & 0 & 0 \\ \frac{1}{A_1 A_2} \frac{\partial A_1}{\partial \alpha_2} & \frac{1}{A_2} \frac{\partial}{\partial \alpha_2} & \frac{1}{A_1} \frac{\partial}{\partial \alpha_1} & -\frac{1}{A_1 A_2} \frac{\partial A_2}{\partial \alpha_1} & 0 & -\frac{1}{R_2} & 0 & 1 & 0 \\ 0 & 0 & 0 & 0 & 0 & 0 & 0 & 0 & 0 \end{bmatrix}^T \quad (3.55)$$

$$\mathbf{D}_\Omega^{\alpha_3} = \begin{bmatrix} 0 & 0 & 0 & 0 & 0 & 0 & 0 & 0 & 0 \\ 0 & 0 & 0 & 0 & 0 & 0 & 0 & 0 & 0 \\ \frac{1}{R_1} & \frac{1}{R_2} & 0 & 0 & \frac{1}{A_1} \frac{\partial}{\partial \alpha_1} & \frac{1}{A_2} \frac{\partial}{\partial \alpha_2} & 0 & 0 & 1 \end{bmatrix}^T \quad (3.56)$$

The generalized strain components defined on the shell middle surface can be obtained from the kinematic equations (3.42)-(3.47) by inserting the definition of the displacement fields (3.22). Recalling that the thickness functions do not depend on  $\alpha_1, \alpha_2$ , the kinematic equations (3.42)-(3.47) become

$$\varepsilon_1 = \frac{1}{H_1} \sum_{\tau=0}^{N+1} \left( \frac{F_\tau^{\alpha_1}}{A_1} \frac{\partial u_1^{(\tau)}}{\partial \alpha_1} + \frac{F_\tau^{\alpha_2} u_2^{(\tau)}}{A_1 A_2} \frac{\partial A_1}{\partial \alpha_2} + \frac{F_\tau^{\alpha_3} u_3^{(\tau)}}{R_1} \right) \quad (3.57)$$

$$\varepsilon_2 = \frac{1}{H_2} \sum_{\tau=0}^{N+1} \left( \frac{F_\tau^{\alpha_2}}{A_2} \frac{\partial u_2^{(\tau)}}{\partial \alpha_2} + \frac{F_\tau^{\alpha_1} u_1^{(\tau)}}{A_1 A_2} \frac{\partial A_2}{\partial \alpha_1} + \frac{F_\tau^{\alpha_3} u_3^{(\tau)}}{R_2} \right) \quad (3.58)$$

$$\gamma_{12} = \frac{1}{H_1} \sum_{\tau=0}^{N+1} \left( \frac{F_\tau^{\alpha_2}}{A_1} \frac{\partial u_2^{(\tau)}}{\partial \alpha_1} - \frac{F_\tau^{\alpha_1} u_1^{(\tau)}}{A_1 A_2} \frac{\partial A_1}{\partial \alpha_2} \right) + \frac{1}{H_2} \sum_{\tau=0}^{N+1} \left( \frac{F_\tau^{\alpha_1}}{A_2} \frac{\partial u_1^{(\tau)}}{\partial \alpha_2} - \frac{F_\tau^{\alpha_2} u_2^{(\tau)}}{A_1 A_2} \frac{\partial A_2}{\partial \alpha_1} \right) \quad (3.59)$$

$$\gamma_{13} = \frac{1}{H_1} \sum_{\tau=0}^{N+1} \left( \frac{F_\tau^{\alpha_3}}{A_1} \frac{\partial u_3^{(\tau)}}{\partial \alpha_1} - \frac{F_\tau^{\alpha_1} u_1^{(\tau)}}{R_1} \right) + \sum_{\tau=0}^{N+1} \frac{\partial F_\tau^{\alpha_1}}{\partial \zeta} u_1^{(\tau)} \quad (3.60)$$

$$\gamma_{23} = \frac{1}{H_2} \sum_{\tau=0}^{N+1} \left( \frac{F_\tau^{\alpha_3}}{A_2} \frac{\partial u_3^{(\tau)}}{\partial \alpha_2} - \frac{F_\tau^{\alpha_2} u_2^{(\tau)}}{R_2} \right) + \sum_{\tau=0}^{N+1} \frac{\partial F_\tau^{\alpha_2}}{\partial \zeta} u_2^{(\tau)} \quad (3.61)$$

$$\varepsilon_3 = \sum_{\tau=0}^{N+1} \frac{\partial F_\tau^{\alpha_3}}{\partial \zeta} u_3^{(\tau)} \quad (3.62)$$

For the sake of conciseness, relations (3.57)-(3.62) can be written also in the following form

$$\varepsilon_1 = \frac{1}{H_1} \sum_{\tau=0}^{N+1} \left( F_\tau^{\alpha_1} \varepsilon_1^{(\tau)\alpha_1} + F_\tau^{\alpha_2} \varepsilon_1^{(\tau)\alpha_2} + F_\tau^{\alpha_3} \varepsilon_1^{(\tau)\alpha_3} \right) \quad (3.63)$$

$$\varepsilon_2 = \frac{1}{H_2} \sum_{\tau=0}^{N+1} \left( F_\tau^{\alpha_2} \varepsilon_2^{(\tau)\alpha_2} + F_\tau^{\alpha_1} \varepsilon_2^{(\tau)\alpha_1} + F_\tau^{\alpha_3} \varepsilon_2^{(\tau)\alpha_3} \right) \quad (3.64)$$

$$\gamma_{12} = \frac{1}{H_1} \sum_{\tau=0}^{N+1} \left( F_\tau^{\alpha_2} \gamma_1^{(\tau)\alpha_2} + F_\tau^{\alpha_1} \gamma_1^{(\tau)\alpha_1} \right) + \frac{1}{H_2} \sum_{\tau=0}^{N+1} \left( F_\tau^{\alpha_1} \gamma_2^{(\tau)\alpha_1} + F_\tau^{\alpha_2} \gamma_2^{(\tau)\alpha_2} \right) \quad (3.65)$$

$$\gamma_{13} = \frac{1}{H_1} \sum_{\tau=0}^{N+1} \left( F_\tau^{\alpha_3} \gamma_{13}^{(\tau)\alpha_3} + F_\tau^{\alpha_1} \gamma_{13}^{(\tau)\alpha_1} \right) + \sum_{\tau=0}^{N+1} \frac{\partial F_\tau^{\alpha_1}}{\partial \zeta} \omega_{13}^{(\tau)\alpha_1} \quad (3.66)$$

$$\gamma_{23} = \frac{1}{H_2} \sum_{\tau=0}^{N+1} \left( F_\tau^{\alpha_3} \gamma_{23}^{(\tau)\alpha_3} + F_\tau^{\alpha_2} \gamma_{23}^{(\tau)\alpha_2} \right) + \sum_{\tau=0}^{N+1} \frac{\partial F_\tau^{\alpha_2}}{\partial \zeta} \omega_{23}^{(\tau)\alpha_2} \quad (3.67)$$

$$\varepsilon_3 = \sum_{\tau=0}^{N+1} \frac{\partial F_\tau^{\alpha_3}}{\partial \zeta} \varepsilon_3^{(\tau)\alpha_3} \quad (3.68)$$

where the generalized strain components have been introduced for each order of kinematic expansion  $\tau$ . The quantities at issue can be collected in the corresponding vector  $\boldsymbol{\varepsilon}^{(\tau)\alpha_i} = \boldsymbol{\varepsilon}^{(\tau)\alpha_i}(\alpha_1, \alpha_2, t)$  defined below

$$\boldsymbol{\varepsilon}^{(\tau)\alpha_i}(\alpha_1, \alpha_2, t) = \left[ \varepsilon_1^{(\tau)\alpha_i} \quad \varepsilon_2^{(\tau)\alpha_i} \quad \gamma_1^{(\tau)\alpha_i} \quad \gamma_2^{(\tau)\alpha_i} \quad \gamma_{13}^{(\tau)\alpha_i} \quad \gamma_{23}^{(\tau)\alpha_i} \quad \omega_{13}^{(\tau)\alpha_i} \quad \omega_{23}^{(\tau)\alpha_i} \quad \varepsilon_3^{(\tau)\alpha_i} \right]^T \quad (3.69)$$

for  $\tau = 0, 1, 2, \dots, N, N+1$  and  $i = 1, 2, 3$ . The definitions of the generalized strain components (3.69) can be easily obtained by comparing relations (3.57)-(3.62) and (3.63)-(3.68)

$$\varepsilon_2^{(\tau)\alpha_1} = \frac{u_1^{(\tau)}}{A_1 A_2} \frac{\partial A_2}{\partial \alpha_1}, \quad \varepsilon_2^{(\tau)\alpha_2} = \frac{1}{A_2} \frac{\partial u_2^{(\tau)}}{\partial \alpha_2}, \quad \varepsilon_2^{(\tau)\alpha_3} = \frac{u_3^{(\tau)}}{R_2} \quad (3.70)$$

$$\varepsilon_2^{(\tau)\alpha_1} = \frac{u_1^{(\tau)}}{A_1 A_2} \frac{\partial A_2}{\partial \alpha_1}, \quad \varepsilon_2^{(\tau)\alpha_2} = \frac{1}{A_2} \frac{\partial u_2^{(\tau)}}{\partial \alpha_2}, \quad \varepsilon_2^{(\tau)\alpha_3} = \frac{u_3^{(\tau)}}{R_2} \quad (3.71)$$

$$\gamma_1^{(\tau)\alpha_1} = -\frac{u_1^{(\tau)}}{A_1 A_2} \frac{\partial A_1}{\partial \alpha_2}, \quad \gamma_1^{(\tau)\alpha_2} = \frac{1}{A_1} \frac{\partial u_2^{(\tau)}}{\partial \alpha_1}, \quad \gamma_1^{(\tau)\alpha_3} = 0 \quad (3.72)$$

$$\gamma_2^{(\tau)\alpha_1} = \frac{1}{A_2} \frac{\partial u_1^{(\tau)}}{\partial \alpha_2}, \quad \gamma_2^{(\tau)\alpha_2} = -\frac{u_2^{(\tau)}}{A_1 A_2} \frac{\partial A_2}{\partial \alpha_1}, \quad \gamma_2^{(\tau)\alpha_3} = 0 \quad (3.73)$$

$$\gamma_{13}^{(\tau)\alpha_1} = -\frac{u_1^{(\tau)}}{R_1}, \quad \gamma_{13}^{(\tau)\alpha_2} = 0, \quad \gamma_{13}^{(\tau)\alpha_3} = \frac{1}{A_1} \frac{\partial u_3^{(\tau)}}{\partial \alpha_1} \quad (3.74)$$

$$\gamma_{23}^{(\tau)\alpha_1} = 0, \quad \gamma_{23}^{(\tau)\alpha_2} = -\frac{u_2^{(\tau)}}{R_2}, \quad \gamma_{23}^{(\tau)\alpha_3} = \frac{1}{A_2} \frac{\partial u_3^{(\tau)}}{\partial \alpha_2} \quad (3.75)$$

$$\omega_{13}^{(\tau)\alpha_1} = u_1^{(\tau)}, \quad \omega_{13}^{(\tau)\alpha_2} = 0, \quad \omega_{13}^{(\tau)\alpha_3} = 0 \quad (3.76)$$

$$\omega_{23}^{(\tau)\alpha_1} = 0, \quad \omega_{23}^{(\tau)\alpha_2} = u_2^{(\tau)}, \quad \omega_{23}^{(\tau)\alpha_3} = 0 \quad (3.77)$$

$$\varepsilon_3^{(\tau)\alpha_1} = 0, \quad \varepsilon_3^{(\tau)\alpha_2} = 0, \quad \varepsilon_3^{(\tau)\alpha_3} = u_3^{(\tau)} \quad (3.78)$$

It should be noted that the recursive features of this approach facilitate the implementation of this higher-order model. This aspect is even more evident if the kinematic equations (3.63)-(3.68) are written as follows

$$\varepsilon_1 = \frac{1}{H_1} \sum_{\tau=0}^{N+1} \sum_{i=1}^3 F_{\tau}^{\alpha_i} \varepsilon_1^{(\tau)\alpha_i} \quad (3.79)$$

$$\varepsilon_2 = \frac{1}{H_2} \sum_{\tau=0}^{N+1} \sum_{i=1}^3 F_{\tau}^{\alpha_i} \varepsilon_2^{(\tau)\alpha_i} \quad (3.80)$$

$$\gamma_{12} = \frac{1}{H_1} \sum_{\tau=0}^{N+1} \sum_{i=1}^3 F_{\tau}^{\alpha_i} \gamma_1^{(\tau)\alpha_i} + \frac{1}{H_2} \sum_{\tau=0}^{N+1} \sum_{i=1}^3 F_{\tau}^{\alpha_i} \gamma_2^{(\tau)\alpha_i} \quad (3.81)$$

$$\gamma_{13} = \frac{1}{H_1} \sum_{\tau=0}^{N+1} \sum_{i=1}^3 F_{\tau}^{\alpha_i} \gamma_{13}^{(\tau)\alpha_i} + \sum_{\tau=0}^{N+1} \sum_{i=1}^3 \frac{\partial F_{\tau}^{\alpha_i}}{\partial \zeta} \omega_{13}^{(\tau)\alpha_i} \quad (3.82)$$

$$\gamma_{23} = \frac{1}{H_2} \sum_{\tau=0}^{N+1} \sum_{i=1}^3 F_{\tau}^{\alpha_i} \gamma_{23}^{(\tau)\alpha_i} + \sum_{\tau=0}^{N+1} \sum_{i=1}^3 \frac{\partial F_{\tau}^{\alpha_i}}{\partial \zeta} \omega_{23}^{(\tau)\alpha_i} \quad (3.83)$$

$$\varepsilon_3 = \sum_{\tau=0}^{N+1} \sum_{i=1}^3 \frac{\partial F_{\tau}^{\alpha_i}}{\partial \zeta} \varepsilon_3^{(\tau)\alpha_i} \quad (3.84)$$

In compact matrix form, relations (3.79)-(3.84) assume the following aspect

$$\boldsymbol{\varepsilon} = \sum_{\tau=0}^{N+1} \sum_{i=1}^3 \mathbf{Z}^{(\tau)\alpha_i} \boldsymbol{\varepsilon}^{(\tau)\alpha_i} \quad (3.85)$$

where the matrix  $\mathbf{Z}^{(\tau)\alpha_i}$ , for  $\tau = 0, 1, 2, \dots, N, N+1$  and  $i = 1, 2, 3$ , is given by

$$\mathbf{Z}^{(\tau)\alpha_i} = \begin{bmatrix} \frac{F_{\tau}^{\alpha_i}}{H_1} & 0 & 0 & 0 & 0 & 0 & 0 & 0 & 0 \\ 0 & \frac{F_{\tau}^{\alpha_i}}{H_2} & 0 & 0 & 0 & 0 & 0 & 0 & 0 \\ 0 & 0 & \frac{F_{\tau}^{\alpha_i}}{H_1} & \frac{F_{\tau}^{\alpha_i}}{H_2} & 0 & 0 & 0 & 0 & 0 \\ 0 & 0 & 0 & 0 & \frac{F_{\tau}^{\alpha_i}}{H_1} & 0 & \frac{\partial F_{\tau}^{\alpha_i}}{\partial \zeta} & 0 & 0 \\ 0 & 0 & 0 & 0 & 0 & \frac{F_{\tau}^{\alpha_i}}{H_2} & 0 & \frac{\partial F_{\tau}^{\alpha_i}}{\partial \zeta} & 0 \\ 0 & 0 & 0 & 0 & 0 & 0 & 0 & 0 & \frac{\partial F_{\tau}^{\alpha_i}}{\partial \zeta} \end{bmatrix} \quad (3.86)$$

Relation (3.85) can be obtained by performing the same procedure in compact matrix form as follows

$$\begin{aligned}
 \boldsymbol{\varepsilon} &= \sum_{\tau=0}^{N+1} \mathbf{D}_{\zeta} \left( \mathbf{D}_{\Omega}^{\alpha_1} + \mathbf{D}_{\Omega}^{\alpha_2} + \mathbf{D}_{\Omega}^{\alpha_3} \right) \mathbf{F}_{\tau} \mathbf{u}^{(\tau)} \\
 &= \sum_{\tau=0}^{N+1} \mathbf{D}_{\zeta} \left( F_{\tau}^{\alpha_1} \mathbf{D}_{\Omega}^{\alpha_1} + F_{\tau}^{\alpha_2} \mathbf{D}_{\Omega}^{\alpha_2} + F_{\tau}^{\alpha_3} \mathbf{D}_{\Omega}^{\alpha_3} \right) \mathbf{u}^{(\tau)} \\
 &= \sum_{\tau=0}^{N+1} \left( \mathbf{D}_{\zeta} F_{\tau}^{\alpha_1} \mathbf{D}_{\Omega}^{\alpha_1} + \mathbf{D}_{\zeta} F_{\tau}^{\alpha_2} \mathbf{D}_{\Omega}^{\alpha_2} + \mathbf{D}_{\zeta} F_{\tau}^{\alpha_3} \mathbf{D}_{\Omega}^{\alpha_3} \right) \mathbf{u}^{(\tau)} \quad (3.87) \\
 &= \sum_{\tau=0}^{N+1} \sum_{i=1}^3 \mathbf{Z}^{(\tau)\alpha_i} \mathbf{D}_{\Omega}^{\alpha_i} \mathbf{u}^{(\tau)} \\
 &= \sum_{\tau=0}^{N+1} \sum_{i=1}^3 \mathbf{Z}^{(\tau)\alpha_i} \boldsymbol{\varepsilon}^{(\tau)\alpha_i}
 \end{aligned}$$

where the compact definition of the generalized strains is also established. One gets

$$\boldsymbol{\varepsilon}^{(\tau)\alpha_i} = \mathbf{D}_{\Omega}^{\alpha_i} \mathbf{u}^{(\tau)} \quad (3.88)$$

for  $\tau = 0, 1, 2, \dots, N, N+1$  and  $i = 1, 2, 3$ . This equation relates the generalized strains in hand with the generalized displacements. These quantities are both defined on the shell middle surface.

The definition of the generalized strain components (3.88) can be written also for the weak formulation. In fact, by recalling the interpolation (3.37), the following relation is achieved

$$\boldsymbol{\varepsilon}^{(\tau)\alpha_i} = \mathbf{D}_{\Omega}^{\alpha_i} \mathbf{N}^T \bar{\mathbf{u}}^{(\tau)} \quad (3.89)$$

for  $\tau = 0, 1, 2, \dots, N, N+1$  and  $i = 1, 2, 3$ . Thus, the generalized strains are directly related to the nodal displacements (3.36). In order to facilitate the treatise, it is convenient to write the kinematic operators (3.54)-(3.56) as follows

$$\mathbf{D}_{\Omega}^{\alpha_1} = \begin{bmatrix} \bar{\mathbf{D}}_{\Omega}^{\alpha_1} & \mathbf{0} & \mathbf{0} \end{bmatrix} \quad (3.90)$$

$$\mathbf{D}_{\Omega}^{\alpha_2} = \begin{bmatrix} \mathbf{0} & \bar{\mathbf{D}}_{\Omega}^{\alpha_2} & \mathbf{0} \end{bmatrix} \quad (3.91)$$

$$\mathbf{D}_{\Omega}^{\alpha_3} = \begin{bmatrix} \mathbf{0} & \mathbf{0} & \bar{\mathbf{D}}_{\Omega}^{\alpha_3} \end{bmatrix} \quad (3.92)$$

in which each component is a column vector of size  $9 \times 1$ . In particular, the following definitions are obtained by comparing (3.54)-(3.56) with (3.90)-(3.92)

$$\bar{\mathbf{D}}_{\Omega}^{\alpha_1} = \begin{bmatrix} \frac{1}{A_1} \frac{\partial}{\partial \alpha_1} & \frac{1}{A_1 A_2} \frac{\partial A_2}{\partial \alpha_1} & -\frac{1}{A_1 A_2} \frac{\partial A_1}{\partial \alpha_2} & \frac{1}{A_2} \frac{\partial}{\partial \alpha_2} & -\frac{1}{R_1} & 0 & 1 & 0 & 0 \end{bmatrix}^T \quad (3.93)$$

$$\bar{\mathbf{D}}_{\Omega}^{\alpha_2} = \begin{bmatrix} \frac{1}{A_1 A_2} \frac{\partial A_1}{\partial \alpha_2} & \frac{1}{A_2} \frac{\partial}{\partial \alpha_2} & \frac{1}{A_1} \frac{\partial}{\partial \alpha_1} & -\frac{1}{A_1 A_2} \frac{\partial A_2}{\partial \alpha_1} & 0 & -\frac{1}{R_2} & 0 & 1 & 0 \end{bmatrix}^T \quad (3.94)$$

$$\bar{\mathbf{D}}_{\Omega}^{\alpha_3} = \begin{bmatrix} \frac{1}{R_1} & \frac{1}{R_2} & 0 & 0 & \frac{1}{A_1} \frac{\partial}{\partial \alpha_1} & \frac{1}{A_2} \frac{\partial}{\partial \alpha_2} & 0 & 0 & 1 \end{bmatrix}^T \quad (3.95)$$

Let us consider at this point equation (3.89). Having in mind definitions (3.93)-(3.95), one gets

$$\boldsymbol{\varepsilon}^{(\tau)\alpha_1} = \bar{\mathbf{D}}_{\Omega}^{\alpha_1} \bar{\mathbf{N}}^T \bar{\mathbf{u}}^{(\tau)} = \mathbf{B}^{\alpha_1} \bar{\mathbf{u}}^{(\tau)} \quad (3.96)$$

$$\boldsymbol{\varepsilon}^{(\tau)\alpha_2} = \bar{\mathbf{D}}_{\Omega}^{\alpha_2} \bar{\mathbf{N}}^T \bar{\mathbf{u}}^{(\tau)} = \mathbf{B}^{\alpha_2} \bar{\mathbf{u}}^{(\tau)} \quad (3.97)$$

$$\boldsymbol{\varepsilon}^{(\tau)\alpha_3} = \bar{\mathbf{D}}_{\Omega}^{\alpha_3} \bar{\mathbf{N}}^T \bar{\mathbf{u}}^{(\tau)} = \mathbf{B}^{\alpha_3} \bar{\mathbf{u}}^{(\tau)} \quad (3.98)$$

for  $\tau = 0, 1, 2, \dots, N, N+1$ . In compact notation, it is possible to write also the following expression

$$\boldsymbol{\varepsilon}^{(\tau)\alpha_i} = \mathbf{B}^{\alpha_i} \bar{\mathbf{u}}^{(\tau)} \quad (3.99)$$

for  $\tau = 0, 1, 2, \dots, N, N+1$  and  $i = 1, 2, 3$ . The differential operators  $\mathbf{B}^{\alpha_i}$ , whose size is  $9 \times (I_N I_M)$ , assume the aspect shown below

$$\mathbf{B}^{\alpha_1} = \begin{bmatrix} \frac{1}{A_1} \mathbf{l}_{\alpha_2} \otimes_k \mathbf{l}_{\alpha_1}^{(1)} \\ \frac{1}{A_1 A_2} \frac{\partial A_2}{\partial \alpha_1} \mathbf{l}_{\alpha_2} \otimes_k \mathbf{l}_{\alpha_1} \\ -\frac{1}{A_1 A_2} \frac{\partial A_1}{\partial \alpha_2} \mathbf{l}_{\alpha_2} \otimes_k \mathbf{l}_{\alpha_1} \\ \frac{1}{A_2} \mathbf{l}_{\alpha_2}^{(1)} \otimes_k \mathbf{l}_{\alpha_1} \\ -\frac{1}{R_1} \mathbf{l}_{\alpha_2} \otimes_k \mathbf{l}_{\alpha_1} \\ \mathbf{0} \\ \mathbf{l}_{\alpha_2} \otimes_k \mathbf{l}_{\alpha_1} \\ \mathbf{0} \\ \mathbf{0} \end{bmatrix}, \quad \mathbf{B}^{\alpha_2} = \begin{bmatrix} \frac{1}{A_1 A_2} \frac{\partial A_1}{\partial \alpha_2} \mathbf{l}_{\alpha_2} \otimes_k \mathbf{l}_{\alpha_1} \\ \frac{1}{A_2} \mathbf{l}_{\alpha_2}^{(1)} \otimes_k \mathbf{l}_{\alpha_1} \\ \frac{1}{A_1} \mathbf{l}_{\alpha_2} \otimes_k \mathbf{l}_{\alpha_1}^{(1)} \\ -\frac{1}{A_1 A_2} \frac{\partial A_2}{\partial \alpha_1} \mathbf{l}_{\alpha_2} \otimes_k \mathbf{l}_{\alpha_1} \\ \mathbf{0} \\ -\frac{1}{R_2} \mathbf{l}_{\alpha_2} \otimes_k \mathbf{l}_{\alpha_1} \\ \mathbf{0} \\ \mathbf{l}_{\alpha_2} \otimes_k \mathbf{l}_{\alpha_1} \\ \mathbf{0} \end{bmatrix}, \quad \mathbf{B}^{\alpha_3} = \begin{bmatrix} \frac{1}{R_1} \mathbf{l}_{\alpha_2} \otimes_k \mathbf{l}_{\alpha_1} \\ \frac{1}{R_2} \mathbf{l}_{\alpha_2} \otimes_k \mathbf{l}_{\alpha_1} \\ \mathbf{0} \\ \mathbf{0} \\ \frac{1}{A_1} \mathbf{l}_{\alpha_2} \otimes_k \mathbf{l}_{\alpha_1}^{(1)} \\ \frac{1}{A_2} \mathbf{l}_{\alpha_2}^{(1)} \otimes_k \mathbf{l}_{\alpha_1} \\ \mathbf{0} \\ \mathbf{0} \\ \mathbf{l}_{\alpha_2} \otimes_k \mathbf{l}_{\alpha_1} \end{bmatrix} \quad (3.100)$$

in which  $\mathbf{l}_{\alpha_1}^{(1)}, \mathbf{l}_{\alpha_2}^{(1)}$  denote the vectors that collect the first-order derivatives of the interpolating functions (3.39)-(3.40) along  $\alpha_1, \alpha_2$  with respect to the same coordinates. These vectors are given by

$$\mathbf{l}_{\alpha_1}^{(1)} = \left[ l_1^{(1)}(\alpha_1) \quad \dots \quad l_f^{(1)}(\alpha_1) \quad \dots \quad l_N^{(1)}(\alpha_1) \right] \quad (3.101)$$

$$\mathbf{l}_{\alpha_2}^{(1)} = \left[ l_1^{(1)}(\alpha_2) \quad \cdots \quad l_g^{(1)}(\alpha_2) \quad \cdots \quad l_{I_M}^{(1)}(\alpha_2) \right] \quad (3.102)$$

where the following derivatives are required

$$l_f^{(1)}(\alpha_1) = \frac{\partial l_f(\alpha_1)}{\partial \alpha_1} \quad (3.103)$$

$$l_g^{(1)}(\alpha_2) = \frac{\partial l_g(\alpha_2)}{\partial \alpha_2} \quad (3.104)$$

For the sake of completeness, the operators  $\mathbf{B}^{\alpha_i}$ , for  $\tau = 0, 1, 2, \dots, N, N+1$  and  $i = 1, 2, 3$ , can be written also in extended notation

$$\mathbf{B}^{\alpha_1} = \begin{bmatrix} \frac{1}{A_1} l_1(\alpha_2) [l_1^{(0)}(\alpha_1) \quad \cdots \quad l_{I_N}^{(0)}(\alpha_1)] & \frac{1}{A_1} l_2(\alpha_2) [l_1^{(0)}(\alpha_1) \quad \cdots \quad l_{I_N}^{(0)}(\alpha_1)] & \cdots & \frac{1}{A_1} l_{I_M}(\alpha_2) [l_1^{(0)}(\alpha_1) \quad \cdots \quad l_{I_N}^{(0)}(\alpha_1)] \\ \frac{1}{A_1 A_2} \frac{\partial A_2}{\partial \alpha_1} l_1(\alpha_2) [l_1(\alpha_1) \quad \cdots \quad l_{I_N}(\alpha_1)] & \frac{1}{A_1 A_2} \frac{\partial A_2}{\partial \alpha_1} l_2(\alpha_2) [l_1(\alpha_1) \quad \cdots \quad l_{I_N}(\alpha_1)] & \cdots & \frac{1}{A_1 A_2} \frac{\partial A_2}{\partial \alpha_1} l_{I_M}(\alpha_2) [l_1(\alpha_1) \quad \cdots \quad l_{I_N}(\alpha_1)] \\ -\frac{1}{A_1 A_2} \frac{\partial A_1}{\partial \alpha_2} l_1(\alpha_2) [l_1(\alpha_1) \quad \cdots \quad l_{I_N}(\alpha_1)] & -\frac{1}{A_1 A_2} \frac{\partial A_1}{\partial \alpha_2} l_2(\alpha_2) [l_1(\alpha_1) \quad \cdots \quad l_{I_N}(\alpha_1)] & \cdots & -\frac{1}{A_1 A_2} \frac{\partial A_1}{\partial \alpha_2} l_{I_M}(\alpha_2) [l_1(\alpha_1) \quad \cdots \quad l_{I_N}(\alpha_1)] \\ \frac{1}{A_2} l_1^{(0)}(\alpha_2) [l_1(\alpha_1) \quad \cdots \quad l_{I_N}(\alpha_1)] & \frac{1}{A_2} l_2^{(0)}(\alpha_2) [l_1(\alpha_1) \quad \cdots \quad l_{I_N}(\alpha_1)] & \cdots & \frac{1}{A_2} l_{I_M}^{(0)}(\alpha_2) [l_1(\alpha_1) \quad \cdots \quad l_{I_N}(\alpha_1)] \\ -\frac{1}{R_1} l_1(\alpha_2) [l_1(\alpha_1) \quad \cdots \quad l_{I_N}(\alpha_1)] & -\frac{1}{R_1} l_2(\alpha_2) [l_1(\alpha_1) \quad \cdots \quad l_{I_N}(\alpha_1)] & \cdots & -\frac{1}{R_1} l_{I_M}(\alpha_2) [l_1(\alpha_1) \quad \cdots \quad l_{I_N}(\alpha_1)] \\ \mathbf{0} & & & \\ l_1(\alpha_2) [l_1(\alpha_1) \quad \cdots \quad l_{I_N}(\alpha_1)] & l_2(\alpha_2) [l_1(\alpha_1) \quad \cdots \quad l_{I_N}(\alpha_1)] & \cdots & l_{I_M}(\alpha_2) [l_1(\alpha_1) \quad \cdots \quad l_{I_N}(\alpha_1)] \\ \mathbf{0} & & & \\ \mathbf{0} & & & \end{bmatrix}$$

$$\mathbf{B}^{\alpha_2} = \begin{bmatrix} \frac{1}{A_1 A_2} \frac{\partial A_1}{\partial \alpha_2} l_1(\alpha_2) [l_1(\alpha_1) \quad \cdots \quad l_{I_N}(\alpha_1)] & \frac{1}{A_1 A_2} \frac{\partial A_1}{\partial \alpha_2} l_2(\alpha_2) [l_1(\alpha_1) \quad \cdots \quad l_{I_N}(\alpha_1)] & \cdots & \frac{1}{A_1 A_2} \frac{\partial A_1}{\partial \alpha_2} l_{I_M}(\alpha_2) [l_1(\alpha_1) \quad \cdots \quad l_{I_N}(\alpha_1)] \\ \frac{1}{A_2} l_1^{(0)}(\alpha_2) [l_1(\alpha_1) \quad \cdots \quad l_{I_N}(\alpha_1)] & \frac{1}{A_2} l_2^{(0)}(\alpha_2) [l_1(\alpha_1) \quad \cdots \quad l_{I_N}(\alpha_1)] & \cdots & \frac{1}{A_2} l_{I_M}^{(0)}(\alpha_2) [l_1(\alpha_1) \quad \cdots \quad l_{I_N}(\alpha_1)] \\ \frac{1}{A_1} l_1(\alpha_2) [l_1^{(0)}(\alpha_1) \quad \cdots \quad l_{I_N}^{(0)}(\alpha_1)] & \frac{1}{A_1} l_2(\alpha_2) [l_1^{(0)}(\alpha_1) \quad \cdots \quad l_{I_N}^{(0)}(\alpha_1)] & \cdots & \frac{1}{A_1} l_{I_M}(\alpha_2) [l_1^{(0)}(\alpha_1) \quad \cdots \quad l_{I_N}^{(0)}(\alpha_1)] \\ -\frac{1}{A_1 A_2} \frac{\partial A_2}{\partial \alpha_1} l_1(\alpha_2) [l_1(\alpha_1) \quad \cdots \quad l_{I_N}(\alpha_1)] & -\frac{1}{A_1 A_2} \frac{\partial A_2}{\partial \alpha_1} l_2(\alpha_2) [l_1(\alpha_1) \quad \cdots \quad l_{I_N}(\alpha_1)] & \cdots & -\frac{1}{A_1 A_2} \frac{\partial A_2}{\partial \alpha_1} l_{I_M}(\alpha_2) [l_1(\alpha_1) \quad \cdots \quad l_{I_N}(\alpha_1)] \\ \mathbf{0} & & & \\ -\frac{1}{R_2} l_1(\alpha_2) [l_1(\alpha_1) \quad \cdots \quad l_{I_N}(\alpha_1)] & -\frac{1}{R_2} l_2(\alpha_2) [l_1(\alpha_1) \quad \cdots \quad l_{I_N}(\alpha_1)] & \cdots & -\frac{1}{R_2} l_{I_M}(\alpha_2) [l_1(\alpha_1) \quad \cdots \quad l_{I_N}(\alpha_1)] \\ \mathbf{0} & & & \\ l_1(\alpha_2) [l_1(\alpha_1) \quad \cdots \quad l_{I_N}(\alpha_1)] & l_2(\alpha_2) [l_1(\alpha_1) \quad \cdots \quad l_{I_N}(\alpha_1)] & \cdots & l_{I_M}(\alpha_2) [l_1(\alpha_1) \quad \cdots \quad l_{I_N}(\alpha_1)] \\ \mathbf{0} & & & \end{bmatrix}$$

$$\mathbf{B}^{\alpha_2} = \begin{bmatrix} \frac{1}{R_1} l_1(\alpha_2) [l_1(\alpha_1) \cdots l_{I_N}(\alpha_1)] & \frac{1}{R_1} l_2(\alpha_2) [l_1(\alpha_1) \cdots l_{I_N}(\alpha_1)] & \cdots & \frac{1}{R_1} l_{I_M}(\alpha_2) [l_1(\alpha_1) \cdots l_{I_N}(\alpha_1)] \\ \frac{1}{R_2} l_1(\alpha_2) [l_1(\alpha_1) \cdots l_{I_N}(\alpha_1)] & \frac{1}{R_2} l_2(\alpha_2) [l_1(\alpha_1) \cdots l_{I_N}(\alpha_1)] & \cdots & \frac{1}{R_2} l_{I_M}(\alpha_2) [l_1(\alpha_1) \cdots l_{I_N}(\alpha_1)] \\ & \mathbf{0} & & \\ & \mathbf{0} & & \\ \frac{1}{A_1} l_1(\alpha_2) [l_1^{(1)}(\alpha_1) \cdots l_{I_N}^{(1)}(\alpha_1)] & \frac{1}{A_1} l_2(\alpha_2) [l_1^{(1)}(\alpha_1) \cdots l_{I_N}^{(1)}(\alpha_1)] & \cdots & \frac{1}{A_1} l_{I_M}(\alpha_2) [l_1^{(1)}(\alpha_1) \cdots l_{I_N}^{(1)}(\alpha_1)] \\ \frac{1}{A_2} l_1^{(1)}(\alpha_2) [l_1(\alpha_1) \cdots l_{I_N}(\alpha_1)] & \frac{1}{A_2} l_2^{(1)}(\alpha_2) [l_1(\alpha_1) \cdots l_{I_N}(\alpha_1)] & \cdots & \frac{1}{A_2} l_{I_M}^{(1)}(\alpha_2) [l_1(\alpha_1) \cdots l_{I_N}(\alpha_1)] \\ & \mathbf{0} & & \\ & \mathbf{0} & & \\ l_1(\alpha_2) [l_1(\alpha_1) \cdots l_{I_N}(\alpha_1)] & l_2(\alpha_2) [l_1(\alpha_1) \cdots l_{I_N}(\alpha_1)] & \cdots & l_{I_M}(\alpha_2) [l_1(\alpha_1) \cdots l_{I_N}(\alpha_1)] \end{bmatrix} \quad (3.105)$$

### 3.1.5 CONSTITUTIVE EQUATIONS

The importance of the constitutive equations has been already highlighted in the previous sections, in which some notes concerning the three-dimensional theory of elasticity have been illustrated.

This section aims to investigate the mechanical behavior of shells made of composite materials. It is well-known that many researchers focused their efforts on the analysis of composite materials to improve the structural response. By employing these materials, in fact, it is possible to obtain higher levels of stiffness and strength, without increasing the structural weight. Analogously, considerable advances have been achieved in terms of thermal properties and fatigue life.

Therefore, it is easy to see a great use of composite materials in many engineering fields that require lighter and more efficient structural elements. For instance, these progresses involve the analysis and manufacturing of aircrafts, aerospace components, as well as sails and boat hulls.

#### 3.1.5.1 Composite materials

As highlighted above, it is possible to achieve enhanced mechanical properties with respect to the ones that characterize conventional materials by using composite materials. In general, composite materials are obtained by combining two or more constituents at different levels,

such as nano-, micro-, and macro-scale. Usually, the aim of composite materials is to improve the mechanical property of basis constituent, called matrix, by inserting different kind of reinforcing phases. Composite materials can be categorized as follows:

- *fibrous composites*, which consist consisting long fibers of a stronger material immersed in a matrix made of another material.
- *granular composites*, which consist of particles of a stronger material immersed in a matrix made of another material.
- *laminated composites*, which consist of several layers made of different materials, including composites of the first two groups.

From the microscopic point of view, composite materials are intrinsically heterogeneous. Nevertheless, from the macroscopic point of view they can be considered as homogeneous, since peculiar homogenization techniques are introduced to evaluate the overall mechanical properties of the composite.

#### *3.1.5.1.1 Fibrous composites*

Let us consider a fiber-reinforced composite. The matrix holds together the various fibers and protects them from the environmental conditions, whereas the fibers give strength and stiffness to the composite. The load transfer is originated from the shear stresses that arise between the matrix and the fibers. These fibers can be placed within the matrix according to specific oriented paths. Thus, the composite is characterized by mechanical properties that depend on the orientation of the fibers. If  $O'\alpha_1\alpha_2\zeta$  denotes the local reference system of any shell element, the fibers can be oriented of a generic angle  $\theta$  with respect to these coordinate system, as depicted in Figure 3.5. Consequently, the material reference system  $O'\hat{\alpha}_1\hat{\alpha}_2\hat{\zeta}$  must be introduced.

A fiber-reinforced composite, in which the fibers are unidirectional as shown in Figure 3.5, can be modeled as an orthotropic medium with two planes of material symmetry, which are parallel and transverse to the directions of the fibers themselves, respectively. The material reference system is placed on the middle surface of the composite.

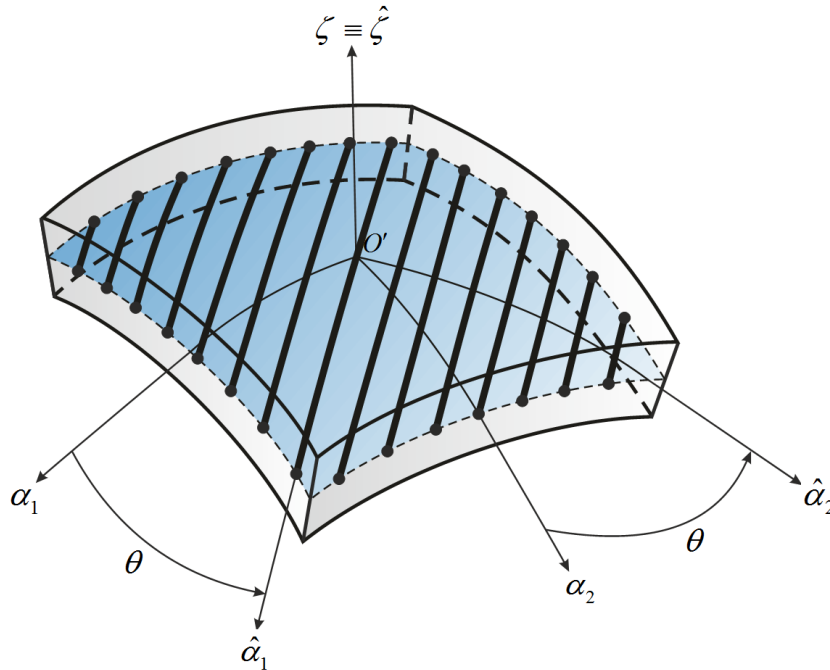


**Figure 3.5** – Material reference system of a fibrous composite with a generic orientation  $\theta$  of the fibers.

In particular, axis  $\hat{\alpha}_1$  is chosen parallel to the fiber direction, axis  $\hat{\alpha}_2$  is orthogonal to the first one and transverse to the fiber direction, whereas axis  $\zeta \equiv \hat{\zeta}$  is normal to the parametric lines of the middle surface. These composites have the maximum strength along the fiber direction, but they show a weak mechanical behavior along the transversal fiber direction.

The overall mechanical properties of a fiber-reinforced composite can be obtained either by a theoretical approach or by appropriate laboratory tests. As far as the theoretical models are concerned, several homogenization techniques can be used. These theories are based on the following hypotheses:

- The composite is linearly elastic from the macroscopic point of view.
- Residual stresses in a stress-free state are not allowed.
- Both the matrix and the reinforcing fibers are linearly elastic, homogeneous and without voids or micro cracks.
- The matrix and the fibers, which are aligned and regularly placed in the matrix, are perfectly bonded together.

In general, reinforcing fibers are assumed to be transversely isotropic, thus five independent elastic constants are required. Their mechanical properties can be expressed as a function of the engineering constants. In particular, the Young's moduli  $E_1^f$ ,  $E_2^f = E_3^f$ , the

shear moduli  $G_{12}^f = G_{13}^f$ ,  $G_{23}^f$ , and the Poisson's ratios  $\nu_{12}^f = \nu_{13}^f$ ,  $\nu_{23}^f$  are required. The other constants can be evaluated by means of relations (3.12). It should be noted that the superscript “ $f$ ” stands for fibers. On the other hand, the matrix can be considered isotropic and its properties are given by the Young's modulus  $E^m$ , the shear modulus  $G^m$ , and the Poisson's ratio  $\nu^m$ , in which the superscript “ $m$ ” stands for matrix. For the sake of completeness, it should be recalled that the shear modulus for an isotropic medium can be computed through expression (3.17).

The rule of mixture represents the easiest and most classical manner approach to evaluate the overall mechanical properties of these composites. The volume fractions of the fibers  $V_f$  and of the matrix  $V_m$  are required for this purpose

$$V_f = \frac{v_f}{v_c}, \quad V_m = \frac{v_m}{v_c} \quad (3.106)$$

where  $v_f$ ,  $v_m$ ,  $v_c$  denote the overall volume of the fibers, of the matrix and of the composite, respectively. The following relation is introduced to relate quantities in (3.106)

$$V_f + V_m = 1 \quad (3.107)$$

At this point, it is possible to evaluate the mechanical properties of the fibrous composite in terms of engineering constants

$$E_1 = E_1^f V_f + E^m V_m \quad (3.108)$$

$$E_2 = E_3 = \frac{E^m}{1 - V_f (1 - E^m / E_2^f)} \quad (3.109)$$

$$G_{12} = G_{13} = \frac{G^m}{1 - V_f (1 - G^m / G_{12}^f)} \quad (3.110)$$

$$G_{23} = \frac{G^m}{1 - V_f (1 - G^m / G_{23}^f)} \quad (3.111)$$

$$\nu_{12} = \nu_{13} = \nu_{12}^f V_f + \nu^m V_m \quad (3.112)$$

$$\nu_{23} = \frac{E_2}{2G_{23}} - 1 \quad (3.113)$$

It can be noted that five independent constants are needed to characterize the mechanical behavior of the composite, if this theoretical approach is employed. More accurate and

complex approaches could be used for the same purpose as highlighted in [209]. Finally, the density of the composite is given by

$$\rho = \rho^f V_f + \rho^m V_m \quad (3.114)$$

in which  $\rho^f, \rho^m$  denote respectively the density of the fiber and of the matrix.

At this point, it could be also specified that the orientation  $\theta$  of the fibers can be defined by some functions to describe curvilinear paths. Consequently, one gets  $\theta = \theta(\alpha_1, \alpha_2)$ . This idea is known in the literature as Variable Angle Tow (VAT) [176-191], as specified in the introduction.

In general, when an arbitrary orientation is chosen, the constitutive laws (3.8) must be written in the geometric reference system. Thus, a transformation of the elastic coefficients is required. Let us consider an orthotropic material whose fiber orientation is given by  $\theta$ . The generalized Hooke law in the material reference system assumes the following aspect

$$\begin{bmatrix} \hat{\sigma}_1 \\ \hat{\sigma}_2 \\ \hat{\tau}_{12} \\ \hat{\tau}_{13} \\ \hat{\tau}_{23} \\ \hat{\sigma}_3 \end{bmatrix} = \begin{bmatrix} C_{11} & C_{12} & 0 & 0 & 0 & C_{13} \\ C_{12} & C_{22} & 0 & 0 & 0 & C_{23} \\ 0 & 0 & C_{66} & 0 & 0 & 0 \\ 0 & 0 & 0 & C_{44} & 0 & 0 \\ 0 & 0 & 0 & 0 & C_{55} & 0 \\ C_{13} & C_{23} & 0 & 0 & 0 & C_{33} \end{bmatrix} \begin{bmatrix} \hat{\epsilon}_1 \\ \hat{\epsilon}_2 \\ \hat{\gamma}_{12} \\ \hat{\gamma}_{13} \\ \hat{\gamma}_{23} \\ \hat{\epsilon}_3 \end{bmatrix} \quad (3.115)$$

In compact notation, one gets

$$\hat{\boldsymbol{\sigma}} = \mathbf{C} \hat{\boldsymbol{\epsilon}} \quad (3.116)$$

where  $\hat{\boldsymbol{\sigma}}, \hat{\boldsymbol{\epsilon}}$  collect the stress and strain components defined in the material reference system  $O' \hat{\alpha}_1 \hat{\alpha}_2 \zeta$ . On the other hand,  $\boldsymbol{\sigma}, \boldsymbol{\epsilon}$  represent the same vector [evaluated in the geometric reference system  $O' \alpha_1 \alpha_2 \zeta$ , as depicted in Figure 3.4. The constitutive relations in this reference system are given by

$$\boldsymbol{\sigma} = \bar{\mathbf{C}} \boldsymbol{\epsilon} \quad (3.117)$$

in which  $\bar{\mathbf{C}}$  is the constitutive. The following transformations allows to compute its elements  $\bar{C}_{ij}$ , which take into account the generic orientation  $\theta$ . In extended notation, relation (3.117) becomes

$$\begin{bmatrix} \sigma_1 \\ \sigma_2 \\ \tau_{12} \\ \tau_{13} \\ \tau_{23} \\ \sigma_3 \end{bmatrix} = \begin{bmatrix} \bar{C}_{11} & \bar{C}_{12} & \bar{C}_{16} & 0 & 0 & \bar{C}_{13} \\ \bar{C}_{12} & \bar{C}_{22} & \bar{C}_{26} & 0 & 0 & \bar{C}_{23} \\ \bar{C}_{16} & \bar{C}_{26} & \bar{C}_{66} & 0 & 0 & \bar{C}_{36} \\ 0 & 0 & 0 & \bar{C}_{44} & \bar{C}_{45} & 0 \\ 0 & 0 & 0 & \bar{C}_{45} & \bar{C}_{55} & 0 \\ \bar{C}_{13} & \bar{C}_{23} & \bar{C}_{36} & 0 & 0 & \bar{C}_{33} \end{bmatrix} \begin{bmatrix} \varepsilon_1 \\ \varepsilon_2 \\ \gamma_{12} \\ \gamma_{13} \\ \gamma_{23} \\ \varepsilon_3 \end{bmatrix} \quad (3.118)$$

where

$$\begin{aligned} \bar{C}_{11} &= C_{11} \cos^4 \theta + 2(C_{12} + 2C_{66}) \cos^2 \theta \sin^2 \theta + C_{22} \sin^4 \theta \\ \bar{C}_{12} &= C_{12} \cos^4 \theta + (C_{11} + C_{22} - 4C_{66}) \cos^2 \theta \sin^2 \theta + C_{12} \sin^4 \theta \\ \bar{C}_{13} &= C_{13} \cos^2 \theta + C_{23} \sin^2 \theta \\ \bar{C}_{16} &= (C_{11} - C_{12} - 2C_{66}) \cos^3 \theta \sin \theta + (C_{12} - C_{22} + 2C_{66}) \cos \theta \sin^3 \theta \\ \bar{C}_{22} &= C_{22} \cos^4 \theta + 2(C_{12} + 2C_{66}) \cos^2 \theta \sin^2 \theta + C_{11} \sin^4 \theta \\ \bar{C}_{23} &= C_{23} \cos^2 \theta + C_{13} \sin^2 \theta \\ \bar{C}_{26} &= (C_{12} - C_{22} + 2C_{66}) \cos^3 \theta \sin \theta + (C_{11} - C_{12} - 2C_{66}) \cos \theta \sin^3 \theta \\ \bar{C}_{33} &= C_{33} \\ \bar{C}_{36} &= (C_{13} - C_{23}) \cos \theta \sin \theta \\ \bar{C}_{66} &= (C_{11} + C_{22} - 2C_{12}) \cos^2 \theta \sin^2 \theta + C_{66} (\cos^2 \theta - \sin^2 \theta)^2 \\ \bar{C}_{44} &= C_{44} \cos^2 \theta + C_{55} \sin^2 \theta \\ \bar{C}_{45} &= (C_{44} - C_{55}) \cos \theta \sin \theta \\ \bar{C}_{55} &= C_{55} \cos^2 \theta + C_{44} \sin^2 \theta \end{aligned} \quad (3.119)$$

The complete treatise concerning these transformations for more general cases can be found in the book by Tornabene et al. [57].

### 3.1.5.1.2 Granular composites

A granular composite is a medium which consist of particles of a stronger material immersed in a matrix made of another material. When the reinforcing phase is defined by a continuous gradual variation of the volume fraction along a particular direction, this medium

is known as Functionally Graded Material (FGM). The FGMs analyzed in this work have a through-the-thickness variation of the mechanical properties in order to reduce thermal stresses, residual stresses and the stress concentrations. These materials are mainly made of isotropic constituents, such as metals and ceramics, and are especially used as thermal barriers in case of high temperature gradients since the ceramics improve the resistance to thermal shocks, whereas the ductility is enhanced by the presence of metals. Due to this gradual variation, the mechanical properties of the composite depend on the thickness coordinate  $\zeta$  of the structure. Since the composite turns out to be isotropic, its mechanical characterization is achieved once the Young's modulus  $E(\zeta)$ , the Poisson's ratio  $\nu(\zeta)$  and the density  $\rho(\zeta)$  are evaluated through a micromechanical approach. Even in this circumstance, the theory of mixture illustrated above can be used. According to this approach, the volume fraction of the metallic phase  $V_M$  and of the ceramic one  $V_C$  are related together as follows

$$V_C + V_M = 1 \quad (3.120)$$

For an isotropic medium, the theory of mixture assume the following aspect

$$\begin{aligned} E(\zeta) &= E_C V_C(\zeta) + E_M V_M(\zeta) \\ \nu(\zeta) &= \nu_C V_C(\zeta) + \nu_M V_M(\zeta) \\ \rho(\zeta) &= \rho_C V_C(\zeta) + \rho_M V_M(\zeta) \end{aligned} \quad (3.121)$$

where the subscripts "C" and "M" denote the properties of the ceramic and the metal, respectively. Several through-the-thickness distributions can be used to define the volume fraction variation  $V_C(\zeta)$ . For example, a five-parameter power law (5P), the Weibull function (W), and the exponential function (E) can be employed to this aim. Their analytical expressions vary according to the position of the stiffer material, which can be placed at the top or at the bottom parts of the structure. The Young's moduli of the isotropic composite in these portions are denoted by  $E_{top}$  and  $E_{bottom}$ , respectively. The expressions of these distributions are presented in Table 3.1 for  $E_{top} > E_{bottom}$  and  $E_{bottom} > E_{top}$ .

**Table 3.1** – Through-the-thickness distributions for the volume fractions of FGM.

$E_{top} > E_{bottom}$	$E_{bottom} > E_{top}$
<i>Five-parameter power law</i>	
$V_c(\zeta) = \left( d - a \left( \frac{1}{2} - \frac{\zeta}{h} \right) + b \left( \frac{1}{2} - \frac{\zeta}{h} \right)^c \right)^p$	$V_c(\zeta) = \left( d - a \left( \frac{1}{2} + \frac{\zeta}{h} \right) + b \left( \frac{1}{2} + \frac{\zeta}{h} \right)^c \right)^p$
<i>Weibull function</i>	
$V_c(\zeta) = 1 - \exp \left( - \left( \frac{1}{a} \left( \frac{1}{2} + \frac{\zeta}{h} \right) \right)^b \right)$	$V_c(\zeta) = \exp \left( - \left( \frac{1}{a} \left( \frac{1}{2} + \frac{\zeta}{h} \right) \right)^b \right)$
<i>Exponential function</i>	
$V_c(\zeta) = \left( \frac{\exp \left( a \left( \frac{1}{2} + \frac{\zeta}{h} \right) \right) - 1}{\left( \exp \left( \frac{a}{2} \right) - 1 \right) \left( \exp \left( a \frac{\zeta}{h} \right) + 1 \right)} \right)^b$	$V_c(\zeta) = 1 - \left( \frac{\exp \left( a \left( \frac{1}{2} + \frac{\zeta}{h} \right) \right) - 1}{\left( \exp \left( \frac{a}{2} \right) - 1 \right) \left( \exp \left( a \frac{\zeta}{h} \right) + 1 \right)} \right)^b$

The various parameters that appear in Table 3.1 define the distributions themselves and have to be specified clearly to define univocally those variations. The following notation can be employed for this purpose

$$FGM_{bottom(dist)(a/b/...)}^{top} \quad (3.122)$$

in which “*top*” and “*bottom*” denote the materials at the top and bottom of the medium, respectively; “*(dist)*” is the law chosen to describe the volume fraction distribution; whereas the quantities in the last brackets on the right stand for the parameters that characterize these distributions. Some examples of volume fraction distributions are depicted in Figure 3.6, for several choices of the parameters included in Table 3.1.

Another example of granular composite is given by polymeric matrix reinforced with Carbon Nanotubes (CNTs). Since their discovery from graphene, those tubular carbon structures have given the possibility to increase the mechanical behavior of composite materials because of their notable physical and chemical properties [192-209]. These materials are also known as nanocomposites due to the nanoscale of the reinforcing phase.

In the following paragraphs, a micromechanics approach is presented to evaluate the overall mechanical properties of a polymer matrix reinforced by CNTs. The matrix is assumed to be isotropic and characterized by the Young’s modulus  $E^m$ , the Poisson’s ratio  $\nu^m$ , and the density  $\rho^m$ . In particular, the Eshelby-Mori-Tanaka scheme is used to compute the mechanical properties of this hybrid matrix improved by CNTs in order to capture and model also the agglomeration of the reinforcing phase [120, 131].

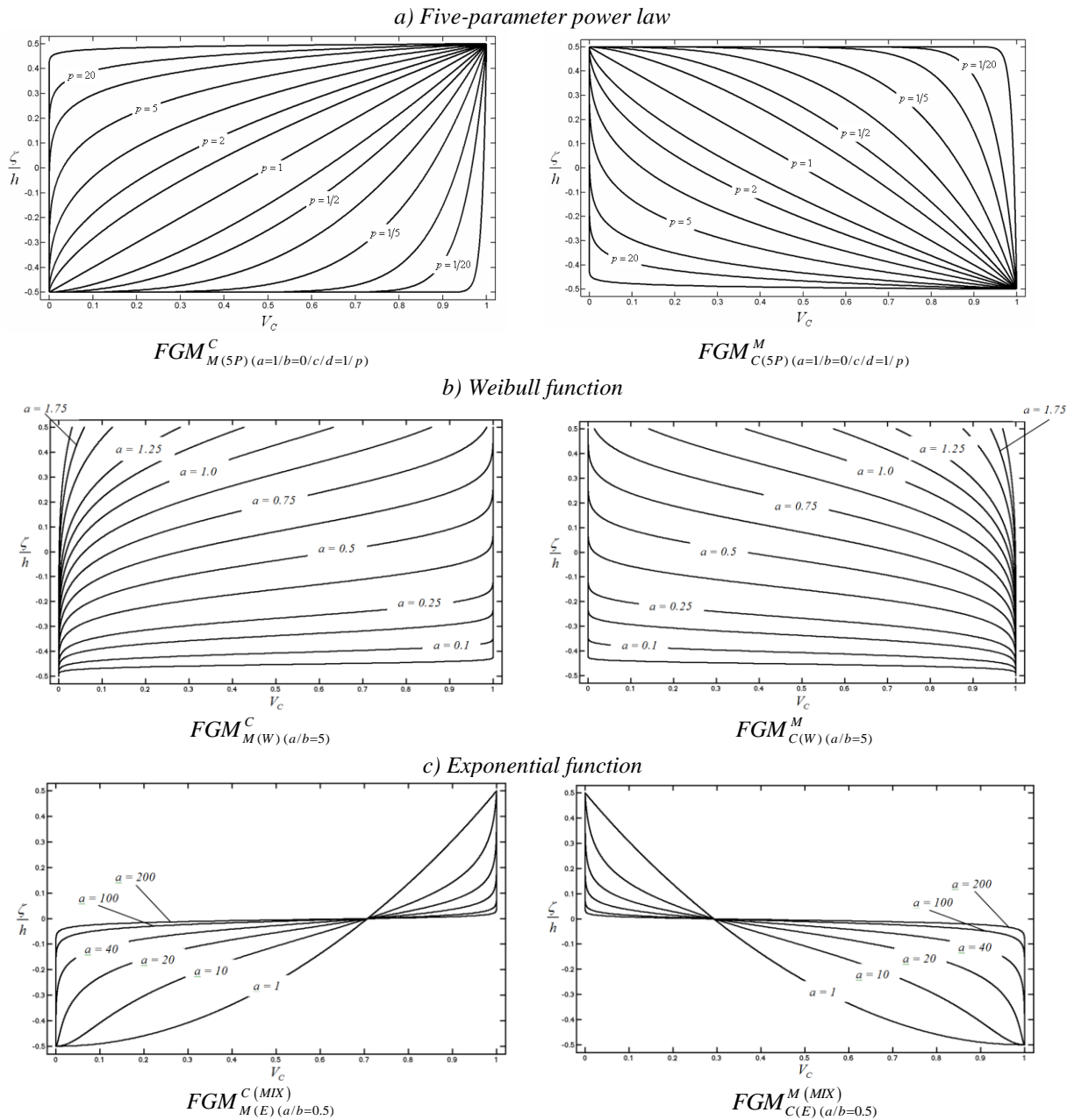


**Figure 3.6** – Graphical representations of the through-the-thickness volume fraction distributions for a FGM.

According to the current approach, CNTs have the tendency to agglomerate if included in a polymer matrix. Consequently, spherical shaped inclusions with higher concentrations of CNTs appear in the composite. Thus, the reinforcing phase can be found both in these inclusions and scattered in the matrix, as depicted in Figure 3.7. For the sake of completeness, it should be specified that this behavior is well-described in the work by Shi et al. [200].

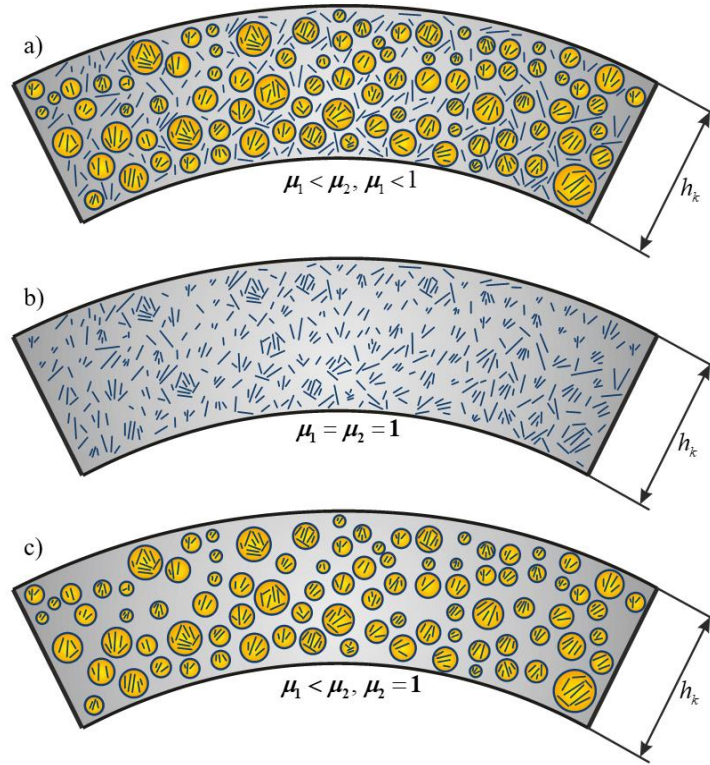


**Figure 3.7** - Agglomeration model: a) partial agglomeration; b) zero agglomeration of CNTs; c) complete agglomeration of CNTs [209].

The total volume of CNTs is given by  $W_r$ . This quantity can be seen as the sum of two contributions, which are the volume of CNTs inside the spherical inclusions  $W_r^{in}$  and scattered in the matrix  $W_r^m$

$$W_r = W_r^{in} + W_r^m \quad (3.123)$$

Consequently, the total volume of representative element assume the following aspect

$$W = W_r + W_m \quad (3.124)$$

where  $W_m$  is volume of the matrix. At this point, the mass fraction of CNTs  $w_r$  and the mass fraction of the matrix  $w_m$  can be computed as follows

$$w_r = \frac{M_r}{M_r + M_m}, \quad w_m = \frac{M_m}{M_r + M_m} \quad (3.125)$$

in which  $M_r$  and  $M_m$  denote respectively the masses of CNTs and of the matrix. Analogously, the volume fraction of CNTs  $V_r$  and the volume fraction of the matrix  $V_m$  can be evaluated as

$$V_r = \frac{W_r}{W}, \quad V_m = \frac{W_m}{W} \quad (3.126)$$

recalling that these quantities are related by means of the following expression

$$V_r + V_m = 1 \quad (3.127)$$

Even the volume fraction of CNTs is given by the summation of the volume fraction of CNT inside the spherical inclusions  $V_r^{in}$  with the volume fraction of CNTs scattered in the matrix  $V_r^m$

$$V_r = V_r^{in} + V_r^m \quad (3.128)$$

If  $\rho_r, \rho_m$  denote respectively the density of CNTs and the density of the polymer matrix, the CNT volume fraction can be expressed as a function of the mass fraction  $w_r$

$$V_r = \left( \frac{\rho_r}{w_r \rho_m} - \frac{\rho_r}{\rho_m} + 1 \right)^{-1} \quad (3.129)$$

According to this micromechanics model, the following two parameters describe the agglomeration of CNTs

$$\mu_1 = \frac{W_{in}}{W}, \quad \mu_2 = \frac{W_r^{in}}{W_r} \quad (3.130)$$

for  $\mu_2 \geq \mu_1$  and  $\mu_1, \mu_2 \in [0,1]$ . It is easy to note that  $\mu_1$  represents the ratio between the spherical inclusion and the total volume of the composite. On the contrary,  $\mu_2$  stands for the ratio between the volume of CNTs within the inclusions and the CNT total volume. Depending on the value of  $\mu_1, \mu_2$ , several mechanical configurations in terms of agglomeration can be achieved. For the sake of completeness, some examples are depicted in Figure 3.6. In general, CNTs can be both contained in the inclusions and scattered in the polymer matrix (Figure 3.7a). This circumstance is obtained by setting  $\mu_1 < \mu_2$  and  $\mu_1 < 1$ . On the other hand, CNTs are completely concentrated in the inclusions for  $\mu_1 = \mu_2 = 1$ , since one gets  $W_r = W_r^{in}$ . In this case, which is shown in Figure 3.7b, the sole inclusions coincide with the reference domain, since  $W_{in} = W$ . Thus, the level of agglomeration is equal to zero. Finally, the complete agglomeration can be obtained for  $\mu_1 < \mu_2$  and  $\mu_2 = 1$ . As depicted in Figure 3.7c, the reinforcing phase is concentrated exclusively in the inclusions.

If relations (3.126), (3.128) and (3.130) are combined together, the following expressions can be obtained as well

$$\frac{W_r^{in}}{W_{in}} = \frac{V_r \mu_2}{\mu_1} \quad (3.131)$$

$$\frac{W_r^m}{W - W_{in}} = \frac{V_r (1 - \mu_2)}{1 - \mu_1} \quad (3.132)$$

In order to evaluate the overall mechanical properties of the composites, an equivalent continuum model for CNTs should be introduced. For this purpose, it can be assumed that a single CNT fiber has a linear-elastic behavior and can be modeled as a homogeneous cylindrical solid, as shown in Figure 3.8. This aspect has been specified also in the work by Odegard et al. [198].

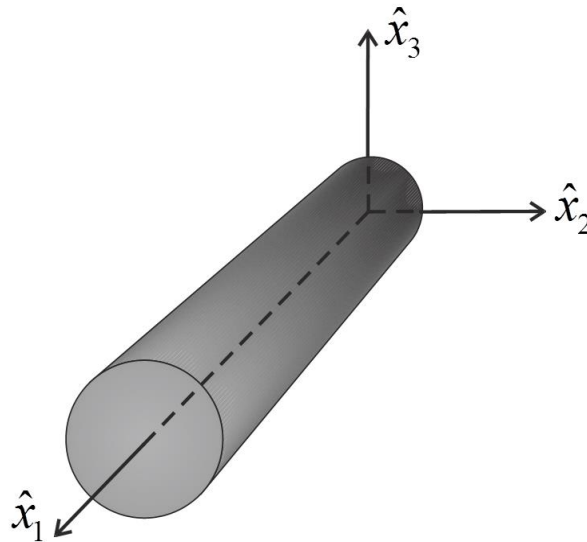


**Figure 3.8** - Continuum equivalent model for a single fiber of CNT [209].

This element can be considered transversely isotropic. In particular, the plane of isotropy is orthogonal to its longitudinal axis (Figure 3.8). Consequently, its mechanical behavior is completely described by five independent constants. As shown in the work by Hashin and Rosen [122], the constitutive laws for such a transversely isotropic medium can be expressed as a function of five elastic moduli  $C_{ij}^r$ . In the local reference system of the element  $O \hat{x}_1 \hat{x}_2 \hat{x}_3$ , the relations between stresses and strains assume the following aspect

$$\begin{bmatrix} \sigma_1^r \\ \sigma_2^r \\ \tau_{12}^r \\ \tau_{13}^r \\ \tau_{23}^r \\ \sigma_3^r \end{bmatrix} = \begin{bmatrix} C_{11}^r & C_{12}^r & 0 & 0 & 0 & C_{12}^r \\ C_{12}^r & C_{22}^r & 0 & 0 & 0 & C_{23}^r \\ 0 & 0 & C_{44}^r & 0 & 0 & 0 \\ 0 & 0 & 0 & C_{44}^r & 0 & 0 \\ 0 & 0 & 0 & 0 & \frac{C_{22}^r - C_{23}^r}{2} & 0 \\ C_{12}^r & C_{23}^r & 0 & 0 & 0 & C_{22}^r \end{bmatrix} \begin{bmatrix} \varepsilon_1^r \\ \varepsilon_2^r \\ \gamma_{12}^r \\ \gamma_{13}^r \\ \gamma_{23}^r \\ \varepsilon_3^r \end{bmatrix} \quad (3.133)$$

in which  $\sigma_1^r, \sigma_2^r, \tau_{12}^r, \tau_{13}^r, \tau_{23}^r, \sigma_3^r$  and  $\varepsilon_1^r, \varepsilon_2^r, \gamma_{12}^r, \gamma_{13}^r, \gamma_{23}^r, \varepsilon_3^r$  are the stress and strain components, respectively. Analogously, the same constitutive equations can be given by using the notation suggested by Hill [123, 124]

$$\begin{bmatrix} \sigma_1^r \\ \sigma_2^r \\ \tau_{12}^r \\ \tau_{13}^r \\ \tau_{23}^r \\ \sigma_3^r \end{bmatrix} = \begin{bmatrix} n_r & l_r & 0 & 0 & 0 & l_r \\ l_r & k_r + m_r & 0 & 0 & 0 & k_r - m_r \\ 0 & 0 & p_r & 0 & 0 & 0 \\ 0 & 0 & 0 & p_r & 0 & 0 \\ 0 & 0 & 0 & 0 & m_r & 0 \\ l_r & k_r - m_r & 0 & 0 & 0 & k_r + m_r \end{bmatrix} \begin{bmatrix} \varepsilon_1^r \\ \varepsilon_2^r \\ \gamma_{12}^r \\ \gamma_{13}^r \\ \gamma_{23}^r \\ \varepsilon_3^r \end{bmatrix} \quad (3.134)$$

where  $k_r, l_r, m_r, n_r, p_r$  are the Hill's elastic moduli. By comparing relations (3.133) and (3.134), the Hill's moduli can be evaluated as a function of the elastic moduli  $C_{ij}^r$

$$k_r = \frac{C_{22}^r + C_{23}^r}{2}, \quad l_r = C_{12}^r, \quad m_r = \frac{C_{22}^r - C_{23}^r}{2}, \quad n_r = C_{11}^r, \quad p_r = C_{44}^r \quad (3.135)$$

The same mechanical behavior can be described also in terms of the engineering constants as follows

$$E_1^r = n_r - \frac{l_r^2}{k_r} = C_{11}^r - \frac{2(C_{12}^r)^2}{C_{22}^r + C_{23}^r} \quad (3.136)$$

$$E_2^r = E_3^r = \frac{4m_r(k_r n_r - l_r^2)}{k_r n_r - l_r^2 + m_r n_r} = \frac{(C_{22}^r - C_{23}^r)(C_{11}^r C_{22}^r + C_{11}^r C_{23}^r - 2(C_{12}^r)^2)}{C_{11}^r C_{22}^r - (C_{12}^r)^2} \quad (3.137)$$

$$\nu_{12}^r = \nu_{13}^r = \frac{l_r}{2k_r} = \frac{C_{12}^r}{C_{22}^r + C_{23}^r} \quad (3.138)$$

$$\nu_{23}^r = \frac{n_r(k_r - m_r) - l_r^2}{n_r(k_r + m_r) - l_r^2} = \frac{C_{11}^r C_{23}^r - (C_{12}^r)^2}{C_{11}^r C_{22}^r - (C_{12}^r)^2} \quad (3.139)$$

$$G_{12}^r = G_{13}^r = p_r = C_{44}^r \quad (3.140)$$

$$G_{23}^r = m_r = \frac{E_2^r}{2(1+\nu_{23}^r)} \quad (3.141)$$

where the superscript “ $r$ ” denotes the mechanical properties of the reinforcing phase at issue. At this point, the Eshelby-Mori-Tanaka approach can be used to evaluate the global properties of this composite, which turns out to be isotropic. The bulk modulus of the spherical inclusions  $K_{in}^*$  is given by

$$K_{in}^* = K^m + \frac{V_r \mu_2 (\delta_r - 3K^m \alpha_r)}{3(\mu_1 - V_r \mu_2 + V_r \mu_2 \alpha_r)} \quad (3.142)$$

whereas their shear modulus  $G_{in}^*$  is given by

$$G_{in}^* = G^m + \frac{V_r \mu_2 (\eta_r - 2G^m \beta_r)}{2(\mu_1 - V_r \mu_2 + V_r \mu_2 \beta_r)} \quad (3.143)$$

whereas  $K^m$  and  $G^m$  are the bulk and the shear moduli of the isotropic matrix, which can be evaluated as follows

$$K^m = \frac{E^m}{3(1-2\nu^m)}, \quad G^m = \frac{E^m}{2(1+\nu^m)} \quad (3.144)$$

On the contrary, the bulk modulus of the matrix in which CNTs are scattered is given by

$$K_{out}^* = K^m + \frac{V_r (1-\mu_2) (\delta_r - 3K^m \alpha_r)}{3(1-\mu_1 - V_r (1-\mu_2) + V_r (1-\mu_2) \alpha_r)} \quad (3.145)$$

Analogously, the following definition allows to compute the corresponding shear modulus

$$G_{out}^* = G^m + \frac{V_r (1-\mu_2) (\eta_r - 2G^m \beta_r)}{2(1-\mu_1 - V_r (1-\mu_2) + V_r (1-\mu_2) \beta_r)} \quad (3.146)$$

The quantities defined below are require to evaluate the elastic properties just introduced

$$\alpha_r = \frac{3(K^m + G^m) + k_r + l_r}{3(G^m + k_r)} \quad (3.147)$$

$$\beta_r = \frac{1}{5} \left( \frac{4G^m + 2k_r + l_r}{3(G^m + k_r)} + \frac{4G^m}{G^m + p_r} + \frac{2(G^m (3K^m + G^m) + G^m (3K^m + 7G^m))}{G^m (3K^m + G^m) + m_r (3K^m + 7G^m)} \right) \quad (3.148)$$

$$\delta_r = \frac{1}{3} \left( n_r + 2l_r + \frac{(2k_r + l_r)(3K^m + G^m - l_r)}{G^m + k_r} \right) \quad (3.149)$$

$$\eta_r = \frac{1}{5} \left( \frac{2}{3}(n_r - l_r) + \frac{8G^m p_r}{G^m + p_r} + \frac{2(k_r - l_r)(2G^m + l_r)}{3(G^m + k_r)} + \frac{8m_r G^m (3K^m + 4G^m)}{3K^m (m_r + G^m) + G^m (7m_r + G^m)} \right) \quad (3.150)$$

The effective bulk modulus  $K$  and the shear modulus  $G$  of this composite are given by

$$K = K_{out}^* \left( 1 + \frac{\mu_1 \left( \frac{K_{in}^*}{K_{out}^*} - 1 \right)}{1 + (1 - \mu_1) \left( \frac{K_{in}^*}{K_{out}^*} - 1 \right) \frac{1 + \nu_{out}^*}{3 - 3\nu_{out}^*}} \right) \quad (3.151)$$

$$G = G_{out}^* \left( 1 + \frac{\mu_1 \left( \frac{G_{in}^*}{G_{out}^*} - 1 \right)}{1 + (1 - \mu_1) \left( \frac{G_{in}^*}{G_{out}^*} - 1 \right) \frac{8 - 10\nu_{out}^*}{15 - 15\nu_{out}^*}} \right) \quad (3.152)$$

where

$$\nu_{out}^* = \frac{3K_{out}^* - 2G_{out}^*}{6K_{out}^* + 2G_{out}^*} \quad (3.153)$$

Finally, the Young's modulus  $E$  and the Poisson's ratio  $\nu$  of the isotropic composite can be computed as follows

$$E = \frac{9KG}{3K + G}, \quad \nu = \frac{3K - 2G}{6K + 2G} \quad (3.154)$$

It should be specified that the density  $\rho$  of this polymer matrix enriched by CNTs is still computed through the rule of mixture

$$\rho = (\rho^r - \rho^m)V_r + \rho^m \quad (3.155)$$

where  $\rho^r$  is the CNT density. Finally, it should be also specified that a continuous gradual variation can be used to describe the volume fraction  $V_r$  of CNTs. Consequently, the class of Functionally Graded Carbon Nanotube (FG-CNT) reinforced composites is achieved. For this purpose, the same distributions listed in Table 3.1 can be employed.

### 3.1.5.1.3 Laminated composites

As specified in the previous sections, a laminated composite is a structure made of  $l$  plies (called also laminae or layers), as depicted in Figure 3.3. The lamina is the fundamental element of a laminate. The following assumptions must be introduced for a laminated composite structure:

- each layer is a continuous body, therefore discontinuities and blanks are not allowed;
- the mechanical behavior of each ply is linear-elastic;
- the laminae are perfectly bonded, thus relative slips between them are not permitted.

Each layer can be isotropic, orthotropic, FGMs, reinforced by CNTs, or a combination of them. The sequence of the various constituents denotes the lamination scheme or the stacking sequence. A complete mechanical characterization of the laminate is performed once the properties, the thickness, and the orientation of each layer are specified. For this purpose, the superscript  $k$  is introduced to specify the  $k$ -th lamina and all its features. For instance, if an isotropic layer is considered, its Young modulus, its Poisson's ratio and its density are indicated respectively by  $E^{(k)}$ ,  $\nu^{(k)}$  e  $\rho^{(k)}$ . As far as an orthotropic layer is concerned, the orientation of the  $k$ -th layer is given by  $\theta^{(k)}$ . For a laminated composite made of  $l$  plies defined by arbitrary orientations of the fibers, the following notation is required to specify univocally the laminate itself

$$\left( \theta^{(1)} / \theta^{(2)} / \dots / \theta^{(k)} / \dots / \theta^{(l)} \right) \quad (3.156)$$

It should be specified that these orientations are listed from the lower layer to the upper one. Finally, it must be mentioned that even the through-the-thickness distributions listed in Table 3.1 assume different notations if applied to the  $k$ -th layer. The volume fraction distributions in hand  $V_C^{(k)}(\zeta)$  are presented in Table 3.2, where it can be noted that each quantity is linked to the  $k$ -th lamina.

**Table 3.2** – Through-the-thickness distributions for the volume fractions of a functionally graded layer.

$E_{top} > E_{bottom}$	$E_{bottom} > E_{top}$
<i>Five-parameter power law</i>	
$V_C^{(k)}(\zeta) = \left( d^{(k)} - a^{(k)} \left( \frac{\zeta_{k+1} - \zeta}{h_k} \right) + b^{(k)} \left( \frac{\zeta_{k+1} - \zeta}{h_k} \right)^{c^{(k)}} \right)^{p^{(k)}}$	$V_C^{(k)}(\zeta) = \left( a^{(k)} - a^{(k)} \left( \frac{\zeta - \zeta_k}{h_k} \right) + b^{(k)} \left( \frac{\zeta - \zeta_k}{h_k} \right)^{c^{(k)}} \right)^{p^{(k)}}$
<i>Weibull function</i>	
$V_C^{(k)}(\zeta) = 1 - \exp \left( - \left( \frac{1}{a^{(k)}} \frac{\zeta - \zeta_k}{h_k} \right)^{b^{(k)}} \right)$	$V_C^{(k)}(\zeta) = \exp \left( - \left( \frac{1}{a^{(k)}} \frac{\zeta - \zeta_k}{h_k} \right)^{b^{(k)}} \right)$
<i>Exponential function</i>	
$V_C^{(k)}(\zeta) = \left( \frac{\exp \left( a^{(k)} \left( \frac{\zeta - \zeta_k - h_k/2 + 1}{h_k} \right) \right) - 1}{\left( \exp \left( \frac{a^{(k)}}{2} \right) - 1 \right) \left( \exp \left( a^{(k)} \frac{\zeta - \zeta_k - h_k/2}{h_k} \right) + 1 \right)} \right)^{b^{(k)}}$	$V_C^{(k)}(\zeta) = 1 - \left( \frac{\exp \left( a^{(k)} \left( \frac{\zeta - \zeta_k - h_k/2 + 1}{h_k} \right) \right) - 1}{\left( \exp \left( \frac{a^{(k)}}{2} \right) - 1 \right) \left( \exp \left( a^{(k)} \frac{\zeta - \zeta_k - h_k/2}{h_k} \right) + 1 \right)} \right)^{b^{(k)}}$

### 3.1.6 EQUATIONS OF MOTION

The equations of motion for a laminated composite doubly-curved shell can be obtained efficiently by means of the Hamilton's variational principle. This approach allows to obtain at the same time both the equations of motions and the natural or static boundary conditions of the problem.

Let us consider an elastic shell which changes its state between two consecutive arbitrary instants, identified by the time variables  $t_1$  and  $t_2$ . The shell is in equilibrium under the action of external applied loads. The equilibrium configuration is denoted by the three-dimensional displacement vector  $\mathbf{U}$ , whereas an arbitrary configuration is identified by the displacement vector  $\mathbf{U} + \delta\mathbf{U}$ , in which  $\delta\mathbf{U}$  is the vector that collects the virtual displacements. The path followed by the body during the dynamic process is ruled by the Hamilton's principle

$$\delta \int_{t_1}^{t_2} (\mathcal{T} - \Pi) dt = 0 \quad \rightarrow \quad \int_{t_1}^{t_2} (\delta\mathcal{T} - \delta\Pi) dt = 0 \quad (3.157)$$

in which  $\mathcal{T}$  is kinetic energy of the system and  $\Pi$  is the total potential energy. On the other hand,  $\delta\mathcal{T}, \delta\Pi$  denote the variations of the kinetic energy and total potential energy, respectively. The Hamilton's variational principle (3.157) specifies that the energy term  $(\mathcal{T} - \Pi)$  has an extreme value, which can be proven to be a minimum. The value of  $t_1, t_2$  can

be chosen arbitrarily, provided that the variations of all the energetic quantities in (3.157) are equal to zero for  $t = t_1$  and  $t = t_2$ . The total potential energy  $\Pi$  is given by the summation of the elastic energy of deformation  $\Phi$  and of the potential of external loads  $H$

$$\Pi = \Phi + H = \Phi - L_e \quad (3.158)$$

It should be noted that the potential of external loads  $H$  is given by the summation of the work done by the volume and surface external loads  $L_e$  changed in sign. Consequently, equation (3.157) becomes

$$\int_{t_1}^{t_2} (\delta T - \delta \Phi + \delta L_e) dt = 0 \quad (3.159)$$

In the following, all the energetic terms that appear in (3.159) will be presented in their explicit form. The elastic energy of deformation  $\Phi$  for a three-dimensional medium is given by

$$\Phi = \frac{1}{2} \int \int \int_{\alpha_1 \alpha_2 \zeta} (\sigma_1 \varepsilon_1 + \sigma_2 \varepsilon_2 + \sigma_3 \varepsilon_3 + \tau_{12} \gamma_{12} + \tau_{13} \gamma_{13} + \tau_{23} \gamma_{23}) A_1 A_2 H_1 H_2 d\alpha_1 d\alpha_2 d\zeta \quad (3.160)$$

Its variation  $\delta \Phi$  can be deduced easily

$$\delta \Phi = \frac{1}{2} \int \int \int_{\alpha_1 \alpha_2 \zeta} (\sigma_1 \delta \varepsilon_1 + \sigma_2 \delta \varepsilon_2 + \sigma_3 \delta \varepsilon_3 + \tau_{12} \delta \gamma_{12} + \tau_{13} \delta \gamma_{13} + \tau_{23} \delta \gamma_{23}) A_1 A_2 H_1 H_2 d\alpha_1 d\alpha_2 d\zeta \quad (3.161)$$

If the elastic body is a laminated composite structure made of  $l$  layers, the variation of the elastic energy of deformation  $\Phi$  becomes

$$\begin{aligned} \delta \Phi = \sum_{k=1}^l \int \int \int_{\alpha_1 \alpha_2 \zeta_k}^{\zeta_{k+1}} & \left( \sigma_1^{(k)} \delta \varepsilon_1^{(k)} + \sigma_2^{(k)} \delta \varepsilon_2^{(k)} + \sigma_3^{(k)} \delta \varepsilon_3^{(k)} + \right. \\ & \left. + \tau_{12}^{(k)} \delta \gamma_{12}^{(k)} + \tau_{13}^{(k)} \delta \gamma_{13}^{(k)} + \tau_{23}^{(k)} \delta \gamma_{23}^{(k)} \right) A_1 A_2 H_1 H_2 d\alpha_1 d\alpha_2 d\zeta \end{aligned} \quad (3.162)$$

where the index  $k$  is used to denote the generic ply. At this point, the kinematic equations (3.79)-(3.84) can be inserted into (3.162)

$$\begin{aligned} \delta \Phi = \sum_{k=1}^l \sum_{\tau=0}^{N+1} \sum_{i=1}^3 \int \int \int_{\alpha_1 \alpha_2 \zeta_k}^{\zeta_{k+1}} & \left( \sigma_1^{(k)} \frac{F_\tau^{\alpha_i} \delta \varepsilon_1^{(\tau)\alpha_i}}{H_1} + \sigma_2^{(k)} \frac{F_\tau^{\alpha_i} \delta \varepsilon_2^{(\tau)\alpha_i}}{H_2} + \sigma_3^{(k)} \frac{\partial F_\tau^{\alpha_i}}{\partial \zeta} \delta \varepsilon_3^{(\tau)\alpha_i} + \right. \\ & + \tau_{12}^{(k)} \frac{F_\tau^{\alpha_i} \delta \gamma_1^{(\tau)\alpha_i}}{H_1} + \tau_{12}^{(k)} \frac{F_\tau^{\alpha_i} \delta \gamma_2^{(\tau)\alpha_i}}{H_2} + \tau_{13}^{(k)} \frac{F_\tau^{\alpha_i} \delta \gamma_{13}^{(\tau)\alpha_i}}{H_1} + \\ & \left. + \tau_{13}^{(k)} \frac{\partial F_\tau^{\alpha_i}}{\partial \zeta} \delta \omega_{13}^{(\tau)\alpha_i} + \tau_{23}^{(k)} \frac{F_\tau^{\alpha_i} \delta \gamma_{23}^{(\tau)\alpha_i}}{H_2} + \tau_{23}^{(k)} \frac{\partial F_\tau^{\alpha_i}}{\partial \zeta} \delta \omega_{23}^{(\tau)\alpha_i} \right) A_1 H_1 A_2 H_2 d\alpha_1 d\alpha_2 d\zeta \end{aligned} \quad (3.163)$$

The integrals that involve the through-the-thickness coordinate  $\zeta$ , as well as all the terms that depend on this coordinate, can be separated to obtain the definitions of the stress resultants or generalized internal forces. These quantities are presented below

$$N_1^{(\tau)\alpha_i} = \sum_{k=1}^l \int_{\zeta_k}^{\zeta_{k+1}} \sigma_1^{(k)} F_\tau^{\alpha_i} H_2 d\zeta \quad (3.164)$$

$$N_2^{(\tau)\alpha_i} = \sum_{k=1}^l \int_{\zeta_k}^{\zeta_{k+1}} \sigma_2^{(k)} F_\tau^{\alpha_i} H_1 d\zeta \quad (3.165)$$

$$N_{12}^{(\tau)\alpha_i} = \sum_{k=1}^l \int_{\zeta_k}^{\zeta_{k+1}} \tau_{12}^{(k)} F_\tau^{\alpha_i} H_2 d\zeta \quad (3.166)$$

$$N_{21}^{(\tau)\alpha_i} = \sum_{k=1}^l \int_{\zeta_k}^{\zeta_{k+1}} \tau_{12}^{(k)} F_\tau^{\alpha_i} H_1 d\zeta \quad (3.167)$$

$$T_1^{(\tau)\alpha_i} = \sum_{k=1}^l \int_{\zeta_k}^{\zeta_{k+1}} \tau_{13}^{(k)} F_\tau^{\alpha_i} H_2 d\zeta \quad (3.168)$$

$$T_2^{(\tau)\alpha_i} = \sum_{k=1}^l \int_{\zeta_k}^{\zeta_{k+1}} \tau_{23}^{(k)} F_\tau^{\alpha_i} H_1 d\zeta \quad (3.169)$$

$$P_1^{(\tau)\alpha_i} = \sum_{k=1}^l \int_{\zeta_k}^{\zeta_{k+1}} \tau_{13}^{(k)} \frac{\partial F_\tau^{\alpha_i}}{\partial \zeta} H_1 H_2 d\zeta \quad (3.170)$$

$$P_2^{(\tau)\alpha_i} = \sum_{k=1}^l \int_{\zeta_k}^{\zeta_{k+1}} \tau_{23}^{(k)} \frac{\partial F_\tau^{\alpha_i}}{\partial \zeta} H_1 H_2 d\zeta \quad (3.171)$$

$$S_3^{(\tau)\alpha_i} = \sum_{k=1}^l \int_{\zeta_k}^{\zeta_{k+1}} \sigma_3^{(k)} \frac{\partial F_\tau^{\alpha_i}}{\partial \zeta} H_1 H_2 d\zeta \quad (3.172)$$

The same procedure can be followed in compact matrix form

$$\begin{aligned} \delta \Phi &= \sum_{k=1}^l \int_{\alpha_1} \int_{\alpha_2} \int_{\zeta_k}^{\zeta_{k+1}} \delta \boldsymbol{\varepsilon}^{(k)T} \boldsymbol{\sigma}^{(k)} A_1 H_1 A_2 H_2 d\zeta d\alpha_2 d\alpha_1 = \\ &= \sum_{k=1}^l \int_{\alpha_1} \int_{\alpha_2} \int_{\zeta_k}^{\zeta_{k+1}} \left( \sum_{\tau=0}^{N+1} \sum_{i=1}^3 \mathbf{Z}^{(\tau)\alpha_i} \delta \boldsymbol{\varepsilon}^{(\tau)\alpha_i} \right)^T \boldsymbol{\sigma}^{(k)} A_1 H_1 A_2 H_2 d\zeta d\alpha_2 d\alpha_1 = \\ &= \sum_{k=1}^l \int_{\alpha_1} \int_{\alpha_2} \int_{\zeta_k}^{\zeta_{k+1}} \left( \sum_{\tau=0}^{N+1} \sum_{i=1}^3 \left( \delta \boldsymbol{\varepsilon}^{(\tau)\alpha_i} \right)^T \left( \mathbf{Z}^{(\tau)\alpha_i} \right)^T \right) \boldsymbol{\sigma}^{(k)} A_1 H_1 A_2 H_2 d\zeta d\alpha_2 d\alpha_1 = \\ &= \sum_{\tau=0}^{N+1} \sum_{i=1}^3 \int_{\alpha_1} \int_{\alpha_2} \left( \delta \boldsymbol{\varepsilon}^{(\tau)\alpha_i} \right)^T \sum_{k=1}^l \int_{\zeta_k}^{\zeta_{k+1}} \left( \mathbf{Z}^{(\tau)\alpha_i} \right)^T \boldsymbol{\sigma}^{(k)} H_1 H_2 d\zeta A_1 A_2 d\alpha_2 d\alpha_1 = \\ &= \sum_{\tau=0}^{N+1} \sum_{i=1}^3 \int_{\alpha_1} \int_{\alpha_2} \left( \delta \boldsymbol{\varepsilon}^{(\tau)\alpha_i} \right)^T \mathbf{S}^{(\tau)\alpha_i} A_1 A_2 d\alpha_2 d\alpha_1 \end{aligned} \quad (3.173)$$

where  $\mathbf{S}^{(\tau)\alpha_i} = \mathbf{S}^{(\tau)\alpha_i}(\alpha_1, \alpha_2, t)$  is the  $\tau$ -th order generalized stress resultant vector that collects the quantities defined in (3.164)-(3.172) and assumes the aspect shown below

$$\mathbf{S}^{(\tau)\alpha_i} = \left[ N_1^{(\tau)\alpha_i} \quad N_2^{(\tau)\alpha_i} \quad N_{12}^{(\tau)\alpha_i} \quad N_{21}^{(\tau)\alpha_i} \quad T_1^{(\tau)\alpha_i} \quad T_2^{(\tau)\alpha_i} \quad P_1^{(\tau)\alpha_i} \quad P_2^{(\tau)\alpha_i} \quad S_3^{(\tau)\alpha_i} \right]^T \quad (3.174)$$

For the sake of conciseness, the variation of the elastic energy of deformation can be written as follows

$$\delta\Phi = \sum_{\tau=0}^{N+1} \sum_{i=1}^3 \int \int_{\alpha_1, \alpha_2} (\delta \boldsymbol{\varepsilon}^{(\tau)\alpha_i})^T \mathbf{S}^{(\tau)\alpha_i} A_1 A_2 d\alpha_1 d\alpha_2 \quad (3.175)$$

From relation (3.173), the following definition can be extracted, for  $\tau=0,1,2,\dots,N,N+1$  and  $i=1,2,3$

$$\mathbf{S}^{(\tau)\alpha_i} = \sum_{\eta=0}^{N+1} \sum_{j=1}^3 \left( \sum_{k=1}^l \int_{\zeta_k}^{\zeta_{k+1}} (\mathbf{Z}^{(\tau)\alpha_i})^T \bar{\mathbf{C}}^{(k)} \mathbf{Z}^{(\eta)\alpha_j} H_1 H_2 d\zeta \right) \boldsymbol{\varepsilon}^{(\eta)\alpha_j} \quad (3.176)$$

in which the constitutive equations (3.117) have been employed. The stiffness matrix (or constitutive operator)  $\mathbf{A}^{(\tau\eta)\alpha_i\alpha_j}$  can be conveniently deduced

$$\mathbf{A}^{(\tau\eta)\alpha_i\alpha_j} = \sum_{k=1}^l \int_{\zeta_k}^{\zeta_{k+1}} (\mathbf{Z}^{(\tau)\alpha_i})^T \bar{\mathbf{C}}^{(k)} \mathbf{Z}^{(\eta)\alpha_j} H_1 H_2 d\zeta \quad (3.177)$$

Equation (3.176) assumes the following aspect

$$\mathbf{S}^{(\tau)\alpha_i} = \sum_{\eta=0}^{N+1} \sum_{j=1}^3 \mathbf{A}^{(\tau\eta)\alpha_i\alpha_j} \boldsymbol{\varepsilon}^{(\eta)\alpha_j} \quad (3.178)$$

for  $\tau=0,1,2,\dots,N,N+1$  and  $i=1,2,3$ . Having in mind the definition of the generalized strains (3.88), the stress resultants can be expressed as a function of the generalized displacements as follows

$$\mathbf{S}^{(\tau)\alpha_i} = \sum_{\eta=0}^{N+1} \sum_{j=1}^3 \mathbf{A}^{(\tau\eta)\alpha_i\alpha_j} \mathbf{D}_{\Omega}^{\alpha_j} \mathbf{u}^{(\eta)} \quad (3.179)$$

for  $\tau=0,1,2,\dots,N,N+1$  and  $i=1,2,3$ . This relation will be useful to apply the natural boundary conditions along the external edges of the structure. It should be noted that this definition involves the derivatives with respect to the principal coordinates of the degrees of freedom of the model. The constitutive operator  $\mathbf{A}^{(\tau\eta)\alpha_i\alpha_j}$  is a  $9 \times 9$  matrix, which takes the following extended form

$$\mathbf{A}^{(\tau\eta)\alpha_i\alpha_j} = \begin{bmatrix} A_{11(20)}^{(\tau\eta)\alpha_i\alpha_j} & A_{12(11)}^{(\tau\eta)\alpha_i\alpha_j} & A_{16(20)}^{(\tau\eta)\alpha_i\alpha_j} & A_{16(11)}^{(\tau\eta)\alpha_i\alpha_j} & 0 & 0 & 0 & 0 & A_{13(10)}^{(\tau\bar{\eta})\alpha_i\alpha_j} \\ A_{12(11)}^{(\tau\eta)\alpha_i\alpha_j} & A_{22(02)}^{(\tau\eta)\alpha_i\alpha_j} & A_{26(11)}^{(\tau\eta)\alpha_i\alpha_j} & A_{26(02)}^{(\tau\eta)\alpha_i\alpha_j} & 0 & 0 & 0 & 0 & A_{23(01)}^{(\tau\bar{\eta})\alpha_i\alpha_j} \\ A_{16(20)}^{(\tau\eta)\alpha_i\alpha_j} & A_{26(11)}^{(\tau\eta)\alpha_i\alpha_j} & A_{66(20)}^{(\tau\eta)\alpha_i\alpha_j} & A_{66(11)}^{(\tau\eta)\alpha_i\alpha_j} & 0 & 0 & 0 & 0 & A_{36(10)}^{(\tau\bar{\eta})\alpha_i\alpha_j} \\ A_{16(11)}^{(\tau\eta)\alpha_i\alpha_j} & A_{26(02)}^{(\tau\eta)\alpha_i\alpha_j} & A_{66(11)}^{(\tau\eta)\alpha_i\alpha_j} & A_{66(02)}^{(\tau\eta)\alpha_i\alpha_j} & 0 & 0 & 0 & 0 & A_{36(01)}^{(\tau\bar{\eta})\alpha_i\alpha_j} \\ 0 & 0 & 0 & 0 & A_{44(20)}^{(\tau\eta)\alpha_i\alpha_j} & A_{45(11)}^{(\tau\eta)\alpha_i\alpha_j} & A_{44(10)}^{(\tau\bar{\eta})\alpha_i\alpha_j} & A_{45(10)}^{(\tau\bar{\eta})\alpha_i\alpha_j} & 0 \\ 0 & 0 & 0 & 0 & A_{45(11)}^{(\tau\eta)\alpha_i\alpha_j} & A_{55(02)}^{(\tau\eta)\alpha_i\alpha_j} & A_{45(01)}^{(\tau\bar{\eta})\alpha_i\alpha_j} & A_{55(01)}^{(\tau\bar{\eta})\alpha_i\alpha_j} & 0 \\ 0 & 0 & 0 & 0 & A_{44(10)}^{(\tau\bar{\eta})\alpha_i\alpha_j} & A_{45(01)}^{(\tau\bar{\eta})\alpha_i\alpha_j} & A_{44(00)}^{(\tau\bar{\eta})\alpha_i\alpha_j} & A_{45(00)}^{(\tau\bar{\eta})\alpha_i\alpha_j} & 0 \\ 0 & 0 & 0 & 0 & A_{45(10)}^{(\tau\bar{\eta})\alpha_i\alpha_j} & A_{55(01)}^{(\tau\bar{\eta})\alpha_i\alpha_j} & A_{45(00)}^{(\tau\bar{\eta})\alpha_i\alpha_j} & A_{55(00)}^{(\tau\bar{\eta})\alpha_i\alpha_j} & 0 \\ A_{13(10)}^{(\tau\bar{\eta})\alpha_i\alpha_j} & A_{23(01)}^{(\tau\bar{\eta})\alpha_i\alpha_j} & A_{36(10)}^{(\tau\bar{\eta})\alpha_i\alpha_j} & A_{36(01)}^{(\tau\bar{\eta})\alpha_i\alpha_j} & 0 & 0 & 0 & 0 & A_{33(00)}^{(\tau\bar{\eta})\alpha_i\alpha_j} \end{bmatrix} \quad (3.180)$$

in which the definitions below are required

$$A_{nm(pq)}^{(\tau\eta)\alpha_i\alpha_j} = \sum_{k=1}^l \int_{\zeta_k}^{\zeta_{k+1}} \bar{B}_{nm}^{(k)} F_{\eta}^{\alpha_j} F_{\tau}^{\alpha_i} \frac{H_1 H_2}{H_1^p H_2^q} d\zeta \quad (3.181)$$

$$A_{nm(pq)}^{(\tau\bar{\eta})\alpha_i\alpha_j} = \sum_{k=1}^l \int_{\zeta_k}^{\zeta_{k+1}} \bar{B}_{nm}^{(k)} F_{\eta}^{\alpha_j} \frac{\partial F_{\tau}^{\alpha_i}}{\partial \zeta} \frac{H_1 H_2}{H_1^p H_2^q} d\zeta \quad (3.182)$$

$$A_{nm(pq)}^{(\tau\bar{\eta})\alpha_i\alpha_j} = \sum_{k=1}^l \int_{\zeta_k}^{\zeta_{k+1}} \bar{B}_{nm}^{(k)} \frac{\partial F_{\eta}^{\alpha_j}}{\partial \zeta} F_{\tau}^{\alpha_i} \frac{H_1 H_2}{H_1^p H_2^q} d\zeta \quad (3.183)$$

$$A_{nm(pq)}^{(\tau\bar{\eta})\alpha_i\alpha_j} = \sum_{k=1}^l \int_{\zeta_k}^{\zeta_{k+1}} \bar{B}_{nm}^{(k)} \frac{\partial F_{\eta}^{\alpha_j}}{\partial \zeta} \frac{\partial F_{\tau}^{\alpha_i}}{\partial \zeta} \frac{H_1 H_2}{H_1^p H_2^q} d\zeta \quad (3.184)$$

for  $\tau, \eta = 0, 1, 2, \dots, N, N+1$ ,  $n, m = 1, 2, \dots, 6$ ,  $p, q = 0, 1, 2$ , and  $i, j = 1, 2, 3$ . The coefficients  $\bar{B}_{nm}^{(k)}$  are defined as shown below to introduce the shear correction factor  $\kappa$

$$\begin{aligned} \bar{B}_{nm}^{(k)} &= \bar{C}_{nm}^{(k)} & \text{for } n, m = 1, 2, 3, 6 \\ \bar{B}_{nm}^{(k)} &= \kappa \bar{C}_{nm}^{(k)} & \text{for } n, m = 4, 5 \end{aligned} \quad (3.185)$$

It should be noted that only lower-order shear deformation theories, such as ED1, EDZ1, ED2, and EDZ2 could require this correction.

Recalling the assumption (3.99), the stress resultants (3.178) assume the following definition according to the current weak formulation, in which the kinematic hypotheses (3.37) are introduced

$$\mathbf{S}^{(\tau)\alpha_i} = \sum_{\eta=0}^{N+1} \sum_{j=1}^3 \mathbf{A}^{(\tau\eta)\alpha_i\alpha_j} \mathbf{B}^{\alpha_j} \bar{\mathbf{u}}^{(\tau)} \quad (3.186)$$

The integral of the variation of the elastic strain energy  $\delta\Phi$  defined in (3.175) with respect to the time variable in the interval  $[t_1, t_2]$  assumes the following aspect

$$\int_{t_1}^{t_2} \delta\Phi dt = \sum_{\tau=0}^{N+1} \sum_{i=1}^3 \int_{t_1}^{t_2} \int_{\alpha_1} \int_{\alpha_2} \left( \delta \mathbf{\epsilon}^{(\tau)\alpha_i} \right)^T \mathbf{S}^{(\tau)\alpha_i} A_1 A_2 d\alpha_1 d\alpha_2 dt \quad (3.187)$$

Having in mind the definitions of the generalized strain components (3.88), one gets

$$\int_{t_1}^{t_2} \delta\Phi dt = \sum_{\tau=0}^{N+1} \sum_{i=1}^3 \int_{t_1}^{t_2} \int_{\alpha_1} \int_{\alpha_2} \left( \delta \left( \mathbf{D}_{\Omega}^{\alpha_i} \mathbf{u}^{(\tau)} \right) \right)^T \mathbf{S}^{(\tau)\alpha_i} A_1 A_2 d\alpha_1 d\alpha_2 dt \quad (3.188)$$

On the other hand, the kinetic energy  $\mathcal{T}$  assumes the following aspect

$$\mathcal{T} = \frac{1}{2} \int_{\alpha_1} \int_{\alpha_2} \int_{\zeta} \rho \left( \dot{U}_1^2 + \dot{U}_2^2 + \dot{U}_3^2 \right) A_1 A_2 H_1 H_2 d\alpha_1 d\alpha_2 d\zeta \quad (3.189)$$

whereas its variation is given by

$$\delta\mathcal{T} = \int_{\alpha_1} \int_{\alpha_2} \int_{\zeta} \rho \left( \dot{U}_1 \delta\dot{U}_1 + \dot{U}_2 \delta\dot{U}_2 + \dot{U}_3 \delta\dot{U}_3 \right) A_1 A_2 H_1 H_2 d\alpha_1 d\alpha_2 d\zeta \quad (3.190)$$

It should be noted that  $\dot{U}_1, \dot{U}_2, \dot{U}_3$  stand for the time derivatives of the three-dimensional displacements collected in (3.1). These velocities can be included in the corresponding vector  $\dot{\mathbf{U}} = \dot{\mathbf{U}}(\alpha_1, \alpha_2, \zeta, t)$  defined below

$$\dot{\mathbf{U}} = \left[ \dot{U}_1(\alpha_1, \alpha_2, \zeta, t) \quad \dot{U}_2(\alpha_1, \alpha_2, \zeta, t) \quad \dot{U}_3(\alpha_1, \alpha_2, \zeta, t) \right]^T \quad (3.191)$$

In matrix form, expression (3.190) becomes

$$\delta\mathcal{T} = \int_{\alpha_1} \int_{\alpha_2} \int_{\zeta} \rho \left( \delta\dot{\mathbf{U}} \right)^T \dot{\mathbf{U}} A_1 A_2 H_1 H_2 d\alpha_1 d\alpha_2 d\zeta \quad (3.192)$$

For a laminated composite structure made of  $l$  layers, the variation of the kinetic energy is given by

$$\delta\mathcal{T} = \sum_{k=1}^l \int_{\zeta_k}^{\zeta_{k+1}} \int_{\alpha_1} \int_{\alpha_2} \rho^{(k)} \left( \delta\dot{\mathbf{U}} \right)^T \dot{\mathbf{U}} A_1 A_2 H_1 H_2 d\alpha_1 d\alpha_2 d\zeta \quad (3.193)$$

Recalling definition (3.159), the integration with respect to the time variable must be computed in the interval  $t_1, t_2$ . By applying the integration by part rule, one gets

$$\int_{t_1}^{t_2} \delta\mathcal{T} dt = \sum_{k=1}^l \int_{t_1}^{t_2} \int_{\zeta_k}^{\zeta_{k+1}} \int_{\alpha_1} \int_{\alpha_2} \rho^{(k)} \left( \delta\dot{\mathbf{U}} \right)^T \dot{\mathbf{U}} A_1 A_2 H_1 H_2 d\alpha_1 d\alpha_2 d\zeta dt =$$

$$\begin{aligned}
&= \sum_{k=1}^l \int_{\zeta_k}^{\zeta_{k+1}} \int_{\alpha_1}^{\alpha_2} \int_{t_1}^{t_2} \rho^{(k)} (\delta \dot{\mathbf{U}})^T \dot{\mathbf{U}} A_1 A_2 H_1 H_2 d\alpha_1 d\alpha_2 d\zeta dt = \\
&= \sum_{k=1}^l \int_{\zeta_k}^{\zeta_{k+1}} \int_{\alpha_1}^{\alpha_2} \rho^{(k)} \left( \left[ (\delta \mathbf{U})^T \dot{\mathbf{U}} \right]_{t_1}^{t_2} - \int_{t_1}^{t_2} (\delta \mathbf{U})^T \ddot{\mathbf{U}} dt \right) A_1 A_2 H_1 H_2 d\alpha_1 d\alpha_2 d\zeta = \\
&= - \sum_{k=1}^l \int_{t_1}^{t_2} \int_{\zeta_k}^{\zeta_{k+1}} \int_{\alpha_1}^{\alpha_2} \rho^{(k)} (\delta \mathbf{U})^T \ddot{\mathbf{U}} A_1 A_2 H_1 H_2 d\alpha_1 d\alpha_2 d\zeta dt \tag{3.194}
\end{aligned}$$

Due to the hypothesis of synchronous motions, the virtual displacements assume a null value at the times  $t_1, t_2$ . This is the assumption that allows to delete the quantities in square brackets in the procedure just shown. Mathematically speaking, the synchronous motion hypothesis can be expressed as  $\delta \dots(t_1) = \delta \dots(t_2) = 0$ . The following relation is achieved by inserting the definition of the displacement field (3.26) into (3.194)

$$\begin{aligned}
\int_{t_1}^{t_2} \delta \mathcal{T} dt &= - \sum_{k=1}^l \int_{t_1}^{t_2} \int_{\zeta_k}^{\zeta_{k+1}} \int_{\alpha_1}^{\alpha_2} \rho^{(k)} \left( \sum_{\tau=0}^{N+1} \mathbf{F}_\tau \delta \mathbf{u}^{(\tau)} \right)^T \left( \sum_{\eta=0}^{N+1} \mathbf{F}_\eta \ddot{\mathbf{u}}^{(\eta)} \right) A_1 A_2 H_1 H_2 d\alpha_1 d\alpha_2 d\zeta dt = \\
&= - \sum_{\eta=0}^{N+1} \sum_{\tau=0}^{N+1} \sum_{k=1}^l \int_{t_1}^{t_2} \int_{\zeta_k}^{\zeta_{k+1}} \int_{\alpha_1}^{\alpha_2} \rho^{(k)} \left( F_\tau^{\alpha_1} F_\eta^{\alpha_1} \ddot{u}_1^{(\eta)} \delta u_1^{(\tau)} + F_\tau^{\alpha_2} F_\eta^{\alpha_2} \ddot{u}_2^{(\eta)} \delta u_2^{(\tau)} + \right. \\
&\quad \left. + F_\tau^{\alpha_3} F_\eta^{\alpha_3} \ddot{u}_3^{(\eta)} \delta u_3^{(\tau)} \right) H_1 H_2 A_1 A_2 d\alpha_1 d\alpha_2 d\zeta dt = \\
&= - \sum_{\tau=0}^{N+1} \int_{t_1}^{t_2} \int_{\alpha_1}^{\alpha_2} \left( \sum_{\eta=0}^{N+1} I^{(\tau\eta)\alpha_1\alpha_1} \ddot{u}_1^{(\eta)} \right) \delta u_1^{(\tau)} + \left( \sum_{\eta=0}^{N+1} I^{(\tau\eta)\alpha_2\alpha_2} \ddot{u}_2^{(\eta)} \right) \delta u_2^{(\tau)} + \\
&\quad + \left( \sum_{\eta=0}^{N+1} I^{(\tau\eta)\alpha_3\alpha_3} \ddot{u}_3^{(\eta)} \right) \delta u_3^{(\tau)} \Big) A_1 A_2 d\alpha_1 d\alpha_2 dt = \\
&= - \sum_{\tau=0}^{N+1} \int_{t_1}^{t_2} \int_{\alpha_1}^{\alpha_2} (\delta \mathbf{u}^{(\tau)})^T \left( \sum_{\eta=0}^{N+1} \mathbf{M}^{(\tau\eta)} \ddot{\mathbf{u}}^{(\eta)} \right) A_1 A_2 d\alpha_1 d\alpha_2 dt = \tag{3.195}
\end{aligned}$$

where the inertia masses  $I^{(\tau\eta)\alpha_i\alpha_i}$  are introduced by means of the following integrals with respect to the thickness coordinate

$$I_0^{(\tau\eta)\alpha_i\alpha_i} = \sum_{k=1}^l \int_{\zeta_k}^{\zeta_{k+1}} \rho^{(k)} F_\tau^{\alpha_i} F_\eta^{\alpha_i} H_1 H_2 d\zeta \tag{3.196}$$

for  $i=1,2,3$ . These quantities can be included in the corresponding mass matrix  $\mathbf{M}^{(\tau\eta)}$  defined below

$$\mathbf{M}^{(\tau\eta)} = \begin{bmatrix} I^{(\tau\eta)\alpha_1\alpha_1} & 0 & 0 \\ 0 & I^{(\tau\eta)\alpha_2\alpha_2} & 0 \\ 0 & 0 & I^{(\tau\eta)\alpha_3\alpha_3} \end{bmatrix} \quad (3.197)$$

for  $\tau, \eta = 0, 1, 2, \dots, N, N+1$ , whose size is  $3 \times 3$ .

As far as the work done by the external loads  $L_e$  is concerned, several kinds of external actions should be considered, which can be classified as volume forces and surface forces. These quantities are applied in each point of the three-dimensional medium or within the external surfaces of the structure, respectively. Since an ESL approach is considered, their effect must be computed on the shell middle surface by means of static equivalence principles. The procedure in hand will be presented in the following taking into account different kinds of loads.

In general, the external forces are characterized by three load components related to each principal direction, for every order of kinematic expansion  $\tau$ . Those quantities can be collected in the corresponding vector  $\tilde{\mathbf{q}}^{(\tau)}$  defined below

$$\tilde{\mathbf{q}}^{(\tau)} = \begin{bmatrix} \tilde{q}_1^{(\tau)} & \tilde{q}_2^{(\tau)} & \tilde{q}_3^{(\tau)} \end{bmatrix}^T \quad (3.198)$$

for  $\tau = 0, 1, 2, \dots, N, N+1$ . Each component  $\tilde{q}_i^{(\tau)}$ , for  $i = 1, 2, 3$ , includes the effects of the surface forces  $q_{isa}^{(\tau)}$ , volume actions  $q_{iva}^{(\tau)}$ , as well as the consequences of an elastic foundation  $q_{if}^{(\tau)}$ . Thus, the vector  $\tilde{\mathbf{q}}^{(\tau)}$  can be written as follows

$$\tilde{\mathbf{q}}^{(\tau)} = \mathbf{q}_{sa}^{(\tau)} + \mathbf{q}_{va}^{(\tau)} + \mathbf{q}_f^{(\tau)} \quad (3.199)$$

in which each vector collects three load components for each order of kinematic expansion. Mathematically speaking, these vectors assume the aspect shown below

$$\mathbf{q}_{sa}^{(\tau)} = \begin{bmatrix} q_{1sa}^{(\tau)} & q_{2sa}^{(\tau)} & q_{3sa}^{(\tau)} \end{bmatrix}^T \quad (3.200)$$

$$\mathbf{q}_{va}^{(\tau)} = \begin{bmatrix} q_{1va}^{(\tau)} & q_{2va}^{(\tau)} & q_{3va}^{(\tau)} \end{bmatrix}^T \quad (3.201)$$

$$\mathbf{q}_f^{(\tau)} = \begin{bmatrix} q_{1f}^{(\tau)} & q_{2f}^{(\tau)} & q_{3f}^{(\tau)} \end{bmatrix}^T \quad (3.202)$$

for  $\tau = 0, 1, 2, \dots, N, N+1$ . The work done by the external loads  $L_e$  must include the contributions of the terms just mentioned, as well as the work done by the stress resultants

applied directly along the external edges of the reference domain, which are  $\bar{N}_1^{(\tau)\alpha_1}$ ,  $\bar{N}_{12}^{(\tau)\alpha_2}$ ,  $\bar{T}_1^{(\tau)\alpha_3}$  if the edge is characterized by constant values of  $\alpha_1$ , or  $\bar{N}_{21}^{(\tau)\alpha_1}$ ,  $\bar{N}_2^{(\tau)\alpha_2}$ ,  $\bar{T}_2^{(\tau)\alpha_3}$  if the edge is characterized by constant values of  $\alpha_2$ . These quantities can be collected in the following vectors

$$\bar{\mathbf{S}}_{\alpha_1}^{(\tau)} = \left[ \bar{N}_1^{(\tau)\alpha_1} \quad \bar{N}_{12}^{(\tau)\alpha_2} \quad \bar{T}_1^{(\tau)\alpha_3} \right]^T \quad (3.203)$$

$$\bar{\mathbf{S}}_{\alpha_2}^{(\tau)} = \left[ \bar{N}_{21}^{(\tau)\alpha_1} \quad \bar{N}_2^{(\tau)\alpha_2} \quad \bar{T}_2^{(\tau)\alpha_3} \right]^T \quad (3.204)$$

All things considered, the work done by the external loads  $L_e$  is given by

$$\begin{aligned} L_e &= L_{es} + L_{ev} + L_{ef} + L_{eb1} + L_{eb2} = \\ &= \sum_{\tau=0}^{N+1} \int \int_{\alpha_1 \alpha_2} \left( q_{1sa}^{(\tau)} u_1^{(\tau)} + q_{2sa}^{(\tau)} u_2^{(\tau)} + q_{3sa}^{(\tau)} u_3^{(\tau)} \right) A_1 A_2 d\alpha_1 d\alpha_2 + \\ &+ \sum_{\tau=0}^{N+1} \int \int_{\alpha_1 \alpha_2} \left( q_{1va}^{(\tau)} u_1^{(\tau)} + q_{2va}^{(\tau)} u_2^{(\tau)} + q_{3va}^{(\tau)} u_3^{(\tau)} \right) A_1 A_2 d\alpha_1 d\alpha_2 + \\ &+ \sum_{\tau=0}^{N+1} \int \int_{\alpha_1 \alpha_2} \left( q_{1f}^{(\tau)} u_1^{(\tau)} + q_{2f}^{(\tau)} u_2^{(\tau)} + q_{3f}^{(\tau)} u_3^{(\tau)} \right) A_1 A_2 d\alpha_1 d\alpha_2 + \\ &+ \sum_{\tau=0}^{N+1} \oint_{\alpha_2} \left( \bar{N}_1^{(\tau)\alpha_1} u_1^{(\tau)} + \bar{N}_{12}^{(\tau)\alpha_2} u_2^{(\tau)} + \bar{T}_1^{(\tau)\alpha_3} u_3^{(\tau)} \right) A_2 d\alpha_2 + \\ &+ \sum_{\tau=0}^{N+1} \oint_{\alpha_1} \left( \bar{N}_{21}^{(\tau)\alpha_1} u_1^{(\tau)} + \bar{N}_2^{(\tau)\alpha_2} u_2^{(\tau)} + \bar{T}_2^{(\tau)\alpha_3} u_3^{(\tau)} \right) A_1 d\alpha_1 dt \end{aligned} \quad (3.205)$$

where  $L_{es}$  and  $L_{ev}$  are the works done by the surface and volume loads,  $L_{ef}$  is the work done by the forces given by the elastic foundation, whereas  $L_{eb1}$  and  $L_{eb2}$  stand for the work done by the stress resultants applied directly along the external edges. The corresponding variation assumes the following aspect

$$\begin{aligned} \delta L_e &= \delta L_{es} + \delta L_{ev} + \delta L_{ef} + \delta L_{eb1} + \delta L_{eb2} = \\ &= \sum_{\tau=0}^{N+1} \int \int_{\alpha_1 \alpha_2} \left( q_{1sa}^{(\tau)} \delta u_1^{(\tau)} + q_{2sa}^{(\tau)} \delta u_2^{(\tau)} + q_{3sa}^{(\tau)} \delta u_3^{(\tau)} \right) A_1 A_2 d\alpha_1 d\alpha_2 + \\ &+ \sum_{\tau=0}^{N+1} \int \int_{\alpha_1 \alpha_2} \left( q_{1va}^{(\tau)} \delta u_1^{(\tau)} + q_{2va}^{(\tau)} \delta u_2^{(\tau)} + q_{3va}^{(\tau)} \delta u_3^{(\tau)} \right) A_1 A_2 d\alpha_1 d\alpha_2 + \\ &+ \sum_{\tau=0}^{N+1} \int \int_{\alpha_1 \alpha_2} \left( q_{1f}^{(\tau)} \delta u_1^{(\tau)} + q_{2f}^{(\tau)} \delta u_2^{(\tau)} + q_{3f}^{(\tau)} \delta u_3^{(\tau)} \right) A_1 A_2 d\alpha_1 d\alpha_2 + \end{aligned}$$

$$\begin{aligned}
 & + \sum_{\tau=0}^{N+1} \oint_{\alpha_2} \left( \bar{N}_1^{(\tau)\alpha_1} \delta u_1^{(\tau)} + \bar{N}_{12}^{(\tau)\alpha_2} \delta u_2^{(\tau)} + \bar{T}_1^{(\tau)\alpha_3} \delta u_3^{(\tau)} \right) A_2 d\alpha_2 + \\
 & + \sum_{\tau=0}^{N+1} \oint_{\alpha_1} \left( \bar{N}_{21}^{(\tau)\alpha_1} \delta u_1^{(\tau)} + \bar{N}_2^{(\tau)\alpha_2} \delta u_2^{(\tau)} + \bar{T}_2^{(\tau)\alpha_3} \delta u_3^{(\tau)} \right) A_1 d\alpha_1
 \end{aligned} \tag{3.206}$$

The integral of the variation of the work done by the external loads  $\delta L_e$  with respect to the time variable in the interval  $[t_1, t_2]$  takes the following form

$$\begin{aligned}
 \int_{t_1}^{t_2} \delta L_e dt & = \sum_{\tau=0}^{N+1} \int_{t_1}^{t_2} \int_{\alpha_1} \int_{\alpha_2} \left( q_{1sa}^{(\tau)} \delta u_1^{(\tau)} + q_{2sa}^{(\tau)} \delta u_2^{(\tau)} + q_{3sa}^{(\tau)} \delta u_3^{(\tau)} \right) A_1 A_2 d\alpha_1 d\alpha_2 dt + \\
 & + \sum_{\tau=0}^{N+1} \int_{t_1}^{t_2} \int_{\alpha_1} \int_{\alpha_2} \left( q_{1va}^{(\tau)} \delta u_1^{(\tau)} + q_{2va}^{(\tau)} \delta u_2^{(\tau)} + q_{3va}^{(\tau)} \delta u_3^{(\tau)} \right) A_1 A_2 d\alpha_1 d\alpha_2 dt + \\
 & + \sum_{\tau=0}^{N+1} \int_{t_1}^{t_2} \int_{\alpha_1} \int_{\alpha_2} \left( q_{1f}^{(\tau)} \delta u_1^{(\tau)} + q_{2f}^{(\tau)} \delta u_2^{(\tau)} + q_{3f}^{(\tau)} \delta u_3^{(\tau)} \right) A_1 A_2 d\alpha_1 d\alpha_2 dt + \\
 & + \sum_{\tau=0}^{N+1} \int_{t_1}^{t_2} \oint_{\alpha_2} \left( \bar{N}_1^{(\tau)\alpha_1} \delta u_1^{(\tau)} + \bar{N}_{12}^{(\tau)\alpha_2} \delta u_2^{(\tau)} + \bar{T}_1^{(\tau)\alpha_3} \delta u_3^{(\tau)} \right) A_2 d\alpha_2 dt + \\
 & + \sum_{\tau=0}^{N+1} \int_{t_1}^{t_2} \oint_{\alpha_1} \left( \bar{N}_{21}^{(\tau)\alpha_1} \delta u_1^{(\tau)} + \bar{N}_2^{(\tau)\alpha_2} \delta u_2^{(\tau)} + \bar{T}_2^{(\tau)\alpha_3} \delta u_3^{(\tau)} \right) A_1 d\alpha_1 dt
 \end{aligned} \tag{3.207}$$

In compact matrix form, one gets

$$\begin{aligned}
 \int_{t_1}^{t_2} \delta L_e dt & = \sum_{\tau=0}^{N+1} \int_{t_1}^{t_2} \int_{\alpha_1} \int_{\alpha_2} \left( \delta \mathbf{u}^{(\tau)} \right)^T \mathbf{q}_{sa}^{(\tau)} A_1 A_2 d\alpha_1 d\alpha_2 dt + \\
 & + \sum_{\tau=0}^{N+1} \int_{t_1}^{t_2} \int_{\alpha_1} \int_{\alpha_2} \left( \delta \mathbf{u}^{(\tau)} \right)^T \mathbf{q}_{va}^{(\tau)} A_1 A_2 d\alpha_1 d\alpha_2 dt + \\
 & + \sum_{\tau=0}^{N+1} \int_{t_1}^{t_2} \int_{\alpha_1} \int_{\alpha_2} \left( \delta \mathbf{u}^{(\tau)} \right)^T \mathbf{q}_f^{(\tau)} A_1 A_2 d\alpha_1 d\alpha_2 dt + \\
 & + \sum_{\tau=0}^{N+1} \int_{t_1}^{t_2} \oint_{\alpha_2} \left( \delta \mathbf{u}^{(\tau)} \right)^T \bar{\mathbf{S}}_{\alpha_1}^{(\tau)} A_2 d\alpha_2 dt + \\
 & + \sum_{\tau=0}^{N+1} \int_{t_1}^{t_2} \oint_{\alpha_1} \left( \delta \mathbf{u}^{(\tau)} \right)^T \bar{\mathbf{S}}_{\alpha_2}^{(\tau)} A_1 d\alpha_1 dt
 \end{aligned} \tag{3.208}$$

At this point, the Hamilton's principle (3.159) can be written as follows

$$\begin{aligned}
 & \int_{t_1}^{t_2} \left( - \sum_{\tau=0}^{N+1} \int_{\alpha_1} \int_{\alpha_2} \left( \delta \mathbf{u}^{(\tau)} \right)^T \left( \sum_{\eta=0}^{N+1} \mathbf{M}^{(\tau\eta)} \ddot{\mathbf{u}}^{(\eta)} \right) A_1 A_2 d\alpha_1 d\alpha_2 + \right. \\
 & \quad \left. - \sum_{\tau=0}^{N+1} \sum_{i=1}^3 \int_{\alpha_1} \int_{\alpha_2} \left( \delta \left( \mathbf{D}_{\Omega}^{\alpha_i} \mathbf{u}^{(\tau)} \right) \right)^T \mathbf{S}^{(\tau)\alpha_i} A_1 A_2 d\alpha_1 d\alpha_2 + \right.
 \end{aligned}$$

$$\begin{aligned}
& + \sum_{\tau=0}^{N+1} \int_{\alpha_1} \int_{\alpha_2} (\delta \mathbf{u}^{(\tau)})^T \mathbf{q}_{sa}^{(\tau)} A_1 A_2 d\alpha_1 d\alpha_2 + \sum_{\tau=0}^{N+1} \int_{\alpha_1} \int_{\alpha_2} (\delta \mathbf{u}^{(\tau)})^T \mathbf{q}_{va}^{(\tau)} A_1 A_2 d\alpha_1 d\alpha_2 + \\
& + \sum_{\tau=0}^{N+1} \int_{\alpha_1} \int_{\alpha_2} (\delta \mathbf{u}^{(\tau)})^T \mathbf{q}_f^{(\tau)} A_1 A_2 d\alpha_1 d\alpha_2 + \sum_{\tau=0}^{N+1} \oint_{\alpha_2} (\delta \mathbf{u}^{(\tau)})^T \bar{\mathbf{S}}_{\alpha_1}^{(\tau)} A_2 d\alpha_2 \\
& + \sum_{\tau=0}^{N+1} \oint_{\alpha_1} (\delta \mathbf{u}^{(\tau)})^T \bar{\mathbf{S}}_{\alpha_2}^{(\tau)} A_1 d\alpha_1 \Big) dt = 0 \tag{3.209}
\end{aligned}$$

Since equation (3.209) must be satisfied for each time interval, the following relation is achieved

$$\begin{aligned}
& - \sum_{\tau=0}^{N+1} \int_{\alpha_1} \int_{\alpha_2} (\delta \mathbf{u}^{(\tau)})^T \left( \sum_{\eta=0}^{N+1} \mathbf{M}^{(\tau\eta)} \ddot{\mathbf{u}}^{(\eta)} \right) A_1 A_2 d\alpha_1 d\alpha_2 + \\
& - \sum_{\tau=0}^{N+1} \sum_{i=1}^3 \int_{\alpha_1} \int_{\alpha_2} (\delta (\mathbf{D}_{\Omega}^{\alpha_i} \mathbf{u}^{(\tau)}))^T \mathbf{S}^{(\tau)\alpha_i} A_1 A_2 d\alpha_1 d\alpha_2 + \\
& + \sum_{\tau=0}^{N+1} \int_{\alpha_1} \int_{\alpha_2} (\delta \mathbf{u}^{(\tau)})^T \mathbf{q}_{sa}^{(\tau)} A_1 A_2 d\alpha_1 d\alpha_2 + \sum_{\tau=0}^{N+1} \int_{\alpha_1} \int_{\alpha_2} (\delta \mathbf{u}^{(\tau)})^T \mathbf{q}_{va}^{(\tau)} A_1 A_2 d\alpha_1 d\alpha_2 + \\
& + \sum_{\tau=0}^{N+1} \int_{\alpha_1} \int_{\alpha_2} (\delta \mathbf{u}^{(\tau)})^T \mathbf{q}_f^{(\tau)} A_1 A_2 d\alpha_1 d\alpha_2 + \sum_{\tau=0}^{N+1} \oint_{\alpha_2} (\delta \mathbf{u}^{(\tau)})^T \bar{\mathbf{S}}_{\alpha_1}^{(\tau)} A_2 d\alpha_2 + \\
& + \sum_{\tau=0}^{N+1} \oint_{\alpha_1} (\delta \mathbf{u}^{(\tau)})^T \bar{\mathbf{S}}_{\alpha_2}^{(\tau)} A_1 d\alpha_1 = 0 \tag{3.210}
\end{aligned}$$

Relation (3.210) could be conveniently written for each order of kinematic expansion  $\tau$ , so that one gets

$$\begin{aligned}
& - \int_{\alpha_1} \int_{\alpha_2} (\delta \mathbf{u}^{(\tau)})^T \left( \sum_{\eta=0}^{N+1} \mathbf{M}^{(\tau\eta)} \ddot{\mathbf{u}}^{(\eta)} \right) A_1 A_2 d\alpha_1 d\alpha_2 + \\
& - \sum_{i=1}^3 \int_{\alpha_1} \int_{\alpha_2} (\delta (\mathbf{D}_{\Omega}^{\alpha_i} \mathbf{u}^{(\tau)}))^T \mathbf{S}^{(\tau)\alpha_i} A_1 A_2 d\alpha_1 d\alpha_2 \\
& + \int_{\alpha_1} \int_{\alpha_2} (\delta \mathbf{u}^{(\tau)})^T \mathbf{q}_{sa}^{(\tau)} A_1 A_2 d\alpha_1 d\alpha_2 + \int_{\alpha_1} \int_{\alpha_2} (\delta \mathbf{u}^{(\tau)})^T \mathbf{q}_{va}^{(\tau)} A_1 A_2 d\alpha_1 d\alpha_2 + \\
& + \int_{\alpha_1} \int_{\alpha_2} (\delta \mathbf{u}^{(\tau)})^T \mathbf{q}_f^{(\tau)} A_1 A_2 d\alpha_1 d\alpha_2 + \oint_{\alpha_2} (\delta \mathbf{u}^{(\tau)})^T \bar{\mathbf{S}}_{\alpha_1}^{(\tau)} A_2 d\alpha_2 \\
& + \oint_{\alpha_1} (\delta \mathbf{u}^{(\tau)})^T \bar{\mathbf{S}}_{\alpha_2}^{(\tau)} A_1 d\alpha_1 = 0 \tag{3.211}
\end{aligned}$$

for  $\tau = 0, 1, 2, \dots, N, N+1$ . Expression (3.211) represents the general form of the Hamilton's principle at issue. Two different path can be pursued now in order to obtain the strong and weak formulations, of the governing equations, respectively.

### 3.1.6.1 Generalized external actions

As mentioned above, different kinds of external loads can be considered in the model. In general, they can be classified as volume and surface forces. In this section, the well-known static equivalence principle is applied in order to obtain the generalized external actions defined in the shell reference domain, which coincides with the middle surface of the structure.

#### 3.1.6.1.1 Surface loads

Surface loads are applied on the external surfaces of the shells, defined respectively by the thickness coordinate  $\zeta = -h/2$  (bottom surface) and  $\zeta = h/2$  (top surface). Three load components can be applied on each surface, which are  $q_{1a}^{(-)}, q_{2a}^{(-)}, q_{3a}^{(-)}$  on the lower surface and  $q_{1a}^{(+)}, q_{2a}^{(+)}, q_{3a}^{(+)}$  on the upper one. The positive directions of these forces are schematically depicted in Figure 3.9.

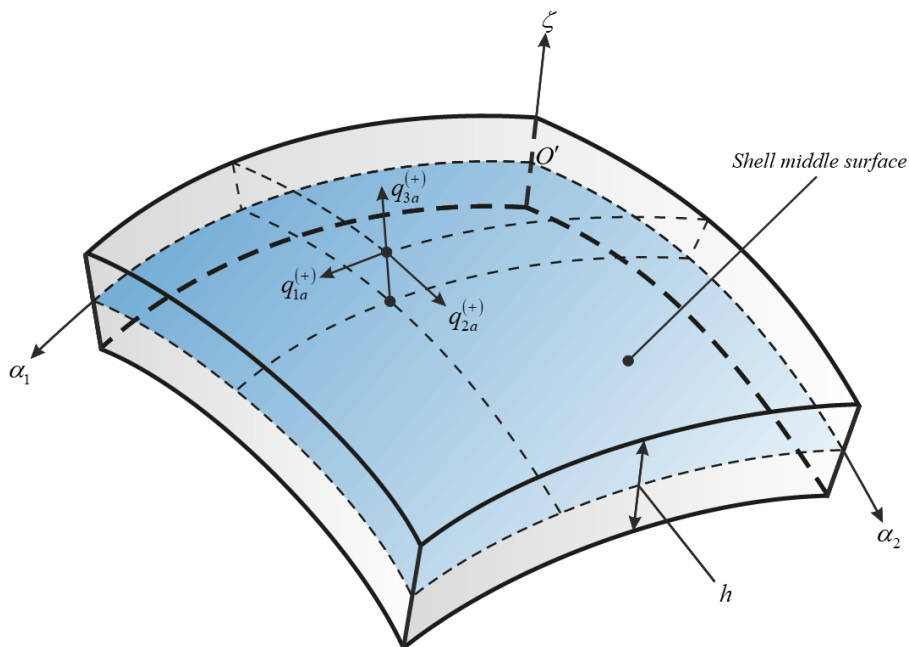


Figure 3.9 – Surface loads applied on the top surface: positive directions.

According to the principle of static equivalence, the work done by the equivalent generalized external loads applied on the shell middle surface must be equal to the work done by external forces acting on the bottom and top surfaces. Without addressing the complete treatise, which can be found in the book by Tornabene et al. [57], the generalized external forces applied on the shell middle surface  $q_{1sa}^{(\tau)}$ ,  $q_{2sa}^{(\tau)}$ ,  $q_{3sa}^{(\tau)}$  are given by

$$\begin{aligned} q_{1sa}^{(\tau)} &= q_{1a}^{(-)} F_{\tau}^{\alpha_1(-)} H_1^{(-)} H_2^{(-)} + q_{1a}^{(+)} F_{\tau}^{\alpha_1(+)} H_1^{(+)} H_2^{(+)} \\ q_{2sa}^{(\tau)} &= q_{2a}^{(-)} F_{\tau}^{\alpha_2(-)} H_1^{(-)} H_2^{(-)} + q_{2a}^{(+)} F_{\tau}^{\alpha_2(+)} H_1^{(+)} H_2^{(+)} \\ q_{3sa}^{(\tau)} &= q_{3a}^{(-)} F_{\tau}^{\alpha_3(-)} H_1^{(-)} H_2^{(-)} + q_{3a}^{(+)} F_{\tau}^{\alpha_3(+)} H_1^{(+)} H_2^{(+)} \end{aligned} \quad (3.212)$$

where  $F_{\tau}^{\alpha_i(-)}$ ,  $F_{\tau}^{\alpha_i(+)}$ , for  $i = 1, 2, 3$ , are the thickness functions evaluated at the bottom and top surfaces, respectively, whereas the geometric parameters  $H_1^{(\pm)}$ ,  $H_2^{(\pm)}$  are defined as follows

$$\begin{aligned} H_1^{(\pm)} &= 1 \pm \frac{h}{2R_1} \\ H_2^{(\pm)} &= 1 \pm \frac{h}{2R_2} \end{aligned} \quad (3.213)$$

according to the definitions shown in (3.49). For the sake of completeness, it should be recalled that point, line, as well as cross loads, can be included in the class of surface actions, as illustrated in the paper by Tornabene et al. [241].

### 3.1.6.1.2 Volume loads

In general, volume forces are proportional to the overall mass of the structure, which can be computed taking into account the density of each layer  $\rho^{(k)}$ , if a laminated composite shell is considered. In order to evaluate these volume loads, the gravitational acceleration  $\mathbf{g}$  must be introduced in the local reference system as follows

$$\mathbf{g} = g_1 \mathbf{t}_1 + g_2 \mathbf{t}_2 + g_3 \mathbf{n} \quad (3.214)$$

where  $\mathbf{t}_1, \mathbf{t}_2, \mathbf{n}$  are the unit normal vectors that identify the principal coordinates  $\alpha_1, \alpha_2, \zeta$ , respectively. The quantities  $g_1, g_2, g_3$  stand for the components of the gravitational acceleration in the local reference system, which can be evaluate as follows

$$\begin{aligned} g_1 &= \mathbf{G}^T \mathbf{t}_1 \\ g_2 &= \mathbf{G}^T \mathbf{t}_2 \\ g_3 &= \mathbf{G}^T \mathbf{n} \end{aligned} \quad (3.215)$$

where  $\mathbf{G}$  is the vector of the gravity defined in the global reference system given by

$$\mathbf{G} = G_1 \mathbf{e}_1 + G_2 \mathbf{e}_2 + G_3 \mathbf{e}_3 \quad (3.216)$$

in which  $\mathbf{e}_i$ , for  $i = 1, 2, 3$ , denote the unit vectors of the global reference system.

Without presenting the complete treatise, which can be found in the book by Tornabene et al. [57], the generalized external forces applied on the shell middle surface related to volume loads can be computed as

$$\begin{aligned} q_{1va}^{(\tau)} &= I_0^{(\tau)\alpha_1} g_1 \\ q_{2va}^{(\tau)} &= I_0^{(\tau)\alpha_2} g_2 \\ q_{3va}^{(\tau)} &= I_0^{(\tau)\alpha_3} g_3 \end{aligned} \quad (3.217)$$

where the following inertia masses  $I_0^{(\tau)\alpha_i}$ , for  $i = 1, 2, 3$ , are required

$$I_0^{(\tau)\alpha_i} = \sum_{k=1}^l \int_{\zeta_k}^{\zeta_{k+1}} \rho^{(k)} F_\tau^{\alpha_i} H_1 H_2 d\zeta \quad (3.218)$$

For the sake of completeness, it should be recalled that seismic actions can be also included in the class of volume forces, as illustrated in the book by Tornabene et al. [57], once the seismic acceleration is well-defined.

### 3.1.6.1.3 Winkler-Pasternak elastic foundation

According to the Winkler-Pasternak model for the elastic foundation, a generic shell structure resting on this kind of foundation can be analyzed by applying uniformly distributed springs at the top and bottom surfaces, depending on the side where the foundation is applied. These springs are characterized by a value of stiffness along each principal direction denoted by  $k_{1f}^{(+)}, k_{1f}^{(-)}, k_{2f}^{(+)}, k_{2f}^{(-)}, k_{3f}^{(+)}, k_{3f}^{(-)}$ , where the subscripts specify the direction, whereas the superscripts stand for the surface of application. If the Pasternak hypotheses are introduced, a shear layer characterized by shear moduli  $G_f^{(+)}, G_f^{(-)}$  can be considered, too.

The inertia features are defined once the density of the foundation at the external surfaces of the elastic foundation  $\rho_f^{(+)}, \rho_f^{(-)}$  is specified. The linear model at issue is depicted in Figure 3.10.

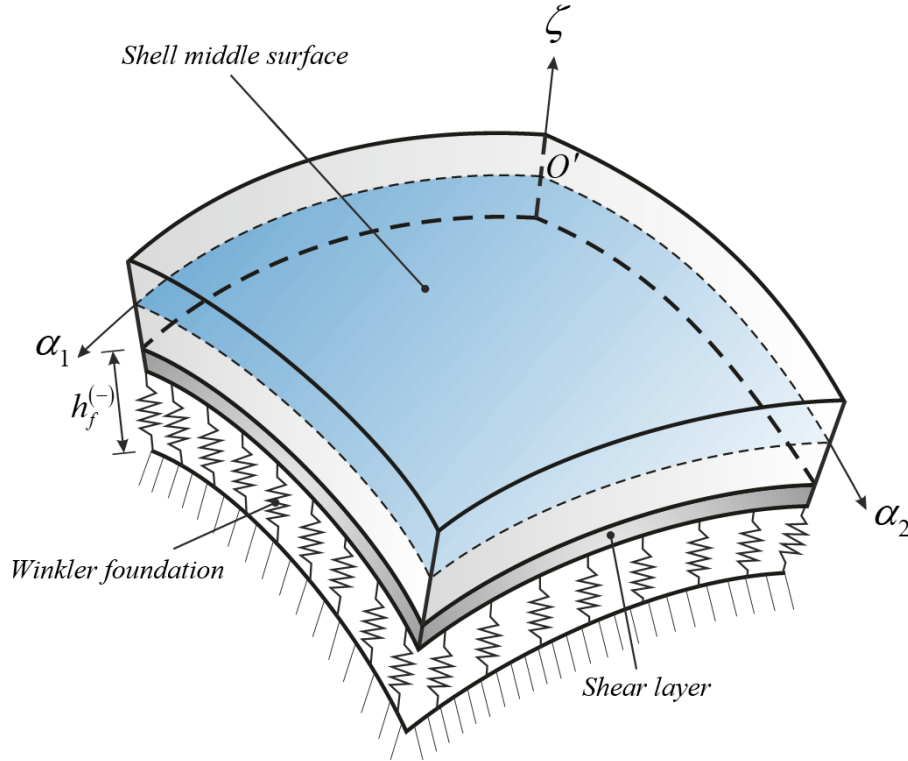


**Figure 3.10** – Winkler-Pasternak foundation applied at the bottom surface of the shell.

Without describing the complete treatise, which are presented in the book by Tornabene et al. [57], the generalized external forces applied on the shell middle surface related to this elastic foundation can be computed as follows

$$\begin{aligned}
 q_{1f}^{(\tau)} &= \sum_{\eta=0}^{N+1} \left( L_{f1}^{(\tau)\alpha_1} u_1^{(\eta)} + I_{f1}^{(\tau)\alpha_1} \ddot{u}_1^{(\eta)} \right) \\
 q_{2f}^{(\tau)} &= \sum_{\eta=0}^{N+1} \left( L_{f2}^{(\tau)\alpha_2} u_2^{(\eta)} + I_{f2}^{(\tau)\alpha_2} \ddot{u}_2^{(\eta)} \right) \\
 q_{3f}^{(\tau)} &= \sum_{\eta=0}^{N+1} \left( L_{f3}^{(\tau)\alpha_3} u_3^{(\eta)} + I_{f3}^{(\tau)\alpha_3} \ddot{u}_3^{(\eta)} \right)
 \end{aligned} \tag{3.219}$$

for  $\tau = 0, 1, 2, \dots, N, N+1$ . The stiffness of the elastic foundation is described through the terms

$L_{f1}^{(\tau)\alpha_1}, L_{f2}^{(\tau)\alpha_2}, L_{f3}^{(\tau)\alpha_3}$ , which are defined by

$$\begin{aligned}
 L_{f1}^{(\tau\eta)\alpha_1} &= -k_{1f}^{(-)} F_{\eta}^{\alpha_1(-)} F_{\tau}^{\alpha_1(-)} H_1^{(-)} H_2^{(-)} - k_{1f}^{(+)} F_{\eta}^{\alpha_1(+)} F_{\tau}^{\alpha_1(+)} H_1^{(+)} H_2^{(+)} \\
 L_{f2}^{(\tau\eta)\alpha_2} &= -k_{2f}^{(-)} F_{\eta}^{\alpha_2(-)} F_{\tau}^{\alpha_2(-)} H_1^{(-)} H_2^{(-)} - k_{2f}^{(+)} F_{\eta}^{\alpha_2(+)} F_{\tau}^{\alpha_2(+)} H_1^{(+)} H_2^{(+)} \\
 L_{f3}^{(\tau\eta)\alpha_3} &= -\left(k_{3f}^{(-)} - G_f^{(-)} \nabla_{(-)}^2\right) F_{\eta}^{\alpha_3(-)} F_{\tau}^{\alpha_3(-)} H_1^{(-)} H_2^{(-)} - \left(k_{3f}^{(+)} - G_f^{(+)} \nabla_{(+)}^2\right) F_{\eta}^{\alpha_3(+)} F_{\tau}^{\alpha_3(+)} H_1^{(+)} H_2^{(+)}
 \end{aligned} \tag{3.220}$$

where the quantities  $\nabla_{(\pm)}^2$  represent the Laplacian operator in curvilinear orthogonal coordinates evaluated at the top and bottom surfaces, respectively, required to describe the shear stiffness of the Pasternak model. Analytically speaking, the Laplacian operator assumes the following aspect

$$\begin{aligned}
 \nabla^2 = & \left( \frac{1}{A_1^2 H_1^2} \frac{\partial^2}{\partial \alpha_1^2} + \frac{1}{A_2^2 H_2^2} \frac{\partial^2}{\partial \alpha_2^2} + \left( \frac{1}{A_1 A_2 H_1} \frac{\partial A_2}{\partial \alpha_1} - \frac{\zeta}{A_1^2 R_2^2 H_1^2 H_2} \frac{\partial R_2}{\partial \alpha_1} + \right. \right. \\
 & \left. \left. - \frac{1}{A_1^3 H_1^2} \frac{\partial A_1}{\partial \alpha_1} + \frac{\zeta}{A_1^2 R_1^2 H_1^3} \frac{\partial R_1}{\partial \alpha_1} \right) \frac{\partial}{\partial \alpha_1} + \left( \frac{1}{A_1 A_2 H_2} \frac{\partial A_1}{\partial \alpha_2} - \frac{\zeta}{A_2^2 R_1^2 H_2^2 H_1} \frac{\partial R_1}{\partial \alpha_2} + \right. \right. \\
 & \left. \left. - \frac{1}{A_2^3 H_2^2} \frac{\partial A_2}{\partial \alpha_2} + \frac{\zeta}{A_2^2 R_2^2 H_2^3} \frac{\partial R_2}{\partial \alpha_2} \right) \frac{\partial}{\partial \alpha_2} \right)
 \end{aligned} \tag{3.221}$$

which must be computed at the external surfaces for  $\zeta = \pm h/2$ , in order to evaluate the corresponding quantities  $\nabla_{(\pm)}^2$ .

On the other hand, the inertia properties in (3.219) are taken into account once the quantities  $I_{f1}^{(\tau\eta)\alpha_1}, I_{f2}^{(\tau\eta)\alpha_2}, I_{f3}^{(\tau\eta)\alpha_3}$  are defined. They are specified below

$$\begin{aligned}
 I_{f1}^{(\tau\eta)\alpha_1} &= -\frac{1}{3} \rho_f^{(-)} h_f^{(-)} F_{\eta}^{\alpha_1(-)} F_{\tau}^{\alpha_1(-)} H_1^{(-)} H_2^{(-)} - \frac{1}{3} \rho_f^{(+)} h_f^{(+)} F_{\eta}^{\alpha_1(+)} F_{\tau}^{\alpha_1(+)} H_1^{(+)} H_2^{(+)} \\
 I_{f2}^{(\tau\eta)\alpha_2} &= -\frac{1}{3} \rho_f^{(-)} h_f^{(-)} F_{\eta}^{\alpha_2(-)} F_{\tau}^{\alpha_2(-)} H_1^{(-)} H_2^{(-)} - \frac{1}{3} \rho_f^{(+)} h_f^{(+)} F_{\eta}^{\alpha_2(+)} F_{\tau}^{\alpha_2(+)} H_1^{(+)} H_2^{(+)} \\
 I_{f3}^{(\tau\eta)\alpha_3} &= -\frac{1}{3} \rho_f^{(-)} h_f^{(-)} F_{\eta}^{\alpha_3(-)} F_{\tau}^{\alpha_3(-)} H_1^{(-)} H_2^{(-)} - \frac{1}{3} \rho_f^{(+)} h_f^{(+)} F_{\eta}^{\alpha_3(+)} F_{\tau}^{\alpha_3(+)} H_1^{(+)} H_2^{(+)}
 \end{aligned} \tag{3.222}$$

The expression (3.219) can be conveniently written in matrix form as follows

$$\begin{bmatrix} q_{1f}^{(\tau)} \\ q_{2f}^{(\tau)} \\ q_{3f}^{(\tau)} \end{bmatrix} = \sum_{\eta=0}^{N+1} \begin{bmatrix} L_{f1}^{(\tau\eta)\alpha_1} & 0 & 0 \\ 0 & L_{f2}^{(\tau\eta)\alpha_2} & 0 \\ 0 & 0 & L_{f3}^{(\tau\eta)\alpha_3} \end{bmatrix} \begin{bmatrix} u_1^{(\eta)} \\ u_2^{(\eta)} \\ u_3^{(\eta)} \end{bmatrix} + \sum_{\eta=0}^{N+1} \begin{bmatrix} I_{f1}^{(\tau\eta)\alpha_1} & 0 & 0 \\ 0 & I_{f2}^{(\tau\eta)\alpha_2} & 0 \\ 0 & 0 & I_{f3}^{(\tau\eta)\alpha_3} \end{bmatrix} \begin{bmatrix} \ddot{u}_1^{(\eta)} \\ \ddot{u}_2^{(\eta)} \\ \ddot{u}_3^{(\eta)} \end{bmatrix} \tag{3.223}$$

Analogously, a compact matrix form can be used too

$$\mathbf{q}_f^{(\tau)} = \sum_{\eta=0}^{N+1} \mathbf{L}_f^{(\tau\eta)} \mathbf{u}^{(\eta)} + \sum_{\eta=0}^{N+1} \mathbf{M}_f^{(\tau\eta)} \ddot{\mathbf{u}}^{(\eta)} \tag{3.224}$$

for  $\tau = 0, 1, 2, \dots, N, N+1$ . The stiffness matrix  $\mathbf{L}_f^{(\tau\eta)}$  and the mass matrix  $\mathbf{M}_f^{(\tau\eta)}$  of the foundation can be easily deduced by comparing equations (3.223) and (3.224). One gets

$$\mathbf{L}_f^{(\tau\eta)} = \begin{bmatrix} L_{f1}^{(\tau\eta)\alpha_1} & 0 & 0 \\ 0 & L_{f2}^{(\tau\eta)\alpha_2} & 0 \\ 0 & 0 & L_{f3}^{(\tau\eta)\alpha_3} \end{bmatrix}, \quad \mathbf{M}_f^{(\tau\eta)} = \begin{bmatrix} I_{f1}^{(\tau\eta)\alpha_1} & 0 & 0 \\ 0 & I_{f2}^{(\tau\eta)\alpha_2} & 0 \\ 0 & 0 & I_{f3}^{(\tau\eta)\alpha_3} \end{bmatrix} \quad (3.225)$$

### 3.1.7 STRONG FORMULATION

The strong form of the governing equations can be deduced directly from the general expression of the Hamilton's variational principle obtained in (3.211). A brief summary of the formulation in hand is only presented in this section. A more complete treatise can be found in the book by Tornabene et al. [57].

Having in mind the Hamilton's principle (3.211), it should be noted that the variation of the derivatives must be performed as far as the elastic energy of deformation  $\delta\Phi$  is concerned. For this purpose, the integration by part rule can be applied. For the sake of conciseness, the procedure is shown in matrix form, but the complete treatise in extended notation is presented in the book by Tornabene et al. [57]. One gets

$$\begin{aligned} \delta\Phi &= \sum_{i=1}^3 \int \int_{\alpha_1 \alpha_2} \left( \delta \left( \mathbf{D}_\Omega^{\alpha_i} \mathbf{u}^{(\tau)} \right) \right)^T \mathbf{S}^{(\tau)\alpha_i} A_1 A_2 d\alpha_1 d\alpha_2 = \\ &= - \sum_{i=1}^3 \int \int_{\alpha_1 \alpha_2} \left( \delta \mathbf{u}^{(\tau)} \right)^T \mathbf{D}_\Omega^{*\alpha_i} \mathbf{S}^{(\tau)\alpha_i} A_1 A_2 d\alpha_1 d\alpha_2 + \\ &\quad + \oint_{\alpha_2} \left( \delta \mathbf{u}^{(\tau)} \right)^T \mathbf{S}_{\alpha_1}^{(\tau)} A_2 d\alpha_2 + \oint_{\alpha_1} \left( \delta \mathbf{u}^{(\tau)} \right)^T \mathbf{S}_{\alpha_2}^{(\tau)} A_1 d\alpha_1 \end{aligned} \quad (3.226)$$

for  $\tau = 0, 1, 2, \dots, N, N+1$ , where  $\mathbf{D}_\Omega^{*\alpha_i}$  stands for the equilibrium operators defined below

$$\mathbf{D}_\Omega^{*\alpha_1} = \begin{bmatrix} \frac{1}{A_1} \frac{\partial}{\partial \alpha_1} + \frac{1}{A_1 A_2} \frac{\partial A_2}{\partial \alpha_1} & -\frac{1}{A_1 A_2} \frac{\partial A_2}{\partial \alpha_1} & \frac{1}{A_1 A_2} \frac{\partial A_1}{\partial \alpha_2} & \frac{1}{A_2} \frac{\partial}{\partial \alpha_2} + \frac{1}{A_1 A_2} \frac{\partial A_1}{\partial \alpha_2} & \frac{1}{R_1} & 0 & -1 & 0 & 0 \\ 0 & 0 & 0 & 0 & 0 & 0 & 0 & 0 & 0 \\ 0 & 0 & 0 & 0 & 0 & 0 & 0 & 0 & 0 \end{bmatrix} \quad (3.227)$$

$$\mathbf{D}_{\Omega}^{*\alpha_2} = \begin{bmatrix} 0 & 0 & 0 & 0 & 0 & 0 & 0 & 0 & 0 & 0 \\ -\frac{1}{A_1 A_2} \frac{\partial A_1}{\partial \alpha_2} & \frac{1}{A_2} \frac{\partial}{\partial \alpha_2} + \frac{1}{A_1 A_2} \frac{\partial A_1}{\partial \alpha_2} & \frac{1}{A_1} \frac{\partial}{\partial \alpha_1} + \frac{1}{A_1 A_2} \frac{\partial A_2}{\partial \alpha_1} & \frac{1}{A_1 A_2} \frac{\partial A_2}{\partial \alpha_1} & 0 & \frac{1}{R_2} & 0 & -1 & 0 \\ 0 & 0 & 0 & 0 & 0 & 0 & 0 & 0 & 0 \end{bmatrix} \quad (3.228)$$

$$\mathbf{D}_{\Omega}^{*\alpha_3} = \begin{bmatrix} 0 & 0 & 0 & 0 & 0 & 0 & 0 & 0 & 0 \\ 0 & 0 & 0 & 0 & 0 & 0 & 0 & 0 & 0 \\ -\frac{1}{R_1} & -\frac{1}{R_2} & 0 & 0 & \frac{1}{A_1} \frac{\partial}{\partial \alpha_1} + \frac{1}{A_1 A_2} \frac{\partial A_2}{\partial \alpha_1} & \frac{1}{A_2} \frac{\partial}{\partial \alpha_2} + \frac{1}{A_1 A_2} \frac{\partial A_1}{\partial \alpha_2} & 0 & 0 & -1 \end{bmatrix} \quad (3.229)$$

On the other hand, the vectors  $\mathbf{S}_{\alpha_1}^{(\tau)}$  and  $\mathbf{S}_{\alpha_2}^{(\tau)}$  collect the resultants of the internal stresses evaluated along the edges of the shell middle surface defined as follows

$$\mathbf{S}_{\alpha_1}^{(\tau)} = \left[ N_1^{(\tau)\alpha_1} \quad N_{12}^{(\tau)\alpha_2} \quad T_1^{(\tau)\alpha_3} \right]^T \quad (3.230)$$

$$\mathbf{S}_{\alpha_2}^{(\tau)} = \left[ N_{21}^{(\tau)\alpha_1} \quad N_2^{(\tau)\alpha_2} \quad T_2^{(\tau)\alpha_3} \right]^T \quad (3.231)$$

for  $\tau = 0, 1, 2, \dots, N, N+1$ . By inserting expression (3.226) into (3.211), one gets

$$\begin{aligned} & - \int_{\alpha_1} \int_{\alpha_2} \left( \delta \mathbf{u}^{(\tau)} \right)^T \left( \sum_{\eta=0}^{N+1} \mathbf{M}^{(\tau\eta)} \ddot{\mathbf{u}}^{(\eta)} \right) A_1 A_2 d\alpha_1 d\alpha_2 + \\ & + \sum_{i=1}^3 \int_{\alpha_1} \int_{\alpha_2} \left( \delta \mathbf{u}^{(\tau)} \right)^T \mathbf{D}_{\Omega}^{*\alpha_i} \mathbf{S}^{(\tau)\alpha_i} A_1 A_2 d\alpha_1 d\alpha_2 + \\ & + \int_{\alpha_1} \int_{\alpha_2} \left( \delta \mathbf{u}^{(\tau)} \right)^T \mathbf{q}_{sa}^{(\tau)} A_1 A_2 d\alpha_1 d\alpha_2 + \int_{\alpha_1} \int_{\alpha_2} \left( \delta \mathbf{u}^{(\tau)} \right)^T \mathbf{q}_{va}^{(\tau)} A_1 A_2 d\alpha_1 d\alpha_2 + \\ & + \int_{\alpha_1} \int_{\alpha_2} \left( \delta \mathbf{u}^{(\tau)} \right)^T \mathbf{q}_f^{(\tau)} A_1 A_2 d\alpha_1 d\alpha_2 + \oint_{\alpha_2} \left( \delta \mathbf{u}^{(\tau)} \right)^T \bar{\mathbf{S}}_{\alpha_1}^{(\tau)} A_2 d\alpha_2 \\ & + \oint_{\alpha_1} \left( \delta \mathbf{u}^{(\tau)} \right)^T \bar{\mathbf{S}}_{\alpha_2}^{(\tau)} A_1 d\alpha_1 - \oint_{\alpha_2} \left( \delta \mathbf{u}^{(\tau)} \right)^T \mathbf{S}_{\alpha_1}^{(\tau)} A_2 d\alpha_2 + \\ & - \oint_{\alpha_1} \left( \delta \mathbf{u}^{(\tau)} \right)^T \mathbf{S}_{\alpha_2}^{(\tau)} A_1 d\alpha_1 = 0 \end{aligned} \quad (3.232)$$

This relation is satisfied once all the multiplicative coefficients of each variation are null, where the variations collected into  $\delta \mathbf{u}^{(\tau)}$  denote the arbitrary generalized displacements. As a result, the motion equation are obtained, as well as the boundary conditions. In particular, three equations of motion are derived for each order of kinematic expansion  $\tau$

$$- \sum_{\eta=0}^{N+1} \mathbf{M}^{(\tau\eta)} \ddot{\mathbf{u}}^{(\eta)} + \sum_{i=1}^3 \mathbf{D}_{\Omega}^{*\alpha_i} \mathbf{S}^{(\tau)\alpha_i} + \mathbf{q}_{sa}^{(\tau)} + \mathbf{q}_{va}^{(\tau)} + \mathbf{q}_f^{(\tau)} = 0 \quad (3.233)$$

At this point, the motion equations can be written as a function of the generalized displacements collected in  $\mathbf{u}^{(\tau)}$  if the definitions of the generalized stress resultants (3.179) are recalled. One gets

$$-\sum_{\eta=0}^{N+1} \mathbf{M}^{(\tau\eta)} \ddot{\mathbf{u}}^{(\eta)} + \sum_{\eta=0}^{N+1} \mathbf{L}^{(\tau\eta)} \mathbf{u}^{(\eta)} + \mathbf{q}_{sa}^{(\tau)} + \mathbf{q}_{va}^{(\tau)} + \mathbf{q}_f^{(\tau)} = 0 \quad (3.234)$$

where the fundamental operator  $\mathbf{L}^{(\tau\eta)}$  has been introduced

$$\mathbf{L}^{(\tau\eta)} = \sum_{i=1}^3 \sum_{j=1}^3 \mathbf{D}_{\Omega}^{*\alpha_i} \mathbf{A}^{(\tau\eta)\alpha_i\alpha_j} \mathbf{D}_{\Omega}^{\alpha_j} = \begin{bmatrix} L_{11}^{(\tau\eta)\alpha_1\alpha_1} & L_{12}^{(\tau\eta)\alpha_1\alpha_2} & L_{13}^{(\tau\eta)\alpha_1\alpha_3} \\ L_{21}^{(\tau\eta)\alpha_2\alpha_1} & L_{22}^{(\tau\eta)\alpha_2\alpha_2} & L_{23}^{(\tau\eta)\alpha_2\alpha_3} \\ L_{31}^{(\tau\eta)\alpha_3\alpha_1} & L_{32}^{(\tau\eta)\alpha_3\alpha_2} & L_{33}^{(\tau\eta)\alpha_3\alpha_3} \end{bmatrix} \quad (3.235)$$

Consequently, by defining  $\mathbf{q}^{(\tau)} = \mathbf{q}_{sa}^{(\tau)} + \mathbf{q}_{va}^{(\tau)}$  and introducing the expressions of the external loads due to an elastic foundation  $\mathbf{q}_f^{(\tau)}$ , equation (3.234) becomes

$$\sum_{\eta=0}^{N+1} (\mathbf{L}^{(\tau\eta)} + \mathbf{L}_f^{(\tau\eta)}) \mathbf{u}^{(\eta)} + \mathbf{q}^{(\tau)} = \sum_{\eta=0}^{N+1} (\mathbf{M}^{(\tau\eta)} - \mathbf{M}_f^{(\tau\eta)}) \ddot{\mathbf{u}}^{(\eta)} \quad (3.236)$$

for  $\tau = 0, 1, 2, \dots, N, N+1$ . Relations (3.236) are known as fundamental equations. A generic element  $L_{fg}^{(\tau\eta)\alpha_i\alpha_j}$  of the fundamental operator defined in (3.235) takes the following aspect for a generic shell structure in a principal curvilinear coordinate system, for  $f, g = 1, 2, 3$ ,  $\tau, \eta = 0, 1, 2, \dots, N, N+1$ , and  $i, j = 1, 2, 3$

$$\begin{aligned} L_{11}^{(\tau\eta)\alpha_1\alpha_1} = & \frac{A_{11(20)}^{(\tau\eta)\alpha_1\alpha_1}}{A_1^2} \frac{\partial^2}{\partial \alpha_1^2} + \left( -\frac{A_{11(20)}^{(\tau\eta)\alpha_1\alpha_1}}{A_1^3} \frac{\partial A_1}{\partial \alpha_1} + \frac{A_{11(20)}^{(\tau\eta)\alpha_1\alpha_1}}{A_1^2 A_2} \frac{\partial A_2}{\partial \alpha_1} + \frac{1}{A_1^2} \frac{\partial A_{11(20)}^{(\tau\eta)\alpha_1\alpha_1}}{\partial \alpha_1} + \frac{1}{A_1 A_2} \frac{\partial A_{16(11)}^{(\tau\eta)\alpha_1\alpha_1}}{\partial \alpha_2} \right) \frac{\partial}{\partial \alpha_1} + \frac{2A_{16(11)}^{(\tau\eta)\alpha_1\alpha_1}}{A_1 A_2} \frac{\partial^2}{\partial \alpha_1 \partial \alpha_2} + \\ & + \frac{A_{66(02)}^{(\tau\eta)\alpha_1\alpha_1}}{A_2^2} \frac{\partial^2}{\partial \alpha_2^2} + \left( -\frac{A_{66(02)}^{(\tau\eta)\alpha_1\alpha_1}}{A_2^3} \frac{\partial A_2}{\partial \alpha_2} + \frac{A_{66(02)}^{(\tau\eta)\alpha_1\alpha_1}}{A_1 A_2^2} \frac{\partial A_1}{\partial \alpha_2} + \frac{1}{A_2^2} \frac{\partial A_{66(02)}^{(\tau\eta)\alpha_1\alpha_1}}{\partial \alpha_2} + \frac{1}{A_1 A_2} \frac{\partial A_{16(11)}^{(\tau\eta)\alpha_1\alpha_1}}{\partial \alpha_1} \right) \frac{\partial}{\partial \alpha_2} + \\ & + A_{12(11)}^{(\tau\eta)\alpha_1\alpha_1} \left( \frac{1}{A_1^2 A_2} \frac{\partial^2 A_2}{\partial \alpha_1^2} - \frac{1}{A_1^3 A_2} \frac{\partial A_1}{\partial \alpha_1} \frac{\partial A_2}{\partial \alpha_1} \right) + A_{16(20)}^{(\tau\eta)\alpha_1\alpha_1} \left( \frac{1}{A_1^3 A_2} \frac{\partial A_1}{\partial \alpha_1} \frac{\partial A_1}{\partial \alpha_2} - \frac{1}{A_1^2 A_2} \frac{\partial^2 A_1}{\partial \alpha_1 \partial \alpha_2} \right) + \\ & + A_{66(11)}^{(\tau\eta)\alpha_1\alpha_1} \left( \frac{1}{A_1 A_2^3} \frac{\partial A_1}{\partial \alpha_2} \frac{\partial A_2}{\partial \alpha_2} - \frac{1}{A_1 A_2^2} \frac{\partial^2 A_1}{\partial \alpha_2^2} \right) + A_{26(02)}^{(\tau\eta)\alpha_1\alpha_1} \left( \frac{1}{A_1 A_2^2} \frac{\partial^2 A_2}{\partial \alpha_1 \partial \alpha_2} - \frac{1}{A_1 A_2^3} \frac{\partial A_2}{\partial \alpha_1} \frac{\partial A_2}{\partial \alpha_2} \right) + \\ & + \left( \frac{1}{A_1^2 A_2} \frac{\partial A_{12(11)}^{(\tau\eta)\alpha_1\alpha_1}}{\partial \alpha_1} + \frac{1}{A_1 A_2^2} \frac{\partial A_{26(02)}^{(\tau\eta)\alpha_1\alpha_1}}{\partial \alpha_2} \right) \frac{\partial A_2}{\partial \alpha_1} - \left( \frac{1}{A_1^2 A_2} \frac{\partial A_{16(20)}^{(\tau\eta)\alpha_1\alpha_1}}{\partial \alpha_1} + \frac{1}{A_1 A_2^2} \frac{\partial A_{66(11)}^{(\tau\eta)\alpha_1\alpha_1}}{\partial \alpha_2} \right) \frac{\partial A_1}{\partial \alpha_2} + \\ & + \frac{2A_{26(11)}^{(\tau\eta)\alpha_1\alpha_1}}{A_1^2 A_2^2} \frac{\partial A_1}{\partial \alpha_2} \frac{\partial A_2}{\partial \alpha_1} - \frac{A_{22(02)}^{(\tau\eta)\alpha_1\alpha_1}}{A_1^2 A_2^2} \left( \frac{\partial A_2}{\partial \alpha_1} \right)^2 - \frac{A_{66(20)}^{(\tau\eta)\alpha_1\alpha_1}}{A_1^2 A_2^2} \left( \frac{\partial A_1}{\partial \alpha_2} \right)^2 - \frac{A_{44(20)}^{(\tau\eta)\alpha_1\alpha_1}}{R_1^2} + \frac{A_{44(10)}^{(\tau\eta)\alpha_1\alpha_1}}{R_1} + \frac{A_{44(10)}^{(\bar{\tau}\eta)\alpha_1\alpha_1}}{R_1} - A_{44(00)}^{(\bar{\tau}\eta)\alpha_1\alpha_1} \end{aligned}$$

$$\begin{aligned}
 L_{12}^{(\tau\eta)\alpha_1\alpha_2} = & \frac{A_{16(20)}^{(\tau\eta)\alpha_1\alpha_2}}{A_1^2} \frac{\partial^2}{\partial \alpha_1^2} + \left( -\frac{A_{16(20)}^{(\tau\eta)\alpha_1\alpha_2}}{A_1^3} \frac{\partial A_1}{\partial \alpha_1} + \frac{A_{11(20)}^{(\tau\eta)\alpha_1\alpha_2} + A_{66(20)}^{(\tau\eta)\alpha_1\alpha_2}}{A_1^2 A_2} \frac{\partial A_1}{\partial \alpha_2} + \frac{A_{16(20)}^{(\tau\eta)\alpha_1\alpha_2} - A_{16(11)}^{(\tau\eta)\alpha_1\alpha_2} - A_{26(11)}^{(\tau\eta)\alpha_1\alpha_2}}{A_1^2 A_2} \frac{\partial A_2}{\partial \alpha_1} + \right. \\
 & \left. + \frac{1}{A_1^2} \frac{\partial A_{16(20)}^{(\tau\eta)\alpha_1\alpha_2}}{\partial \alpha_1} + \frac{1}{A_1 A_2} \frac{\partial A_{66(11)}^{(\tau\eta)\alpha_1\alpha_2}}{\partial \alpha_2} \right) \frac{\partial}{\partial \alpha_1} + \frac{A_{12(11)}^{(\tau\eta)\alpha_1\alpha_2} + A_{66(11)}^{(\tau\eta)\alpha_1\alpha_2}}{A_1 A_2} \frac{\partial^2}{\partial \alpha_1 \partial \alpha_2} + \frac{A_{26(02)}^{(\tau\eta)\alpha_1\alpha_2}}{A_2^2} \frac{\partial^2}{\partial \alpha_2^2} + \\
 & + \left( -\frac{A_{26(02)}^{(\tau\eta)\alpha_1\alpha_2}}{A_2^3} \frac{\partial A_2}{\partial \alpha_2} - \frac{A_{22(02)}^{(\tau\eta)\alpha_1\alpha_2} + A_{66(02)}^{(\tau\eta)\alpha_1\alpha_2}}{A_1 A_2^2} \frac{\partial A_2}{\partial \alpha_1} + \frac{A_{26(02)}^{(\tau\eta)\alpha_1\alpha_2} + A_{16(11)}^{(\tau\eta)\alpha_1\alpha_2} + A_{26(11)}^{(\tau\eta)\alpha_1\alpha_2}}{A_1 A_2^2} \frac{\partial A_1}{\partial \alpha_2} + \right. \\
 & \left. + \frac{1}{A_2^2} \frac{\partial A_{26(02)}^{(\tau\eta)\alpha_1\alpha_2}}{\partial \alpha_2} + \frac{1}{A_1 A_2} \frac{\partial A_{12(11)}^{(\tau\eta)\alpha_1\alpha_2}}{\partial \alpha_1} \right) \frac{\partial}{\partial \alpha_2} + A_{11(20)}^{(\tau\eta)\alpha_1\alpha_2} \left( \frac{1}{A_1^2 A_2} \frac{\partial^2 A_1}{\partial \alpha_1 \partial \alpha_2} - \frac{1}{A_1^3 A_2} \frac{\partial A_1}{\partial \alpha_1} \frac{\partial A_1}{\partial \alpha_2} \right) + \\
 & + A_{16(11)}^{(\tau\eta)\alpha_1\alpha_2} \left( \frac{1}{A_1 A_2^2} \frac{\partial^2 A_1}{\partial \alpha_2^2} - \frac{1}{A_1 A_2^3} \frac{\partial A_1}{\partial \alpha_2} \frac{\partial A_2}{\partial \alpha_2} + \frac{1}{A_1^3 A_2} \frac{\partial A_1}{\partial \alpha_1} \frac{\partial A_2}{\partial \alpha_1} - \frac{1}{A_1^2 A_2} \frac{\partial^2 A_2}{\partial \alpha_1^2} \right) + \\
 & + A_{66(02)}^{(\tau\eta)\alpha_1\alpha_2} \left( \frac{1}{A_1 A_2^3} \frac{\partial A_2}{\partial \alpha_1} \frac{\partial A_2}{\partial \alpha_2} - \frac{1}{A_1 A_2^2} \frac{\partial^2 A_2}{\partial \alpha_1 \partial \alpha_2} \right) + \left( \frac{1}{A_1^2 A_2} \frac{\partial A_{11(20)}^{(\tau\eta)\alpha_1\alpha_2}}{\partial \alpha_1} + \frac{1}{A_1 A_2^2} \frac{\partial A_{16(11)}^{(\tau\eta)\alpha_1\alpha_2}}{\partial \alpha_2} \right) \frac{\partial A_1}{\partial \alpha_2} + \\
 & - \left( \frac{1}{A_1^2 A_2} \frac{\partial A_{16(11)}^{(\tau\eta)\alpha_1\alpha_2}}{\partial \alpha_1} + \frac{1}{A_1 A_2^2} \frac{\partial A_{66(02)}^{(\tau\eta)\alpha_1\alpha_2}}{\partial \alpha_2} \right) \frac{\partial A_2}{\partial \alpha_1} - \frac{A_{12(11)}^{(\tau\eta)\alpha_1\alpha_2} + A_{66(11)}^{(\tau\eta)\alpha_1\alpha_2}}{A_1^2 A_2^2} \frac{\partial A_1}{\partial \alpha_2} \frac{\partial A_2}{\partial \alpha_1} + \frac{A_{26(02)}^{(\tau\eta)\alpha_1\alpha_2}}{A_1^2 A_2^2} \left( \frac{\partial A_2}{\partial \alpha_1} \right)^2 + \\
 & + \frac{A_{16(20)}^{(\tau\eta)\alpha_1\alpha_2}}{A_1^2 A_2^2} \left( \frac{\partial A_1}{\partial \alpha_2} \right)^2 - \frac{A_{45(11)}^{(\tau\eta)\alpha_1\alpha_2}}{R_1 R_2} + \frac{A_{45(10)}^{(\tau\eta)\alpha_1\alpha_2}}{R_1} + \frac{A_{45(01)}^{(\tau\eta)\alpha_1\alpha_2}}{R_2} - A_{45(00)}^{(\tau\eta)\alpha_1\alpha_2}
 \end{aligned}$$

$$\begin{aligned}
 L_{13}^{(\tau\eta)\alpha_1\alpha_3} = & \left( \frac{A_{11(20)}^{(\tau\eta)\alpha_1\alpha_3} + A_{44(20)}^{(\tau\eta)\alpha_1\alpha_3}}{A_1 R_1} + \frac{A_{12(11)}^{(\tau\eta)\alpha_1\alpha_3}}{A_1 R_2} + \frac{A_{13(10)}^{(\tau\eta)\alpha_1\alpha_3} - A_{44(10)}^{(\tau\eta)\alpha_1\alpha_3}}{A_1} \right) \frac{\partial}{\partial \alpha_1} + \\
 & + \left( \frac{A_{16(11)}^{(\tau\eta)\alpha_1\alpha_3} + A_{45(11)}^{(\tau\eta)\alpha_1\alpha_3}}{A_2 R_1} + \frac{A_{26(02)}^{(\tau\eta)\alpha_1\alpha_3}}{A_2 R_2} + \frac{A_{36(01)}^{(\tau\eta)\alpha_1\alpha_3} - A_{45(01)}^{(\tau\eta)\alpha_1\alpha_3}}{A_2} \right) \frac{\partial}{\partial \alpha_2} + \\
 & + \left( \frac{A_{11(20)}^{(\tau\eta)\alpha_1\alpha_3} - A_{12(11)}^{(\tau\eta)\alpha_1\alpha_3}}{A_1 A_2 R_1} + \frac{A_{12(11)}^{(\tau\eta)\alpha_1\alpha_3} - A_{22(02)}^{(\tau\eta)\alpha_1\alpha_3}}{A_1 A_2 R_2} + \frac{A_{13(10)}^{(\tau\eta)\alpha_1\alpha_3} - A_{23(01)}^{(\tau\eta)\alpha_1\alpha_3}}{A_1 A_2} \right) \frac{\partial A_2}{\partial \alpha_1} + \\
 & + \left( \frac{A_{16(11)}^{(\tau\eta)\alpha_1\alpha_3} + A_{16(20)}^{(\tau\eta)\alpha_1\alpha_3}}{A_1 A_2 R_1} + \frac{A_{26(02)}^{(\tau\eta)\alpha_1\alpha_3} + A_{26(11)}^{(\tau\eta)\alpha_1\alpha_3}}{A_1 A_2 R_2} + \frac{A_{36(01)}^{(\tau\eta)\alpha_1\alpha_3} + A_{36(10)}^{(\tau\eta)\alpha_1\alpha_3}}{A_1 A_2} \right) \frac{\partial A_1}{\partial \alpha_2} + \\
 & + \frac{1}{A_1 R_1} \frac{\partial A_{11(20)}^{(\tau\eta)\alpha_1\alpha_3}}{\partial \alpha_1} + \frac{1}{A_1 R_2} \frac{\partial A_{12(11)}^{(\tau\eta)\alpha_1\alpha_3}}{\partial \alpha_1} + \frac{1}{A_2 R_1} \frac{\partial A_{16(11)}^{(\tau\eta)\alpha_1\alpha_3}}{\partial \alpha_2} + \frac{1}{A_2 R_2} \frac{\partial A_{26(02)}^{(\tau\eta)\alpha_1\alpha_3}}{\partial \alpha_2} + \\
 & + \frac{1}{A_1} \frac{\partial A_{13(10)}^{(\tau\eta)\alpha_1\alpha_3}}{\partial \alpha_1} + \frac{1}{A_2} \frac{\partial A_{36(01)}^{(\tau\eta)\alpha_1\alpha_3}}{\partial \alpha_2} - \frac{A_{11(20)}^{(\tau\eta)\alpha_1\alpha_3}}{A_1 R_1^2} \frac{\partial R_1}{\partial \alpha_1} - \frac{A_{12(11)}^{(\tau\eta)\alpha_1\alpha_3}}{A_1 R_2^2} \frac{\partial R_2}{\partial \alpha_1} - \frac{A_{16(11)}^{(\tau\eta)\alpha_1\alpha_3}}{A_2 R_1^2} \frac{\partial R_1}{\partial \alpha_2} - \frac{A_{26(02)}^{(\tau\eta)\alpha_1\alpha_3}}{A_2 R_2^2} \frac{\partial R_2}{\partial \alpha_2}
 \end{aligned}$$

$$\begin{aligned}
 L_{21}^{(\tau\eta)\alpha_2\alpha_1} = & \frac{A_{16(20)}^{(\tau\eta)\alpha_2\alpha_1}}{A_1^2} \frac{\partial^2}{\partial \alpha_1^2} + \left( -\frac{A_{16(20)}^{(\tau\eta)\alpha_2\alpha_1}}{A_1^3} \frac{\partial A_1}{\partial \alpha_1} - \frac{A_{11(20)}^{(\tau\eta)\alpha_2\alpha_1} + A_{66(20)}^{(\tau\eta)\alpha_2\alpha_1}}{A_1^2 A_2} \frac{\partial A_1}{\partial \alpha_2} + \frac{A_{16(20)}^{(\tau\eta)\alpha_2\alpha_1} + A_{16(11)}^{(\tau\eta)\alpha_2\alpha_1} + A_{26(11)}^{(\tau\eta)\alpha_2\alpha_1}}{A_1^2 A_2} \frac{\partial A_2}{\partial \alpha_1} + \right. \\
 & \left. + \frac{1}{A_1^2} \frac{\partial A_{16(20)}^{(\tau\eta)\alpha_2\alpha_1}}{\partial \alpha_1} + \frac{1}{A_1 A_2} \frac{\partial A_{12(11)}^{(\tau\eta)\alpha_2\alpha_1}}{\partial \alpha_2} \right) \frac{\partial}{\partial \alpha_1} + \frac{A_{12(11)}^{(\tau\eta)\alpha_2\alpha_1} + A_{66(11)}^{(\tau\eta)\alpha_2\alpha_1}}{A_1 A_2} \frac{\partial^2}{\partial \alpha_1 \partial \alpha_2} + \frac{A_{26(02)}^{(\tau\eta)\alpha_2\alpha_1}}{A_2^2} \frac{\partial^2}{\partial \alpha_2^2} +
 \end{aligned}$$

$$\begin{aligned}
& + \left( -\frac{A_{26(02)}^{(\tau\eta)\alpha_2\alpha_1}}{A_2^3} \frac{\partial A_2}{\partial \alpha_2} + \frac{A_{22(02)}^{(\tau\eta)\alpha_2\alpha_1} + A_{66(02)}^{(\tau\eta)\alpha_2\alpha_1}}{A_1 A_2^2} \frac{\partial A_2}{\partial \alpha_1} + \frac{A_{26(02)}^{(\tau\eta)\alpha_2\alpha_1} - A_{16(11)}^{(\tau\eta)\alpha_2\alpha_1} - A_{26(11)}^{(\tau\eta)\alpha_2\alpha_1}}{A_1 A_2^2} \frac{\partial A_1}{\partial \alpha_2} + \right. \\
& + \left. \frac{1}{A_2^2} \frac{\partial A_{26(02)}^{(\tau\eta)\alpha_2\alpha_1}}{\partial \alpha_2} + \frac{1}{A_1 A_2} \frac{\partial A_{66(11)}^{(\tau\eta)\alpha_2\alpha_1}}{\partial \alpha_1} \right) \frac{\partial}{\partial \alpha_2} - A_{66(20)}^{(\tau\eta)\alpha_2\alpha_1} \left( \frac{1}{A_1^2 A_2} \frac{\partial^2 A_1}{\partial \alpha_1 \partial \alpha_2} - \frac{1}{A_1^3 A_2} \frac{\partial A_1}{\partial \alpha_1} \frac{\partial A_1}{\partial \alpha_2} \right) + \\
& - A_{26(11)}^{(\tau\eta)\alpha_2\alpha_1} \left( \frac{1}{A_1 A_2^2} \frac{\partial^2 A_1}{\partial \alpha_2^2} - \frac{1}{A_1 A_2^3} \frac{\partial A_1}{\partial \alpha_2} \frac{\partial A_2}{\partial \alpha_2} + \frac{1}{A_1^3 A_2} \frac{\partial A_1}{\partial \alpha_1} \frac{\partial A_2}{\partial \alpha_1} - \frac{1}{A_1^2 A_2} \frac{\partial^2 A_2}{\partial \alpha_1^2} \right) + \\
& - A_{22(02)}^{(\tau\eta)\alpha_2\alpha_1} \left( \frac{1}{A_1 A_2^3} \frac{\partial A_2}{\partial \alpha_1} \frac{\partial A_2}{\partial \alpha_2} - \frac{1}{A_1 A_2^2} \frac{\partial^2 A_2}{\partial \alpha_1 \partial \alpha_2} \right) - \left( \frac{1}{A_1^2 A_2} \frac{\partial A_{66(20)}^{(\tau\eta)\alpha_2\alpha_1}}{\partial \alpha_1} + \frac{1}{A_1 A_2^2} \frac{\partial A_{26(11)}^{(\tau\eta)\alpha_2\alpha_1}}{\partial \alpha_2} \right) \frac{\partial A_1}{\partial \alpha_2} + \\
& + \left( \frac{1}{A_1^2 A_2} \frac{\partial A_{26(11)}^{(\tau\eta)\alpha_2\alpha_1}}{\partial \alpha_1} + \frac{1}{A_1 A_2^2} \frac{\partial A_{22(02)}^{(\tau\eta)\alpha_2\alpha_1}}{\partial \alpha_2} \right) \frac{\partial A_2}{\partial \alpha_1} - \frac{A_{12(11)}^{(\tau\eta)\alpha_2\alpha_1} + A_{66(11)}^{(\tau\eta)\alpha_2\alpha_1}}{A_1^2 A_2^2} \frac{\partial A_1}{\partial \alpha_2} \frac{\partial A_2}{\partial \alpha_1} + \frac{A_{26(02)}^{(\tau\eta)\alpha_2\alpha_1}}{A_1^2 A_2^2} \left( \frac{\partial A_2}{\partial \alpha_1} \right)^2 + \\
& + \frac{A_{16(20)}^{(\tau\eta)\alpha_2\alpha_1}}{A_1^2 A_2^2} \left( \frac{\partial A_1}{\partial \alpha_2} \right)^2 - \frac{A_{45(11)}^{(\tau\eta)\alpha_2\alpha_1}}{R_1 R_2} + \frac{A_{45(10)}^{(\tau\eta)\alpha_2\alpha_1}}{R_1} + \frac{A_{45(01)}^{(\tau\eta)\alpha_2\alpha_1}}{R_2} - A_{45(00)}^{(\tau\eta)\alpha_2\alpha_1} \\
L_{22}^{(\tau\eta)\alpha_2\alpha_2} & = \frac{A_{66(20)}^{(\tau\eta)\alpha_2\alpha_2}}{A_1^2} \frac{\partial^2}{\partial \alpha_1^2} + \left( -\frac{A_{66(20)}^{(\tau\eta)\alpha_2\alpha_2}}{A_1^3} \frac{\partial A_1}{\partial \alpha_1} + \frac{A_{66(20)}^{(\tau\eta)\alpha_2\alpha_2}}{A_1^2 A_2} \frac{\partial A_2}{\partial \alpha_1} + \frac{1}{A_1^2} \frac{\partial A_{66(20)}^{(\tau\eta)\alpha_2\alpha_2}}{\partial \alpha_1} + \frac{1}{A_1 A_2} \frac{\partial A_{26(11)}^{(\tau\eta)\alpha_2\alpha_2}}{\partial \alpha_2} \right) \frac{\partial}{\partial \alpha_1} + \\
& + \frac{2A_{26(11)}^{(\tau\eta)\alpha_2\alpha_2}}{A_1 A_2} \frac{\partial^2}{\partial \alpha_1 \partial \alpha_2} + \frac{A_{22(02)}^{(\tau\eta)\alpha_2\alpha_2}}{A_2^2} \frac{\partial^2}{\partial \alpha_2^2} + \left( -\frac{A_{22(02)}^{(\tau\eta)\alpha_2\alpha_2}}{A_2^3} \frac{\partial A_2}{\partial \alpha_2} + \frac{A_{22(02)}^{(\tau\eta)\alpha_2\alpha_2}}{A_1 A_2^2} \frac{\partial A_1}{\partial \alpha_2} + \frac{1}{A_2^2} \frac{\partial A_{22(02)}^{(\tau\eta)\alpha_2\alpha_2}}{\partial \alpha_2} + \right. \\
& + \left. \frac{1}{A_1 A_2} \frac{\partial A_{26(11)}^{(\tau\eta)\alpha_2\alpha_2}}{\partial \alpha_1} \right) \frac{\partial}{\partial \alpha_2} - A_{66(11)}^{(\tau\eta)\alpha_2\alpha_2} \left( \frac{1}{A_1^2 A_2} \frac{\partial^2 A_2}{\partial \alpha_1^2} - \frac{1}{A_1^3 A_2} \frac{\partial A_1}{\partial \alpha_1} \frac{\partial A_2}{\partial \alpha_1} \right) + \\
& - A_{16(20)}^{(\tau\eta)\alpha_2\alpha_2} \left( \frac{1}{A_1^3 A_2} \frac{\partial A_1}{\partial \alpha_1} \frac{\partial A_1}{\partial \alpha_2} - \frac{1}{A_1^2 A_2} \frac{\partial^2 A_1}{\partial \alpha_1 \partial \alpha_2} \right) - A_{12(11)}^{(\tau\eta)\alpha_2\alpha_2} \left( \frac{1}{A_1 A_2^3} \frac{\partial A_1}{\partial \alpha_2} \frac{\partial A_2}{\partial \alpha_2} - \frac{1}{A_1 A_2^2} \frac{\partial^2 A_1}{\partial \alpha_2^2} \right) + \\
& - A_{26(02)}^{(\tau\eta)\alpha_2\alpha_2} \left( \frac{1}{A_1 A_2^2} \frac{\partial^2 A_2}{\partial \alpha_1 \partial \alpha_2} - \frac{1}{A_1 A_2^3} \frac{\partial A_2}{\partial \alpha_1} \frac{\partial A_2}{\partial \alpha_2} \right) - \left( \frac{1}{A_1^2 A_2} \frac{\partial A_{66(11)}^{(\tau\eta)\alpha_2\alpha_2}}{\partial \alpha_1} + \frac{1}{A_1 A_2^2} \frac{\partial A_{26(02)}^{(\tau\eta)\alpha_2\alpha_2}}{\partial \alpha_2} \right) \frac{\partial A_2}{\partial \alpha_1} + \\
& + \left( \frac{1}{A_1^2 A_2} \frac{\partial A_{16(20)}^{(\tau\eta)\alpha_2\alpha_2}}{\partial \alpha_1} + \frac{1}{A_1 A_2^2} \frac{\partial A_{12(11)}^{(\tau\eta)\alpha_2\alpha_2}}{\partial \alpha_2} \right) \frac{\partial A_1}{\partial \alpha_2} + \frac{2A_{16(11)}^{(\tau\eta)\alpha_2\alpha_2}}{A_1^2 A_2^2} \frac{\partial A_1}{\partial \alpha_2} \frac{\partial A_2}{\partial \alpha_1} - \frac{A_{66(02)}^{(\tau\eta)\alpha_2\alpha_2}}{A_1^2 A_2^2} \left( \frac{\partial A_2}{\partial \alpha_1} \right)^2 + \\
& - \frac{A_{11(20)}^{(\tau\eta)\alpha_2\alpha_2}}{A_1^2 A_2^2} \left( \frac{\partial A_1}{\partial \alpha_2} \right)^2 - \frac{A_{55(02)}^{(\tau\eta)\alpha_2\alpha_2}}{R_2^2} + \frac{A_{55(01)}^{(\tau\eta)\alpha_2\alpha_2} + A_{55(01)}^{(\tau\eta)\alpha_2\alpha_2}}{R_2} - A_{55(00)}^{(\tau\eta)\alpha_2\alpha_2} \\
L_{23}^{(\tau\eta)\alpha_2\alpha_3} & = \left( \frac{A_{16(20)}^{(\tau\eta)\alpha_2\alpha_3}}{A_1 R_1} + \frac{A_{26(11)}^{(\tau\eta)\alpha_2\alpha_3} + A_{45(11)}^{(\tau\eta)\alpha_2\alpha_3}}{A_1 R_2} + \frac{A_{36(10)}^{(\tau\eta)\alpha_2\alpha_3} - A_{45(10)}^{(\tau\eta)\alpha_2\alpha_3}}{A_1} \right) \frac{\partial}{\partial \alpha_1} + \\
& + \left( \frac{A_{12(11)}^{(\tau\eta)\alpha_2\alpha_3}}{A_2 R_1} + \frac{A_{22(02)}^{(\tau\eta)\alpha_2\alpha_3} + A_{55(02)}^{(\tau\eta)\alpha_2\alpha_3}}{A_2 R_2} + \frac{A_{23(01)}^{(\tau\eta)\alpha_2\alpha_3} - A_{55(01)}^{(\tau\eta)\alpha_2\alpha_3}}{A_2} \right) \frac{\partial}{\partial \alpha_2} + \\
& + \left( \frac{A_{16(20)}^{(\tau\eta)\alpha_2\alpha_3} + A_{16(11)}^{(\tau\eta)\alpha_2\alpha_3}}{A_1 A_2 R_1} + \frac{A_{26(11)}^{(\tau\eta)\alpha_2\alpha_3} + A_{26(02)}^{(\tau\eta)\alpha_2\alpha_3}}{A_1 A_2 R_2} + \frac{A_{36(10)}^{(\tau\eta)\alpha_2\alpha_3} + A_{36(01)}^{(\tau\eta)\alpha_2\alpha_3}}{A_1 A_2} \right) \frac{\partial A_2}{\partial \alpha_1} +
\end{aligned}$$

$$\begin{aligned}
 & + \left( \frac{A_{12(11)}^{(\tau\eta)\alpha_2\alpha_3} - A_{11(02)}^{(\tau\eta)\alpha_2\alpha_3}}{A_1 A_2 R_1} + \frac{A_{22(02)}^{(\tau\eta)\alpha_2\alpha_3} - A_{12(11)}^{(\tau\eta)\alpha_2\alpha_3}}{A_1 A_2 R_2} + \frac{A_{23(01)}^{(\tau\bar{\eta})\alpha_2\alpha_3} - A_{13(10)}^{(\tau\bar{\eta})\alpha_2\alpha_3}}{A_1 A_2} \right) \frac{\partial A_1}{\partial \alpha_2} + \\
 & + \frac{1}{A_1 R_1} \frac{\partial A_{16(20)}^{(\tau\eta)\alpha_2\alpha_3}}{\partial \alpha_1} + \frac{1}{A_1 R_2} \frac{\partial A_{26(11)}^{(\tau\eta)\alpha_2\alpha_3}}{\partial \alpha_1} + \frac{1}{A_2 R_1} \frac{\partial A_{12(11)}^{(\tau\eta)\alpha_2\alpha_3}}{\partial \alpha_2} + \frac{1}{A_2 R_2} \frac{\partial A_{22(02)}^{(\tau\eta)\alpha_2\alpha_3}}{\partial \alpha_2} + \\
 & + \frac{1}{A_1} \frac{\partial A_{36(10)}^{(\tau\bar{\eta})\alpha_2\alpha_3}}{\partial \alpha_1} + \frac{1}{A_2} \frac{\partial A_{23(01)}^{(\tau\bar{\eta})\alpha_2\alpha_3}}{\partial \alpha_2} - \frac{A_{16(20)}^{(\tau\eta)\alpha_2\alpha_3}}{A_1 R_1^2} \frac{\partial R_1}{\partial \alpha_1} - \frac{A_{26(11)}^{(\tau\eta)\alpha_2\alpha_3}}{A_1 R_2^2} \frac{\partial R_2}{\partial \alpha_1} - \frac{A_{12(11)}^{(\tau\eta)\alpha_2\alpha_3}}{A_2 R_1^2} \frac{\partial R_1}{\partial \alpha_2} - \frac{A_{22(02)}^{(\tau\eta)\alpha_2\alpha_3}}{A_2 R_2^2} \frac{\partial R_2}{\partial \alpha_2} \\
 \\
 L_{31}^{(\tau\eta)\alpha_3\alpha_1} & = - \left( \frac{A_{11(20)}^{(\tau\eta)\alpha_3\alpha_1} + A_{44(20)}^{(\tau\eta)\alpha_3\alpha_1}}{A_1 R_1} + \frac{A_{12(11)}^{(\tau\eta)\alpha_3\alpha_1}}{A_1 R_2} + \frac{A_{13(10)}^{(\tau\bar{\eta})\alpha_3\alpha_1} - A_{44(10)}^{(\tau\bar{\eta})\alpha_3\alpha_1}}{A_1} \right) \frac{\partial}{\partial \alpha_1} + \\
 & - \left( \frac{A_{16(11)}^{(\tau\eta)\alpha_3\alpha_1} + A_{45(11)}^{(\tau\eta)\alpha_3\alpha_1}}{A_2 R_1} + \frac{A_{26(02)}^{(\tau\eta)\alpha_3\alpha_1}}{A_2 R_2} + \frac{A_{36(01)}^{(\tau\bar{\eta})\alpha_3\alpha_1} - A_{45(01)}^{(\tau\bar{\eta})\alpha_3\alpha_1}}{A_2} \right) \frac{\partial}{\partial \alpha_2} + \\
 & + \left( \frac{A_{44(20)}^{(\tau\eta)\alpha_3\alpha_1} + A_{12(11)}^{(\tau\eta)\alpha_3\alpha_1}}{A_1 A_2 R_1} - \frac{A_{22(02)}^{(\tau\eta)\alpha_3\alpha_1}}{A_1 A_2 R_2} + \frac{A_{44(10)}^{(\tau\bar{\eta})\alpha_3\alpha_1} - A_{23(01)}^{(\tau\bar{\eta})\alpha_3\alpha_1}}{A_1 A_2} \right) \frac{\partial A_2}{\partial \alpha_1} + \\
 & + \left( \frac{A_{16(20)}^{(\tau\eta)\alpha_3\alpha_1} - A_{45(11)}^{(\tau\eta)\alpha_3\alpha_1}}{A_1 A_2 R_1} + \frac{A_{26(11)}^{(\tau\eta)\alpha_3\alpha_1}}{A_1 A_2 R_2} + \frac{A_{45(01)}^{(\tau\bar{\eta})\alpha_3\alpha_1} + A_{36(10)}^{(\tau\bar{\eta})\alpha_3\alpha_1}}{A_1 A_2} \right) \frac{\partial A_1}{\partial \alpha_2} + \\
 & - \frac{1}{A_1 R_1} \frac{\partial A_{44(20)}^{(\tau\eta)\alpha_3\alpha_1}}{\partial \alpha_1} + \frac{1}{A_1} \frac{\partial A_{44(10)}^{(\tau\bar{\eta})\alpha_3\alpha_1}}{\partial \alpha_1} - \frac{1}{A_2 R_1} \frac{\partial A_{45(11)}^{(\tau\eta)\alpha_3\alpha_1}}{\partial \alpha_2} + \\
 & + \frac{1}{A_2} \frac{\partial A_{45(01)}^{(\tau\bar{\eta})\alpha_3\alpha_1}}{\partial \alpha_2} + \frac{A_{44(20)}^{(\tau\eta)\alpha_3\alpha_1}}{A_1 R_1^2} \frac{\partial R_1}{\partial \alpha_1} + \frac{A_{45(11)}^{(\tau\eta)\alpha_3\alpha_1}}{A_2 R_1^2} \frac{\partial R_1}{\partial \alpha_2} \\
 \\
 L_{32}^{(\tau\eta)\alpha_3\alpha_2} & = - \left( \frac{A_{16(20)}^{(\tau\eta)\alpha_3\alpha_2}}{A_1 R_1} + \frac{A_{26(11)}^{(\tau\eta)\alpha_3\alpha_2} + A_{45(11)}^{(\tau\eta)\alpha_3\alpha_2}}{A_1 R_2} + \frac{A_{36(10)}^{(\tau\bar{\eta})\alpha_3\alpha_2} - A_{45(10)}^{(\tau\bar{\eta})\alpha_3\alpha_2}}{A_1} \right) \frac{\partial}{\partial \alpha_1} + \\
 & - \left( \frac{A_{12(20)}^{(\tau\eta)\alpha_3\alpha_2}}{A_2 R_1} + \frac{A_{22(02)}^{(\tau\eta)\alpha_3\alpha_2} + A_{55(02)}^{(\tau\eta)\alpha_3\alpha_2}}{A_2 R_2} + \frac{A_{23(01)}^{(\tau\bar{\eta})\alpha_3\alpha_2} - A_{55(01)}^{(\tau\bar{\eta})\alpha_3\alpha_2}}{A_2} \right) \frac{\partial}{\partial \alpha_2} + \\
 & + \left( \frac{A_{16(11)}^{(\tau\eta)\alpha_3\alpha_2}}{A_1 A_2 R_1} + \frac{A_{26(02)}^{(\tau\eta)\alpha_3\alpha_2} - A_{45(11)}^{(\tau\eta)\alpha_3\alpha_2}}{A_1 A_2 R_2} + \frac{A_{45(10)}^{(\tau\bar{\eta})\alpha_3\alpha_2} + A_{36(01)}^{(\tau\bar{\eta})\alpha_3\alpha_2}}{A_1 A_2} \right) \frac{\partial A_2}{\partial \alpha_1} + \\
 & + \left( \frac{A_{11(20)}^{(\tau\eta)\alpha_3\alpha_2}}{A_1 A_2 R_1} - \frac{A_{12(11)}^{(\tau\eta)\alpha_3\alpha_2} + A_{55(02)}^{(\tau\eta)\alpha_3\alpha_2}}{A_1 A_2 R_2} + \frac{A_{55(01)}^{(\tau\bar{\eta})\alpha_3\alpha_2} - A_{13(10)}^{(\tau\bar{\eta})\alpha_3\alpha_2}}{A_1 A_2} \right) \frac{\partial A_1}{\partial \alpha_2} + \\
 & - \frac{1}{A_1 R_2} \frac{\partial A_{45(11)}^{(\tau\eta)\alpha_3\alpha_2}}{\partial \alpha_1} + \frac{1}{A_1} \frac{\partial A_{45(10)}^{(\tau\bar{\eta})\alpha_3\alpha_2}}{\partial \alpha_1} - \frac{1}{A_2 R_2} \frac{\partial A_{55(02)}^{(\tau\eta)\alpha_3\alpha_2}}{\partial \alpha_2} + \\
 & + \frac{1}{A_2} \frac{\partial A_{55(01)}^{(\tau\bar{\eta})\alpha_3\alpha_2}}{\partial \alpha_2} + \frac{A_{45(11)}^{(\tau\eta)\alpha_3\alpha_2}}{A_1 R_2^2} \frac{\partial R_2}{\partial \alpha_1} + \frac{A_{55(02)}^{(\tau\eta)\alpha_3\alpha_2}}{A_2 R_2^2} \frac{\partial R_2}{\partial \alpha_2} \\
 \\
 L_{33}^{(\tau\eta)\alpha_3\alpha_3} & = \frac{A_{44(20)}^{(\tau\eta)\alpha_3\alpha_3}}{A_1^2} \frac{\partial^2}{\partial \alpha_1^2} + \left( - \frac{A_{44(20)}^{(\tau\eta)\alpha_3\alpha_3}}{A_1^3} \frac{\partial A_1}{\partial \alpha_1} + \frac{A_{44(20)}^{(\tau\eta)\alpha_3\alpha_3}}{A_1^2 A_2} \frac{\partial A_2}{\partial \alpha_1} + \frac{1}{A_1^2} \frac{\partial A_{44(20)}^{(\tau\eta)\alpha_3\alpha_3}}{\partial \alpha_1} + \frac{1}{A_1 A_2} \frac{\partial A_{45(11)}^{(\tau\eta)\alpha_3\alpha_3}}{\partial \alpha_2} \right) \frac{\partial}{\partial \alpha_1} +
 \end{aligned}$$

$$\begin{aligned}
 & + \frac{2A_{45(11)}^{(\tau\eta)\alpha_3\alpha_3}}{A_1A_2} \frac{\partial^2}{\partial\alpha_1\partial\alpha_2} + \frac{A_{55(02)}^{(\tau\eta)\alpha_3\alpha_3}}{A_2^2} \frac{\partial^2}{\partial\alpha_2^2} + \\
 & + \left( -\frac{A_{55(02)}^{(\tau\eta)\alpha_3\alpha_3}}{A_2^3} \frac{\partial A_2}{\partial\alpha_2} + \frac{A_{55(02)}^{(\tau\eta)\alpha_3\alpha_3}}{A_1A_2^2} \frac{\partial A_1}{\partial\alpha_2} + \frac{1}{A_2^2} \frac{\partial A_{55(02)}^{(\tau\eta)\alpha_3\alpha_3}}{\partial\alpha_2} + \frac{1}{A_1A_2} \frac{\partial A_{45(11)}^{(\tau\eta)\alpha_3\alpha_3}}{\partial\alpha_1} \right) \frac{\partial}{\partial\alpha_2} + \\
 & - \frac{A_{11(20)}^{(\tau\eta)\alpha_3\alpha_3}}{R_1^2} - \frac{A_{22(02)}^{(\tau\eta)\alpha_3\alpha_3}}{R_2^2} - \frac{2A_{12(11)}^{(\tau\eta)\alpha_3\alpha_3}}{R_1R_2} - \frac{A_{13(10)}^{(\tau\eta)\alpha_3\alpha_3} + A_{13(10)}^{(\bar{\tau}\eta)\alpha_3\alpha_3}}{R_1} - \frac{A_{23(01)}^{(\tau\eta)\alpha_3\alpha_3} + A_{23(01)}^{(\bar{\tau}\eta)\alpha_3\alpha_3}}{R_2} - A_{33(00)}^{(\bar{\tau}\eta)\alpha_3\alpha_3}
 \end{aligned} \tag{3.237}$$

A simpler expression of the fundamental equations (3.236) can be obtained if the effect of the elastic foundation is neglected as follows

$$\sum_{\eta=0}^{N+1} \mathbf{L}^{(\tau\eta)} \mathbf{u}^{(\eta)} + \mathbf{q}^{(\tau)} = \sum_{\eta=0}^{N+1} \mathbf{M}^{(\tau\eta)} \ddot{\mathbf{u}}^{(\eta)} \tag{3.238}$$

It should be noted that the maximum order of expansion  $N$  defines the number of equations. In particular, the total number of equations is equal to  $3 \times (N+2)$  for a theory that embeds the Murakami's function.

For the sake of clarity, the complete system of fundamental equations (3.238) can be written in matrix form as follows

$$\begin{aligned}
 & \begin{bmatrix} \mathbf{L}^{(00)} & \mathbf{L}^{(01)} & \dots & \dots & \mathbf{L}^{(0(N))} & \mathbf{L}^{(0(N+1))} \\ \mathbf{L}^{(10)} & \mathbf{L}^{(11)} & \dots & \dots & \mathbf{L}^{(1(N))} & \mathbf{L}^{(1(N+1))} \\ \vdots & \vdots & \ddots & & \vdots & \vdots \\ \vdots & \vdots & & \ddots & \vdots & \vdots \\ \mathbf{L}^{((N)0)} & \mathbf{L}^{((N)1)} & \dots & \dots & \mathbf{L}^{((N)(N))} & \mathbf{L}^{((N)(N+1))} \\ \mathbf{L}^{((N+1)0)} & \mathbf{L}^{((N+1)1)} & \dots & \dots & \mathbf{L}^{((N+1)(N))} & \mathbf{L}^{((N+1)(N+1))} \end{bmatrix} \begin{bmatrix} \mathbf{u}^{(0)} \\ \mathbf{u}^{(1)} \\ \vdots \\ \vdots \\ \mathbf{u}^{(N)} \\ \mathbf{u}^{(N+1)} \end{bmatrix} + \begin{bmatrix} \mathbf{q}^{(0)} \\ \mathbf{q}^{(1)} \\ \vdots \\ \vdots \\ \mathbf{q}^{(N)} \\ \mathbf{q}^{(N+1)} \end{bmatrix} = \\
 & = \begin{bmatrix} \mathbf{M}^{(00)} & \mathbf{M}^{(01)} & \dots & \dots & \mathbf{M}^{(0(N))} & \mathbf{M}^{(0(N+1))} \\ \mathbf{M}^{(10)} & \mathbf{M}^{(11)} & \dots & \dots & \mathbf{M}^{(1(N))} & \mathbf{M}^{(1(N+1))} \\ \vdots & \vdots & \ddots & & \vdots & \vdots \\ \vdots & \vdots & & \ddots & \vdots & \vdots \\ \mathbf{M}^{((N)0)} & \mathbf{M}^{((N)1)} & \dots & \dots & \mathbf{M}^{((N)(N))} & \mathbf{M}^{((N)(N+1))} \\ \mathbf{M}^{((N+1)0)} & \mathbf{M}^{((N+1)1)} & \dots & \dots & \mathbf{M}^{((N+1)(N))} & \mathbf{M}^{((N+1)(N+1))} \end{bmatrix} \begin{bmatrix} \ddot{\mathbf{u}}^{(0)} \\ \ddot{\mathbf{u}}^{(1)} \\ \vdots \\ \vdots \\ \ddot{\mathbf{u}}^{(N)} \\ \ddot{\mathbf{u}}^{(N+1)} \end{bmatrix}
 \end{aligned} \tag{3.239}$$

Finally, it should be recalled that the differential system at issue can be solved only if the proper boundary conditions are enforced. The Hamilton's principle provide the following equations

$$\oint_{\alpha_2} (\delta \mathbf{u}^{(\tau)})^T (\bar{\mathbf{S}}_{\alpha_1}^{(\tau)} - \mathbf{S}_{\alpha_1}^{(\tau)}) A_2 d\alpha_2 + \oint_{\alpha_1} (\delta \mathbf{u}^{(\tau)})^T (\bar{\mathbf{S}}_{\alpha_2}^{(\tau)} - \mathbf{S}_{\alpha_2}^{(\tau)}) A_1 d\alpha_1 \tag{3.240}$$

These integrals must be equal to zero, too. Thus, one gets

$$\begin{aligned} & \left( \delta \mathbf{u}^{(\tau)} \right)^T \left( \bar{\mathbf{S}}_{\alpha_1}^{(\tau)} - \mathbf{S}_{\alpha_1}^{(\tau)} \right) \\ & \left( \delta \mathbf{u}^{(\tau)} \right)^T \left( \bar{\mathbf{S}}_{\alpha_2}^{(\tau)} - \mathbf{S}_{\alpha_2}^{(\tau)} \right) \end{aligned} \quad (3.241)$$

Relations (3.241) provide the boundary conditions along the external edges of the middle surface. For constant values of  $\alpha_1$  the conditions at issue are given by

$$\mathbf{u}^{(\tau)} = \mathbf{0} \quad \text{or} \quad \bar{\mathbf{S}}_{\alpha_1}^{(\tau)} = \mathbf{S}_{\alpha_1}^{(\tau)} \quad (3.242)$$

On the other hand, for constant values of  $\alpha_2$  these conditions become

$$\mathbf{u}^{(\tau)} = \mathbf{0} \quad \text{or} \quad \bar{\mathbf{S}}_{\alpha_2}^{(\tau)} = \mathbf{S}_{\alpha_2}^{(\tau)} \quad (3.243)$$

Several kinds of boundary conditions can be obtained by combining properly relations (3.242) and (3.243) along the four edges of the reference domain.

For the sake of completeness, it should be specified that the generalized stresses in (3.242)-(3.243) involve the natural (or force) boundary conditions, whereas the generalized displacements are needed for the essential (or geometric) boundary conditions. Since both displacements and stress resultants appear in the boundary conditions, the continuity requirement of this strong formulation is  $C^1$ . The natural boundary conditions can be written by means of definition (3.179).

Finally, it should be noted at this point that a numerical technique must be employed to evaluate all the matrices and vectors that appear in (3.236). These quantities can be obtained by approximating directly the derivatives with respect to the coordinates  $\alpha_1, \alpha_2$ . For this purpose, the DQ method presented in the first chapter is employed to get the discrete form of the governing equations.

### 3.1.7.1 Governing equations for distorted domains

The coordinate change illustrated in the previous chapter must be considered to deal with distorted domain. Thus, the differential operators (3.237) have to be modified accordingly. In particular, as shown in the previous chapter, the first-order derivatives with respect to the principal curvilinear coordinates become

$$\frac{\partial}{\partial \alpha_1} = \xi_{1,\alpha_1} \frac{\partial}{\partial \xi_1} + \xi_{2,\alpha_1} \frac{\partial}{\partial \xi_2} \quad (3.244)$$

$$\frac{\partial}{\partial \alpha_2} = \xi_{1,\alpha_2} \frac{\partial}{\partial \xi_1} + \xi_{2,\alpha_2} \frac{\partial}{\partial \xi_2} \quad (3.245)$$

As far as the second-order and mixed derivatives are concerned, the following substitution must be performed

$$\frac{\partial^2}{\partial \alpha_1^2} = \xi_{1,\alpha_1}^2 \frac{\partial^2}{\partial \xi_1^2} + \xi_{2,\alpha_1}^2 \frac{\partial^2}{\partial \xi_2^2} + 2\xi_{1,\alpha_1} \xi_{2,\alpha_1} \frac{\partial^2}{\partial \xi_1 \partial \xi_2} + \xi_{1,\alpha_1 \alpha_1} \frac{\partial}{\partial \xi_1} + \xi_{2,\alpha_1 \alpha_1} \frac{\partial}{\partial \xi_2} \quad (3.246)$$

$$\frac{\partial^2}{\partial \alpha_2^2} = \xi_{1,\alpha_2}^2 \frac{\partial^2}{\partial \xi_1^2} + \xi_{2,\alpha_2}^2 \frac{\partial^2}{\partial \xi_2^2} + 2\xi_{1,\alpha_2} \xi_{2,\alpha_2} \frac{\partial^2}{\partial \xi_1 \partial \xi_2} + \xi_{1,\alpha_2 \alpha_2} \frac{\partial}{\partial \xi_1} + \xi_{2,\alpha_2 \alpha_2} \frac{\partial}{\partial \xi_2} \quad (3.247)$$

$$\begin{aligned} \frac{\partial^2}{\partial \alpha_1 \partial \alpha_2} &= \xi_{1,\alpha_1} \xi_{1,\alpha_2} \frac{\partial^2}{\partial \xi_1^2} + \xi_{2,\alpha_1} \xi_{2,\alpha_2} \frac{\partial^2}{\partial \xi_2^2} + \\ &+ \left( \xi_{1,\alpha_1} \xi_{2,\alpha_2} + \xi_{1,\alpha_2} \xi_{2,\alpha_1} \right) \frac{\partial^2}{\partial \xi_1 \partial \xi_2} + \xi_{1,\alpha_1 \alpha_2} \frac{\partial}{\partial \xi_1} + \xi_{2,\alpha_1 \alpha_2} \frac{\partial}{\partial \xi_2} \end{aligned} \quad (3.248)$$

where  $\xi_1, \xi_2$  stand for the natural coordinates defined in the intervals  $\xi_1 \in [-1, 1]$  and  $\xi_2 \in [-1, 1]$ , respectively. The meaning of the various quantities that appear in (3.244)-(3.248) is explained in the previous chapter. In other words, the derivatives at issue are written in the computational element (or master element).

It should be noted that both the stress resultants and displacement components involved in the boundary conditions (3.242)-(3.243) must be modified to take into account distorted domains. For this purpose, the outward unit vectors  $\mathbf{n}_n$ ,  $\mathbf{n}_s$ ,  $\mathbf{n}_\zeta$  along each edge of the irregular domain are required, as shown in Figure 3.11.

These vectors are computed as the direction cosines of the three corresponding directions. In particular, each vector is fully described once its three components are introduced

$$\begin{aligned} \mathbf{n}_n &= [n_{n1} \quad n_{n2} \quad n_{n3}]^T \\ \mathbf{n}_s &= [n_{s1} \quad n_{s2} \quad n_{s3}]^T \\ \mathbf{n}_\zeta &= [n_{\zeta 1} \quad n_{\zeta 2} \quad n_{\zeta 3}]^T \end{aligned} \quad (3.249)$$

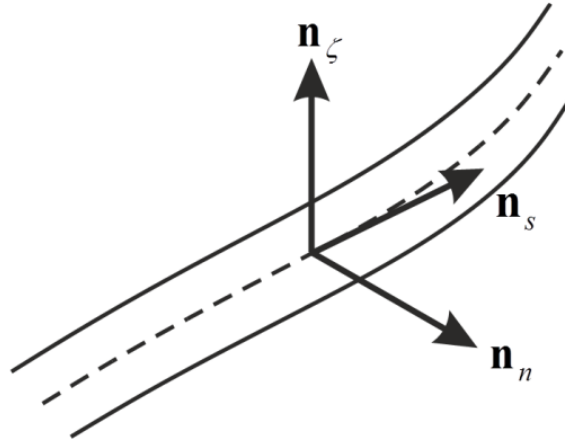


Figure 3.11 – Outward unit normal vectors for a generic edge [62].

The quantities in (3.249) allow to evaluate the generalized displacements along a generic edge  $u_n^{(\tau)}$ ,  $u_s^{(\tau)}$  and  $u_\zeta^{(\tau)}$  as follows, for  $\tau = 0, 1, 2, \dots, N, N+1$

$$\begin{aligned} u_n^{(\tau)} &= n_{n1}u_1^{(\tau)} + n_{n2}u_2^{(\tau)} \\ u_s^{(\tau)} &= n_{s1}u_1^{(\tau)} + n_{s2}u_2^{(\tau)} \\ u_\zeta^{(\tau)} &= u_3^{(\tau)} \end{aligned} \quad (3.250)$$

Analogously, the generalized stress resultants  $N_n^{(\tau)\alpha_1}$ ,  $N_{ns}^{(\tau)\alpha_2}$  and  $T_\zeta^{(\tau)\alpha_3}$  can be computed as shown below, for  $\tau = 0, 1, 2, \dots, N, N+1$

$$\begin{aligned} N_n^{(\tau)\alpha_1} &= N_1^{(\tau)\alpha_1}n_{n1}^2 + N_2^{(\tau)\alpha_1}n_{n2}^2 + N_{12}^{(\tau)\alpha_1}n_{n1}n_{n2} + N_{21}^{(\tau)\alpha_1}n_{n1}n_{n2} \\ N_{ns}^{(\tau)\alpha_2} &= N_1^{(\tau)\alpha_2}n_{n1}n_{s1} + N_2^{(\tau)\alpha_2}n_{n2}n_{s2} + N_{12}^{(\tau)\alpha_2}n_{n1}n_{s2} + N_{21}^{(\tau)\alpha_2}n_{n2}n_{s1} \\ T_\zeta^{(\tau)\alpha_3} &= T_1^{(\tau)\alpha_3}n_{n1} + T_2^{(\tau)\alpha_3}n_{n2} \end{aligned} \quad (3.251)$$

Several kinds of restraints can be enforced by applying the proper boundary conditions and using the quantities just introduced.

### 3.1.7.2 Discrete form of the governing equations

By means of the DQ method, the partial derivatives that describe the mechanical behavior of laminated composite doubly-curved shells are written in each sampling point of the domain. Consequently, the fundamental equations (3.236) must be written in discrete form by applying directly the definition of the DQ method illustrated in the first chapter.

### 3.1.8 WEAK FORMULATION

In order to obtain the weak form of the governing equations, the kinematic assumption concerning the displacement field (3.37) must be recalled and inserted into the general expression of the Hamilton's principle (3.211). Let us consider first the term related to the variation of the kinetic energy  $\delta\mathcal{T}$ . Having in mind the definition (3.37), one gets

$$\begin{aligned}
\delta\mathcal{T} &= \int_{\alpha_1} \int_{\alpha_2} \left( \delta\mathbf{u}^{(\tau)} \right)^T \left( \sum_{\eta=0}^{N+1} \mathbf{M}^{(\tau\eta)} \ddot{\mathbf{u}}^{(\eta)} \right) A_1 A_2 d\alpha_1 d\alpha_2 = \\
&= \int_{\alpha_1} \int_{\alpha_2} \left( \mathbf{N}^T \delta\bar{\mathbf{u}}^{(\tau)} \right)^T \left( \sum_{\eta=0}^{N+1} \mathbf{M}^{(\tau\eta)} \mathbf{N}^T \ddot{\mathbf{u}}^{(\eta)} \right) A_1 A_2 d\alpha_1 d\alpha_2 = \\
&= \int_{\alpha_1} \int_{\alpha_2} \left( \delta\bar{\mathbf{u}}^{(\tau)} \right)^T \mathbf{N} \left( \sum_{\eta=0}^{N+1} \mathbf{M}^{(\tau\eta)} \mathbf{N}^T \ddot{\mathbf{u}}^{(\eta)} \right) A_1 A_2 d\alpha_1 d\alpha_2 = \\
&= \int_{\alpha_1} \int_{\alpha_2} \left( \delta\bar{\mathbf{u}}^{(\tau)} \right)^T \left( \sum_{\eta=0}^{N+1} \mathbf{N} \mathbf{M}^{(\tau\eta)} \mathbf{N}^T \ddot{\mathbf{u}}^{(\eta)} \right) A_1 A_2 d\alpha_1 d\alpha_2 = \\
&= \left( \delta\bar{\mathbf{u}}^{(\tau)} \right)^T \sum_{\eta=0}^{N+1} \left( \int_{\alpha_1} \int_{\alpha_2} \mathbf{N} \mathbf{M}^{(\tau\eta)} \mathbf{N}^T A_1 A_2 d\alpha_1 d\alpha_2 \right) \ddot{\mathbf{u}}^{(\eta)} = \\
&= \left( \delta\bar{\mathbf{u}}^{(\tau)} \right)^T \sum_{\eta=0}^{N+1} \bar{\mathbf{M}}^{(\tau\eta)} \ddot{\mathbf{u}}^{(\eta)} \tag{3.252}
\end{aligned}$$

where  $\bar{\mathbf{M}}^{(\tau\eta)}$  is the mass matrix of size  $(3I_N I_M) \times (3I_N I_M)$  defined below

$$\bar{\mathbf{M}}^{(\tau\eta)} = \int_{\alpha_1} \int_{\alpha_2} \begin{bmatrix} \bar{\mathbf{N}} I_0^{(\tau\eta)\alpha_1\alpha_1} \bar{\mathbf{N}}^T & \mathbf{0} & \mathbf{0} \\ \mathbf{0} & \bar{\mathbf{N}} I_0^{(\tau\eta)\alpha_2\alpha_2} \bar{\mathbf{N}}^T & \mathbf{0} \\ \mathbf{0} & \mathbf{0} & \bar{\mathbf{N}} I_0^{(\tau\eta)\alpha_3\alpha_3} \bar{\mathbf{N}}^T \end{bmatrix} A_1 A_2 d\alpha_1 d\alpha_2 \tag{3.253}$$

Let us take into account now the quantities that come from the variation of the elastic energy  $\delta\Phi$ . Recalling assumption (3.37) and having in mind definitions (3.89) and (3.99), the variation at issue becomes

$$\begin{aligned}
\delta\Phi &= \sum_{i=1}^3 \int_{\alpha_1} \int_{\alpha_2} \left( \delta \left( \mathbf{D}_{\Omega}^{\alpha_i} \mathbf{u}^{(\tau)} \right) \right)^T \mathbf{S}^{(\tau)\alpha_i} A_1 A_2 d\alpha_1 d\alpha_2 = \\
&= \sum_{i=1}^3 \int_{\alpha_1} \int_{\alpha_2} \left( \delta \left( \mathbf{D}_{\Omega}^{\alpha_i} \mathbf{N}^T \bar{\mathbf{u}}^{(\tau)} \right) \right)^T \mathbf{S}^{(\tau)\alpha_i} A_1 A_2 d\alpha_1 d\alpha_2 = \\
&= \sum_{i=1}^3 \int_{\alpha_1} \int_{\alpha_2} \left( \delta\bar{\mathbf{u}}^{(\tau)} \right)^T \left( \mathbf{D}_{\Omega}^{\alpha_i} \mathbf{N}^T \right)^T \mathbf{S}^{(\tau)\alpha_i} A_1 A_2 d\alpha_1 d\alpha_2 =
\end{aligned}$$

$$= \sum_{i=1}^3 \int_{\alpha_1} \int_{\alpha_2} \left( \delta \bar{\mathbf{u}}^{(\tau)} \right)^T \left( \mathbf{B}^{\alpha_i} \right)^T \mathbf{S}^{(\tau)\alpha_i} A_1 A_2 d\alpha_1 d\alpha_2 \quad (3.254)$$

in which the operators  $\mathbf{B}^{\alpha_i}$ , for  $i=1,2,3$ , assume the same meaning shown in (3.100). The same procedure can be performed for the terms linked to the work done by the external loads. The contribution due to the surface loads collected in  $\mathbf{q}_{sa}^{(\tau)}$  assumes the following aspect

$$\begin{aligned} \delta L_{es} &= \int_{\alpha_1} \int_{\alpha_2} \left( \delta \mathbf{u}^{(\tau)} \right)^T \mathbf{q}_{sa}^{(\tau)} A_1 A_2 d\alpha_1 d\alpha_2 = \\ &= \int_{\alpha_1} \int_{\alpha_2} \left( \mathbf{N}^T \delta \bar{\mathbf{u}}^{(\tau)} \right)^T \mathbf{q}_{sa}^{(\tau)} A_1 A_2 d\alpha_1 d\alpha_2 = \\ &= \int_{\alpha_1} \int_{\alpha_2} \left( \delta \bar{\mathbf{u}}^{(\tau)} \right)^T \mathbf{N} \mathbf{q}_{sa}^{(\tau)} A_1 A_2 d\alpha_1 d\alpha_2 = \\ &= \left( \delta \bar{\mathbf{u}}^{(\tau)} \right)^T \int_{\alpha_1} \int_{\alpha_2} \mathbf{N} \mathbf{q}_{sa}^{(\tau)} A_1 A_2 d\alpha_1 d\alpha_2 = \\ &= \left( \delta \bar{\mathbf{u}}^{(\tau)} \right)^T \mathbf{Q}_{sa}^{(\tau)} \end{aligned} \quad (3.255)$$

where  $\mathbf{Q}_{sa}^{(\tau)}$  is the vector of the surface loads of size  $(3I_N I_M) \times 1$  defined below

$$\mathbf{Q}_{sa}^{(\tau)} = \int_{\alpha_1} \int_{\alpha_2} \begin{bmatrix} \bar{\mathbf{N}} q_{1sa}^{(\tau)} \\ \bar{\mathbf{N}} q_{2sa}^{(\tau)} \\ \bar{\mathbf{N}} q_{3sa}^{(\tau)} \end{bmatrix} A_1 A_2 d\alpha_1 d\alpha_2 \quad (3.256)$$

Analogously, as far as the volume forces are concerned, one gets

$$\begin{aligned} \delta L_{ev} &= \int_{\alpha_1} \int_{\alpha_2} \left( \delta \mathbf{u}^{(\tau)} \right)^T \mathbf{q}_{va}^{(\tau)} A_1 A_2 d\alpha_1 d\alpha_2 = \\ &= \int_{\alpha_1} \int_{\alpha_2} \left( \mathbf{N}^T \delta \bar{\mathbf{u}}^{(\tau)} \right)^T \mathbf{q}_{va}^{(\tau)} A_1 A_2 d\alpha_1 d\alpha_2 = \\ &= \int_{\alpha_1} \int_{\alpha_2} \left( \delta \bar{\mathbf{u}}^{(\tau)} \right)^T \mathbf{N} \mathbf{q}_{va}^{(\tau)} A_1 A_2 d\alpha_1 d\alpha_2 = \\ &= \left( \delta \bar{\mathbf{u}}^{(\tau)} \right)^T \int_{\alpha_1} \int_{\alpha_2} \mathbf{N} \mathbf{q}_{va}^{(\tau)} A_1 A_2 d\alpha_1 d\alpha_2 = \\ &= \left( \delta \bar{\mathbf{u}}^{(\tau)} \right)^T \mathbf{Q}_{va}^{(\tau)} \end{aligned} \quad (3.257)$$

where  $\mathbf{Q}_{va}^{(\tau)}$  denotes the vector of the volume forces of size  $(3I_N I_M) \times 1$  defined below

$$\mathbf{Q}_{va}^{(\tau)} = \int \int_{\alpha_1 \alpha_2} \begin{bmatrix} \bar{\mathbf{N}}q_{1va}^{(\tau)} \\ \bar{\mathbf{N}}q_{2va}^{(\tau)} \\ \bar{\mathbf{N}}q_{3va}^{(\tau)} \end{bmatrix} A_1 A_2 d\alpha_1 d\alpha_2 \quad (3.258)$$

The effect of the Winkler-Pasternak elastic foundation can be analyzed now, having in mind definitions (3.224). Starting from equation (3.211), the contribution of the foundation assumes the following aspect

$$\begin{aligned} \delta L_{ef} &= \int \int_{\alpha_1 \alpha_2} (\delta \mathbf{u}^{(\tau)})^T \mathbf{q}_f^{(\tau)} A_1 A_2 d\alpha_1 d\alpha_2 = \\ &= \int \int_{\alpha_1 \alpha_2} (\delta \mathbf{u}^{(\tau)})^T \left( \sum_{\eta=0}^{N+1} \mathbf{L}_f^{(\tau\eta)} \mathbf{u}^{(\eta)} \right) A_1 A_2 d\alpha_1 d\alpha_2 + \\ &\quad + \int \int_{\alpha_1 \alpha_2} (\delta \mathbf{u}^{(\tau)})^T \left( \sum_{\eta=0}^{N+1} \mathbf{M}_f^{(\tau\eta)} \ddot{\mathbf{u}}^{(\eta)} \right) A_1 A_2 d\alpha_1 d\alpha_2 = \\ &= \int \int_{\alpha_1 \alpha_2} (\mathbf{N}^T \delta \bar{\mathbf{u}}^{(\tau)})^T \left( \sum_{\eta=0}^{N+1} \mathbf{L}_f^{(\tau\eta)} \mathbf{N}^T \bar{\mathbf{u}}^{(\eta)} \right) A_1 A_2 d\alpha_1 d\alpha_2 + \\ &\quad + \int \int_{\alpha_1 \alpha_2} (\mathbf{N}^T \delta \bar{\mathbf{u}}^{(\tau)})^T \left( \sum_{\eta=0}^{N+1} \mathbf{M}_f^{(\tau\eta)} \mathbf{N}^T \ddot{\bar{\mathbf{u}}}^{(\eta)} \right) A_1 A_2 d\alpha_1 d\alpha_2 = \\ &= \int \int_{\alpha_1 \alpha_2} (\delta \bar{\mathbf{u}}^{(\tau)})^T \mathbf{N} \left( \sum_{\eta=0}^{N+1} \mathbf{L}_f^{(\tau\eta)} \mathbf{N}^T \bar{\mathbf{u}}^{(\eta)} \right) A_1 A_2 d\alpha_1 d\alpha_2 + \\ &\quad + \int \int_{\alpha_1 \alpha_2} (\delta \bar{\mathbf{u}}^{(\tau)})^T \mathbf{N} \left( \sum_{\eta=0}^{N+1} \mathbf{M}_f^{(\tau\eta)} \mathbf{N}^T \ddot{\bar{\mathbf{u}}}^{(\eta)} \right) A_1 A_2 d\alpha_1 d\alpha_2 = \\ &= \int \int_{\alpha_1 \alpha_2} (\delta \bar{\mathbf{u}}^{(\tau)})^T \left( \sum_{\eta=0}^{N+1} \mathbf{N} \mathbf{L}_f^{(\tau\eta)} \mathbf{N}^T \bar{\mathbf{u}}^{(\eta)} \right) A_1 A_2 d\alpha_1 d\alpha_2 + \\ &\quad + \int \int_{\alpha_1 \alpha_2} (\delta \bar{\mathbf{u}}^{(\tau)})^T \left( \sum_{\eta=0}^{N+1} \mathbf{N} \mathbf{M}_f^{(\tau\eta)} \mathbf{N}^T \ddot{\bar{\mathbf{u}}}^{(\eta)} \right) A_1 A_2 d\alpha_1 d\alpha_2 = \\ &= (\delta \bar{\mathbf{u}}^{(\tau)})^T \sum_{\eta=0}^{N+1} \int \int_{\alpha_1 \alpha_2} \left( \sum_{\eta=0}^{N+1} \mathbf{N} \mathbf{L}_f^{(\tau\eta)} \mathbf{N}^T A_1 A_2 d\alpha_1 d\alpha_2 \right) \bar{\mathbf{u}}^{(\eta)} + \\ &\quad + (\delta \bar{\mathbf{u}}^{(\tau)})^T \sum_{\eta=0}^{N+1} \int \int_{\alpha_1 \alpha_2} \left( \sum_{\eta=0}^{N+1} \mathbf{N} \mathbf{M}_f^{(\tau\eta)} \mathbf{N}^T A_1 A_2 d\alpha_1 d\alpha_2 \right) \ddot{\bar{\mathbf{u}}}^{(\eta)} = \\ &= (\delta \bar{\mathbf{u}}^{(\tau)})^T \sum_{\eta=0}^{N+1} \mathbf{K}_f^{(\tau\eta)} \bar{\mathbf{u}}^{(\eta)} + (\delta \bar{\mathbf{u}}^{(\tau)})^T \sum_{\eta=0}^{N+1} \bar{\mathbf{M}}_f^{(\tau\eta)} \ddot{\bar{\mathbf{u}}}^{(\eta)} \quad (3.259) \end{aligned}$$

where  $\mathbf{K}_f^{(\tau\eta)}$  and  $\bar{\mathbf{M}}_f^{(\tau\eta)}$  represent respectively the stiffness and mass matrices of the foundation, whose size is given by  $(3I_N I_M) \times (3I_N I_M)$  for both of them. In particular, the

stiffness operator is defined as follows

$$\mathbf{K}_f^{(\tau\eta)} = \int_{\alpha_1} \int_{\alpha_2} \begin{bmatrix} \bar{\mathbf{N}} L_{f1}^{(\tau\eta)\alpha_1} \bar{\mathbf{N}}^T & \mathbf{0} & \mathbf{0} \\ \mathbf{0} & \bar{\mathbf{N}} L_{f2}^{(\tau\eta)\alpha_2} \bar{\mathbf{N}}^T & \mathbf{0} \\ \mathbf{0} & \mathbf{0} & \bar{\mathbf{N}} L_{f3}^{(\tau\eta)\alpha_3} \bar{\mathbf{N}}^T \end{bmatrix} A_1 A_2 d\alpha_1 d\alpha_2 \quad (3.260)$$

whereas the mass matrix  $\bar{\mathbf{M}}_f^{(\tau\eta)}$  becomes

$$\mathbf{M}_f^{(\tau\eta)} = \int_{\alpha_1} \int_{\alpha_2} \begin{bmatrix} \bar{\mathbf{N}} I_{f1}^{(\tau\eta)\alpha_1} \bar{\mathbf{N}}^T & \mathbf{0} & \mathbf{0} \\ \mathbf{0} & \bar{\mathbf{N}} I_{f2}^{(\tau\eta)\alpha_2} \bar{\mathbf{N}}^T & \mathbf{0} \\ \mathbf{0} & \mathbf{0} & \bar{\mathbf{N}} I_{f3}^{(\tau\eta)\alpha_3} \bar{\mathbf{N}}^T \end{bmatrix} A_1 A_2 d\alpha_1 d\alpha_2 \quad (3.261)$$

for  $\tau, \eta = 0, 1, 2, \dots, N, N+1$ . Finally, the effect of the external loads applied directly on the external edges must be considered. As far as the edges identified by  $\alpha_1$  constants are concerned, one gets

$$\begin{aligned} \delta L_{eb1} &= \oint_{\alpha_2} \left( \delta \mathbf{u}^{(\tau)} \right)^T \bar{\mathbf{S}}_{\alpha_1}^{(\tau)} A_2 d\alpha_2 = \\ &= \oint_{\alpha_2} \left( \mathbf{N}^T \delta \bar{\mathbf{u}}^{(\tau)} \right)^T \bar{\mathbf{S}}_{\alpha_1}^{(\tau)} A_2 d\alpha_2 = \\ &= \oint_{\alpha_2} \left( \delta \bar{\mathbf{u}}^{(\tau)} \right)^T \mathbf{N} \bar{\mathbf{S}}_{\alpha_1}^{(\tau)} A_2 d\alpha_2 = \\ &= \left( \delta \bar{\mathbf{u}}^{(\tau)} \right)^T \oint_{\alpha_2} \mathbf{N} \bar{\mathbf{S}}_{\alpha_1}^{(\tau)} A_2 d\alpha_2 = \\ &= \left( \delta \bar{\mathbf{u}}^{(\tau)} \right)^T \bar{\mathbf{Q}}_{\alpha_1}^{(\tau)} \end{aligned} \quad (3.262)$$

where  $\bar{\mathbf{Q}}_{\alpha_1}^{(\tau)}$  is the vector of size  $(3I_N I_M) \times 1$  which collects their contribution defined below

$$\bar{\mathbf{Q}}_{\alpha_1}^{(\tau)} = \oint_{\alpha_2} \begin{bmatrix} \bar{\mathbf{N}} \bar{\mathbf{N}}_1^{(\tau)\alpha_1} \\ \bar{\mathbf{N}} \bar{\mathbf{N}}_{12}^{(\tau)\alpha_2} \\ \bar{\mathbf{N}} \bar{\mathbf{T}}_1^{(\tau)\alpha_3} \end{bmatrix} A_2 d\alpha_2 \quad (3.263)$$

Analogously, the contribution of the external forces applied directly on the external edges characterized by  $\alpha_2$  constants is given by

$$\begin{aligned} \delta L_{eb1} &= \oint_{\alpha_1} \left( \delta \mathbf{u}^{(\tau)} \right)^T \bar{\mathbf{S}}_{\alpha_2}^{(\tau)} A_1 d\alpha_1 = \\ &= \oint_{\alpha_1} \left( \mathbf{N}^T \delta \bar{\mathbf{u}}^{(\tau)} \right)^T \bar{\mathbf{S}}_{\alpha_2}^{(\tau)} A_1 d\alpha_1 = \end{aligned}$$

$$\begin{aligned}
&= \oint_{\alpha_1} \left( \delta \bar{\mathbf{u}}^{(\tau)} \right)^T \mathbf{N} \bar{\mathbf{S}}_{\alpha_2}^{(\tau)} A_1 d\alpha_1 = \\
&= \left( \delta \bar{\mathbf{u}}^{(\tau)} \right)^T \oint_{\alpha_1} \mathbf{N} \bar{\mathbf{S}}_{\alpha_2}^{(\tau)} A_1 d\alpha_1 = \\
&= \left( \delta \bar{\mathbf{u}}^{(\tau)} \right)^T \bar{\mathbf{Q}}_{\alpha_2}^{(\tau)} \quad (3.264)
\end{aligned}$$

where  $\bar{\mathbf{Q}}_{\alpha_2}^{(\tau)}$  represents the vector of size  $(3I_N I_M) \times 1$  that includes these contributions defined below

$$\bar{\mathbf{Q}}_{\alpha_2}^{(\tau)} = \oint_{\alpha_1} \begin{bmatrix} \bar{\mathbf{N}} \bar{\mathbf{N}}_{21}^{(\tau) \alpha_1} \\ \bar{\mathbf{N}} \bar{\mathbf{N}}_2^{(\tau) \alpha_2} \\ \bar{\mathbf{N}} \bar{\mathbf{T}}_2^{(\tau) \alpha_3} \end{bmatrix} A_1 d\alpha_1 \quad (3.265)$$

All things considered, the Hamilton's principle (3.211) assumes the following aspect if the weak formulation of the governing equation is pursued

$$\begin{aligned}
\left( \delta \bar{\mathbf{u}}^{(\tau)} \right)^T \left( - \sum_{\eta=0}^{N+1} \bar{\mathbf{M}}^{(\tau \eta)} \ddot{\bar{\mathbf{u}}}^{(\eta)} + \sum_{\eta=0}^{N+1} \bar{\mathbf{M}}_f^{(\tau \eta)} \ddot{\bar{\mathbf{u}}}^{(\eta)} - \sum_{i=1}^3 \int_{\alpha_1} \int_{\alpha_2} \left( \mathbf{B}^{\alpha_i} \right)^T \mathbf{S}^{(\tau) \alpha_i} A_1 A_2 d\alpha_1 d\alpha_2 + \right. \\
\left. + \sum_{\eta=0}^{N+1} \mathbf{K}_f^{(\tau \eta)} \bar{\mathbf{u}}^{(\eta)} + \mathbf{Q}_{sa}^{(\tau)} + \mathbf{Q}_{va}^{(\tau)} + \bar{\mathbf{Q}}_{\alpha_1}^{(\tau)} + \bar{\mathbf{Q}}_{\alpha_2}^{(\tau)} \right) = \mathbf{0} \quad (3.266)
\end{aligned}$$

for  $\tau = 0, 1, 2, \dots, N, N+1$ . Since the vector  $\delta \bar{\mathbf{u}}^{(\tau)}$  collects arbitrary generalized nodal displacements, equation (3.266) is satisfied only if these quantities are equal to zero. By assuming  $\mathbf{Q}^{(\tau)} = \mathbf{Q}_{sa}^{(\tau)} + \mathbf{Q}_{va}^{(\tau)} + \bar{\mathbf{Q}}_{\alpha_1}^{(\tau)} + \bar{\mathbf{Q}}_{\alpha_2}^{(\tau)}$ , the weak formulation of the governing motion equations are obtained as follows

$$\sum_{i=1}^3 \int_{\alpha_1} \int_{\alpha_2} \left( \mathbf{B}^{\alpha_i} \right)^T \mathbf{S}^{(\tau) \alpha_i} A_1 A_2 d\alpha_1 d\alpha_2 + \sum_{\eta=0}^{N+1} \bar{\mathbf{M}}^{(\tau \eta)} \ddot{\bar{\mathbf{u}}}^{(\eta)} = \mathbf{Q}^{(\tau)} + \sum_{\eta=0}^{N+1} \mathbf{K}_f^{(\tau \eta)} \bar{\mathbf{u}}^{(\eta)} + \sum_{\eta=0}^{N+1} \bar{\mathbf{M}}_f^{(\tau \eta)} \ddot{\bar{\mathbf{u}}}^{(\eta)} \quad (3.267)$$

The integral form of the weak formulation can be easily noted in (3.267). Nevertheless, a more compact system of equations can be obtained by recalling the definition of the generalized stress resultants (3.186). Let us consider the first term in (3.267). One gets

$$\begin{aligned}
&\sum_{i=1}^3 \int_{\alpha_1} \int_{\alpha_2} \left( \mathbf{B}^{\alpha_i} \right)^T \mathbf{S}^{(\tau) \alpha_i} A_1 A_2 d\alpha_1 d\alpha_2 = \\
&= \sum_{\eta=0}^{N+1} \left( \sum_{i=1}^3 \sum_{j=1}^3 \int_{\alpha_1} \int_{\alpha_2} \left( \mathbf{B}^{\alpha_i} \right)^T \mathbf{A}^{(\tau \eta) \alpha_i \alpha_j} \mathbf{B}^{\alpha_j} A_1 A_2 d\alpha_1 d\alpha_2 \right) \bar{\mathbf{u}}^{(\tau)}
\end{aligned}$$

$$= \sum_{\eta=0}^{N+1} \mathbf{K}^{(\tau\eta)} \bar{\mathbf{u}}^{(\tau)} \quad (3.268)$$

where  $\mathbf{K}^{(\tau\eta)}$  is the stiffness matrix of size  $(3I_N I_M) \times (3I_N I_M)$  defined below

$$\mathbf{K}^{(\tau\eta)} = \int \int_{\alpha_1 \alpha_2} \begin{bmatrix} (\mathbf{B}^{\alpha_1})^T \mathbf{A}^{(\tau\eta)\alpha_1\alpha_1} \mathbf{B}^{\alpha_1} & (\mathbf{B}^{\alpha_1})^T \mathbf{A}^{(\tau\eta)\alpha_1\alpha_2} \mathbf{B}^{\alpha_2} & (\mathbf{B}^{\alpha_1})^T \mathbf{A}^{(\tau\eta)\alpha_1\alpha_3} \mathbf{B}^{\alpha_3} \\ (\mathbf{B}^{\alpha_2})^T \mathbf{A}^{(\tau\eta)\alpha_2\alpha_1} \mathbf{B}^{\alpha_1} & (\mathbf{B}^{\alpha_2})^T \mathbf{A}^{(\tau\eta)\alpha_2\alpha_2} \mathbf{B}^{\alpha_2} & (\mathbf{B}^{\alpha_2})^T \mathbf{A}^{(\tau\eta)\alpha_2\alpha_3} \mathbf{B}^{\alpha_3} \\ (\mathbf{B}^{\alpha_3})^T \mathbf{A}^{(\tau\eta)\alpha_3\alpha_1} \mathbf{B}^{\alpha_1} & (\mathbf{B}^{\alpha_3})^T \mathbf{A}^{(\tau\eta)\alpha_3\alpha_2} \mathbf{B}^{\alpha_2} & (\mathbf{B}^{\alpha_3})^T \mathbf{A}^{(\tau\eta)\alpha_3\alpha_3} \mathbf{B}^{\alpha_3} \end{bmatrix} A_1 A_2 d\alpha_1 d\alpha_2 \quad (3.269)$$

The matrix product in the stiffness matrix (3.269) can be computed as follows, for  $\tau, \eta = 0, 1, 2, \dots, N, N+1$ , by means of the Kronecker product “ $\otimes_k$ ”. The operators at issue are listed by column for conciseness purposes.

*First column of the stiffness matrix*

$$\begin{aligned} (\mathbf{B}^{\alpha_1})^T \mathbf{A}^{(\tau\eta)\alpha_1\alpha_1} \mathbf{B}^{\alpha_1} &= \frac{A_{11(20)}^{(\tau\eta)\alpha_1\alpha_1}}{A_1^2} \left( (\mathbf{l}_{\alpha_2})^T \mathbf{l}_{\alpha_2} \right) \otimes_k \left( (\mathbf{l}_{\alpha_1}^{(1)})^T \mathbf{l}_{\alpha_1}^{(1)} \right) + \frac{A_{66(02)}^{(\tau\eta)\alpha_1\alpha_1}}{A_2^2} \left( (\mathbf{l}_{\alpha_2}^{(1)})^T \mathbf{l}_{\alpha_2}^{(1)} \right) \otimes_k \left( (\mathbf{l}_{\alpha_1})^T \mathbf{l}_{\alpha_1} \right) + \\ &+ \frac{A_{16(11)}^{(\tau\eta)\alpha_1\alpha_1}}{A_1 A_2} \left( \left( (\mathbf{l}_{\alpha_2})^T \mathbf{l}_{\alpha_2}^{(1)} \right) \otimes_k \left( (\mathbf{l}_{\alpha_1}^{(1)})^T \mathbf{l}_{\alpha_1} \right) + \left( (\mathbf{l}_{\alpha_2}^{(1)})^T \mathbf{l}_{\alpha_2} \right) \otimes_k \left( (\mathbf{l}_{\alpha_1})^T \mathbf{l}_{\alpha_1}^{(1)} \right) \right) + \\ &+ \left( \frac{A_{12(11)}^{(\tau\eta)\alpha_1\alpha_1}}{A_1^2 A_2} \frac{\partial A_2}{\partial \alpha_1} - \frac{A_{16(20)}^{(\tau\eta)\alpha_1\alpha_1}}{A_1^2 A_2} \frac{\partial A_1}{\partial \alpha_2} \right) \left( \left( (\mathbf{l}_{\alpha_2})^T \mathbf{l}_{\alpha_2} \right) \otimes_k \left( (\mathbf{l}_{\alpha_1}^{(1)})^T \mathbf{l}_{\alpha_1} \right) + \left( (\mathbf{l}_{\alpha_2}^{(1)})^T \mathbf{l}_{\alpha_2} \right) \otimes_k \left( (\mathbf{l}_{\alpha_1})^T \mathbf{l}_{\alpha_1}^{(1)} \right) \right) + \\ &+ \left( \frac{A_{26(02)}^{(\tau\eta)\alpha_1\alpha_1}}{A_1 A_2^2} \frac{\partial A_2}{\partial \alpha_1} - \frac{A_{66(11)}^{(\tau\eta)\alpha_1\alpha_1}}{A_1 A_2^2} \frac{\partial A_1}{\partial \alpha_2} \right) \left( \left( (\mathbf{l}_{\alpha_2})^T \mathbf{l}_{\alpha_2}^{(1)} \right) \otimes_k \left( (\mathbf{l}_{\alpha_1})^T \mathbf{l}_{\alpha_1} \right) + \left( (\mathbf{l}_{\alpha_2}^{(1)})^T \mathbf{l}_{\alpha_2} \right) \otimes_k \left( (\mathbf{l}_{\alpha_1})^T \mathbf{l}_{\alpha_1}^{(1)} \right) \right) + \\ &+ \left( \frac{A_{22(02)}^{(\tau\eta)\alpha_1\alpha_1}}{A_1^2 A_2^2} \left( \frac{\partial A_2}{\partial \alpha_1} \right)^2 + \frac{A_{66(20)}^{(\tau\eta)\alpha_1\alpha_1}}{A_1^2 A_2^2} \left( \frac{\partial A_1}{\partial \alpha_2} \right)^2 - \frac{2A_{26(11)}^{(\tau\eta)\alpha_1\alpha_1}}{A_1^2 A_2^2} \frac{\partial A_1}{\partial \alpha_2} \frac{\partial A_2}{\partial \alpha_1} + \frac{A_{44(20)}^{(\tau\eta)\alpha_1\alpha_1}}{R_1^2} + \right. \\ &\left. - \frac{A_{44(10)}^{(\tau\eta)\alpha_1\alpha_1} + A_{44(10)}^{(\bar{\tau}\eta)\alpha_1\alpha_1}}{R_1} + A_{44(00)}^{(\bar{\tau}\eta)\alpha_1\alpha_1} \right) \left( (\mathbf{l}_{\alpha_2})^T \mathbf{l}_{\alpha_2} \right) \otimes_k \left( (\mathbf{l}_{\alpha_1})^T \mathbf{l}_{\alpha_1} \right) \\ (\mathbf{B}^{\alpha_2})^T \mathbf{A}^{(\tau\eta)\alpha_2\alpha_1} \mathbf{B}^{\alpha_1} &= \frac{A_{16(20)}^{(\tau\eta)\alpha_2\alpha_1}}{A_1^2} \left( (\mathbf{l}_{\alpha_2})^T \mathbf{l}_{\alpha_2} \right) \otimes_k \left( (\mathbf{l}_{\alpha_1}^{(1)})^T \mathbf{l}_{\alpha_1}^{(1)} \right) + \frac{A_{26(02)}^{(\tau\eta)\alpha_2\alpha_1}}{A_2^2} \left( (\mathbf{l}_{\alpha_2}^{(1)})^T \mathbf{l}_{\alpha_2}^{(1)} \right) \otimes_k \left( (\mathbf{l}_{\alpha_1})^T \mathbf{l}_{\alpha_1} \right) + \\ &+ \frac{A_{66(11)}^{(\tau\eta)\alpha_2\alpha_1}}{A_1 A_2} \left( (\mathbf{l}_{\alpha_2})^T \mathbf{l}_{\alpha_2}^{(1)} \right) \otimes_k \left( (\mathbf{l}_{\alpha_1}^{(1)})^T \mathbf{l}_{\alpha_1} \right) + \frac{A_{12(11)}^{(\tau\eta)\alpha_2\alpha_1}}{A_1 A_2} \left( (\mathbf{l}_{\alpha_2}^{(1)})^T \mathbf{l}_{\alpha_2} \right) \otimes_k \left( (\mathbf{l}_{\alpha_1})^T \mathbf{l}_{\alpha_1}^{(1)} \right) + \\ &+ \left( \frac{A_{26(11)}^{(\tau\eta)\alpha_2\alpha_1}}{A_1^2 A_2} \frac{\partial A_2}{\partial \alpha_1} - \frac{A_{66(20)}^{(\tau\eta)\alpha_2\alpha_1}}{A_1^2 A_2} \frac{\partial A_1}{\partial \alpha_2} \right) \left( (\mathbf{l}_{\alpha_2})^T \mathbf{l}_{\alpha_2} \right) \otimes_k \left( (\mathbf{l}_{\alpha_1}^{(1)})^T \mathbf{l}_{\alpha_1} \right) + \\ &+ \left( \frac{A_{11(20)}^{(\tau\eta)\alpha_2\alpha_1}}{A_1^2 A_2} \frac{\partial A_1}{\partial \alpha_2} - \frac{A_{16(11)}^{(\tau\eta)\alpha_2\alpha_1}}{A_1^2 A_2} \frac{\partial A_2}{\partial \alpha_1} \right) \left( (\mathbf{l}_{\alpha_2}^{(1)})^T \mathbf{l}_{\alpha_2} \right) \otimes_k \left( (\mathbf{l}_{\alpha_1})^T \mathbf{l}_{\alpha_1}^{(1)} \right) + \end{aligned}$$

$$\begin{aligned}
& + \left( \frac{A_{16(11)}^{(\tau\eta)\alpha_2\alpha_1}}{A_1 A_2^2} \frac{\partial A_1}{\partial \alpha_2} - \frac{A_{66(02)}^{(\tau\eta)\alpha_2\alpha_1}}{A_1 A_2^2} \frac{\partial A_2}{\partial \alpha_1} \right) \left( (\mathbf{l}_{\alpha_2})^T \mathbf{l}_{\alpha_2}^{(1)} \right) \otimes_k \left( (\mathbf{l}_{\alpha_1})^T \mathbf{l}_{\alpha_1} \right) + \\
& + \left( \frac{A_{22(02)}^{(\tau\eta)\alpha_2\alpha_1}}{A_1 A_2^2} \frac{\partial A_2}{\partial \alpha_1} - \frac{A_{26(11)}^{(\tau\eta)\alpha_2\alpha_1}}{A_1 A_2^2} \frac{\partial A_1}{\partial \alpha_2} \right) \left( (\mathbf{l}_{\alpha_2}^{(1)})^T \mathbf{l}_{\alpha_2} \right) \otimes_k \left( (\mathbf{l}_{\alpha_1})^T \mathbf{l}_{\alpha_1} \right) + \\
& + \left( \frac{A_{66(11)}^{(\tau\eta)\alpha_2\alpha_1}}{A_1^2 A_2^2} \frac{\partial A_1}{\partial \alpha_2} \frac{\partial A_2}{\partial \alpha_1} - \frac{A_{26(02)}^{(\tau\eta)\alpha_2\alpha_1}}{A_1^2 A_2^2} \left( \frac{\partial A_2}{\partial \alpha_1} \right)^2 + \frac{A_{12(11)}^{(\tau\eta)\alpha_2\alpha_1}}{A_1^2 A_2^2} \frac{\partial A_2}{\partial \alpha_1} \frac{\partial A_1}{\partial \alpha_2} - \frac{A_{16(20)}^{(\tau\eta)\alpha_2\alpha_1}}{A_1^2 A_2^2} \left( \frac{\partial A_1}{\partial \alpha_2} \right)^2 \right) + \\
& + \left. \frac{A_{45(11)}^{(\tau\eta)\alpha_2\alpha_1}}{R_2 R_1} - \frac{A_{45(01)}^{(\tau\eta)\alpha_2\alpha_1}}{R_2} - \frac{A_{45(10)}^{(\tau\eta)\alpha_2\alpha_1}}{R_1} + A_{45(00)}^{(\tau\eta)\alpha_2\alpha_1} \right) \left( (\mathbf{l}_{\alpha_2})^T \mathbf{l}_{\alpha_2} \right) \otimes_k \left( (\mathbf{l}_{\alpha_1})^T \mathbf{l}_{\alpha_1} \right) \\
(\mathbf{B}^{\alpha_3})^T \mathbf{A}^{(\tau\eta)\alpha_3\alpha_1} \mathbf{B}^{\alpha_1} & = \left( -\frac{A_{44(20)}^{(\tau\eta)\alpha_3\alpha_1}}{A_1 R_1} + \frac{A_{44(10)}^{(\tau\eta)\alpha_3\alpha_1}}{A_1} \right) \left( (\mathbf{l}_{\alpha_2})^T \mathbf{l}_{\alpha_2} \right) \otimes_k \left( (\mathbf{l}_{\alpha_1}^{(1)})^T \mathbf{l}_{\alpha_1} \right) + \\
& + \left( \frac{A_{11(20)}^{(\tau\eta)\alpha_3\alpha_1}}{A_1 R_1} + \frac{A_{12(11)}^{(\tau\eta)\alpha_3\alpha_1}}{A_1 R_2} + \frac{A_{13(10)}^{(\tau\eta)\alpha_3\alpha_1}}{A_1} \right) \left( (\mathbf{l}_{\alpha_2})^T \mathbf{l}_{\alpha_2} \right) \otimes_k \left( (\mathbf{l}_{\alpha_1})^T \mathbf{l}_{\alpha_1}^{(1)} \right) + \\
& + \left( \frac{A_{16(11)}^{(\tau\eta)\alpha_3\alpha_1}}{A_2 R_1} + \frac{A_{26(02)}^{(\tau\eta)\alpha_3\alpha_1}}{A_2 R_2} + \frac{A_{36(01)}^{(\tau\eta)\alpha_3\alpha_1}}{A_2} \right) \left( (\mathbf{l}_{\alpha_2})^T \mathbf{l}_{\alpha_2}^{(1)} \right) \otimes_k \left( (\mathbf{l}_{\alpha_1})^T \mathbf{l}_{\alpha_1} \right) + \\
& + \left( -\frac{A_{45(11)}^{(\tau\eta)\alpha_3\alpha_1}}{A_2 R_1} + \frac{A_{45(01)}^{(\tau\eta)\alpha_3\alpha_1}}{A_2} \right) \left( (\mathbf{l}_{\alpha_2}^{(1)})^T \mathbf{l}_{\alpha_2} \right) \otimes_k \left( (\mathbf{l}_{\alpha_1})^T \mathbf{l}_{\alpha_1} \right) + \left( \frac{A_{12(11)}^{(\tau\eta)\alpha_3\alpha_1}}{A_1 A_2 R_1} + \frac{A_{22(02)}^{(\tau\eta)\alpha_3\alpha_1}}{A_1 A_2 R_2} + \frac{A_{23(01)}^{(\tau\eta)\alpha_3\alpha_1}}{A_1 A_2} \right) \frac{\partial A_2}{\partial \alpha_1} + \\
& - \left( \frac{A_{16(20)}^{(\tau\eta)\alpha_3\alpha_1}}{A_1 A_2 R_1} + \frac{A_{26(11)}^{(\tau\eta)\alpha_3\alpha_1}}{A_1 A_2 R_2} + \frac{A_{36(10)}^{(\tau\eta)\alpha_3\alpha_1}}{A_1 A_2} \right) \frac{\partial A_1}{\partial \alpha_2} \left( (\mathbf{l}_{\alpha_2})^T \mathbf{l}_{\alpha_2} \right) \otimes_k \left( (\mathbf{l}_{\alpha_1})^T \mathbf{l}_{\alpha_1} \right)
\end{aligned}$$

Second column of the stiffness matrix

$$\begin{aligned}
(\mathbf{B}^{\alpha_1})^T \mathbf{A}^{(\tau\eta)\alpha_1\alpha_2} \mathbf{B}^{\alpha_2} & = \frac{A_{16(20)}^{(\tau\eta)\alpha_1\alpha_2}}{A_1^2} \left( (\mathbf{l}_{\alpha_2})^T \mathbf{l}_{\alpha_2} \right) \otimes_k \left( (\mathbf{l}_{\alpha_1}^{(1)})^T \mathbf{l}_{\alpha_1} \right) + \frac{A_{26(02)}^{(\tau\eta)\alpha_1\alpha_2}}{A_2^2} \left( (\mathbf{l}_{\alpha_2}^{(1)})^T \mathbf{l}_{\alpha_2} \right) \otimes_k \left( (\mathbf{l}_{\alpha_1})^T \mathbf{l}_{\alpha_1} \right) + \\
& + \frac{A_{12(11)}^{(\tau\eta)\alpha_1\alpha_2}}{A_1 A_2} \left( (\mathbf{l}_{\alpha_2})^T \mathbf{l}_{\alpha_2}^{(1)} \right) \otimes_k \left( (\mathbf{l}_{\alpha_1}^{(1)})^T \mathbf{l}_{\alpha_1} \right) + \frac{A_{66(11)}^{(\tau\eta)\alpha_1\alpha_2}}{A_1 A_2} \left( (\mathbf{l}_{\alpha_2}^{(1)})^T \mathbf{l}_{\alpha_2} \right) \otimes_k \left( (\mathbf{l}_{\alpha_1})^T \mathbf{l}_{\alpha_1} \right) + \\
& + \left( \frac{A_{11(20)}^{(\tau\eta)\alpha_1\alpha_2}}{A_1^2 A_2} \frac{\partial A_1}{\partial \alpha_2} - \frac{A_{16(11)}^{(\tau\eta)\alpha_1\alpha_2}}{A_1^2 A_2} \frac{\partial A_2}{\partial \alpha_1} \right) \left( (\mathbf{l}_{\alpha_2})^T \mathbf{l}_{\alpha_2} \right) \otimes_k \left( (\mathbf{l}_{\alpha_1}^{(1)})^T \mathbf{l}_{\alpha_1} \right) + \\
& + \left( \frac{A_{26(11)}^{(\tau\eta)\alpha_1\alpha_2}}{A_1^2 A_2} \frac{\partial A_2}{\partial \alpha_1} - \frac{A_{66(20)}^{(\tau\eta)\alpha_1\alpha_2}}{A_1^2 A_2} \frac{\partial A_1}{\partial \alpha_2} \right) \left( (\mathbf{l}_{\alpha_2})^T \mathbf{l}_{\alpha_2} \right) \otimes_k \left( (\mathbf{l}_{\alpha_1})^T \mathbf{l}_{\alpha_1}^{(1)} \right) + \\
& + \left( \frac{A_{22(02)}^{(\tau\eta)\alpha_1\alpha_2}}{A_1 A_2^2} \frac{\partial A_2}{\partial \alpha_1} - \frac{A_{26(11)}^{(\tau\eta)\alpha_1\alpha_2}}{A_1 A_2^2} \frac{\partial A_1}{\partial \alpha_2} \right) \left( (\mathbf{l}_{\alpha_2}^{(1)})^T \mathbf{l}_{\alpha_2} \right) \otimes_k \left( (\mathbf{l}_{\alpha_1})^T \mathbf{l}_{\alpha_1} \right) + \\
& + \left( \frac{A_{16(11)}^{(\tau\eta)\alpha_1\alpha_2}}{A_1 A_2^2} \frac{\partial A_1}{\partial \alpha_2} - \frac{A_{66(02)}^{(\tau\eta)\alpha_1\alpha_2}}{A_1 A_2^2} \frac{\partial A_2}{\partial \alpha_1} \right) \left( (\mathbf{l}_{\alpha_2}^{(1)})^T \mathbf{l}_{\alpha_2} \right) \otimes_k \left( (\mathbf{l}_{\alpha_1})^T \mathbf{l}_{\alpha_1} \right) +
\end{aligned}$$

$$\begin{aligned}
 & + \left( \frac{A_{12(11)}^{(\tau\eta)\alpha_1\alpha_2}}{A_1^2 A_2^2} \frac{\partial A_1}{\partial \alpha_2} \frac{\partial A_2}{\partial \alpha_1} - \frac{A_{26(02)}^{(\tau\eta)\alpha_1\alpha_2}}{A_1^2 A_2^2} \left( \frac{\partial A_2}{\partial \alpha_1} \right)^2 + \frac{A_{66(11)}^{(\tau\eta)\alpha_1\alpha_2}}{A_1^2 A_2^2} \frac{\partial A_2}{\partial \alpha_1} \frac{\partial A_1}{\partial \alpha_2} - \frac{A_{16(20)}^{(\tau\eta)\alpha_1\alpha_2}}{A_1^2 A_2^2} \left( \frac{\partial A_1}{\partial \alpha_2} \right)^2 \right. \\
 & \left. + \frac{A_{45(11)}^{(\tau\eta)\alpha_1\alpha_2}}{R_1 R_2} - \frac{A_{45(10)}^{(\tau\eta)\alpha_1\alpha_2}}{R_1} - \frac{A_{45(10)}^{(\bar{\tau}\eta)\alpha_1\alpha_2}}{R_2} + A_{45(00)}^{(\bar{\tau}\eta)\alpha_1\alpha_2} \right) \left( (\mathbf{l}_{\alpha_2})^T \mathbf{l}_{\alpha_2} \right) \otimes_k \left( (\mathbf{l}_{\alpha_1})^T \mathbf{l}_{\alpha_1} \right) \\
 (\mathbf{B}^{\alpha_2})^T \mathbf{A}^{(\tau\eta)\alpha_2\alpha_2} \mathbf{B}^{\alpha_2} & = \frac{A_{66(20)}^{(\tau\eta)\alpha_2\alpha_2}}{A_1^2} \left( (\mathbf{l}_{\alpha_2})^T \mathbf{l}_{\alpha_2} \right) \otimes_k \left( (\mathbf{l}_{\alpha_1}^{(1)})^T \mathbf{l}_{\alpha_1}^{(1)} \right) + \frac{A_{22(02)}^{(\tau\eta)\alpha_2\alpha_2}}{A_2^2} \left( (\mathbf{l}_{\alpha_2}^{(1)})^T \mathbf{l}_{\alpha_2}^{(1)} \right) \otimes_k \left( (\mathbf{l}_{\alpha_1})^T \mathbf{l}_{\alpha_1} \right) + \\
 & + \frac{A_{26(11)}^{(\tau\eta)\alpha_2\alpha_2}}{A_1 A_2} \left( \left( (\mathbf{l}_{\alpha_2})^T \mathbf{l}_{\alpha_2}^{(1)} \right) \otimes_k \left( (\mathbf{l}_{\alpha_1}^{(1)})^T \mathbf{l}_{\alpha_1} \right) + \left( (\mathbf{l}_{\alpha_2}^{(1)})^T \mathbf{l}_{\alpha_2} \right) \otimes_k \left( (\mathbf{l}_{\alpha_1})^T \mathbf{l}_{\alpha_1}^{(1)} \right) \right) + \\
 & + \left( \frac{A_{16(20)}^{(\tau\eta)\alpha_2\alpha_2}}{A_1^2 A_2} \frac{\partial A_1}{\partial \alpha_2} - \frac{A_{66(11)}^{(\tau\eta)\alpha_2\alpha_2}}{A_1^2 A_2} \frac{\partial A_2}{\partial \alpha_1} \right) \left( \left( (\mathbf{l}_{\alpha_2})^T \mathbf{l}_{\alpha_2} \right) \otimes_k \left( (\mathbf{l}_{\alpha_1}^{(1)})^T \mathbf{l}_{\alpha_1} \right) + \left( (\mathbf{l}_{\alpha_2}^{(1)})^T \mathbf{l}_{\alpha_2} \right) \otimes_k \left( (\mathbf{l}_{\alpha_1})^T \mathbf{l}_{\alpha_1}^{(1)} \right) \right) + \\
 & + \left( \frac{A_{12(11)}^{(\tau\eta)\alpha_2\alpha_2}}{A_1 A_2^2} \frac{\partial A_1}{\partial \alpha_2} - \frac{A_{26(02)}^{(\tau\eta)\alpha_2\alpha_2}}{A_1 A_2^2} \frac{\partial A_2}{\partial \alpha_1} \right) \left( \left( (\mathbf{l}_{\alpha_2})^T \mathbf{l}_{\alpha_2}^{(1)} \right) \otimes_k \left( (\mathbf{l}_{\alpha_1})^T \mathbf{l}_{\alpha_1} \right) + \left( (\mathbf{l}_{\alpha_2}^{(1)})^T \mathbf{l}_{\alpha_2} \right) \otimes_k \left( (\mathbf{l}_{\alpha_1})^T \mathbf{l}_{\alpha_1}^{(1)} \right) \right) + \\
 & + \left( \frac{A_{66(02)}^{(\tau\eta)\alpha_2\alpha_2}}{A_1^2 A_2^2} \left( \frac{\partial A_2}{\partial \alpha_1} \right)^2 + \frac{A_{11(20)}^{(\tau\eta)\alpha_2\alpha_2}}{A_1^2 A_2^2} \left( \frac{\partial A_1}{\partial \alpha_2} \right)^2 - \frac{2A_{16(11)}^{(\tau\eta)\alpha_2\alpha_2}}{A_1^2 A_2^2} \frac{\partial A_1}{\partial \alpha_2} \frac{\partial A_2}{\partial \alpha_1} + \right. \\
 & \left. + \frac{A_{55(02)}^{(\tau\eta)\alpha_2\alpha_2}}{R_2^2} - \frac{A_{55(01)}^{(\tau\eta)\alpha_2\alpha_2}}{R_2} + A_{55(01)}^{(\bar{\tau}\eta)\alpha_2\alpha_2} + A_{55(00)}^{(\bar{\tau}\eta)\alpha_2\alpha_2} \right) \left( (\mathbf{l}_{\alpha_2})^T \mathbf{l}_{\alpha_2} \right) \otimes_k \left( (\mathbf{l}_{\alpha_1})^T \mathbf{l}_{\alpha_1} \right) \\
 (\mathbf{B}^{\alpha_3})^T \mathbf{A}^{(\tau\eta)\alpha_3\alpha_2} \mathbf{B}^{\alpha_2} & = \left( -\frac{A_{45(11)}^{(\tau\eta)\alpha_3\alpha_2}}{A_1 R_2} + \frac{A_{45(10)}^{(\tau\eta)\alpha_3\alpha_2}}{A_1} \right) \left( (\mathbf{l}_{\alpha_2})^T \mathbf{l}_{\alpha_2} \right) \otimes_k \left( (\mathbf{l}_{\alpha_1}^{(1)})^T \mathbf{l}_{\alpha_1} \right) + \\
 & + \left( \frac{A_{16(20)}^{(\tau\eta)\alpha_3\alpha_2}}{A_1 R_1} + \frac{A_{26(11)}^{(\tau\eta)\alpha_3\alpha_2}}{A_1 R_2} + \frac{A_{36(10)}^{(\tau\eta)\alpha_3\alpha_2}}{A_1} \right) \left( (\mathbf{l}_{\alpha_2})^T \mathbf{l}_{\alpha_2} \right) \otimes_k \left( (\mathbf{l}_{\alpha_1})^T \mathbf{l}_{\alpha_1}^{(1)} \right) + \\
 & + \left( \frac{A_{12(11)}^{(\tau\eta)\alpha_3\alpha_2}}{A_2 R_1} + \frac{A_{22(02)}^{(\tau\eta)\alpha_3\alpha_2}}{A_2 R_2} + \frac{A_{23(01)}^{(\tau\eta)\alpha_3\alpha_2}}{A_2} \right) \left( (\mathbf{l}_{\alpha_2})^T \mathbf{l}_{\alpha_2}^{(1)} \right) \otimes_k \left( (\mathbf{l}_{\alpha_1})^T \mathbf{l}_{\alpha_1} \right) + \\
 & + \left( -\frac{A_{55(02)}^{(\tau\eta)\alpha_3\alpha_2}}{A_2 R_2} + \frac{A_{55(01)}^{(\tau\eta)\alpha_3\alpha_2}}{A_2} \right) \left( (\mathbf{l}_{\alpha_2}^{(1)})^T \mathbf{l}_{\alpha_2} \right) \otimes_k \left( (\mathbf{l}_{\alpha_1})^T \mathbf{l}_{\alpha_1} \right) + \left( \left( \frac{A_{11(20)}^{(\tau\eta)\alpha_3\alpha_2}}{A_1 A_2 R_1} + \frac{A_{12(11)}^{(\tau\eta)\alpha_3\alpha_2}}{A_1 A_2 R_2} + \frac{A_{13(10)}^{(\tau\eta)\alpha_3\alpha_2}}{A_1 A_2} \right) \frac{\partial A_1}{\partial \alpha_2} + \right. \\
 & \left. - \left( \frac{A_{16(11)}^{(\tau\eta)\alpha_3\alpha_2}}{A_1 A_2 R_1} + \frac{A_{26(02)}^{(\tau\eta)\alpha_3\alpha_2}}{A_1 A_2 R_2} + \frac{A_{36(01)}^{(\tau\eta)\alpha_3\alpha_2}}{A_1 A_2} \right) \frac{\partial A_2}{\partial \alpha_1} \right) \left( (\mathbf{l}_{\alpha_2})^T \mathbf{l}_{\alpha_2} \right) \otimes_k \left( (\mathbf{l}_{\alpha_1})^T \mathbf{l}_{\alpha_1} \right)
 \end{aligned}$$

*Third column of the stiffness matrix*

$$\begin{aligned}
 (\mathbf{B}^{\alpha_1})^T \mathbf{A}^{(\tau\eta)\alpha_1\alpha_3} \mathbf{B}^{\alpha_3} & = \left( \frac{A_{11(20)}^{(\tau\eta)\alpha_1\alpha_3}}{A_1 R_1} + \frac{A_{12(11)}^{(\tau\eta)\alpha_1\alpha_3}}{A_1 R_2} + \frac{A_{13(10)}^{(\tau\eta)\alpha_1\alpha_3}}{A_1} \right) \left( (\mathbf{l}_{\alpha_2})^T \mathbf{l}_{\alpha_2} \right) \otimes_k \left( (\mathbf{l}_{\alpha_1}^{(1)})^T \mathbf{l}_{\alpha_1} \right) + \\
 & + \left( \frac{A_{44(10)}^{(\tau\eta)\alpha_1\alpha_3}}{A_1} - \frac{A_{44(20)}^{(\tau\eta)\alpha_1\alpha_3}}{A_1 R_1} \right) \left( (\mathbf{l}_{\alpha_2})^T \mathbf{l}_{\alpha_2} \right) \otimes_k \left( (\mathbf{l}_{\alpha_1})^T \mathbf{l}_{\alpha_1}^{(1)} \right) +
 \end{aligned}$$

$$\begin{aligned}
& + \left( \frac{A_{45(01)}^{(\bar{\tau}\eta)\alpha_1\alpha_3}}{A_2} - \frac{A_{45(11)}^{(\tau\eta)\alpha_1\alpha_3}}{A_2 R_1} \right) \left( (\mathbf{l}_{\alpha_2})^T \mathbf{l}_{\alpha_2}^{(1)} \right) \otimes_k \left( (\mathbf{l}_{\alpha_1})^T \mathbf{l}_{\alpha_1} \right) + \\
& + \left( \frac{A_{16(11)}^{(\tau\eta)\alpha_1\alpha_3}}{A_2 R_1} + \frac{A_{26(02)}^{(\tau\eta)\alpha_1\alpha_3}}{A_2 R_2} + \frac{A_{36(01)}^{(\bar{\tau}\eta)\alpha_1\alpha_3}}{A_2} \right) \left( (\mathbf{l}_{\alpha_2}^{(1)})^T \mathbf{l}_{\alpha_2} \right) \otimes_k \left( (\mathbf{l}_{\alpha_1})^T \mathbf{l}_{\alpha_1} \right) + \\
& + \left( \frac{A_{12(11)}^{(\tau\eta)\alpha_1\alpha_3}}{A_1 A_2 R_1} + \frac{A_{22(02)}^{(\tau\eta)\alpha_1\alpha_3}}{A_1 A_2 R_2} + \frac{A_{23(01)}^{(\bar{\tau}\eta)\alpha_1\alpha_3}}{A_1 A_2} \right) \frac{\partial A_2}{\partial \alpha_1} - \left( \frac{A_{16(20)}^{(\tau\eta)\alpha_1\alpha_3}}{A_1 A_2 R_1} + \frac{A_{26(11)}^{(\tau\eta)\alpha_1\alpha_3}}{A_1 A_2 R_2} + \frac{A_{36(10)}^{(\bar{\tau}\eta)\alpha_1\alpha_3}}{A_1 A_2} \right) \frac{\partial A_1}{\partial \alpha_2} \left( (\mathbf{l}_{\alpha_2})^T \mathbf{l}_{\alpha_2} \right) \otimes_k \left( (\mathbf{l}_{\alpha_1})^T \mathbf{l}_{\alpha_1} \right) \\
(\mathbf{B}^{\alpha_2})^T \mathbf{A}^{(\tau\eta)\alpha_2\alpha_3} \mathbf{B}^{\alpha_3} & = \left( \frac{A_{16(20)}^{(\tau\eta)\alpha_2\alpha_3}}{A_1 R_1} + \frac{A_{26(11)}^{(\tau\eta)\alpha_2\alpha_3}}{A_1 R_2} + \frac{A_{36(10)}^{(\bar{\tau}\eta)\alpha_2\alpha_3}}{A_1} \right) \left( (\mathbf{l}_{\alpha_2})^T \mathbf{l}_{\alpha_2} \right) \otimes_k \left( (\mathbf{l}_{\alpha_1}^{(1)})^T \mathbf{l}_{\alpha_1} \right) + \\
& + \left( \frac{A_{45(10)}^{(\bar{\tau}\eta)\alpha_2\alpha_3}}{A_1} - \frac{A_{45(11)}^{(\tau\eta)\alpha_2\alpha_3}}{A_1 R_2} \right) \left( (\mathbf{l}_{\alpha_2})^T \mathbf{l}_{\alpha_2} \right) \otimes_k \left( (\mathbf{l}_{\alpha_1})^T \mathbf{l}_{\alpha_1}^{(1)} \right) + \\
& + \left( \frac{A_{55(01)}^{(\bar{\tau}\eta)\alpha_2\alpha_3}}{A_2} - \frac{A_{55(02)}^{(\tau\eta)\alpha_2\alpha_3}}{A_2 R_2} \right) \left( (\mathbf{l}_{\alpha_2})^T \mathbf{l}_{\alpha_2}^{(1)} \right) \otimes_k \left( (\mathbf{l}_{\alpha_1})^T \mathbf{l}_{\alpha_1} \right) + \\
& + \left( \frac{A_{12(11)}^{(\tau\eta)\alpha_2\alpha_3}}{A_2 R_1} + \frac{A_{22(02)}^{(\tau\eta)\alpha_2\alpha_3}}{A_2 R_2} + \frac{A_{23(01)}^{(\bar{\tau}\eta)\alpha_2\alpha_3}}{A_2} \right) \left( (\mathbf{l}_{\alpha_2}^{(1)})^T \mathbf{l}_{\alpha_2} \right) \otimes_k \left( (\mathbf{l}_{\alpha_1})^T \mathbf{l}_{\alpha_1} \right) + \\
& + \left( \frac{A_{11(20)}^{(\tau\eta)\alpha_2\alpha_3}}{A_1 A_2 R_1} + \frac{A_{12(11)}^{(\tau\eta)\alpha_2\alpha_3}}{A_1 A_2 R_2} + \frac{A_{13(10)}^{(\bar{\tau}\eta)\alpha_2\alpha_3}}{A_1 A_2} \right) \frac{\partial A_1}{\partial \alpha_2} - \left( \frac{A_{16(11)}^{(\tau\eta)\alpha_2\alpha_3}}{A_1 A_2 R_1} + \frac{A_{26(02)}^{(\tau\eta)\alpha_2\alpha_3}}{A_1 A_2 R_2} + \frac{A_{36(01)}^{(\bar{\tau}\eta)\alpha_2\alpha_3}}{A_1 A_2} \right) \frac{\partial A_2}{\partial \alpha_1} \left( (\mathbf{l}_{\alpha_2})^T \mathbf{l}_{\alpha_2} \right) \otimes_k \left( (\mathbf{l}_{\alpha_1})^T \mathbf{l}_{\alpha_1} \right) \\
(\mathbf{B}^{\alpha_3})^T \mathbf{A}^{(\tau\eta)\alpha_3\alpha_3} \mathbf{B}^{\alpha_3} & = \frac{A_{44(20)}^{(\tau\eta)\alpha_3\alpha_3}}{A_1^2} \left( (\mathbf{l}_{\alpha_2})^T \mathbf{l}_{\alpha_2} \right) \otimes_k \left( (\mathbf{l}_{\alpha_1}^{(1)})^T \mathbf{l}_{\alpha_1}^{(1)} \right) + \frac{A_{55(02)}^{(\tau\eta)\alpha_3\alpha_3}}{A_2^2} \left( (\mathbf{l}_{\alpha_2}^{(1)})^T \mathbf{l}_{\alpha_2}^{(1)} \right) \otimes_k \left( (\mathbf{l}_{\alpha_1})^T \mathbf{l}_{\alpha_1} \right) + \\
& + \frac{A_{45(11)}^{(\tau\eta)\alpha_3\alpha_3}}{A_1 A_2} \left( \left( (\mathbf{l}_{\alpha_2})^T \mathbf{l}_{\alpha_2}^{(1)} \right) \otimes_k \left( (\mathbf{l}_{\alpha_1}^{(1)})^T \mathbf{l}_{\alpha_1} \right) + \left( (\mathbf{l}_{\alpha_2}^{(1)})^T \mathbf{l}_{\alpha_2} \right) \otimes_k \left( (\mathbf{l}_{\alpha_1})^T \mathbf{l}_{\alpha_1}^{(1)} \right) \right) + \\
& + \left( \frac{A_{11(20)}^{(\tau\eta)\alpha_3\alpha_3}}{R_1^2} + \frac{A_{22(02)}^{(\tau\eta)\alpha_3\alpha_3}}{R_2^2} + \frac{2A_{12(11)}^{(\tau\eta)\alpha_3\alpha_3}}{R_1 R_2} + \frac{A_{13(10)}^{(\bar{\tau}\eta)\alpha_3\alpha_3} + A_{13(10)}^{(\tau\eta)\alpha_3\alpha_3}}{R_1} \right) + \\
& + \frac{A_{23(01)}^{(\bar{\tau}\eta)\alpha_3\alpha_3} + A_{23(01)}^{(\tau\eta)\alpha_3\alpha_3}}{R_2} + A_{33(00)}^{(\bar{\tau}\eta)\alpha_3\alpha_3} \left( (\mathbf{l}_{\alpha_2})^T \mathbf{l}_{\alpha_2} \right) \otimes_k \left( (\mathbf{l}_{\alpha_1})^T \mathbf{l}_{\alpha_1} \right)
\end{aligned}$$

Due to definition (3.268), the fundamental equations (3.267) can be written in terms only of the generalized displacements collected in  $\bar{\mathbf{u}}^{(\eta)}$ . Thus, the fundamental equations assume the following aspect

$$\sum_{\eta=0}^{N+1} \left( \mathbf{K}^{(\tau\eta)} - \mathbf{K}_f^{(\tau\eta)} \right) \bar{\mathbf{u}}^{(\eta)} + \sum_{\eta=0}^{N+1} \left( \bar{\mathbf{M}}^{(\tau\eta)} - \bar{\mathbf{M}}_f^{(\tau\eta)} \right) \ddot{\bar{\mathbf{u}}}^{(\eta)} = \mathbf{Q}^{(\tau)} \quad (3.270)$$

for  $\tau = 0, 1, 2, \dots, N, N+1$ . Equation (3.270) represents the fundamental nucleus of the weak formulation linked to the  $\tau$ -th order of kinematic expansion. A simpler expression is obtained if the effect of the elastic foundation is neglected

$$\sum_{\eta=0}^{N+1} \mathbf{K}^{(\tau\eta)} \bar{\mathbf{u}}^{(\eta)} + \sum_{\eta=0}^{N+1} \bar{\mathbf{M}}^{(\tau\eta)} \ddot{\mathbf{u}}^{(\eta)} = \mathbf{Q}^{(\tau)} \quad (3.271)$$

In order to understand more clearly the meaning of this nucleus, the extended matrix form of (3.271) is shown below for a kinematic model of order  $N$ , embedding the Murakami's function

$$\begin{aligned} & \begin{bmatrix} \mathbf{K}^{(00)} & \mathbf{K}^{(01)} & \dots & \dots & \mathbf{K}^{(0(N))} & \mathbf{K}^{(0(N+1))} \\ \mathbf{K}^{(10)} & \mathbf{K}^{(11)} & \dots & \dots & \mathbf{K}^{(1(N))} & \mathbf{K}^{(1(N+1))} \\ \vdots & \vdots & \ddots & & \vdots & \vdots \\ \vdots & \vdots & & \ddots & \vdots & \vdots \\ \mathbf{K}^{((N)0)} & \mathbf{K}^{((N)1)} & \dots & \dots & \mathbf{K}^{((N)(N))} & \mathbf{K}^{((N)(N+1))} \\ \mathbf{K}^{((N+1)0)} & \mathbf{K}^{((N+1)1)} & \dots & \dots & \mathbf{K}^{((N+1)(N))} & \mathbf{K}^{((N+1)(N+1))} \end{bmatrix} \begin{bmatrix} \bar{\mathbf{u}}^{(0)} \\ \bar{\mathbf{u}}^{(1)} \\ \vdots \\ \vdots \\ \bar{\mathbf{u}}^{(N)} \\ \bar{\mathbf{u}}^{(N+1)} \end{bmatrix} + \\ & + \begin{bmatrix} \bar{\mathbf{M}}^{(00)} & \bar{\mathbf{M}}^{(01)} & \dots & \dots & \bar{\mathbf{M}}^{(0(N))} & \bar{\mathbf{M}}^{(0(N+1))} \\ \bar{\mathbf{M}}^{(10)} & \bar{\mathbf{M}}^{(11)} & \dots & \dots & \bar{\mathbf{M}}^{(1(N))} & \bar{\mathbf{M}}^{(1(N+1))} \\ \vdots & \vdots & \ddots & & \vdots & \vdots \\ \vdots & \vdots & & \ddots & \vdots & \vdots \\ \bar{\mathbf{M}}^{((N)0)} & \bar{\mathbf{M}}^{((N)1)} & \dots & \dots & \bar{\mathbf{M}}^{((N)(N))} & \bar{\mathbf{M}}^{((N)(N+1))} \\ \bar{\mathbf{M}}^{((N+1)0)} & \bar{\mathbf{M}}^{((N+1)1)} & \dots & \dots & \bar{\mathbf{M}}^{((N+1)(N))} & \bar{\mathbf{M}}^{((N+1)(N+1))} \end{bmatrix} \begin{bmatrix} \ddot{\mathbf{u}}^{(0)} \\ \ddot{\mathbf{u}}^{(1)} \\ \vdots \\ \vdots \\ \ddot{\mathbf{u}}^{(N)} \\ \ddot{\mathbf{u}}^{(N+1)} \end{bmatrix} = \begin{bmatrix} \mathbf{Q}^{(0)} \\ \mathbf{Q}^{(1)} \\ \vdots \\ \vdots \\ \mathbf{Q}^{(N)} \\ \mathbf{Q}^{(N+1)} \end{bmatrix} \quad (3.272) \end{aligned}$$

The essential (or geometric) boundary conditions only can be obtained from equation (3.266). In particular, one gets

$$\bar{\mathbf{u}}^{(\tau)} = \mathbf{0} \quad (3.273)$$

for each order of kinematic expansion  $\tau$ . The continuity requirement is clearly  $C^0$ , since the natural (or force) boundary conditions are not involved. Nevertheless, a  $C^1$  weak formulation can be obtained if the natural boundary conditions obtained for the strong formulation and presented in (3.242)-(3.243) are introduced in the model. Definition (3.186) will be used for this purpose.

Finally, it should be noted at this point that a numerical technique must be used to compute all the matrices and vectors that appear in (3.272). These quantities can be achieved by performing the integration with respect to the coordinates  $\alpha_1, \alpha_2$ , in the intervals  $\alpha_1 \in [\alpha_1^0, \alpha_1^1]$  and  $\alpha_2 \in [\alpha_2^0, \alpha_2^1]$ . For this purpose, the IQ method presented in the first chapter is introduced to obtain the discrete form of the governing equations.

### 3.1.8.1 Governing equations for distorted domains

The definitions of the stiffness matrix, the mass matrix, and the load vectors, must be modified in order to analyze the mechanical behavior of shell structures characterized by distorted domains, according to what has been shown in the previous chapter. For this purpose, the meaning of the Jacobian matrix  $\mathbf{J}$  must be recalled, since the integrals at issue are evaluated in the computational element (or master element), described through the natural coordinates  $\xi_1, \xi_2$  defined in the intervals  $\xi_1 \in [-1, 1]$  and  $\xi_2 \in [-1, 1]$ , respectively.

As far as the stiffness matrix  $\mathbf{K}^{(\tau\eta)}$  is concerned, the coordinate change at issue leads to the following definition

$$\mathbf{K}^{(\tau\eta)} = \int_{-1}^1 \int_{-1}^1 \begin{bmatrix} (\mathbf{B}^{\alpha_1})^T \mathbf{A}^{(\tau\eta)\alpha_1} \mathbf{B}^{\alpha_1} & (\mathbf{B}^{\alpha_1})^T \mathbf{A}^{(\tau\eta)\alpha_1\alpha_2} \mathbf{B}^{\alpha_2} & (\mathbf{B}^{\alpha_1})^T \mathbf{A}^{(\tau\eta)\alpha_1\alpha_3} \mathbf{B}^{\alpha_3} \\ (\mathbf{B}^{\alpha_2})^T \mathbf{A}^{(\tau\eta)\alpha_2\alpha_1} \mathbf{B}^{\alpha_1} & (\mathbf{B}^{\alpha_2})^T \mathbf{A}^{(\tau\eta)\alpha_2\alpha_2} \mathbf{B}^{\alpha_2} & (\mathbf{B}^{\alpha_2})^T \mathbf{A}^{(\tau\eta)\alpha_2\alpha_3} \mathbf{B}^{\alpha_3} \\ (\mathbf{B}^{\alpha_3})^T \mathbf{A}^{(\tau\eta)\alpha_3\alpha_1} \mathbf{B}^{\alpha_1} & (\mathbf{B}^{\alpha_3})^T \mathbf{A}^{(\tau\eta)\alpha_3\alpha_2} \mathbf{B}^{\alpha_2} & (\mathbf{B}^{\alpha_3})^T \mathbf{A}^{(\tau\eta)\alpha_3\alpha_3} \mathbf{B}^{\alpha_3} \end{bmatrix} A_1 A_2 \det(\mathbf{J}) d\xi_1 d\xi_2 \quad (3.274)$$

where  $\det(\mathbf{J})$  stands for the determinant of the Jacobian matrix. Analogously, the mass matrix  $\bar{\mathbf{M}}^{(\tau\eta)}$  for a distorted geometry becomes

$$\bar{\mathbf{M}}^{(\tau\eta)} = \int_{-1}^1 \int_{-1}^1 \begin{bmatrix} \bar{\mathbf{N}} I_0^{(\tau\eta)\alpha_1} \bar{\mathbf{N}}^T & \mathbf{0} & \mathbf{0} \\ \mathbf{0} & \bar{\mathbf{N}} I_0^{(\tau\eta)\alpha_2} \bar{\mathbf{N}}^T & \mathbf{0} \\ \mathbf{0} & \mathbf{0} & \bar{\mathbf{N}} I_0^{(\tau\eta)\alpha_3} \bar{\mathbf{N}}^T \end{bmatrix} A_1 A_2 \det(\mathbf{J}) d\xi_1 d\xi_2 \quad (3.275)$$

The same approach can be pursued also for the stiffness and inertia matrices related to the effect of the elastic foundation, which assume the following aspect

$$\mathbf{K}_f^{(\tau\eta)} = \int_{-1}^1 \int_{-1}^1 \begin{bmatrix} \bar{\mathbf{N}} L_{f1}^{(\tau\eta)\alpha_1} \bar{\mathbf{N}}^T & \mathbf{0} & \mathbf{0} \\ \mathbf{0} & \bar{\mathbf{N}} L_{f2}^{(\tau\eta)\alpha_2} \bar{\mathbf{N}}^T & \mathbf{0} \\ \mathbf{0} & \mathbf{0} & \bar{\mathbf{N}} L_{f3}^{(\tau\eta)\alpha_3} \bar{\mathbf{N}}^T \end{bmatrix} A_1 A_2 \det(\mathbf{J}) d\xi_1 d\xi_2 \quad (3.276)$$

$$\mathbf{M}_f^{(\tau\eta)} = \int_{-1}^1 \int_{-1}^1 \begin{bmatrix} \bar{\mathbf{N}} I_0^{(\tau\eta)\alpha_1} \bar{\mathbf{N}}^T & \mathbf{0} & \mathbf{0} \\ \mathbf{0} & \bar{\mathbf{N}} I_0^{(\tau\eta)\alpha_2} \bar{\mathbf{N}}^T & \mathbf{0} \\ \mathbf{0} & \mathbf{0} & \bar{\mathbf{N}} I_0^{(\tau\eta)\alpha_3} \bar{\mathbf{N}}^T \end{bmatrix} A_1 A_2 \det(\mathbf{J}) d\xi_1 d\xi_2 \quad (3.277)$$

Analogously, the determinant of the Jacobian matrix related to the coordinate change at issue is required also to compute the vectors that collect the surface and volume forces.

In particular, one gets respectively

$$\mathbf{Q}_{sa}^{(\tau)} = \int_{-1}^1 \int_{-1}^1 \begin{bmatrix} \bar{\mathbf{N}}q_{1sa}^{(\tau)} \\ \bar{\mathbf{N}}q_{2sa}^{(\tau)} \\ \bar{\mathbf{N}}q_{3sa}^{(\tau)} \end{bmatrix} A_1 A_2 \det(\mathbf{J}) d\xi_1 d\xi_2 \quad (3.278)$$

$$\mathbf{Q}_{va}^{(\tau)} = \int_{-1}^1 \int_{-1}^1 \begin{bmatrix} \bar{\mathbf{N}}q_{1va}^{(\tau)} \\ \bar{\mathbf{N}}q_{2va}^{(\tau)} \\ \bar{\mathbf{N}}q_{3va}^{(\tau)} \end{bmatrix} A_1 A_2 \det(\mathbf{J}) d\xi_1 d\xi_2 \quad (3.279)$$

A different procedure must be followed to evaluate the vectors that include the external forces applied directly along the external edges, since a one-dimensional integral is involved, as shown by the definitions (3.263) and (3.265). In addition, it should be recalled that these forces are applied along a generic edge, thus the components that must be considered can be computed as shown in (3.251). In other words, the external loads applied along a generic edge, which is identified by the outward unit vector  $\mathbf{n}_n$ , are given by  $\bar{N}_n^{(\tau)\alpha_1}, \bar{N}_{ns}^{(\tau)\alpha_2}, \bar{T}_\zeta^{(\tau)\alpha_3}$ , which can be collected in the corresponding vector

$$\bar{\mathbf{S}}_n^{(\tau)} = \left[ \bar{N}_n^{(\tau)\alpha_1} \quad \bar{N}_{ns}^{(\tau)\alpha_2} \quad \bar{T}_\zeta^{(\tau)\alpha_3} \right]^T \quad (3.280)$$

for  $\tau = 0, 1, 2, \dots, N, N+1$ . Having in mind definitions (3.263) and (3.265), their contribution along a generic curved edge identified by the outward unit vector  $\mathbf{n}_n$  can be evaluated by means of the following one-dimensional integral

$$\bar{\mathbf{Q}}_n^{(\tau)} = \oint_{s_n} \begin{bmatrix} \bar{\mathbf{N}}\bar{N}_n^{(\tau)\alpha_1} \\ \bar{\mathbf{N}}\bar{N}_{ns}^{(\tau)\alpha_2} \\ \bar{\mathbf{N}}\bar{T}_\zeta^{(\tau)\alpha_3} \end{bmatrix} ds_n \quad (3.281)$$

where  $s_n$  is the curvilinear abscissa defined along the external edge. If the contribution of the four curved edges is considered, the integral in (3.281) can be written as follows

$$\bar{\mathbf{Q}}_{n(i)}^{(\tau)} = \int_0^{L_{(i)}} \begin{bmatrix} \bar{\mathbf{N}}\bar{N}_n^{(\tau)\alpha_1} \\ \bar{\mathbf{N}}\bar{N}_{ns}^{(\tau)\alpha_2} \\ \bar{\mathbf{N}}\bar{T}_\zeta^{(\tau)\alpha_3} \end{bmatrix} ds_{n(i)} \quad (3.282)$$

for  $i=1, 2, 3, 4$ . The length of the edges at issue is given by  $L_{(i)}$ . Through a change of

variables, the integration (3.282) can be performed in the interval  $[-1,1]$  as shown below

$$\bar{\mathbf{Q}}_{n(i)}^{(\tau)} = \int_{-1}^1 \begin{bmatrix} \bar{\mathbf{N}}\bar{\mathbf{N}}_n^{(\tau)\alpha_1} \\ \bar{\mathbf{N}}\bar{\mathbf{N}}_{ns}^{(\tau)\alpha_2} \\ \bar{\mathbf{N}}\bar{\mathbf{T}}_\zeta^{(\tau)\alpha_3} \end{bmatrix} \frac{L_{(i)}}{2} d\eta_{(i)} \quad (3.283)$$

in which  $\eta_{(i)}$  the curvilinear abscissa used as variable of integration, for  $i=1,2,3,4$ . At this point, the length  $L_{(i)}$  of each edge is required in order to compute the previous integrals. As shown in the previous chapter, the length of a generic curve lying on a curved surface is described by the following expression

$$L_{(i)} = \int_{-1}^1 \sqrt{A_1^2 \left( \frac{d\alpha_1}{d\xi_j} \right)^2 + A_2^2 \left( \frac{d\alpha_2}{d\xi_j} \right)^2} d\xi_j \quad (3.284)$$

for  $i=1,2,3,4$  and  $j=1,2$ . This relation can be used to evaluate distances in a distorted domain, having in mind that each edge is defined by peculiar functions described by the natural coordinates of the parent space  $\xi_1, \xi_2$ . In particular, each edge can be obtained by assuming the boundary values of these coordinates, which are  $\xi_1 = \pm 1$  and  $\xi_2 = \pm 1$ . Thus, the lengths of the four edges can be computed as follows

$$\text{edge(1)} \rightarrow \xi_2 = -1 \rightarrow L_{(1)} = \int_{-1}^1 \sqrt{A_1^2 \left( \frac{d\alpha_1}{d\xi_1} \right)^2 + A_2^2 \left( \frac{d\alpha_2}{d\xi_1} \right)^2} d\xi_1 \quad (3.285)$$

$$\text{edge(2)} \rightarrow \xi_1 = 1 \rightarrow L_{(2)} = \int_{-1}^1 \sqrt{A_1^2 \left( \frac{d\alpha_1}{d\xi_2} \right)^2 + A_2^2 \left( \frac{d\alpha_2}{d\xi_2} \right)^2} d\xi_2 \quad (3.286)$$

$$\text{edge(3)} \rightarrow \xi_2 = 1 \rightarrow L_{(3)} = \int_{-1}^1 \sqrt{A_1^2 \left( \frac{d\alpha_1}{d\xi_1} \right)^2 + A_2^2 \left( \frac{d\alpha_2}{d\xi_1} \right)^2} d\xi_1 \quad (3.287)$$

$$\text{edge(4)} \rightarrow \xi_1 = -1 \rightarrow L_{(4)} = \int_{-1}^1 \sqrt{A_1^2 \left( \frac{d\alpha_1}{d\xi_2} \right)^2 + A_2^2 \left( \frac{d\alpha_2}{d\xi_2} \right)^2} d\xi_2 \quad (3.288)$$

If an isogeometric mapping is employed to describe arbitrarily shaped domains, the coordinates  $\alpha_1, \alpha_2$  assume the following aspect along the boundary edges

$$\text{edge(1)} \rightarrow \xi_2 = -1 \rightarrow \begin{aligned} \alpha_1 &= \alpha_1(\xi_1, -1) = \bar{\alpha}_{1(1)}(\xi_1) \\ \alpha_2 &= \alpha_2(\xi_1, -1) = \bar{\alpha}_{2(1)}(\xi_1) \end{aligned} \quad (3.289)$$

$$\begin{aligned} \text{edge}(2) \rightarrow \xi_1 = 1 \rightarrow \alpha_1 = \alpha_1(1, \xi_2) = \bar{\alpha}_{1(2)}(\xi_2) \\ \alpha_2 = \alpha_2(1, \xi_2) = \bar{\alpha}_{2(2)}(\xi_2) \end{aligned} \quad (3.290)$$

$$\begin{aligned} \text{edge}(3) \rightarrow \xi_2 = 1 \rightarrow \alpha_1 = \alpha_1(\xi_1, 1) = \bar{\alpha}_{1(3)}(\xi_1) \\ \alpha_2 = \alpha_2(\xi_1, 1) = \bar{\alpha}_{2(3)}(\xi_1) \end{aligned} \quad (3.291)$$

$$\begin{aligned} \text{edge}(4) \rightarrow \xi_1 = -1 \rightarrow \alpha_1 = \alpha_1(-1, \xi_2) = \bar{\alpha}_{1(4)}(\xi_2) \\ \alpha_2 = \alpha_2(-1, \xi_2) = \bar{\alpha}_{2(4)}(\xi_2) \end{aligned} \quad (3.292)$$

in which  $\bar{\alpha}_{1(1)}, \bar{\alpha}_{1(2)}, \bar{\alpha}_{1(3)}, \bar{\alpha}_{1(4)}$  and  $\bar{\alpha}_{2(1)}, \bar{\alpha}_{2(2)}, \bar{\alpha}_{2(3)}, \bar{\alpha}_{2(4)}$  are the parametric curves that allow to describe the arbitrary shape of each edge. At this point, the integrals in (3.285)-(3.288) can be easily evaluated to obtain the lengths of the four edges. As a consequence, the stress resultants along the boundaries (3.283) can be computed, too. In particular, one gets

$$\text{edge}(1) \rightarrow \bar{\mathbf{Q}}_{n(1)}^{(\tau)} = \frac{L^{(1)}}{2} \int_{-1}^1 \begin{bmatrix} \bar{\mathbf{N}}\bar{\mathbf{N}}_n^{(\tau)\alpha_1} \\ \bar{\mathbf{N}}\bar{\mathbf{N}}_{ns}^{(\tau)\alpha_2} \\ \bar{\mathbf{N}}\bar{\mathbf{T}}_\zeta^{(\tau)\alpha_3} \end{bmatrix} d\eta_{(1)} \quad (3.293)$$

$$\text{edge}(2) \rightarrow \bar{\mathbf{Q}}_{n(2)}^{(\tau)} = \frac{L^{(2)}}{2} \int_{-1}^1 \begin{bmatrix} \bar{\mathbf{N}}\bar{\mathbf{N}}_n^{(\tau)\alpha_1} \\ \bar{\mathbf{N}}\bar{\mathbf{N}}_{ns}^{(\tau)\alpha_2} \\ \bar{\mathbf{N}}\bar{\mathbf{T}}_\zeta^{(\tau)\alpha_3} \end{bmatrix} d\eta_{(2)} \quad (3.294)$$

$$\text{edge}(3) \rightarrow \bar{\mathbf{Q}}_{n(3)}^{(\tau)} = \frac{L^{(3)}}{2} \int_{-1}^1 \begin{bmatrix} \bar{\mathbf{N}}\bar{\mathbf{N}}_n^{(\tau)\alpha_1} \\ \bar{\mathbf{N}}\bar{\mathbf{N}}_{ns}^{(\tau)\alpha_2} \\ \bar{\mathbf{N}}\bar{\mathbf{T}}_\zeta^{(\tau)\alpha_3} \end{bmatrix} d\eta_{(3)} \quad (3.295)$$

$$\text{edge}(4) \rightarrow \bar{\mathbf{Q}}_{n(4)}^{(\tau)} = \frac{L^{(4)}}{2} \int_{-1}^1 \begin{bmatrix} \bar{\mathbf{N}}\bar{\mathbf{N}}_n^{(\tau)\alpha_1} \\ \bar{\mathbf{N}}\bar{\mathbf{N}}_{ns}^{(\tau)\alpha_2} \\ \bar{\mathbf{N}}\bar{\mathbf{T}}_\zeta^{(\tau)\alpha_3} \end{bmatrix} d\eta_{(4)} \quad (3.296)$$

### 3.1.8.2 Discrete form of the governing equations

The definitions presented in the previous section must be written in discrete form and evaluated in each point of the reference domain, identified by the coordinates  $\alpha_{1f}, \alpha_{2g}$  introduced in (3.31)-(3.32).

For this purpose, the IQ method is used. In the following, the discrete forms of the definitions in hand will be obtained for regular and distorted domains.

### 3.1.8.2.1 Discrete equations for regular domains

By means of the IQ method, the two-dimensional integral that defines the stiffness matrix  $\mathbf{K}^{(\tau\eta)}$  can be written in discrete form and evaluated in each point of the reference domain. The operator (3.269) assumes the following aspect

$$\mathbf{K}^{(\tau\eta)} = \sum_{f=1}^{I_N} \sum_{g=1}^{I_M} w_f^{I_N} w_g^{I_M} A_{1(fg)} A_{2(fg)} \begin{bmatrix} (\mathbf{B}^{\alpha_1})^T \mathbf{A}^{(\tau\eta)\alpha_1\alpha_1} \mathbf{B}^{\alpha_1} & (\mathbf{B}^{\alpha_1})^T \mathbf{A}^{(\tau\eta)\alpha_1\alpha_2} \mathbf{B}^{\alpha_2} & (\mathbf{B}^{\alpha_1})^T \mathbf{A}^{(\tau\eta)\alpha_1\alpha_3} \mathbf{B}^{\alpha_3} \\ (\mathbf{B}^{\alpha_2})^T \mathbf{A}^{(\tau\eta)\alpha_2\alpha_1} \mathbf{B}^{\alpha_1} & (\mathbf{B}^{\alpha_2})^T \mathbf{A}^{(\tau\eta)\alpha_2\alpha_2} \mathbf{B}^{\alpha_2} & (\mathbf{B}^{\alpha_2})^T \mathbf{A}^{(\tau\eta)\alpha_2\alpha_3} \mathbf{B}^{\alpha_3} \\ (\mathbf{B}^{\alpha_3})^T \mathbf{A}^{(\tau\eta)\alpha_3\alpha_1} \mathbf{B}^{\alpha_1} & (\mathbf{B}^{\alpha_3})^T \mathbf{A}^{(\tau\eta)\alpha_3\alpha_2} \mathbf{B}^{\alpha_2} & (\mathbf{B}^{\alpha_3})^T \mathbf{A}^{(\tau\eta)\alpha_3\alpha_3} \mathbf{B}^{\alpha_3} \end{bmatrix}_{(fg)} \quad (3.297)$$

for  $\tau, \eta = 0, 1, 2, \dots, N, N+1$ . It should be recalled that  $w_f^{I_N}, w_g^{I_M}$  represent the weighting coefficients for the integration in the physical domain, whereas  $A_{1(fg)}, A_{2(fg)}$  denote the values that the Lamè parameters assume in each discrete point of the domain.

Analogously, the same procedure is performed for the mass matrix  $\bar{\mathbf{M}}^{(\tau\eta)}$  defined in (3.261), which becomes

$$\bar{\mathbf{M}}^{(\tau\eta)} = \sum_{f=1}^{I_N} \sum_{g=1}^{I_M} w_f^{I_N} w_g^{I_M} A_{1(fg)} A_{2(fg)} \begin{bmatrix} \bar{\mathbf{N}} I_0^{(\tau\eta)\alpha_1\alpha_1} \bar{\mathbf{N}}^T & \mathbf{0} & \mathbf{0} \\ \mathbf{0} & \bar{\mathbf{N}} I_0^{(\tau\eta)\alpha_2\alpha_2} \bar{\mathbf{N}}^T & \mathbf{0} \\ \mathbf{0} & \mathbf{0} & \bar{\mathbf{N}} I_0^{(\tau\eta)\alpha_3\alpha_3} \bar{\mathbf{N}}^T \end{bmatrix}_{(fg)} \quad (3.298)$$

for  $\tau, \eta = 0, 1, 2, \dots, N, N+1$ . In a similar manner, the stiffness matrix and the inertia matrix of the elastic foundation, defined respectively in (3.260) and (3.261), can be written in discrete form as follows

$$\mathbf{K}_f^{(\tau\eta)} = \sum_{f=1}^{I_N} \sum_{g=1}^{I_M} w_f^{I_N} w_g^{I_M} A_{1(fg)} A_{2(fg)} \begin{bmatrix} \bar{\mathbf{N}} L_{f1}^{(\tau\eta)\alpha_1} \bar{\mathbf{N}}^T & \mathbf{0} & \mathbf{0} \\ \mathbf{0} & \bar{\mathbf{N}} L_{f2}^{(\tau\eta)\alpha_2} \bar{\mathbf{N}}^T & \mathbf{0} \\ \mathbf{0} & \mathbf{0} & \bar{\mathbf{N}} L_{f3}^{(\tau\eta)\alpha_3} \bar{\mathbf{N}}^T \end{bmatrix}_{(fg)} \quad (3.299)$$

$$\mathbf{M}_f^{(\tau\eta)} = \sum_{f=1}^{I_N} \sum_{g=1}^{I_M} w_f^{I_N} w_g^{I_M} A_{1(fg)} A_{2(fg)} \begin{bmatrix} \bar{\mathbf{N}} I_0^{(\tau\eta)\alpha_1} \bar{\mathbf{N}}^T & \mathbf{0} & \mathbf{0} \\ \mathbf{0} & \bar{\mathbf{N}} I_0^{(\tau\eta)\alpha_2} \bar{\mathbf{N}}^T & \mathbf{0} \\ \mathbf{0} & \mathbf{0} & \bar{\mathbf{N}} I_0^{(\tau\eta)\alpha_3} \bar{\mathbf{N}}^T \end{bmatrix}_{(fg)} \quad (3.300)$$

for  $\tau, \eta = 0, 1, 2, \dots, N, N+1$ . On the other hand, the discrete vectors of the surface loads and the volume forces assume the following aspect

$$\mathbf{Q}_{sa}^{(\tau)} = \sum_{f=1}^{I_N} \sum_{g=1}^{I_M} w_f^{I_N} w_g^{I_M} A_{1(fg)} A_{2(fg)} \begin{bmatrix} \bar{\mathbf{N}}q_{1sa}^{(\tau)} \\ \bar{\mathbf{N}}q_{2sa}^{(\tau)} \\ \bar{\mathbf{N}}q_{3sa}^{(\tau)} \end{bmatrix}_{(fg)} \quad (3.301)$$

$$\mathbf{Q}_{va}^{(\tau)} = \sum_{f=1}^{I_N} \sum_{g=1}^{I_M} w_f^{I_N} w_g^{I_M} A_{1(fg)} A_{2(fg)} \begin{bmatrix} \bar{\mathbf{N}}q_{1va}^{(\tau)} \\ \bar{\mathbf{N}}q_{2va}^{(\tau)} \\ \bar{\mathbf{N}}q_{3va}^{(\tau)} \end{bmatrix}_{(fg)} \quad (3.302)$$

Finally, the discrete vectors of the forces applied directly on the edges for constant values of  $\alpha_1$ , which are defined in (3.263), are given by

$$\bar{\mathbf{Q}}_{\alpha_1}^{(\tau)} \Big|_{\alpha_1=\alpha_1^0} = \sum_{g=1}^{I_M} w_g^{I_M} A_{2(1g)} \begin{bmatrix} \bar{\mathbf{N}}\bar{\mathbf{N}}_1^{(\tau)\alpha_1} \\ \bar{\mathbf{N}}\bar{\mathbf{N}}_{12}^{(\tau)\alpha_2} \\ \bar{\mathbf{N}}\bar{\mathbf{T}}_1^{(\tau)\alpha_3} \end{bmatrix}_{(1g)}, \quad \bar{\mathbf{Q}}_{\alpha_1}^{(\tau)} \Big|_{\alpha_1=\alpha_1^1} = \sum_{g=1}^{I_M} w_g^{I_M} A_{2(I_N g)} \begin{bmatrix} \bar{\mathbf{N}}\bar{\mathbf{N}}_1^{(\tau)\alpha_1} \\ \bar{\mathbf{N}}\bar{\mathbf{N}}_{12}^{(\tau)\alpha_2} \\ \bar{\mathbf{N}}\bar{\mathbf{T}}_1^{(\tau)\alpha_3} \end{bmatrix}_{(I_N g)} \quad (3.303)$$

whereas the ones for  $\alpha_2$  constants, defined in (3.265), can be computed as follows

$$\bar{\mathbf{Q}}_{\alpha_2}^{(\tau)} \Big|_{\alpha_2=\alpha_2^0} = \sum_{f=1}^{I_N} w_f^{I_N} A_{1(f1)} \begin{bmatrix} \bar{\mathbf{N}}\bar{\mathbf{N}}_1^{(\tau)\alpha_1} \\ \bar{\mathbf{N}}\bar{\mathbf{N}}_{12}^{(\tau)\alpha_2} \\ \bar{\mathbf{N}}\bar{\mathbf{T}}_1^{(\tau)\alpha_3} \end{bmatrix}_{(f1)}, \quad \bar{\mathbf{Q}}_{\alpha_2}^{(\tau)} \Big|_{\alpha_2=\alpha_2^1} = \sum_{f=1}^{I_N} w_f^{I_N} A_{1(fI_N)} \begin{bmatrix} \bar{\mathbf{N}}\bar{\mathbf{N}}_1^{(\tau)\alpha_1} \\ \bar{\mathbf{N}}\bar{\mathbf{N}}_{12}^{(\tau)\alpha_2} \\ \bar{\mathbf{N}}\bar{\mathbf{T}}_1^{(\tau)\alpha_3} \end{bmatrix}_{(fI_N)} \quad (3.304)$$

It should be noted that the discrete forms shown in (3.303)-(3.304) require only one weighting coefficient since a one-dimensional integral have to be solved.

### 3.1.8.2.2 Discrete equations for distorted domains

As shown above, the Jacobian determinant is required to write the governing equations for distorted domains. Thus, in the corresponding discrete forms, even the Jacobian determinant must be computed in each discrete point of the domain.

The stiffness matrix  $\mathbf{K}^{(\tau\eta)}$  introduced in (3.274) can be written in discrete form and evaluated in each point of the reference domain as follows

$$\mathbf{K}^{(\tau\eta)} = \sum_{f=1}^{I_N} \sum_{g=1}^{I_M} \tilde{w}_f^{I_N} \tilde{w}_g^{I_M} A_{1(fg)} A_{2(fg)} \det(\mathbf{J})_{(fg)} \begin{bmatrix} (\mathbf{B}^{\alpha_1})^T \mathbf{A}^{(\tau\eta)\alpha_1} \mathbf{B}^{\alpha_1} & (\mathbf{B}^{\alpha_1})^T \mathbf{A}^{(\tau\eta)\alpha_1\alpha_2} \mathbf{B}^{\alpha_2} & (\mathbf{B}^{\alpha_1})^T \mathbf{A}^{(\tau\eta)\alpha_1\alpha_3} \mathbf{B}^{\alpha_3} \\ (\mathbf{B}^{\alpha_2})^T \mathbf{A}^{(\tau\eta)\alpha_2\alpha_1} \mathbf{B}^{\alpha_1} & (\mathbf{B}^{\alpha_2})^T \mathbf{A}^{(\tau\eta)\alpha_2\alpha_2} \mathbf{B}^{\alpha_2} & (\mathbf{B}^{\alpha_2})^T \mathbf{A}^{(\tau\eta)\alpha_2\alpha_3} \mathbf{B}^{\alpha_3} \\ (\mathbf{B}^{\alpha_3})^T \mathbf{A}^{(\tau\eta)\alpha_3\alpha_1} \mathbf{B}^{\alpha_1} & (\mathbf{B}^{\alpha_3})^T \mathbf{A}^{(\tau\eta)\alpha_3\alpha_2} \mathbf{B}^{\alpha_2} & (\mathbf{B}^{\alpha_3})^T \mathbf{A}^{(\tau\eta)\alpha_3\alpha_3} \mathbf{B}^{\alpha_3} \end{bmatrix}_{(fg)} \quad (3.305)$$

for  $\tau, \eta = 0, 1, 2, \dots, N, N+1$ , in which  $\tilde{w}_f^{I_N} \tilde{w}_g^{I_M}$  are the weighting coefficients for the integration in the parent space, whereas  $\det(\mathbf{J})_{(fg)}$  is the value that the determinant of the Jacobian matrix assume in each discrete node of the domain.

As far as the mass matrix  $\bar{\mathbf{M}}^{(\tau\eta)}$  defined in (3.275) is concerned, the corresponding discrete form is given by

$$\bar{\mathbf{M}}^{(\tau\eta)} = \sum_{f=1}^{I_N} \sum_{g=1}^{I_M} \tilde{w}_f^{I_N} \tilde{w}_g^{I_M} A_{1(fg)} A_{2(fg)} \det(\mathbf{J})_{(fg)} \begin{bmatrix} \bar{\mathbf{N}} I_0^{(\tau\eta)\alpha_1} \bar{\mathbf{N}}^T & \mathbf{0} & \mathbf{0} \\ \mathbf{0} & \bar{\mathbf{N}} I_0^{(\tau\eta)\alpha_2} \bar{\mathbf{N}}^T & \mathbf{0} \\ \mathbf{0} & \mathbf{0} & \bar{\mathbf{N}} I_0^{(\tau\eta)\alpha_3} \bar{\mathbf{N}}^T \end{bmatrix}_{(fg)} \quad (3.306)$$

for  $\tau, \eta = 0, 1, 2, \dots, N, N+1$ . At this point, the stiffness matrix and the inertia matrix of the foundation, whose definitions are shown respectively in (3.276) and (3.277), assume the following discrete aspect

$$\mathbf{K}_f^{(\tau\eta)} = \sum_{f=1}^{I_N} \sum_{g=1}^{I_M} \tilde{w}_f^{I_N} \tilde{w}_g^{I_M} A_{1(fg)} A_{2(fg)} \det(\mathbf{J})_{(fg)} \begin{bmatrix} \bar{\mathbf{N}} L_{f1}^{(\tau\eta)\alpha_1} \bar{\mathbf{N}}^T & \mathbf{0} & \mathbf{0} \\ \mathbf{0} & \bar{\mathbf{N}} L_{f2}^{(\tau\eta)\alpha_2} \bar{\mathbf{N}}^T & \mathbf{0} \\ \mathbf{0} & \mathbf{0} & \bar{\mathbf{N}} L_{f3}^{(\tau\eta)\alpha_3} \bar{\mathbf{N}}^T \end{bmatrix}_{(fg)} \quad (3.307)$$

$$\mathbf{M}_f^{(\tau\eta)} = \sum_{f=1}^{I_N} \sum_{g=1}^{I_M} \tilde{w}_f^{I_N} \tilde{w}_g^{I_M} A_{1(fg)} A_{2(fg)} \det(\mathbf{J})_{(fg)} \begin{bmatrix} \bar{\mathbf{N}} I_0^{(\tau\eta)\alpha_1} \bar{\mathbf{N}}^T & \mathbf{0} & \mathbf{0} \\ \mathbf{0} & \bar{\mathbf{N}} I_0^{(\tau\eta)\alpha_2} \bar{\mathbf{N}}^T & \mathbf{0} \\ \mathbf{0} & \mathbf{0} & \bar{\mathbf{N}} I_0^{(\tau\eta)\alpha_3} \bar{\mathbf{N}}^T \end{bmatrix}_{(fg)} \quad (3.308)$$

for  $\tau, \eta = 0, 1, 2, \dots, N, N+1$ . Analogously, the discrete vectors of the surface loads and the volume forces, defined respectively in (3.278) and (3.279), are given by

$$\mathbf{Q}_{sa}^{(\tau)} = \sum_{f=1}^{I_N} \sum_{g=1}^{I_M} w_f^{I_N} w_g^{I_M} A_{1(fg)} A_{2(fg)} \det(\mathbf{J})_{(fg)} \begin{bmatrix} \bar{\mathbf{N}} q_{1sa}^{(\tau)} \\ \bar{\mathbf{N}} q_{2sa}^{(\tau)} \\ \bar{\mathbf{N}} q_{3sa}^{(\tau)} \end{bmatrix}_{(fg)} \quad (3.309)$$

$$\mathbf{Q}_{va}^{(\tau)} = \sum_{f=1}^{I_N} \sum_{g=1}^{I_M} w_f^{I_N} w_g^{I_M} A_{1(fg)} A_{2(fg)} \det(\mathbf{J})_{(fg)} \begin{bmatrix} \bar{\mathbf{N}}q_{1va}^{(\tau)} \\ \bar{\mathbf{N}}q_{2va}^{(\tau)} \\ \bar{\mathbf{N}}q_{3va}^{(\tau)} \end{bmatrix}_{(fg)} \quad (3.310)$$

Finally, the external loads applied along the curved boundaries defined in (3.293)-(3.296) assume the discrete forms shown below

$$\text{edge(1)} \rightarrow \bar{\mathbf{Q}}_{n(1)}^{(\tau)} = \frac{L_{(1)}}{2} \sum_{f=1}^{I_N} \tilde{w}_f^{I_N} A_{1(f1)} \begin{bmatrix} \bar{\mathbf{N}}\bar{\mathbf{N}}_n^{(\tau)\alpha_1} \\ \bar{\mathbf{N}}\bar{\mathbf{N}}_{ns}^{(\tau)\alpha_2} \\ \bar{\mathbf{N}}\bar{\mathbf{T}}_\zeta^{(\tau)\alpha_3} \end{bmatrix}_{(f1)} \quad (3.311)$$

$$\text{edge(2)} \rightarrow \bar{\mathbf{Q}}_{n(2)}^{(\tau)} = \frac{L_{(2)}}{2} \sum_{g=1}^{I_M} \tilde{w}_g^{I_M} A_{2(I_N g)} \begin{bmatrix} \bar{\mathbf{N}}\bar{\mathbf{N}}_n^{(\tau)\alpha_1} \\ \bar{\mathbf{N}}\bar{\mathbf{N}}_{ns}^{(\tau)\alpha_2} \\ \bar{\mathbf{N}}\bar{\mathbf{T}}_\zeta^{(\tau)\alpha_3} \end{bmatrix}_{(I_N g)} \quad (3.312)$$

$$\text{edge(3)} \rightarrow \bar{\mathbf{Q}}_{n(3)}^{(\tau)} = \frac{L_{(3)}}{2} \sum_{f=1}^{I_N} \tilde{w}_f^{I_N} A_{1(fI_M)} \begin{bmatrix} \bar{\mathbf{N}}\bar{\mathbf{N}}_n^{(\tau)\alpha_1} \\ \bar{\mathbf{N}}\bar{\mathbf{N}}_{ns}^{(\tau)\alpha_2} \\ \bar{\mathbf{N}}\bar{\mathbf{T}}_\zeta^{(\tau)\alpha_3} \end{bmatrix}_{(fI_M)} \quad (3.313)$$

$$\text{edge(4)} \rightarrow \bar{\mathbf{Q}}_{n(4)}^{(\tau)} = \frac{L_{(4)}}{2} \sum_{g=1}^{I_M} \tilde{w}_g^{I_M} A_{2(1g)} \begin{bmatrix} \bar{\mathbf{N}}\bar{\mathbf{N}}_n^{(\tau)\alpha_1} \\ \bar{\mathbf{N}}\bar{\mathbf{N}}_{ns}^{(\tau)\alpha_2} \\ \bar{\mathbf{N}}\bar{\mathbf{T}}_\zeta^{(\tau)\alpha_3} \end{bmatrix}_{(1g)} \quad (3.314)$$

At this point, both the strong and weak formulations have been presented. For the sake of clarity, the procedures shown in this chapter that allow to obtain the governing equations at issue are summarized in the graph depicted in Figure 3.12.

It can be noted from Figure 3.12 that the weak formulation with  $C^1$  compatibility conditions is an hybrid approach, since both the IQ and DQ methods are involved to obtain the governing equations. In particular, the DQ method is required to enforce the natural boundary conditions that are obtained for the strong formulation.

Finally, the equations that govern the mechanical problem at issue can be summarized in the scheme of physical theories, for both the strong and weak formulations, as shown in Figures 3.13 and 3.14, if the contributions of the elastic foundations are neglected.

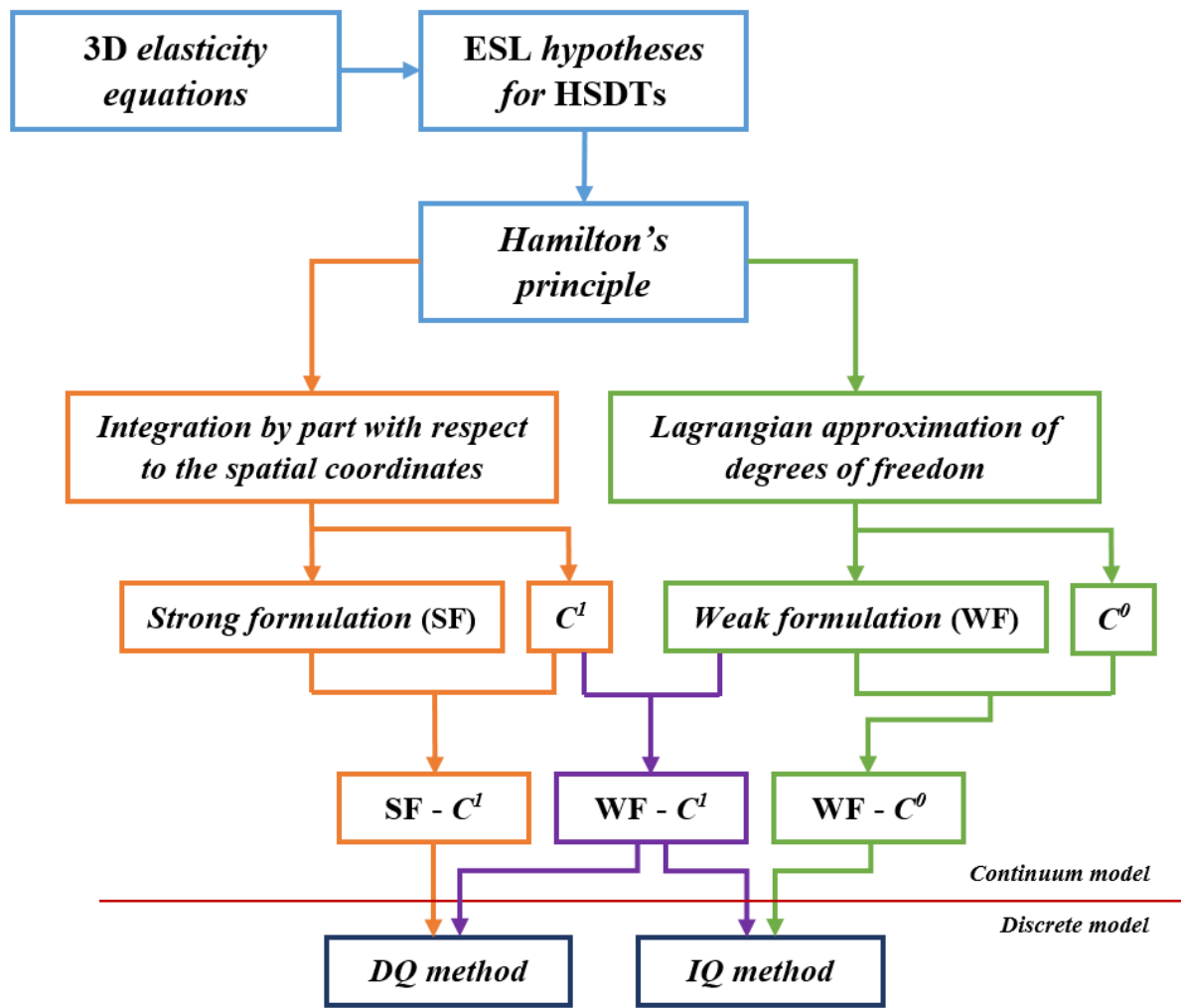


Figure 3.12 – Comparison between the strong and weak formulations.

For this purpose, the momentum vector per unit surface  $\Lambda^{(\tau)}$  must be introduced as follows

$$\Lambda^{(\tau)} = \sum_{\eta=0}^{N+1} \mathbf{M}^{(\tau\eta)} \dot{\mathbf{u}}^{(\eta)} \quad (3.315)$$

for  $\tau = 0, 1, 2, \dots, N, N+1$ , as constitutive equation. The vector  $\dot{\mathbf{u}}^{(\eta)}$  collects the velocity components, which can be computed as the time derivative of the corresponding generalized displacements

$$\dot{\mathbf{u}}^{(\tau)} = \frac{\partial \mathbf{u}^{(\tau)}}{\partial t} \quad (3.316)$$

At this point, the vector of inertial forces per unit surface  $\mathbf{f}_I$  can be evaluated as the time derivative of  $\Lambda^{(\tau)}$ , changed in sign

$$\mathbf{f}_I = -\frac{\partial \Lambda^{(\tau)}}{\partial t} = -\sum_{\eta=0}^{N+1} \mathbf{M}^{(\tau\eta)} \ddot{\mathbf{u}}^{(\eta)} \quad (3.317)$$

Definitions (3.315)-(3.317) are valid for the strong formulation. The same quantities are required also for the corresponding weak formulation. In particular, one gets

$$\Lambda^{(\tau)} = \sum_{\eta=0}^{N+1} \bar{\mathbf{M}}^{(\tau\eta)} \dot{\mathbf{u}}^{(\eta)} \quad (3.318)$$

$$\dot{\mathbf{u}}^{(\tau)} = \frac{\partial \bar{\mathbf{u}}^{(\tau)}}{\partial t} \quad (3.319)$$

$$\mathbf{f}_I = -\frac{\partial \Lambda^{(\tau)}}{\partial t} = -\sum_{\eta=0}^{N+1} \bar{\mathbf{M}}^{(\tau\eta)} \ddot{\mathbf{u}}^{(\eta)} \quad (3.320)$$

for  $\tau = 0, 1, 2, \dots, N, N+1$ .

## 3.2 EXTERNAL RESTRAINTS

The governing equations deduced in the previous sections can be solved once the proper boundary conditions (natural or essential) are enforced. These conditions assume different aspects according to the kind of restraint, which can be fully clamped (C), free (F), or simply-supported (S). In particular, one gets the following conditions for  $\tau = 0, 1, 2, \dots, N, N+1$

*Clamped edge boundary conditions*

$$u_1^{(\tau)} = u_2^{(\tau)} = u_3^{(\tau)} = 0 \quad \text{for } \alpha_1 = \alpha_1^0 \text{ or } \alpha_1 = \alpha_1^1, \alpha_2^0 \leq \alpha_2 \leq \alpha_2^1 \quad (3.321)$$

$$u_1^{(\tau)} = u_2^{(\tau)} = u_3^{(\tau)} = 0 \quad \text{for } \alpha_2 = \alpha_2^0 \text{ or } \alpha_2 = \alpha_2^1, \alpha_1^0 \leq \alpha_1 \leq \alpha_1^1 \quad (3.322)$$

*Free edge boundary conditions*

$$N_1^{(\tau)\alpha_1} = 0, N_{12}^{(\tau)\alpha_2} = 0, T_1^{(\tau)\alpha_3} = 0 \quad \text{for } \alpha_1 = \alpha_1^0 \text{ or } \alpha_1 = \alpha_1^1, \alpha_2^0 \leq \alpha_2 \leq \alpha_2^1 \quad (3.323)$$

$$N_{21}^{(\tau)\alpha_1} = 0, N_2^{(\tau)\alpha_2} = 0, T_2^{(\tau)\alpha_3} = 0 \quad \text{for } \alpha_2 = \alpha_2^0 \text{ or } \alpha_2 = \alpha_2^1, \alpha_1^0 \leq \alpha_1 \leq \alpha_1^1 \quad (3.324)$$

*Simply-supported boundary conditions*

$$N_1^{(\tau)\alpha_1} = 0, \quad u_2^{(\tau)} = u_3^{(\tau)} = 0 \quad \text{for } \alpha_1 = \alpha_1^0 \text{ or } \alpha_1 = \alpha_1^1, \alpha_2^0 \leq \alpha_2 \leq \alpha_2^1 \quad (3.325)$$

$$N_2^{(\tau)\alpha_2} = 0, \quad u_1^{(\tau)} = u_3^{(\tau)} = 0 \quad \text{for } \alpha_2 = \alpha_2^0 \text{ or } \alpha_2 = \alpha_2^1, \alpha_1^0 \leq \alpha_1 \leq \alpha_1^1 \quad (3.326)$$

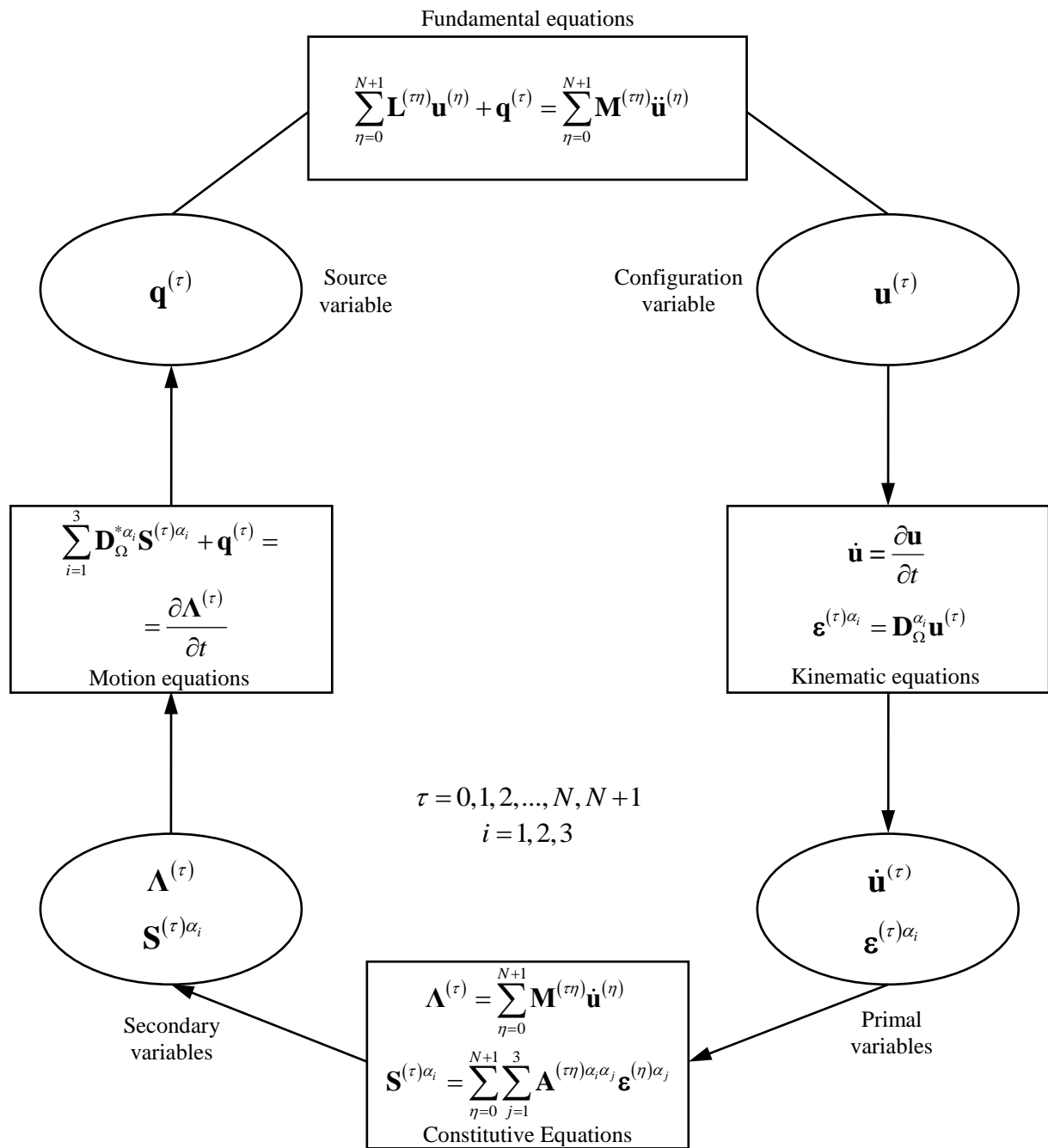


Figure 3.13 – Scheme of physical theories for the higher-order strong formulation.

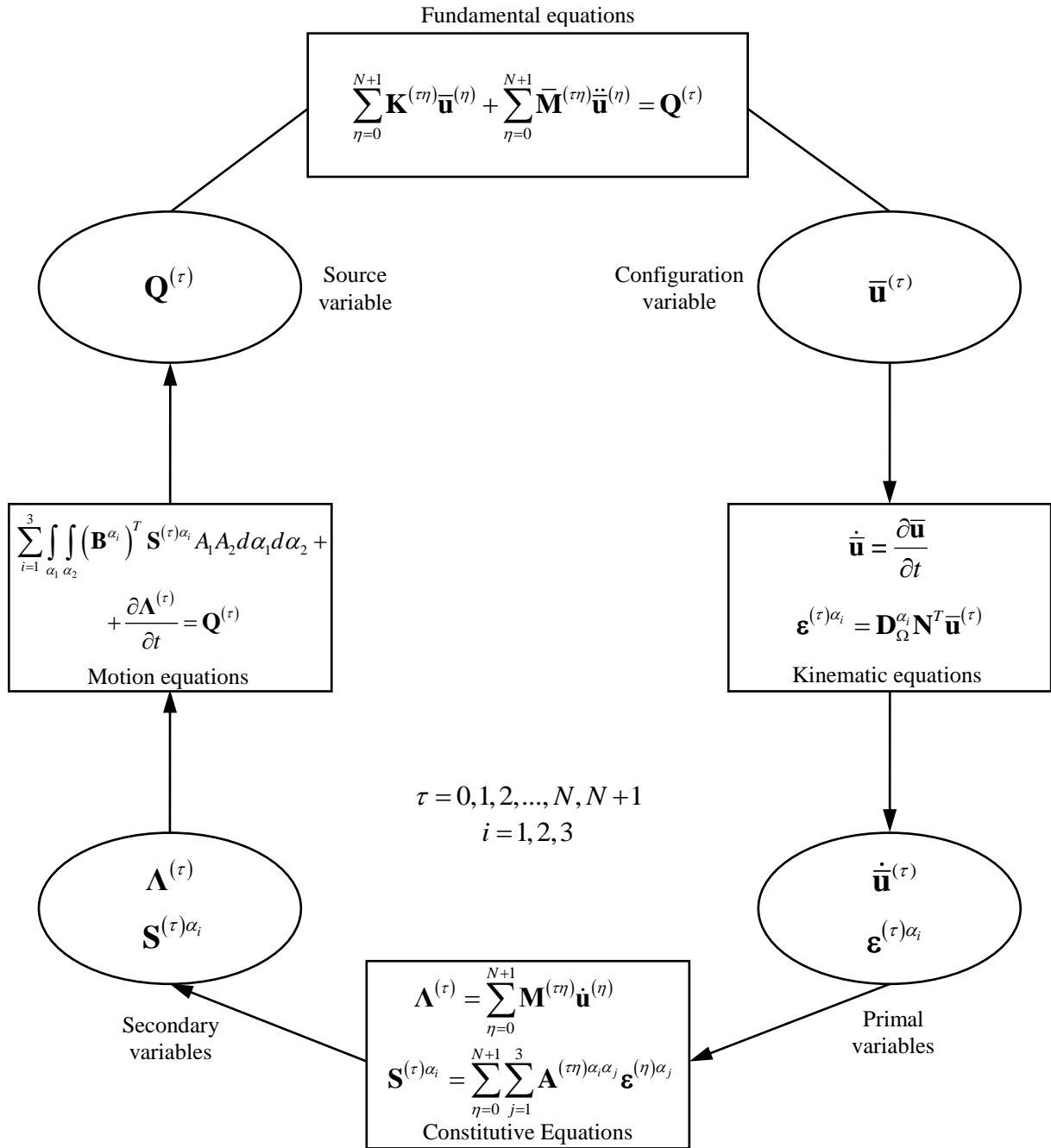


Figure 3.14 – Scheme of physical theories for the higher-order weak formulation.

It is convenient at this point to introduce a notation to identify univocally each external side of the domain, where the boundary conditions are applied. In particular, each side is denoted by a cardinal direction, according to the scheme defined below

$$\begin{array}{lll}
 \alpha_2 = \alpha_2^0 & \alpha_1^0 \leq \alpha_1 \leq \alpha_1^1 & \text{West edge (W)} \\
 \alpha_2 = \alpha_2^1 & \alpha_1^0 \leq \alpha_1 \leq \alpha_1^1 & \text{East edge (E)} \\
 \alpha_2^0 \leq \alpha_2 \leq \alpha_2^1 & \alpha_1 = \alpha_1^0 & \text{North edge (N)} \\
 \alpha_2^0 \leq \alpha_2 \leq \alpha_2^1 & \alpha_1 = \alpha_1^1 & \text{South edge (S)}
 \end{array} \tag{3.327}$$

The boundary conditions are specified by following the order WSEN. It should be recalled once again that the natural boundary conditions are enforced only for  $C^1$  formulations. Finally, conditions (3.321)-(3.326) must be applied also along the external edges of irregular domains, by using the displacements and stress resultants introduced in (3.250) and (3.251), respectively.

### 3.2.1 CONTINUITY CONDITIONS

The boundary conditions assume a different meaning if the structure has a closing edge, as in the case of complete shells of revolution or toroidal shells. In general, it is more appropriate talking about continuity conditions instead of boundary conditions, since these conditions are required to satisfy the structural congruence. The conditions at issue are written in terms of both stress resultants and generalized displacements, for  $\tau = 0, 1, 2, \dots, N, N+1$ . If the closing edge is the one defined by  $\alpha_2^0 = \alpha_2^1$ , one gets

$$\begin{array}{ll}
 N_{21}^{(\tau)\alpha_1}(\alpha_1, \alpha_2^0, t) = N_{21}^{(\tau)\alpha_1}(\alpha_1, \alpha_2^1, t), & u_1^{(\tau)}(\alpha_1, \alpha_2^0, t) = u_1^{(\tau)}(\alpha_1, \alpha_2^1, t) \\
 N_2^{(\tau)\alpha_2}(\alpha_1, \alpha_2^0, t) = N_2^{(\tau)\alpha_2}(\alpha_1, \alpha_2^1, t), & u_2^{(\tau)}(\alpha_1, \alpha_2^0, t) = u_2^{(\tau)}(\alpha_1, \alpha_2^1, t) \\
 T_2^{(\tau)\alpha_3}(\alpha_1, \alpha_2^0, t) = T_2^{(\tau)\alpha_3}(\alpha_1, \alpha_2^1, t), & u_3^{(\tau)}(\alpha_1, \alpha_2^0, t) = u_3^{(\tau)}(\alpha_1, \alpha_2^1, t)
 \end{array} \tag{3.328}$$

Analogously, if the closing edge is the one denoted by  $\alpha_1^0 = \alpha_1^1$ , the continuity conditions are given by

$$\begin{aligned}
 N_1^{(\tau)\alpha_1}(\alpha_1^0, \alpha_2, t) &= N_1^{(\tau)\alpha_1}(\alpha_1^1, \alpha_2, t), & u_1^{(\tau)}(\alpha_1^0, \alpha_2, t) &= u_1^{(\tau)}(\alpha_1^1, \alpha_2, t) \\
 N_{12}^{(\tau)\alpha_2}(\alpha_1^0, \alpha_2, t) &= N_{12}^{(\tau)\alpha_2}(\alpha_1^1, \alpha_2, t), & u_2^{(\tau)}(\alpha_1^0, \alpha_2, t) &= u_2^{(\tau)}(\alpha_1^1, \alpha_2, t) \\
 T_1^{(\tau)\alpha_3}(\alpha_1^0, \alpha_2, t) &= T_1^{(\tau)\alpha_3}(\alpha_1^1, \alpha_2, t), & u_3^{(\tau)}(\alpha_1^0, \alpha_2, t) &= u_3^{(\tau)}(\alpha_1^1, \alpha_2, t)
 \end{aligned} \tag{3.329}$$

Relations (3.328)-(3.329) must be applied independently from the formulation of the governing equations.

### **3.3 REMARKS ON FIRST-ORDER THEORIES**

The well-known Reissner-Mindlin Theory or First-order Shear Deformation Theory (FSDT) for doubly-curved shells can be obtained directly from higher-models, following the same procedure illustrated in the book by Tornabene et al. [57]. The weak formulation for the FSDT can be easily deduced by setting properly the matrices and vectors that appear in the governing equations.

As far as the well-known Kirchhoff-Love theory for thin plates and shells is concerned, it cannot be obtained directly from the present higher-order formulation. Nevertheless, by setting the shear correction factor equal to  $\kappa = 10^6$  in the Reissner-Mindlin theory, the FSDT tends to the Kirchhoff-Love model, since the transverse shear stresses are neglected.



# *Chapter 4*

## *Numerical Applications: Free Vibration Analysis*

The fundamental system of equations that governs the mechanical behavior of laminated composite shell structures has been obtained in the previous chapter, in the framework of weak and strong formulations. The numerical techniques illustrated in the first chapter allow to obtain the discrete form of the governing equations.

The main aim of this chapter is to evaluate the natural frequency of several structures to investigate the accuracy, stability and reliability of the present formulations. Firstly, the procedure to get the natural frequencies, as well as the corresponding mode shapes, is presented. Then, several tests and numerical applications are shown.

### **4.1 MOTION EQUATIONS**

The motion equations that describe the dynamic behavior of composite shell structures can be obtained directly from the fundamental system presented in the previous chapter, by setting the external load vectors equal to zero. For the sake of conciseness, the effect of the Winkler –

Pasternak elastic foundation is neglected, too. The natural frequencies can be achieved by using the well-known method of variable separation. The solution procedure is briefly shown for both the strong and weak formulations.

#### 4.1.1 STRONG FORMULATION

According to the assumptions just introduced, the strong form of the governing equation is given by the following relation, for each order of kinematic expansion  $\tau$

$$\sum_{\eta=0}^{N+1} \mathbf{L}^{(\tau\eta)} \mathbf{u}^{(\eta)} = \sum_{\eta=0}^{N+1} \mathbf{M}^{(\tau\eta)} \ddot{\mathbf{u}}^{(\eta)} \quad (4.1)$$

The solution of the dynamic problem at issue can be pursued by setting

$$\mathbf{u}^{(\tau)}(\alpha_1, \alpha_2, t) = \mathbf{U}^{(\tau)}(\alpha_1, \alpha_2) e^{i\omega t} \quad (4.2)$$

for  $\tau = 0, 1, 2, \dots, N, N+1$ , in which  $\omega$  denotes the circular frequencies of the structures which allows to compute the natural frequencies as  $f = \omega/2\pi$ . On the other hand,  $\mathbf{U}^{(\tau)}$  collects the mode amplitudes and it is defined as follows

$$\mathbf{U}^{(\tau)} = \left[ U_1^{(\tau)} \quad U_2^{(\tau)} \quad U_3^{(\tau)} \right]^T \quad (4.3)$$

for  $\tau = 0, 1, 2, \dots, N, N+1$ . The size of  $\mathbf{U}^{(\tau)}$  is  $3 \times 1$ , for each order of kinematic expansion. By inserting the definition (4.2) and performing its second-order derivative with respect to the time variable  $t$ , the previous relation becomes

$$\sum_{\eta=0}^{N+1} \mathbf{L}^{(\tau\eta)} \mathbf{U}^{(\tau)} + \omega^2 \sum_{\eta=0}^{N+1} \mathbf{M}^{(\tau\eta)} \mathbf{U}^{(\tau)} = \mathbf{0} \quad (4.4)$$

for  $\tau = 0, 1, 2, \dots, N, N+1$ . At this point, the discrete form of equation (4.4) can be carried out by applying the DQ method to approximate directly the derivatives with respect to the geometric coordinates of the reference domain. One gets

$$\mathbf{K}\boldsymbol{\delta} = \omega^2 \mathbf{M}\boldsymbol{\delta} \quad (4.5)$$

where  $\mathbf{K}$  and  $\mathbf{M}$  are the discrete global stiffness and mass matrices, respectively, whose size is clearly given by  $3I_N I_M (N+2) \times 3I_N I_M (N+2)$ . On the other hand,  $\boldsymbol{\delta}$  is the discrete vector of mode amplitudes, whose size is  $3I_N I_M (N+2) \times 1$ .

### 4.1.2 WEAK FORMULATION

Analogously, following the assumptions introduced before, the weak form of the governing equation can be written as follows, for each order of kinematic expansion  $\tau$

$$\sum_{\eta=0}^{N+1} \mathbf{K}^{(\tau\eta)} \bar{\mathbf{u}}^{(\eta)} + \sum_{\eta=0}^{N+1} \bar{\mathbf{M}}^{(\tau\eta)} \ddot{\bar{\mathbf{u}}}^{(\eta)} = \mathbf{0} \quad (4.6)$$

The solution of the dynamic problem consider in this chapter can be achieved by setting

$$\bar{\mathbf{u}}^{(\tau)}(\alpha_{1f}, \alpha_{2g}, t) = \bar{\mathbf{U}}^{(\tau)}(\alpha_{1f}, \alpha_{2g}) e^{i\omega t} \quad (4.7)$$

for  $\tau = 0, 1, 2, \dots, N, N+1$ , where  $\bar{\mathbf{U}}^{(\tau)}$  is the vector that collects the modal displacement in every discrete node of the domain, for each circular frequency  $\omega$  of the structure, defined below

$$\begin{aligned} \bar{\mathbf{U}}^{(\tau)} &= \left[ \bar{\mathbf{U}}_1^{(\tau)} \quad \bar{\mathbf{U}}_2^{(\tau)} \quad \bar{\mathbf{U}}_3^{(\tau)} \right]^T = \\ &= \left[ \left[ U_{1(11)}^{(\tau)} \quad \dots \quad U_{1(I_N1)}^{(\tau)} \mid U_{1(12)}^{(\tau)} \quad \dots \quad U_{1(I_N2)}^{(\tau)} \mid \dots \mid U_{1(1I_M)}^{(\tau)} \quad \dots \quad U_{1(I_N I_M)}^{(\tau)} \mid \dots \right. \right. \\ &\quad \dots \mid U_{2(11)}^{(\tau)} \quad \dots \quad U_{2(I_N1)}^{(\tau)} \mid U_{2(12)}^{(\tau)} \quad \dots \quad U_{2(I_N2)}^{(\tau)} \mid \dots \mid U_{2(1I_M)}^{(\tau)} \quad \dots \quad U_{2(I_N I_M)}^{(\tau)} \mid \dots \\ &\quad \left. \dots \mid U_{3(11)}^{(\tau)} \quad \dots \quad U_{3(I_N1)}^{(\tau)} \mid U_{3(12)}^{(\tau)} \quad \dots \quad U_{3(I_N2)}^{(\tau)} \mid \dots \mid U_{3(1I_M)}^{(\tau)} \quad \dots \quad U_{3(I_N I_M)}^{(\tau)} \right] \right]^T \end{aligned} \quad (4.8)$$

It should be noted that these nodal quantities are listed following the order provided in Figure 1.2. In general,  $U_{k(fg)}^{(\tau)}$  represents the generic  $k$ -th element of  $\bar{\mathbf{U}}^{(\tau)}$  linked to the point of coordinates  $\alpha_{1f}, \alpha_{2g}$ . The size of  $\bar{\mathbf{U}}^{(\tau)}$  is  $(3I_N I_M) \times 1$ , for each order of kinematic expansion.

By inserting the definition (4.7) and performing its second-order derivative with respect to the time variable  $t$ , the previous relation assumes the following aspect

$$\sum_{\eta=0}^{N+1} \mathbf{K}^{(\tau\eta)} \bar{\mathbf{U}}^{(\eta)} = \omega^2 \sum_{\eta=0}^{N+1} \bar{\mathbf{M}}^{(\tau\eta)} \bar{\mathbf{U}}^{(\eta)} \quad (4.9)$$

for  $\tau = 0, 1, 2, \dots, N, N+1$ . Once the stiffness matrix and the mass matrix are computed by means of the IQ method for each order of kinematic expansion, the discrete global system of governing equations is obtained. One gets

$$\mathbf{K}\delta = \omega^2 \mathbf{M}\delta \quad (4.10)$$

where  $\mathbf{K}$  and  $\mathbf{M}$  are the discrete global stiffness and mass matrices, respectively, whose size is given by  $3I_N I_M (N+2) \times 3I_N I_M (N+2)$ . On the other hand,  $\boldsymbol{\delta}$  is the discrete vector of mode amplitudes, whose size is  $3I_N I_M (N+2) \times 1$ .

It can be easily noted that expressions (4.5) and (4.10) are equivalent, even if the various quantities are computed in a completely different manner. In any circumstance, these relations represent the discrete equation of the free vibration frequencies, which is algebraically a generalized linear eigenvalue problem.

### 4.1.3 SOLUTION OF THE EIGENVALUE PROBLEM

As specified above, equations (4.5) and (4.10) represent a generalized linear eigenvalue problem. By definition, the eigenvalues  $\omega_k$  are evidently the circular frequencies, whereas the corresponding eigenvectors  $\boldsymbol{\delta}_k$  denote the mode shape vector. It should be recalled that the maximum number of eigenvalues and eigenvectors that can be computed depends on the number of sampling points of the discrete grid distribution.

The well-known kinematic condensation can be used to reduce the size of the dynamic problem at issue. For this purpose, the vector  $\boldsymbol{\delta}$  is divided into two parts, so that the vector of the modal displacements linked to each discrete point placed within the reference domain, denoted by  $\boldsymbol{\delta}_d$ , is separated from the one that collects the modal displacements of the points placed along the external edges, denoted by  $\boldsymbol{\delta}_b$ . Consequently, one gets  $\boldsymbol{\delta} = [\boldsymbol{\delta}_b \quad \boldsymbol{\delta}_d]^T$ .

Once the classification at issue is introduced, the same scheme is employed to partition the discrete stiffness and mass matrices as follows

$$\begin{bmatrix} \mathbf{K}_{bb} & \mathbf{K}_{bd} \\ \mathbf{K}_{db} & \mathbf{K}_{dd} \end{bmatrix} \begin{bmatrix} \boldsymbol{\delta}_b \\ \boldsymbol{\delta}_d \end{bmatrix} = \omega^2 \begin{bmatrix} \mathbf{0} & \mathbf{0} \\ \mathbf{0} & \mathbf{M}_{dd} \end{bmatrix} \begin{bmatrix} \boldsymbol{\delta}_b \\ \boldsymbol{\delta}_d \end{bmatrix} \quad (4.11)$$

The stiffness and inertia matrices related to the internal points of the domain are denoted by  $\mathbf{K}_{dd}, \mathbf{M}_{dd}$ . On the other hand, the subscript “ $b$ ” specifies the stiffness and inertia contributions that involve the boundary points. In other words, the operators  $\mathbf{K}_{bb}, \mathbf{K}_{bd}, \mathbf{K}_{db}$  are linked to the application of boundary conditions, since the corresponding displacements

are the ones defined along the boundary points. Due to the numerical techniques employed in these circumstances, the boundary conditions involve both the boundary points and the inner ones (included respectively in  $\delta_b$  and  $\delta_d$ ).

At this point, it should be recalled that the natural boundary conditions are replaced by the corresponding field equations if a  $C^0$  formulation is considered. On the other hand, the essential boundary conditions are applied in the same manner for both  $C^0$  and  $C^1$  schemes.

Equation (4.11) can be conveniently written in extend form as follows

$$\begin{aligned} \mathbf{K}_{bb}\delta_b + \mathbf{K}_{bd}\delta_d &= \mathbf{0} \\ \mathbf{K}_{db}\delta_b + \mathbf{K}_{dd}\delta_d &= \omega^2\mathbf{M}_{dd}\delta_d \end{aligned} \quad (4.12)$$

The definition of  $\delta_b$  can be easily deduced from the first vector equation

$$\delta_b = -\mathbf{K}_{bb}^{-1}\mathbf{K}_{bd}\delta_d \quad (4.13)$$

and inserted into the second one in order to obtain the following relation

$$\left(\mathbf{M}_{dd}^{-1}\left(\mathbf{K}_{dd} - \mathbf{K}_{db}\mathbf{K}_{bb}^{-1}\mathbf{K}_{bd}\right) - \omega^2\mathbf{I}\right)\delta_d = \mathbf{0} \quad (4.14)$$

in which  $\mathbf{I}$  is the identity matrix. The size of the eigenvalue problem (4.14) is  $3(I_N - 2)(I_M - 2)(N + 2) \times 3(I_N - 2)(I_M - 2)(N + 2)$ , which is noticeably lower than the one that characterize the previous eigenvalue problems (4.5) and (4.10). By solving the dynamic problem (4.14), the circular frequencies  $\omega_k$  and the corresponding mode shapes  $\delta_k$  are obtained. Finally, the natural frequencies  $f_k$  are achieved recalling that  $f_k = \omega_k / 2\pi$ .

## 4.2 NUMERICAL APPLICATIONS

In this section, the numerical solutions of various tests and applications are presented. The approaches presented in the previous chapters are implemented in a MATLAB code to solve both the strong and weak formulations of the governing equations. For this purpose, the DQ and IQ are employed.

### 4.2.1 CONVERGENCE ANALYSIS

The main aim of this paragraph is to present a set of convergence analyses in order to investigate the effect on the numerical solutions of the choice of both discrete grid distributions and basis functions. For this purpose, a simply-supported (SSSS) square plate of side  $L_x = L_y = 1\text{m}$  and thickness  $h = 0.1\text{m}$  is considered. The results of this investigation are graphically shown for the first natural frequency only, but similar behaviors can be obtained for higher frequencies, too.

The accuracy of the numerical approaches under consideration are presented in terms of relative error  $\varepsilon_1$ , which is defined as follows

$$\varepsilon_1 = \frac{f_1}{f_{1,exact}} - 1 \quad (4.15)$$

in which  $f_1$  is the first natural frequency of the structure obtained by means of the DQ and the IQ methods, whereas  $f_{1,exact}$  is the exact solution for the first frequency provided by Reddy [145]. The convergence analyses at issue are achieved by taking into account each basis function presented in the first chapter for the polynomial approximation. Once the basis function is set, all the discrete grid are employed to get the numerical solution.

The convergence analyses are carried out for both isotropic and laminated configurations. As far as the isotropic medium is concerned, the layer is made of Aluminum ( $E = 70\text{GPa}$ ,  $\nu = 0.3$ ,  $\rho = 2707\text{kg/m}^3$ ). On the other hand, the stacking sequence of the second case is (0/90/90/0), in which the four layers have the same thickness and are all made of Graphite-Epoxy ( $E_1 = 137.9\text{GPa}$ ,  $E_2 = E_3 = 8.96\text{GPa}$ ,  $G_{12} = G_{13} = 7.1\text{GPa}$ ,  $G_{23} = 6.21\text{GPa}$ ,  $\nu_{12} = \nu_{13} = 0.3$ ,  $\nu_{23} = 0.49$ ,  $\rho = 1450\text{kg/m}^3$ ). The results for the isotropic plate are shown in Figures 4.1-4.6, whereas the ones for the laminated composite structure are presented in Figures 4.7-4.12. The solutions are obtained by means of the strong formulation, weak formulation with  $C^1$  boundary conditions, and weak formulation with  $C^0$  boundary conditions. The chosen basis function is specified on the top of each plot. Each convergence analysis is performed by using all the grid distributions introduced in the first chapter. These grid distributions are specified in the legend of the various plots.

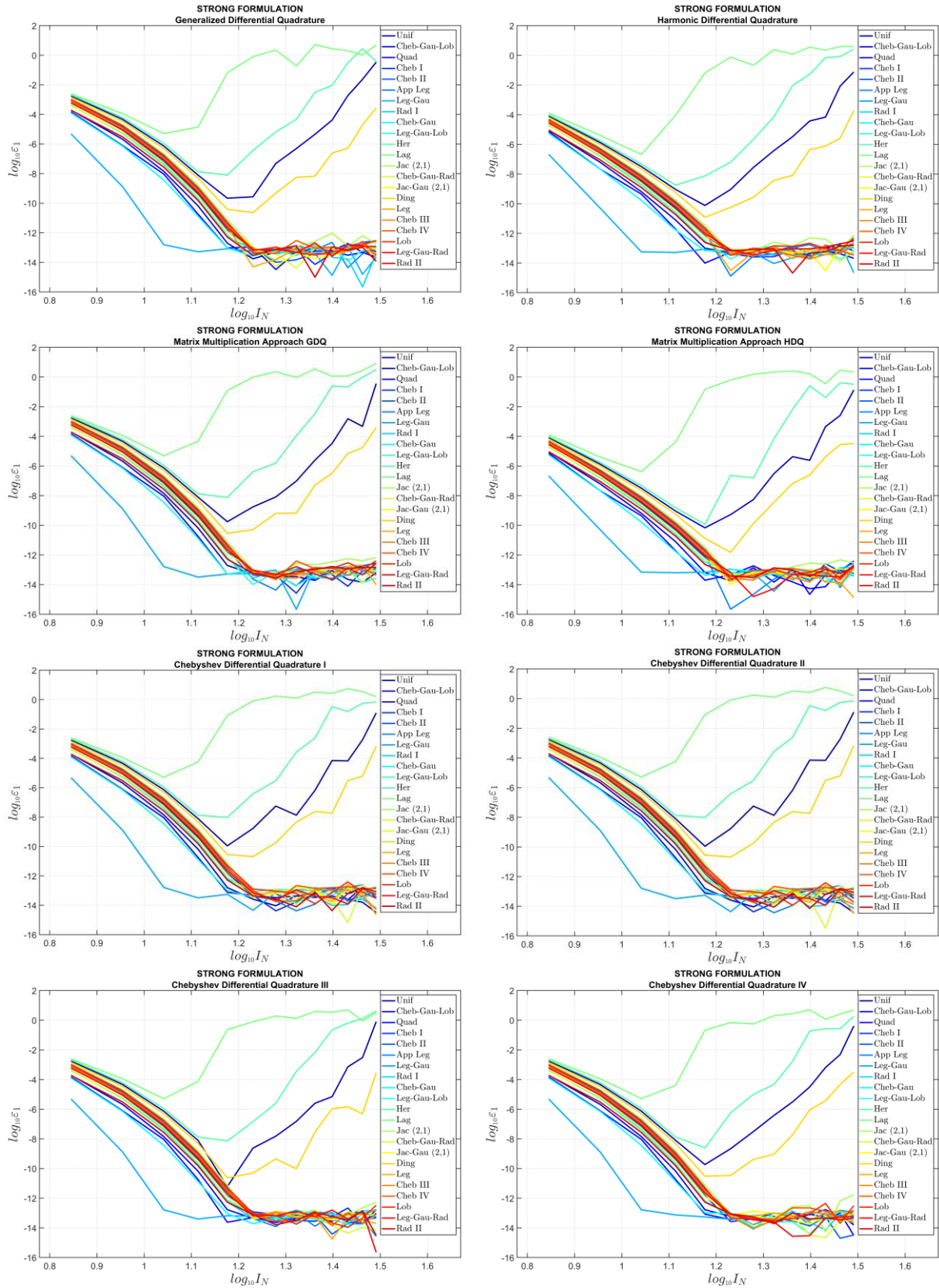
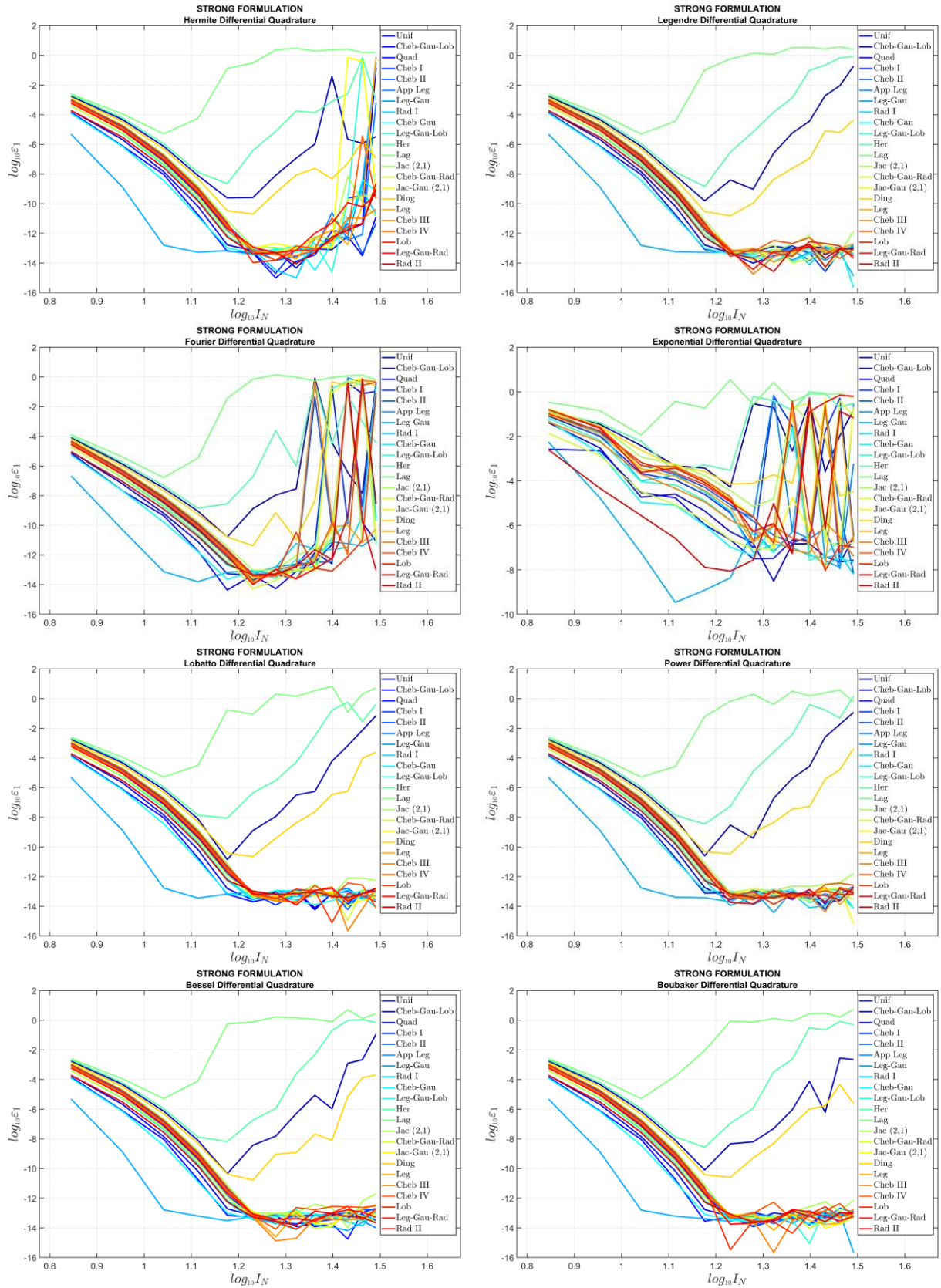
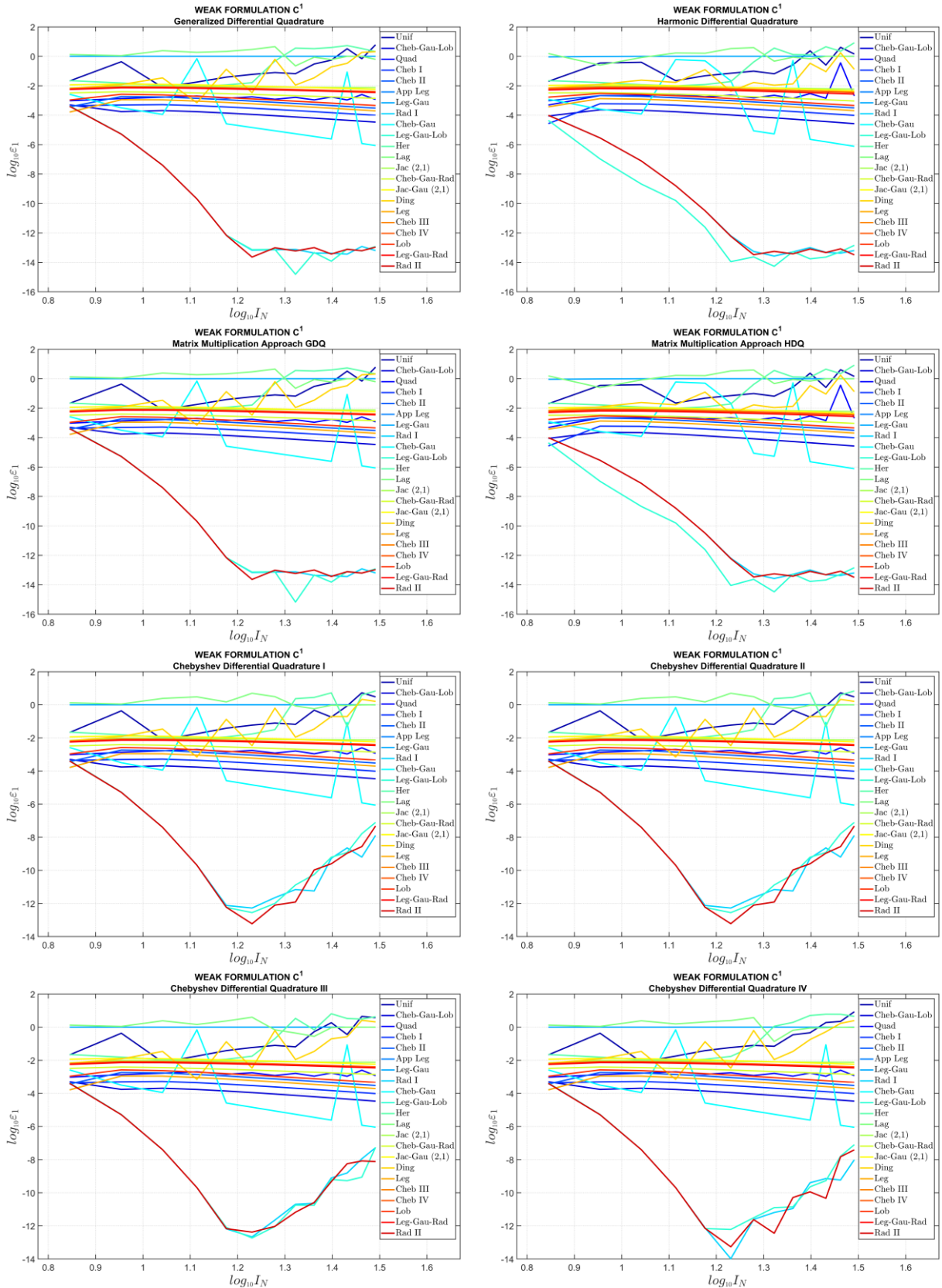


Figure 4.1 – Convergence behavior of the first natural frequency for a SSSS isotropic square plate in the framework of the Reissner-Mindlin theory (FSDT): strong formulation (part 1) [15].



**Figure 4.2** – Convergence behavior of the first natural frequency for a SSSS isotropic square plate in the framework of the Reissner-Mindlin theory (FSDT): strong formulation (part 2) [15].



**Figure 4.3** – Convergence behavior of the first natural frequency for a SSSS isotropic square plate in the framework of the Reissner-Mindlin theory (FSDT): weak formulation with  $C^1$  boundary conditions (part 1) [15].

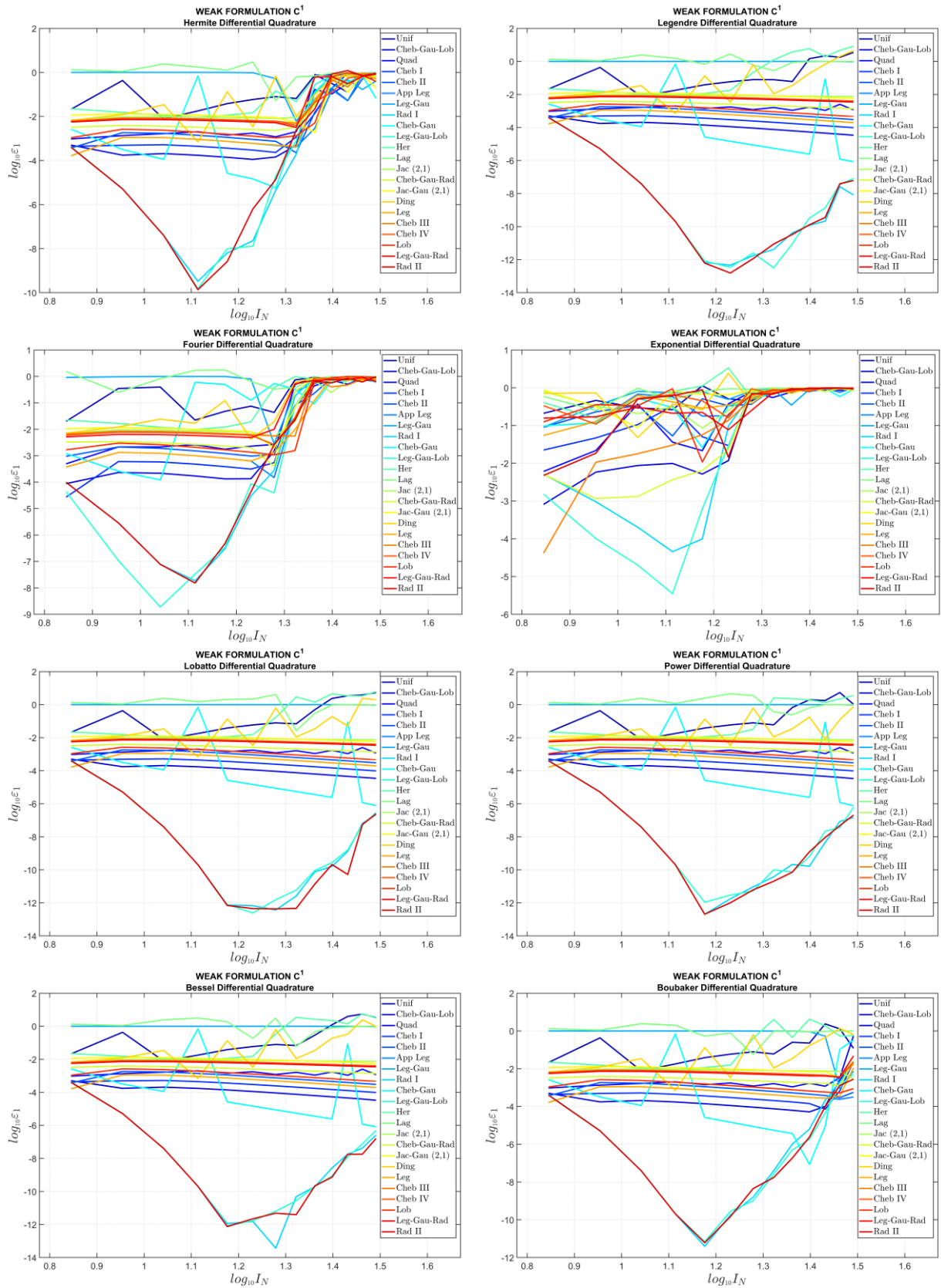


**Figure 4.4** – Convergence behavior of the first natural frequency for a SSSS isotropic square plate in the framework of the Reissner-Mindlin theory (FSDT): weak formulation with  $C^1$  boundary conditions (part 2) [15].

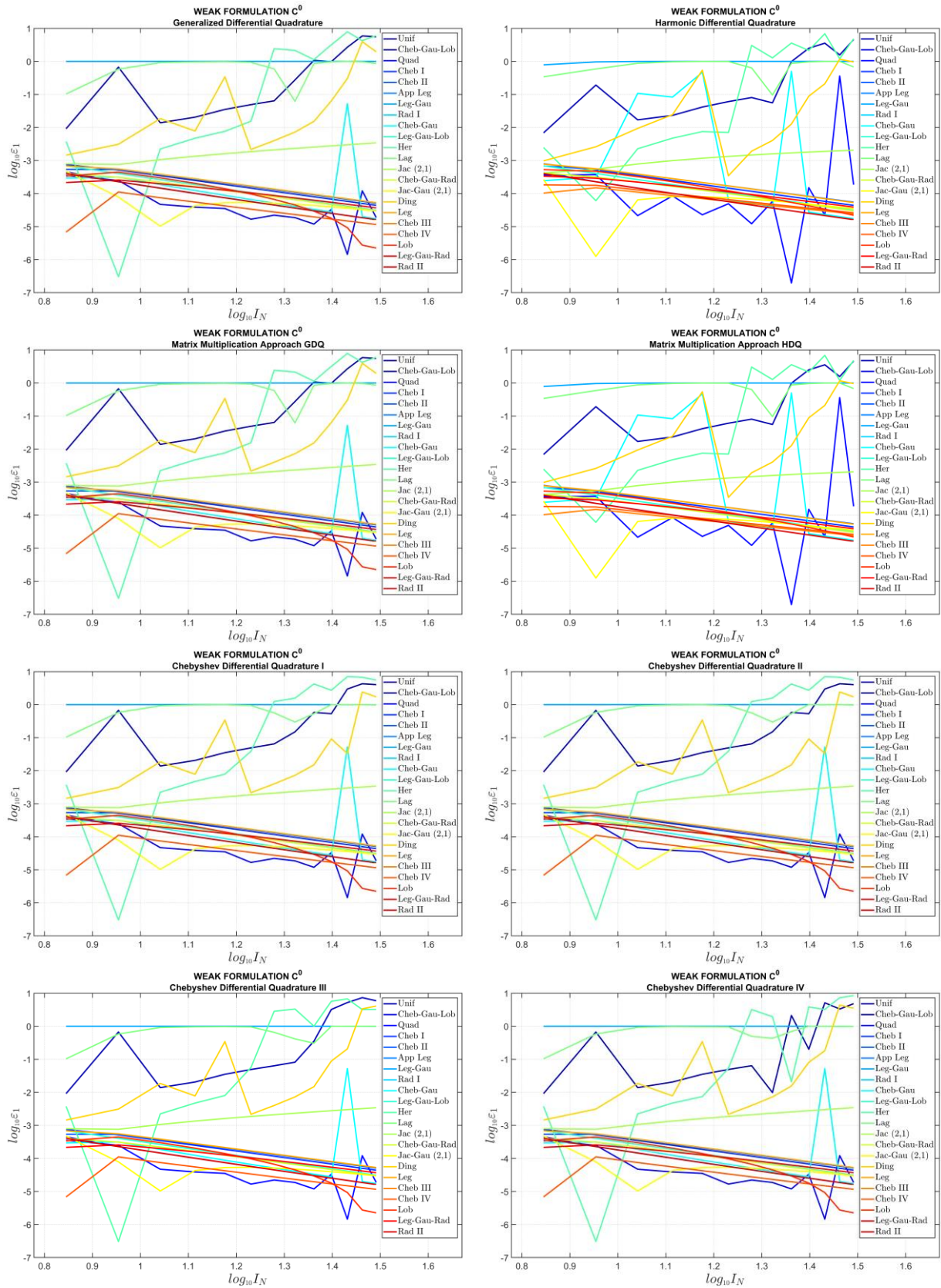


**Figure 4.5** – Convergence behavior of the first natural frequency for a SSSS isotropic square plate in the framework of the Reissner-Mindlin theory (FSDT): weak formulation with  $C^0$  boundary conditions (part 1) [15].

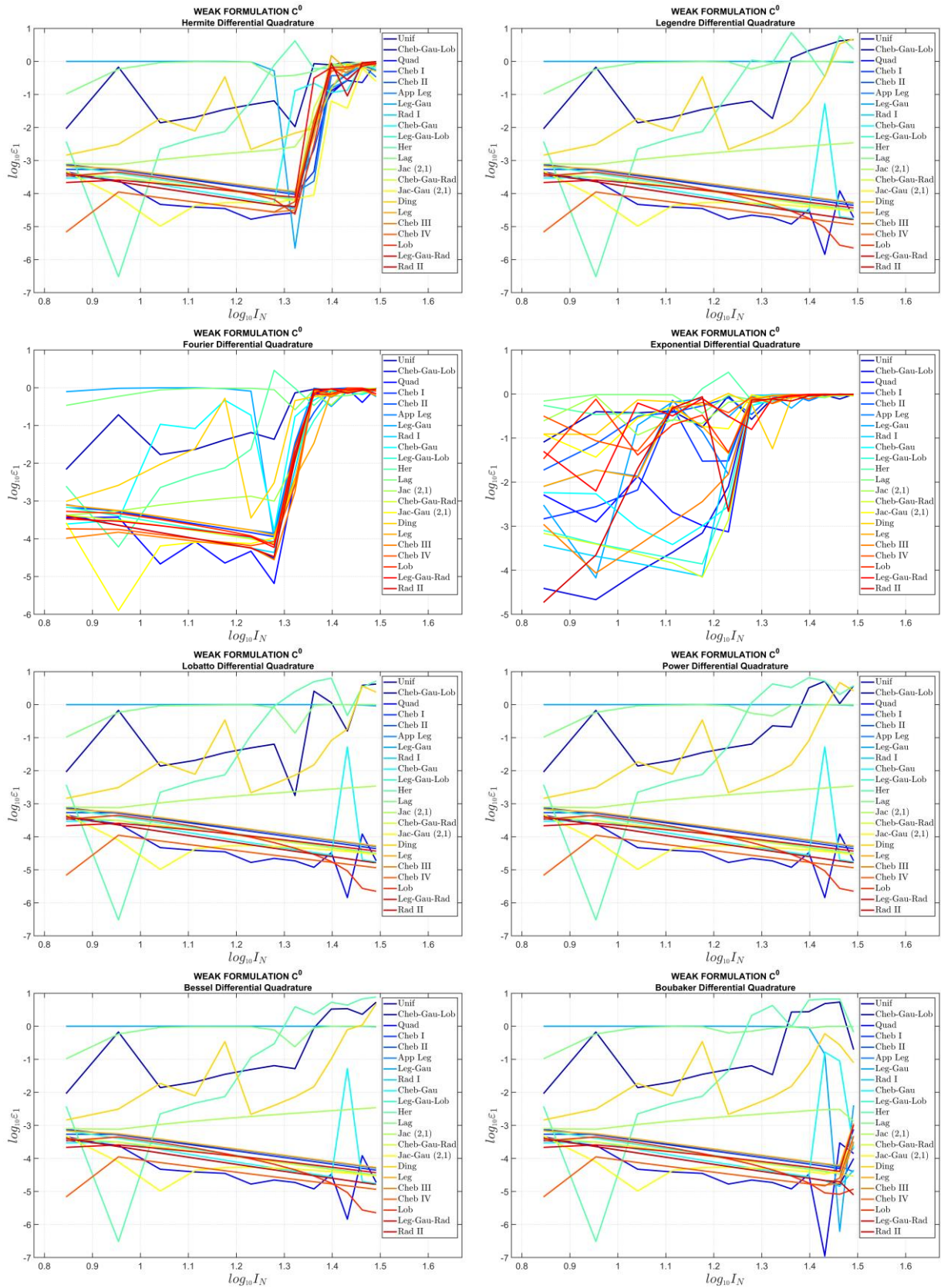


**Figure 4.6** – Convergence behavior of the first natural frequency for a SSSS isotropic square plate in the framework of the Reissner-Mindlin theory (FSDT): weak formulation with  $C^0$  boundary conditions (part 2) [15].

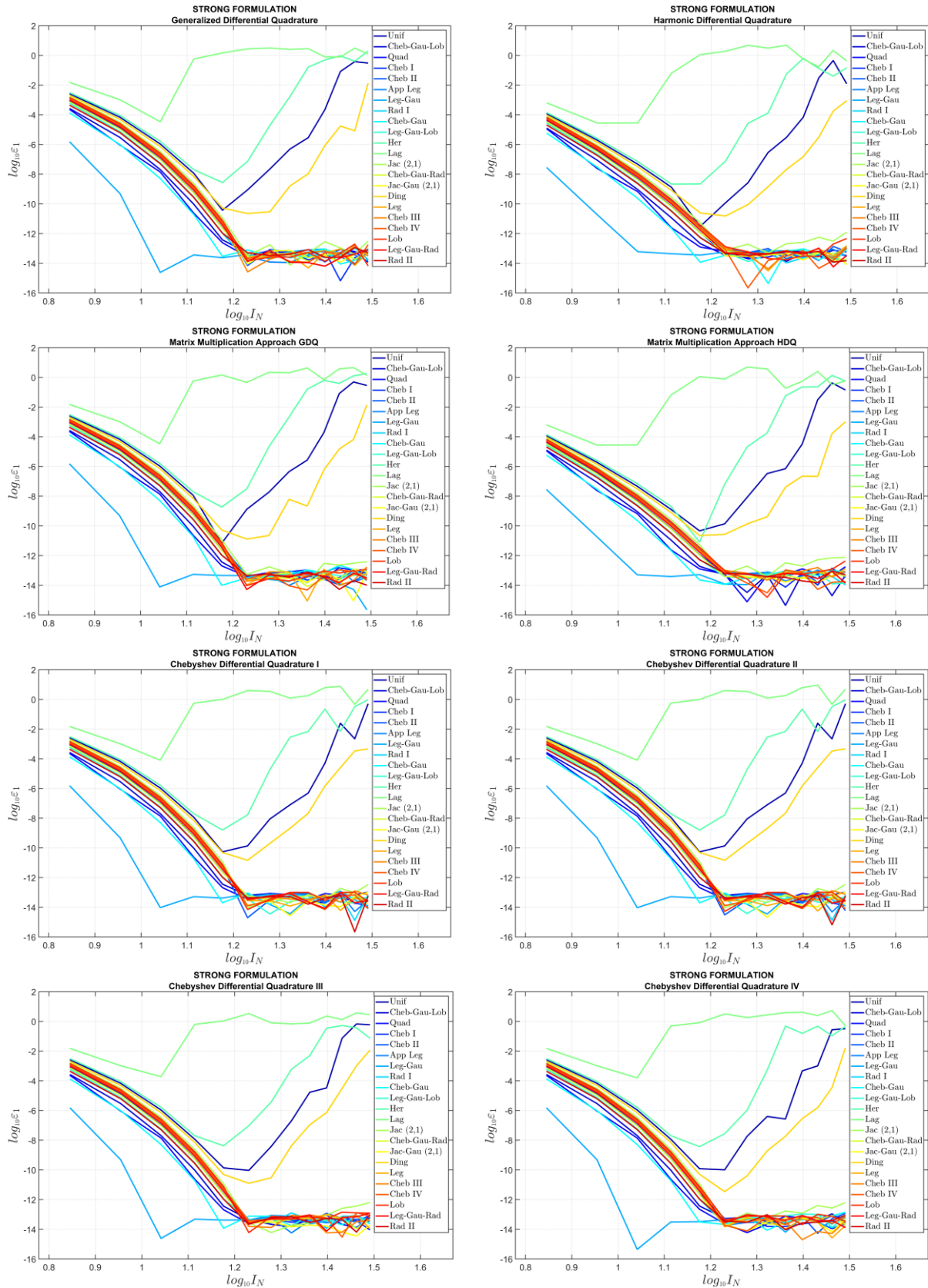


**Figure 4.7** – Convergence behavior of the first natural frequency for a SSSS laminated square plate in the framework of the Reissner-Mindlin theory (FSDT): strong formulation (part 1) [15].

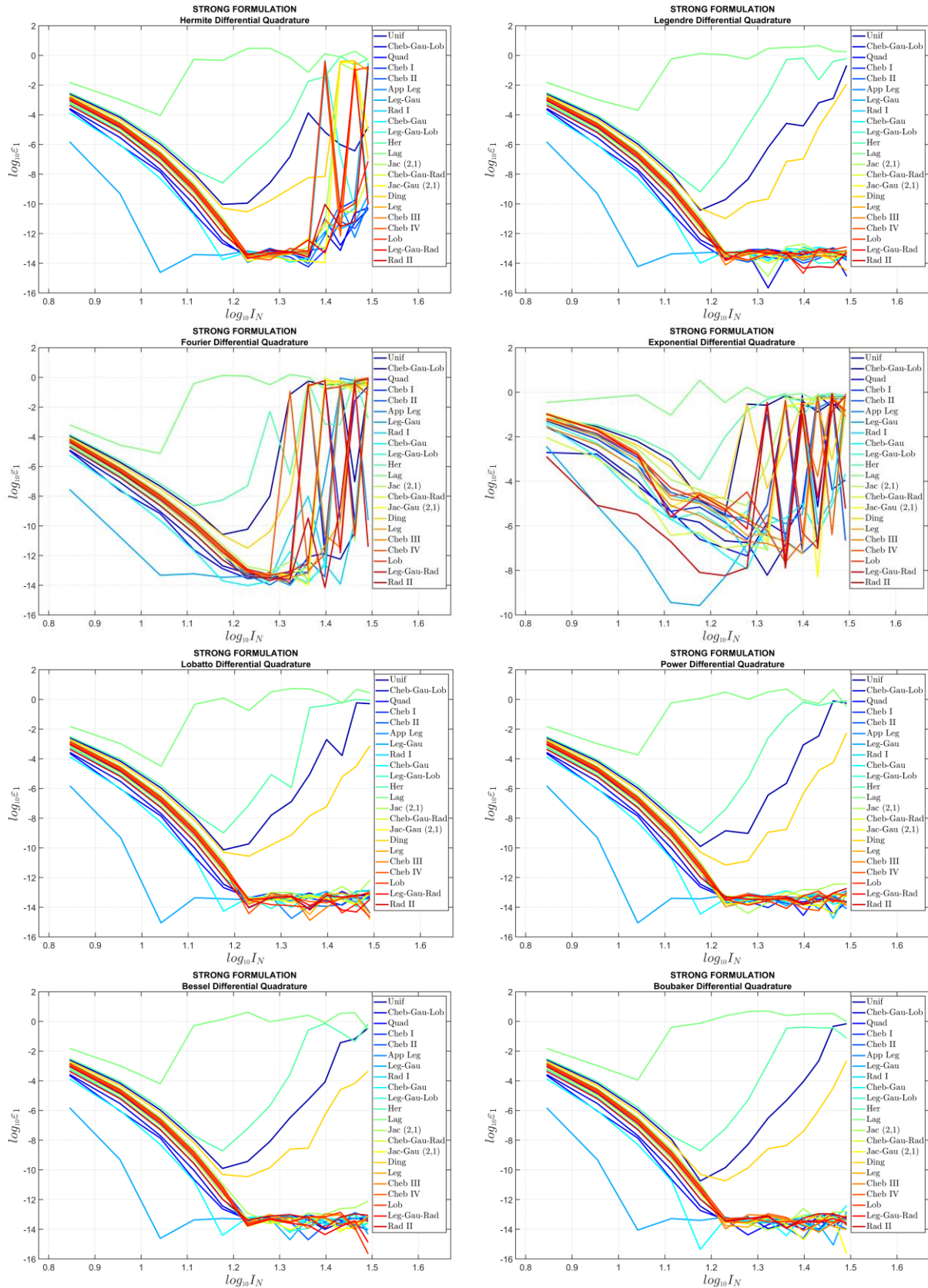


**Figure 4.8** – Convergence behavior of the first natural frequency for a SSSS laminated square plate in the framework of the Reissner-Mindlin theory (FSDT): strong formulation (part 2) [15].

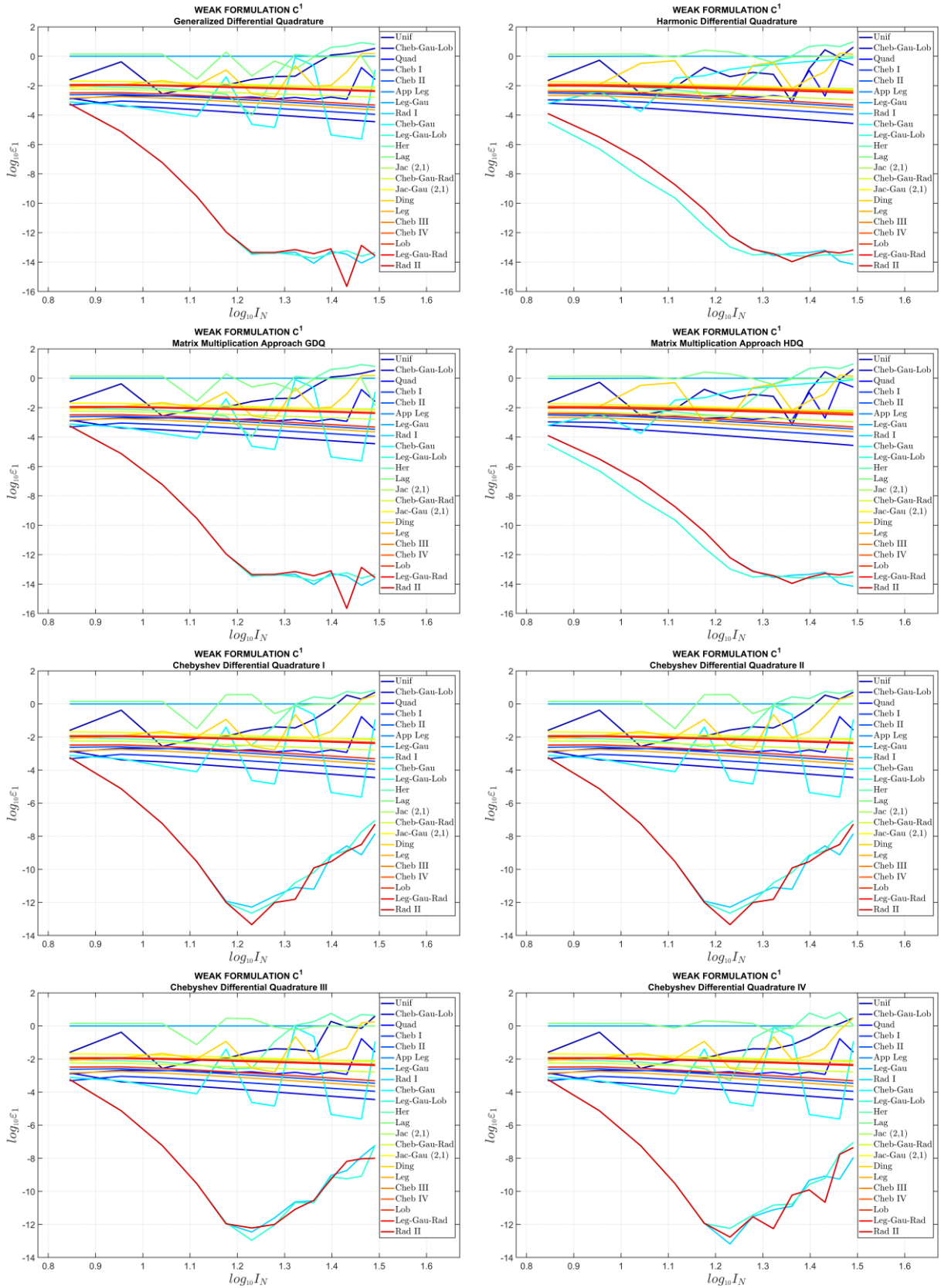


**Figure 4.9** – Convergence behavior of the first natural frequency for a SSSS laminated square plate in the framework of the Reissner-Mindlin theory (FSDT): weak formulation with  $C^1$  boundary conditions (part 1) [15].

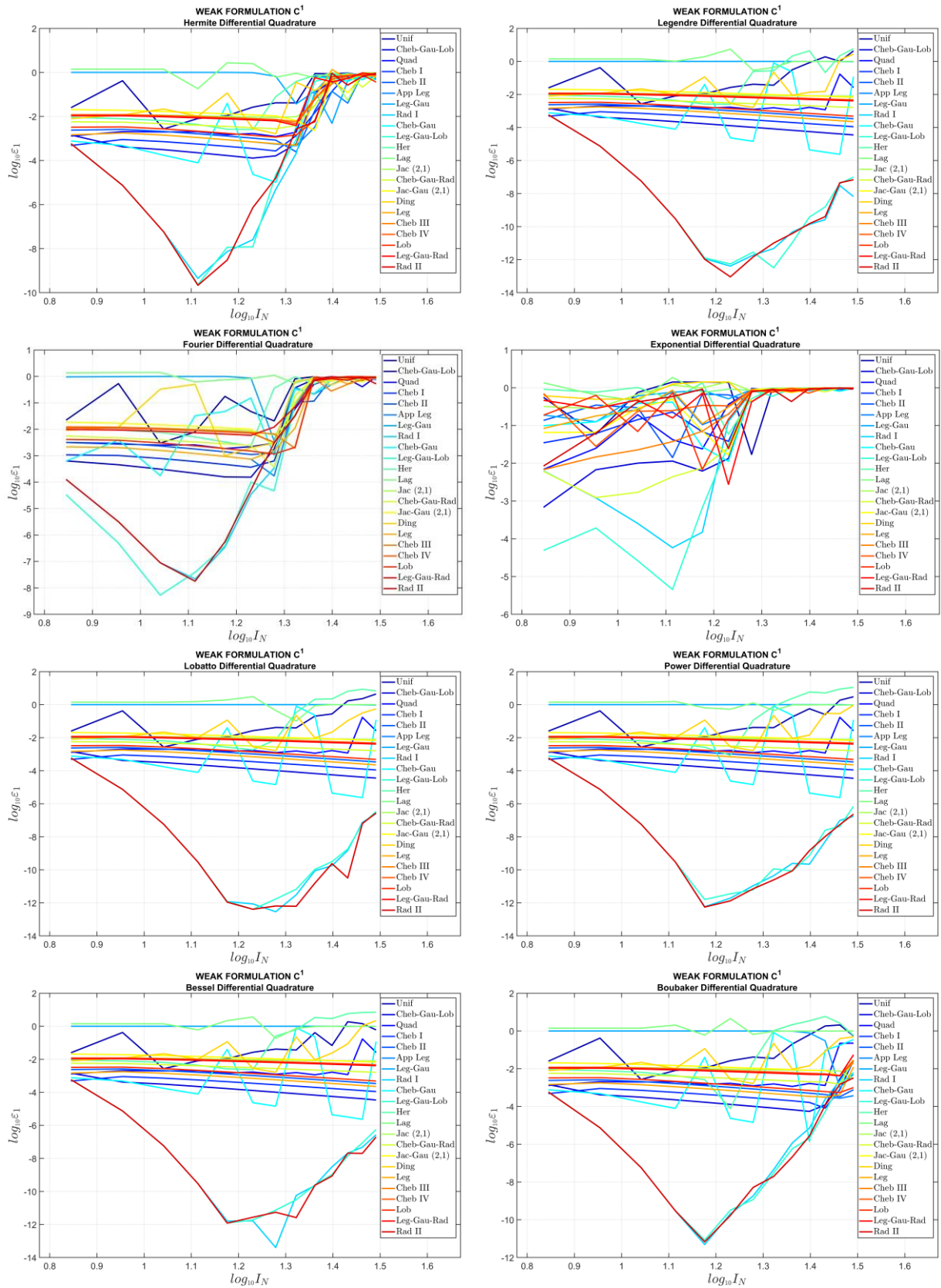


**Figure 4.10** – Convergence behavior of the first natural frequency for a SSSS laminated square plate in the framework of the Reissner-Mindlin theory (FSDT): weak formulation with  $C^1$  boundary conditions (part 2) [15].

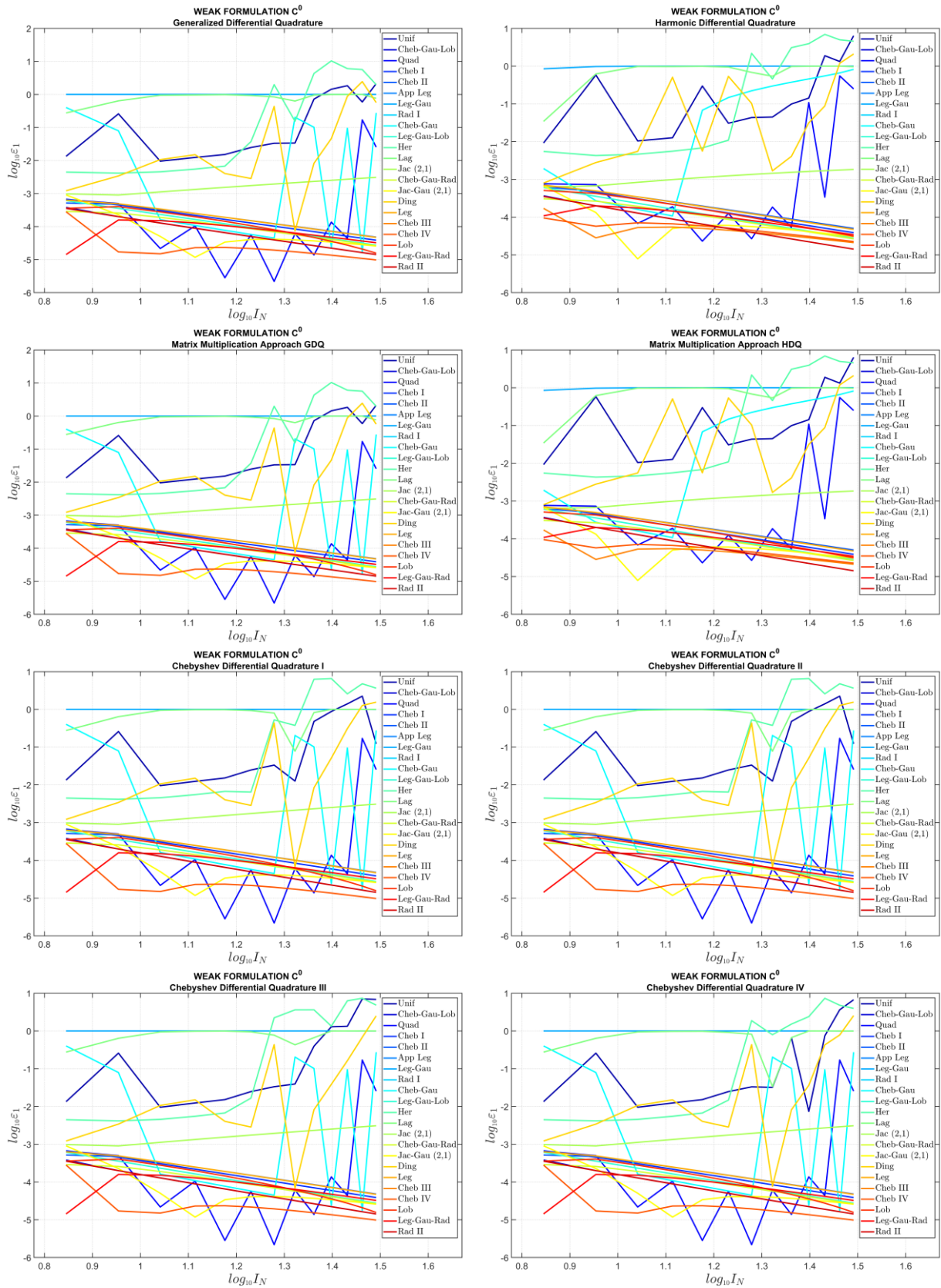


**Figure 4.11** – Convergence behavior of the first natural frequency for a SSSS laminated square plate in the framework of the Reissner-Mindlin theory (FSDT): weak formulation with  $C^0$  boundary conditions (part 1) [15].

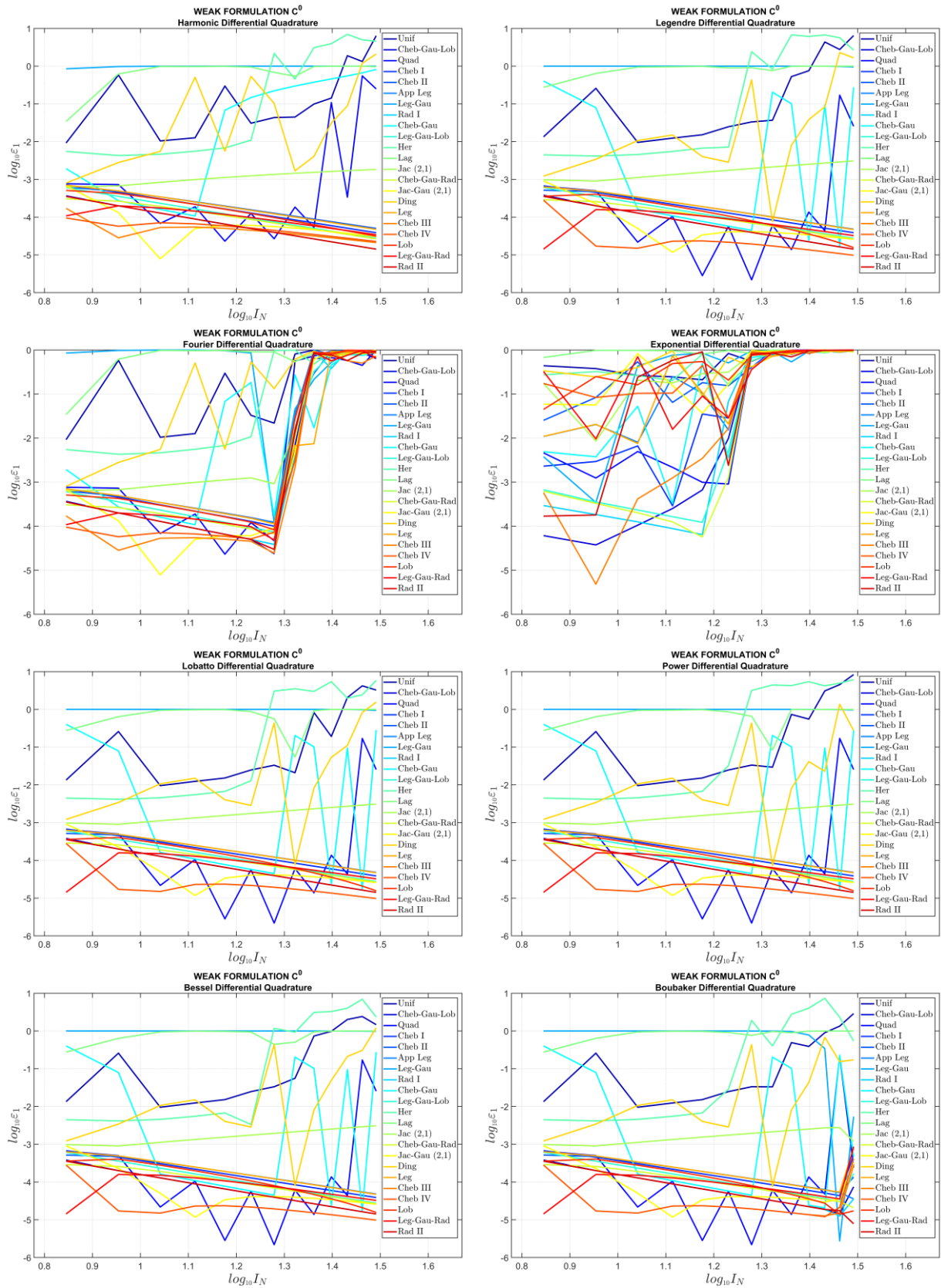


**Figure 4.12** – Convergence behavior of the first natural frequency for a SSSS laminated square plate in the framework of the Reissner-Mindlin theory (FSDT): weak formulation with  $C^0$  boundary conditions (part 2) [15].

The following aspects can be noted by observing the graphs depicted in Figures 4.1-4.12:

- The choice of the basis function define the accuracy and stability of the numerical approach. By choosing particular basis functions, in fact, the numerical results can diverge from the exact solutions since the coefficient matrix could be ill-conditioned. Therefore, the numerical error increases when the inversion of this matrix is carried out. In general, this aspect is unavoidable when the inversion of the matrix is required and an exact expression for the weighting coefficients is not available. Having in mind Figures 4.1-4.12, it is easy to note a fast detachment of the curves from higher values of accuracy if the number of discrete points is increased. On the other hand, more accurate results are obtained when the recursive formulae given by Shu are used [44].
- Analogously, better results can be achieved by setting properly the discrete grid distribution. In general, the Uniform, Hermite, Laguerre and Ding distributions are not accurate for any choice of basis functions.
- The SF is characterized by a geometric convergence independently from the grid distribution, except from the aforementioned ones, for those basis functions that allow the evaluation of the weighting coefficients through recursive formulations. Generally speaking, a noticeably level of accuracy ( $\approx 10^{-13} \div 10^{-14}$  in logarithmic scale) can be reached for a reduced number of grid points ( $I_N = I_M = 15$ ).
- The weak formulation with  $C^0$  boundary conditions is characterized by a linear or algebraic convergence. Nevertheless, the accuracy that can be achieved is extremely lower than the other approaches ( $\approx 10^{-4} \div 10^{-5}$  in logarithmic scale), independently from both the grid distributions and basis functions. Due to the linear convergence behavior, the same accuracy of the other approaches could be reached by increasing excessively the number of grid points.
- The weak formulation with  $C^1$  boundary conditions shows an intermediate behavior, if compared to the previous approaches. In particular, the same accuracy of the strong formulation ( $\approx 10^{-13} \div 10^{-14}$  in logarithmic scale) is reached with a geometric convergence behavior only for the Legendre-Gauss-Lobatto distribution, for almost all the basis functions. On the other hand, a linear convergence behavior as the one that characterize the weak formulation with  $C^0$  boundary conditions can be observed

for the other grid distributions and the accuracy is consequently lower ( $\approx 10^{-4} \div 10^{-5}$  in logarithmic scale).

- Once the machine epsilon is reached, the curves oscillate randomly about this value. Thus, the so-called “Roundoff Plateau” can be easily identified, as illustrated in the book by Boyd [37]. The weak formulation with  $C^0$  boundary conditions could show the same behavior if the number of grid points is increased noticeably.
- The same accuracy is obtained for both the isotropic and composite structures.

For the sake of completeness, the first ten natural frequencies for both the isotropic and laminated plates are shown also in Table 4.1 and Table 4.2, respectively.

**Table 4.1** - Convergence analysis for the first ten natural frequencies [Hz] of a SSSS isotropic square plate. The Lagrange polynomials are employed as basis functions [15].

$f$	$I_N = 11$	$I_N = 15$	$I_N = 21$	$I_N = 25$	$I_N = 31$	Exact [145]
Strong formulation (Cheb-Gau-Lob grid distribution)						
1	466.9278	466.9278	466.9278	466.9278	466.9278	466.9278
2	1113.9183	1113.9347	1113.9347	1113.9347	1113.9347	1113.9347
3	1113.9183	1113.9347	1113.9347	1113.9347	1113.9347	1113.9347
4	1576.8422	1576.8422	1576.8422	1576.8422	1576.8422	1576.8422
5	1576.8422	1576.8422	1576.8422	1576.8422	1576.8422	1576.8422
6	1709.3428	1709.3621	1709.3621	1709.3621	1709.3621	1709.3621
7	2082.1916	2082.6997	2082.7004	2082.7004	2082.7004	2082.7004
8	2082.1916	2082.6997	2082.7004	2082.7004	2082.7004	2082.7004
9	2229.9917	2229.9916	2229.9916	2229.9916	2229.9916	2229.9916
10	2612.4496	2612.8314	2612.8319	2612.8319	2612.8319	2612.8319
Weak formulation $C^1$ (Leg-Gau-Lob grid distribution)						
1	466.9279	466.9278	466.9278	466.9278	466.9278	466.9278
2	1113.8926	1113.9347	1113.9347	1113.9347	1113.9347	1113.9347
3	1113.8926	1113.9347	1113.9347	1113.9347	1113.9347	1113.9347
4	1576.8422	1576.8422	1576.8422	1576.8422	1576.8422	1576.8422
5	1576.8422	1576.8422	1576.8422	1576.8422	1576.8422	1576.8422
6	1709.3138	1709.3621	1709.3621	1709.3621	1709.3621	1709.3621
7	2081.2550	2082.6980	2082.7004	2082.7004	2082.7004	2082.7004
8	2081.2550	2082.6980	2082.7004	2082.7004	2082.7004	2082.7004
9	2229.9918	2229.9916	2229.9916	2229.9916	2229.9916	2229.9916
10	2611.7773	2612.8302	2612.8319	2612.8319	2612.8319	2612.8319
Weak formulation $C^0$ (Cheb III grid distribution)						
1	466.9962	466.9626	466.9449	466.9396	466.9354	466.9278
2	1114.2696	1114.1095	1114.0207	1113.9945	1113.9730	1113.9347
3	1114.2696	1114.1095	1114.0207	1113.9945	1113.9730	1113.9347
4	1584.8338	1580.8933	1578.8201	1578.2143	1577.7196	1576.8422
5	1584.8338	1580.8933	1578.8201	1578.2143	1577.7196	1576.8422
6	1710.0687	1709.7338	1709.5447	1709.4890	1709.4433	1709.3621
7	2083.8990	2083.2224	2082.9554	2082.8775	2082.8137	2082.7004
8	2083.8992	2083.2224	2082.9554	2082.8775	2082.8137	2082.7004
9	2252.7772	2241.4944	2235.5965	2233.8775	2232.4752	2229.9916
10	2614.6673	2613.5847	2613.1996	2613.0873	2612.9953	2612.8319

**Table 4.2** - Convergence analysis for the first ten natural frequencies [Hz] of a SSSS laminated square plate. The Lagrange polynomials are employed as basis functions [15].

$f$	$I_N = 11$	$I_N = 15$	$I_N = 21$	$I_N = 25$	$I_N = 31$	Exact [145]
Strong formulation (Cheb-Gau-Lob grid distribution)						
1	465.8828	465.8828	465.8828	465.8828	465.8828	465.8828
2	869.9711	869.9811	869.9811	869.9811	869.9811	869.9811
3	1106.4077	1106.4077	1106.4077	1106.4077	1106.4077	1106.4077
4	1106.4077	1106.4077	1106.4077	1106.4077	1106.4077	1106.4077
5	1312.0560	1312.0604	1312.0604	1312.0604	1312.0604	1312.0604
6	1550.5355	1550.5443	1550.5443	1550.5443	1550.5443	1550.5443
7	1565.8220	1566.1922	1566.1927	1566.1927	1566.1927	1566.1927
8	2065.4520	2065.7236	2065.7240	2065.7240	2065.7240	2065.7240
9	2212.8145	2212.8153	2212.8153	2212.8153	2212.8153	2212.8153
10	2212.8145	2212.8153	2212.8153	2212.8153	2212.8153	2212.8153
Weak formulation $C^1$ (Leg-Gau-Lob grid distribution)						
1	465.8828	465.8828	465.8828	465.8828	465.8828	465.8828
2	869.9555	869.9811	869.9811	869.9811	869.9811	869.9811
3	1106.4077	1106.4077	1106.4077	1106.4077	1106.4077	1106.4077
4	1106.4077	1106.4077	1106.4077	1106.4077	1106.4077	1106.4077
5	1312.0508	1312.0604	1312.0604	1312.0604	1312.0604	1312.0604
6	1550.5234	1550.5443	1550.5443	1550.5443	1550.5443	1550.5443
7	1565.1392	1566.1909	1566.1927	1566.1927	1566.1927	1566.1927
8	2064.9614	2065.7227	2065.7240	2065.7240	2065.7240	2065.7240
9	2212.8153	2212.8153	2212.8153	2212.8153	2212.8153	2212.8153
10	2212.8153	2212.8153	2212.8153	2212.8153	2212.8153	2212.8153
Weak formulation $C^0$ (Cheb III grid distribution)						
1	465.8898	465.8937	465.8908	465.8891	465.8873	465.8828
2	869.5735	869.7744	869.8880	869.9194	869.9438	869.9811
3	1121.8495	1114.8500	1110.7820	1109.5155	1108.4439	1106.4077
4	1121.8507	1114.8504	1110.7821	1109.5155	1108.4439	1106.4077
5	1310.4150	1311.2929	1311.7201	1311.8332	1311.9206	1312.0604
6	1549.1640	1549.8872	1550.2557	1550.3526	1550.4273	1550.5443
7	1563.1132	1565.8444	1566.0617	1566.1103	1566.1463	1566.1927
8	2061.4567	2065.0975	2065.4758	2065.5627	2065.6286	2065.7240
9	2239.4078	2227.8053	2220.7425	2218.4826	2216.5490	2212.8153
10	2239.4539	2227.8190	2220.7461	2218.4845	2216.5498	2212.8153

## 4.2.2 COMPARISON WITH THE FEM

The same simply-supported plate of the previous section is considered also in this paragraph. In particular, two mechanical configurations are investigated: isotropic (one layer made of Aluminum) and laminated (four layers of equal thickness made of Graphite-Epoxy, in which (0/90/0/90) denotes the stacking sequence). The convergence analyses are performed considering five ratios  $h/R$ . As far as the present approach is concerned, both the strong and weak formulations are taken into account. For this purpose, the Lagrange

polynomials are used as basis functions. The grid distributions chosen for these tests are the ones that have provided the best results in the previous applications, which are the Chebyshev-Gauss-Lobatto for the strong formulation, the Legendre-Gauss-Lobatto for the weak formulation with  $C^1$  boundary conditions, and the Chebyshev of third kind for the weak formulation with  $C^0$  boundary conditions. The present solution is obtained in the framework of the Reissner-Mindlin theory.

In this circumstance, the convergence analyses are performed also by means a commercial code that implements the Finite Element Method (FEM). In particular, the software Strand7 is used to this aim [251]. Three kinds of quadrilateral finite elements are employed, respectively with 4 nodes (Quad4), 8 nodes (Quad8), and 9 nodes (Quad9).

In these applications, the convergence behavior of the relative error (4.15) is plotted with respect to the degrees of freedom of each two-dimensional model (dofs), for the first four natural frequencies. The results are presented in graphical form in Figures 4.13-4.17. The following aspects can be observed:

- The strong formulation and the weak formulation with  $C^1$  boundary conditions reach the maximum level of accuracy for a reduced number of dofs. These approaches are both characterized by a geometric convergence, as in the previous applications, for each ratio  $h/R$ . On the other hand, the weak formulation with  $C^0$  boundary conditions shows a linear convergence for each ratio  $h/R$ .
- The accuracy of the present approaches increases for higher-values of thickness. Nevertheless, the proposed method is characterized by an excellent accuracy for both thin and thick structures.
- The present formulations converge more quickly than the FEM, which is characterized by a lower level of accuracy reached in a rather linear manner. In general, a huge number of dofs is required to reach a higher accuracy, if compared to the strong formulation and the weak formulation with  $C^1$  boundary conditions.
- The accuracy of the FEM decreases noticeably for the laminated composite structures. In general, the FEM show a better behavior for thinner plates. This feature is particularly evident for the laminated case.
- In some circumstances, it can be observed that the results provided by the commercial software reach the convergence for a different value from the exact one.

$h/L = 0.005$

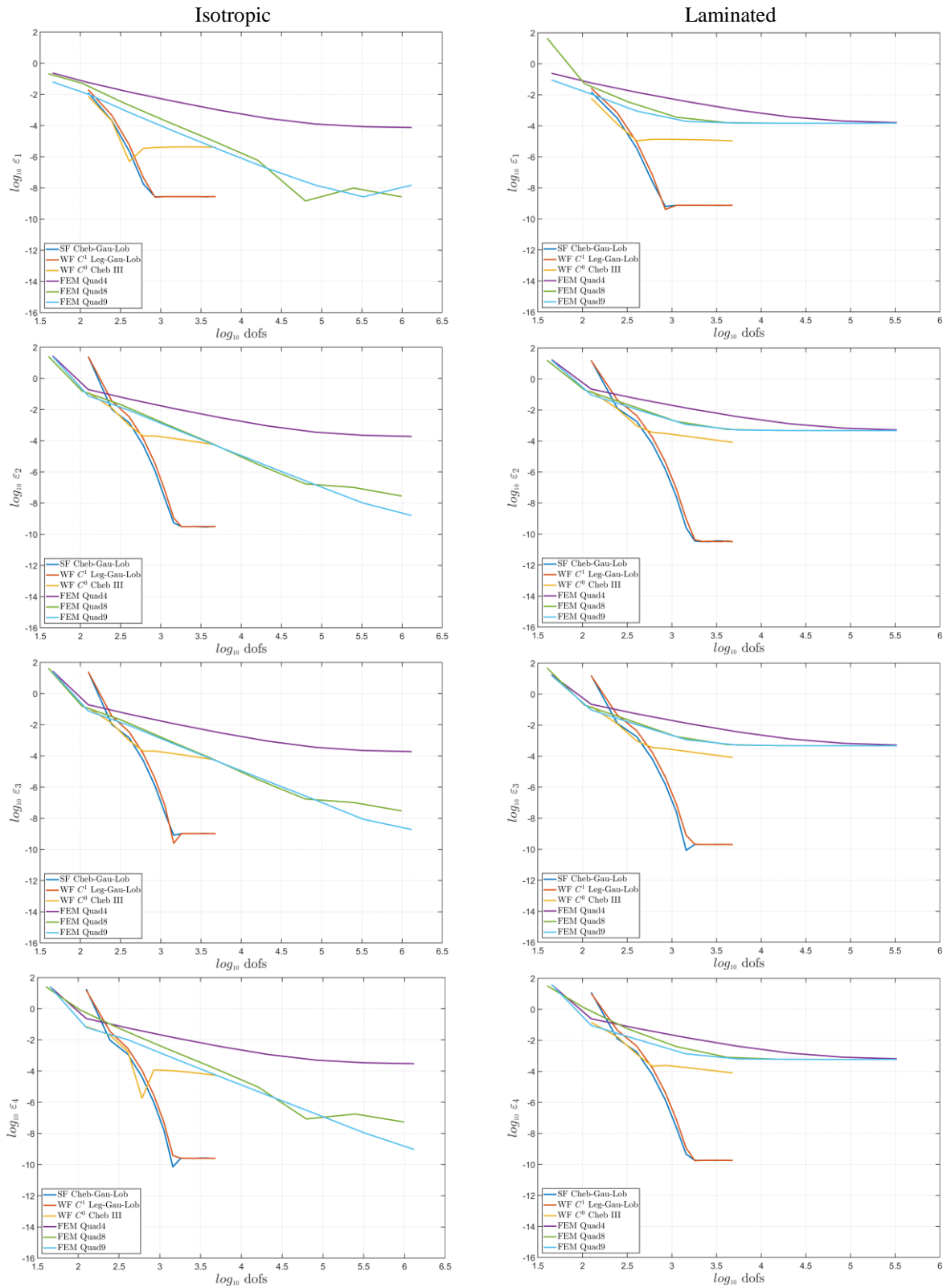


**Figure 4.13** – Convergence behavior of the first four natural frequencies for both isotropic and laminated plates with  $h/L=0.005$  and comparison with the results provided by the FEM (Strand7).

$h/L = 0.01$

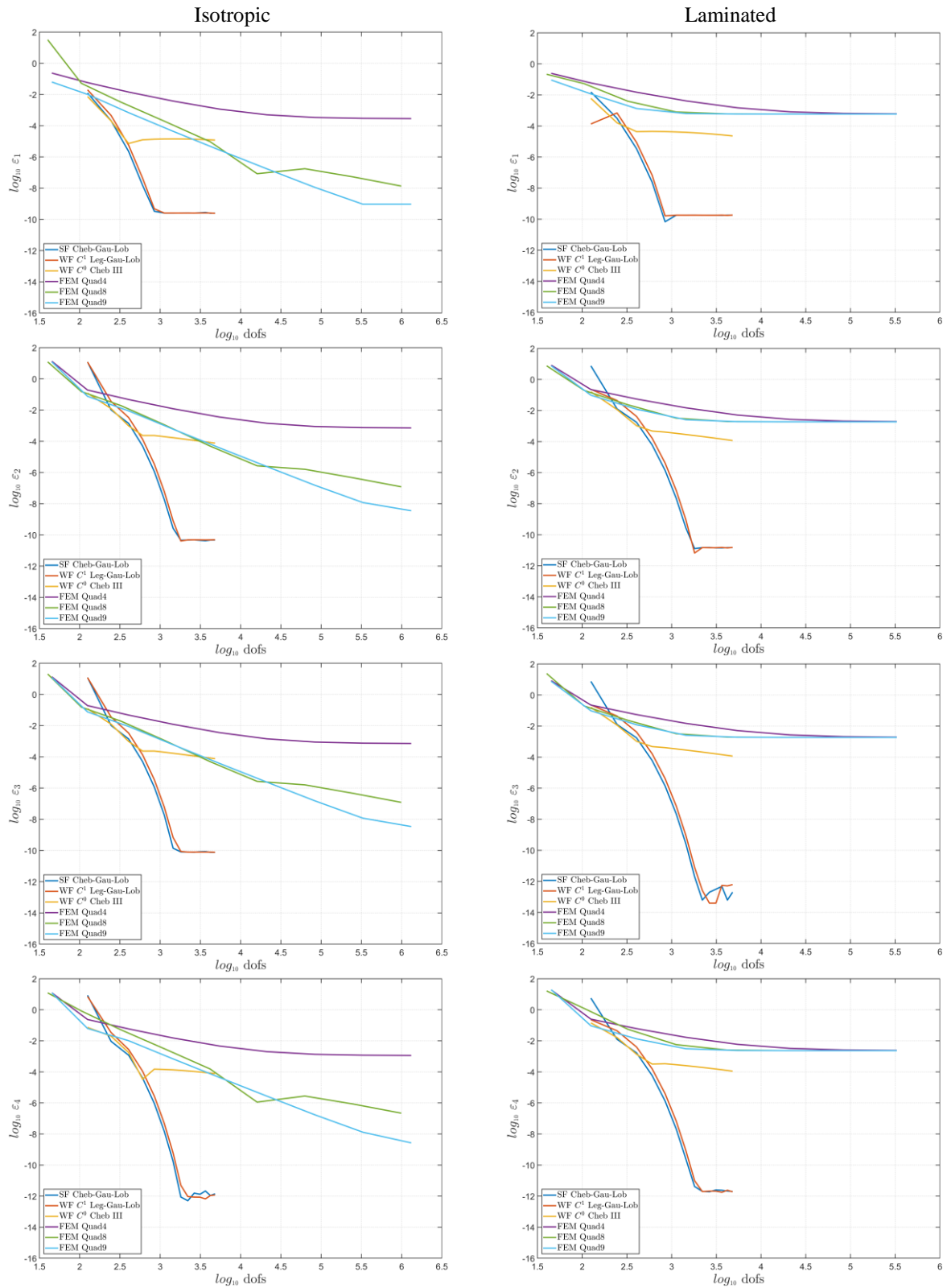


**Figure 4.14** – Convergence behavior of the first four natural frequencies for both isotropic and laminated plates with  $h/L = 0.01$  and comparison with the results provided by the FEM (Strand7).

$h/L = 0.05$

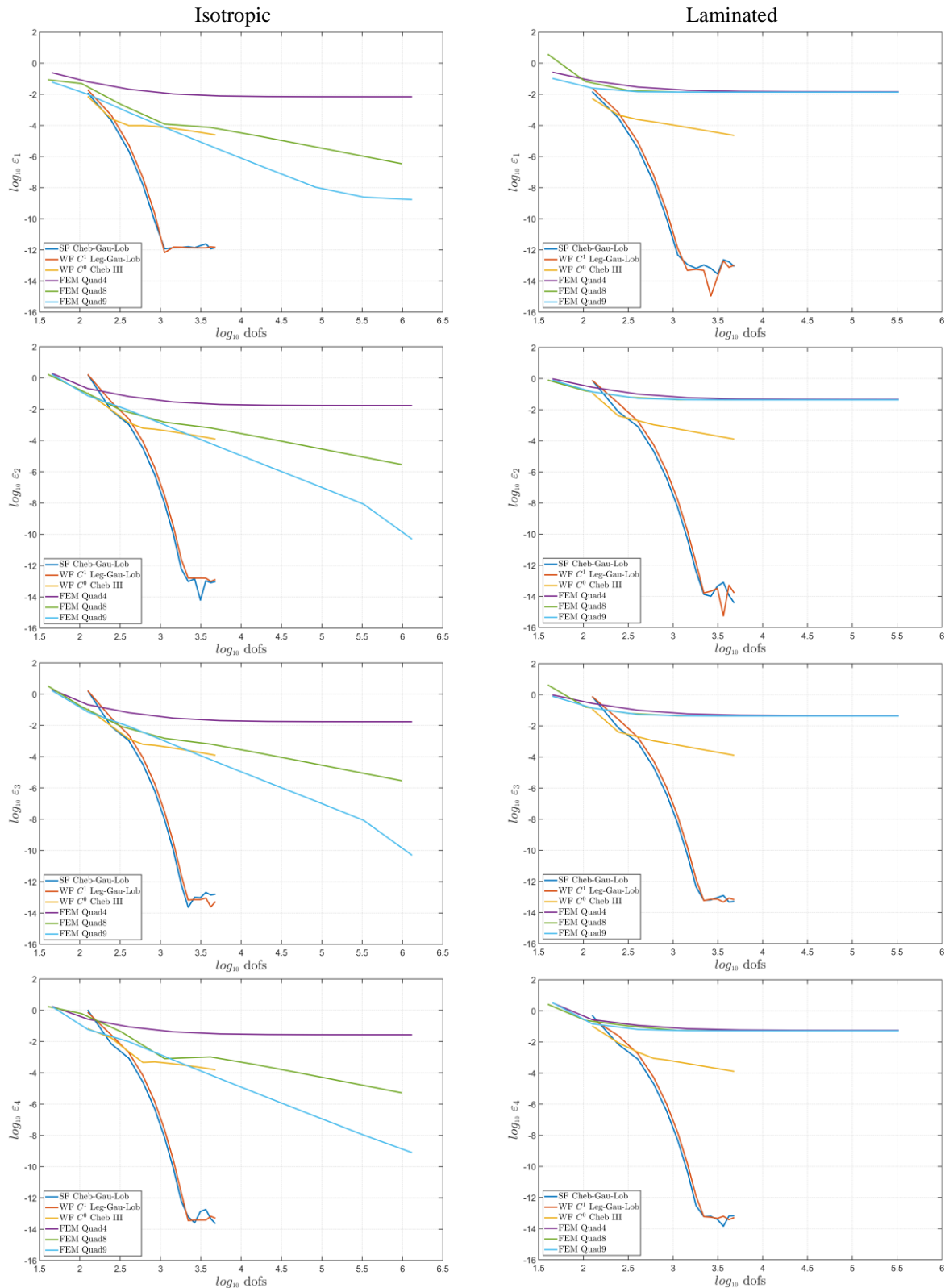


**Figure 4.15** – Convergence behavior of the first four natural frequencies for both isotropic and laminated plates with  $h/L = 0.05$  and comparison with the results provided by the FEM (Strand7).

$h/L = 0.1$

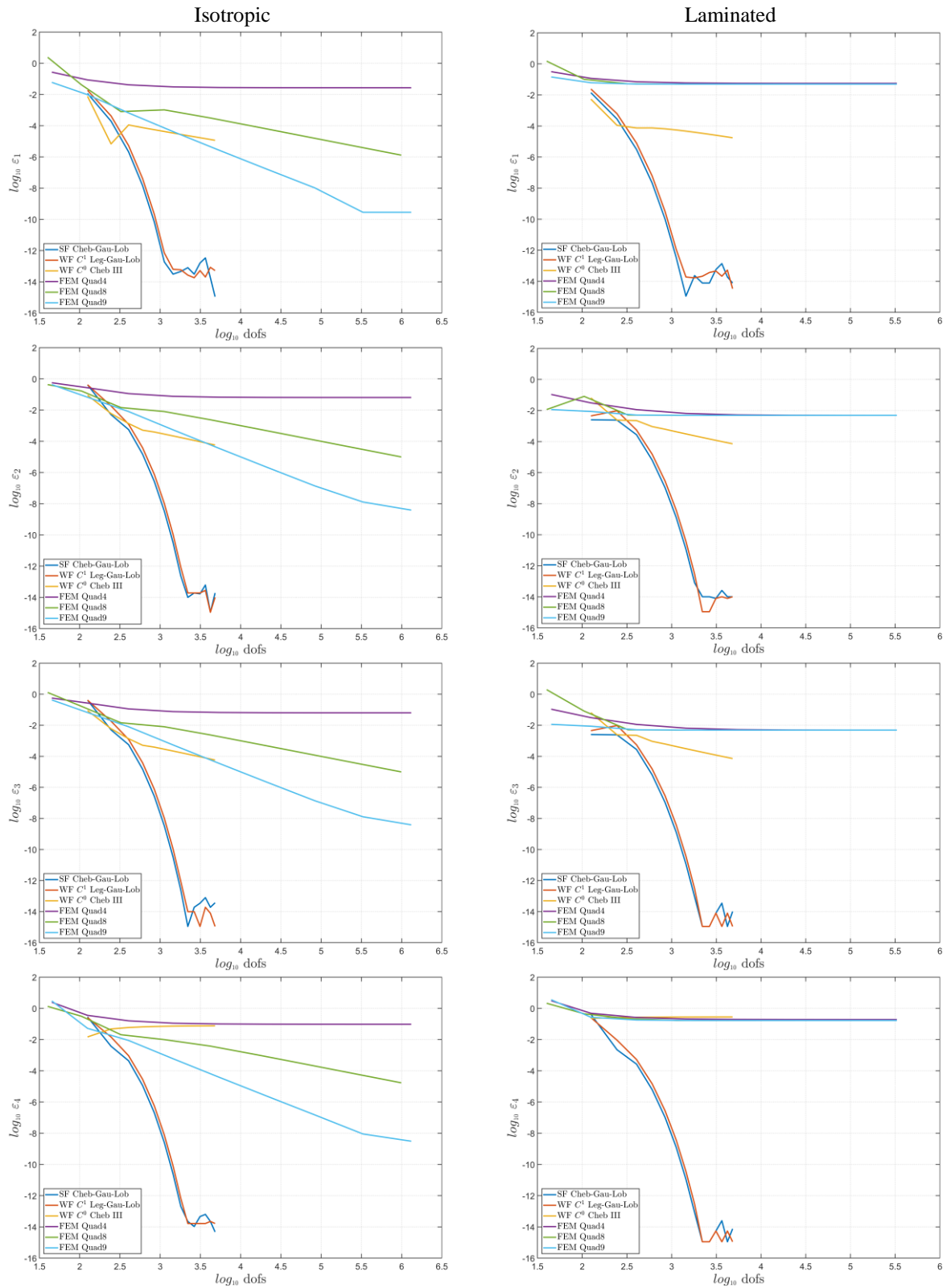


**Figure 4.16** – Convergence behavior of the first four natural frequencies for both isotropic and laminated plates with  $h/L = 0.1$  and comparison with the results provided by the FEM (Strand7).

$h/L = 0.2$

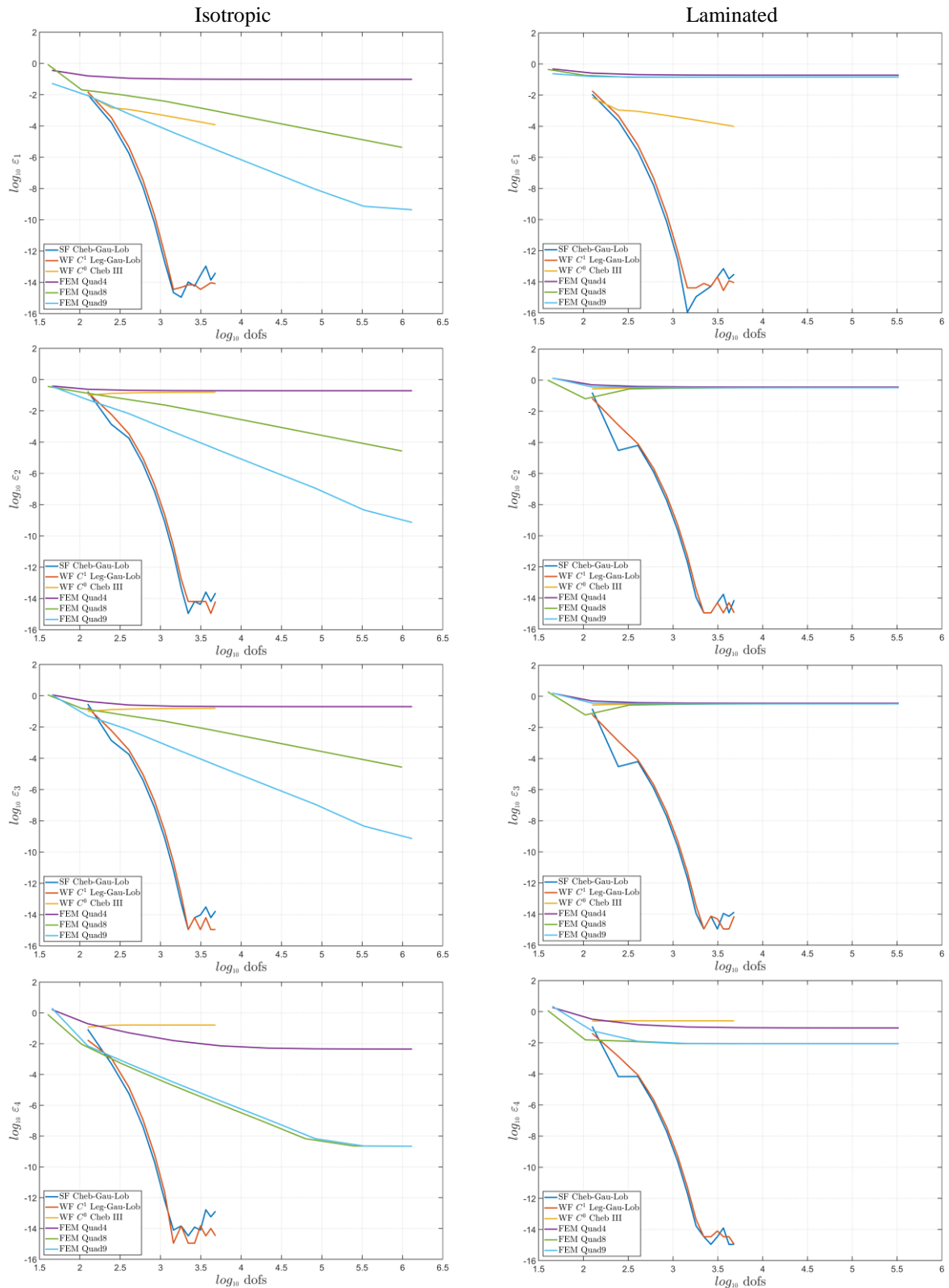


**Figure 4.17** – Convergence behavior of the first four natural frequencies for both isotropic and laminated plates with  $h/L = 0.2$  and comparison with the results provided by the FEM (Strand7).

### 4.2.3 HIGHER-ORDER SHEAR DEFORMATION THEORIES

In the present section, the weak formulation of the governing equations is solved by means of the IQ method to obtain the natural frequencies of several laminated composite shells (Figure 4.18). For this purpose, the Lagrange polynomials are used as basis functions and the Legendre-Gauss-Lobatto grid is employed, since  $C^1$  type of continuity condition is enforced. In the previous sections, in fact, this combination has proven to be the most accurate and stable, as far as the weak formulation is concerned.

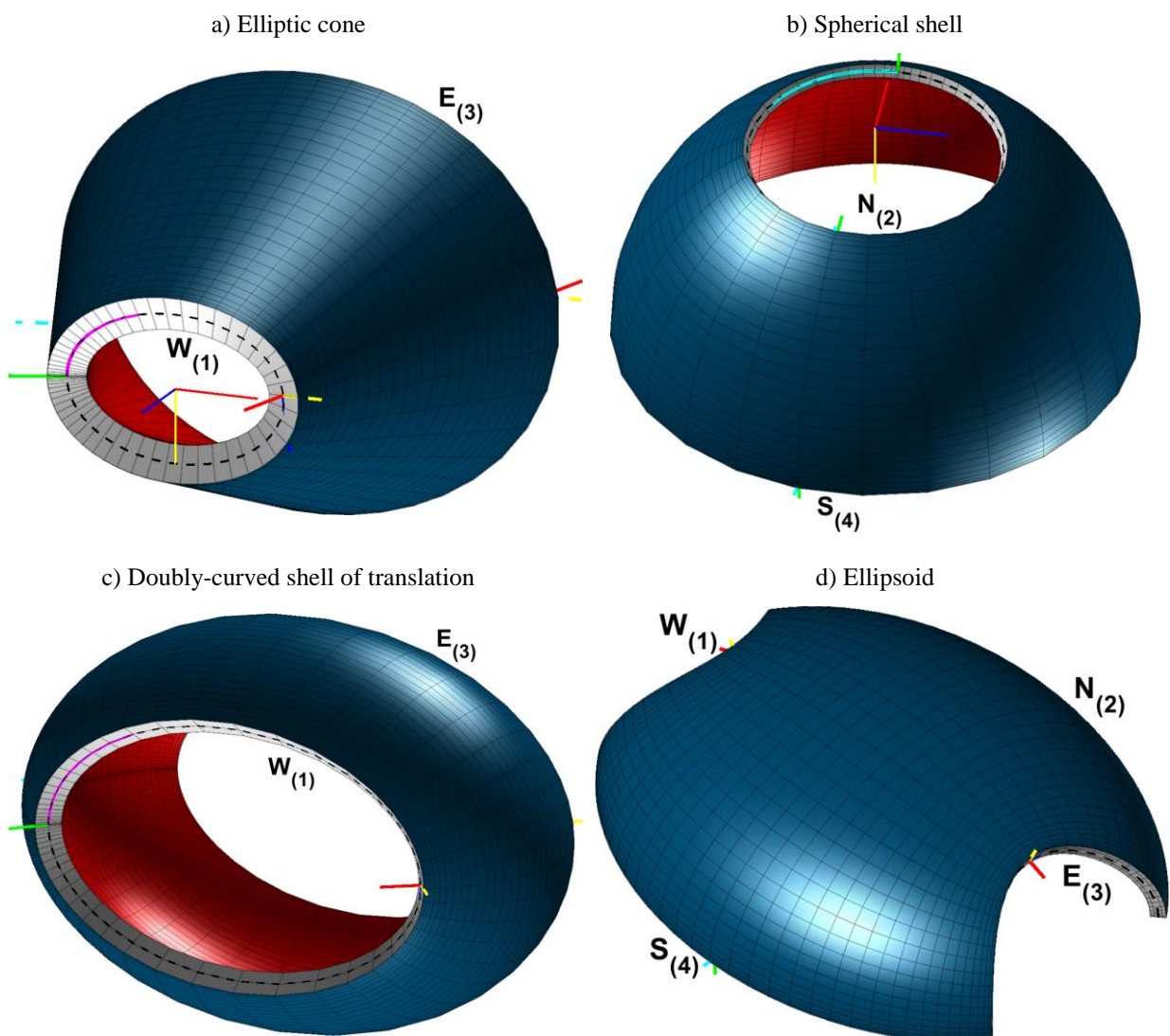


**Figure 4.18** – Laminated composite shells structures: discrete representation and edge identification.

Several HSDTs are considered in this circumstance. In order to prove the reliability of the current numerical approach, the comparison with the solution obtained through a commercial FEM code is performed in each test. The four structures analyzed in this paragraph are an elliptic cone, a spherical shell, a doubly-curved shell of translation (obtained by sliding an elliptic curve along another ellipse), and an ellipsoid. The reference domains of these shells are fully described once the position vectors and the required geometric parameters are specified as in Table 4.3. On the other hand, their first ten natural frequencies are shown in Tables 4.4-4.7, together with the mechanical properties, the stacking sequences, and the number of discrete points  $I_N, I_M$ . It should be specified that considerably higher values of  $I_N, I_M$  are chosen to obtain an extremely accurate description of these curved surfaces. Finally, the first three mode shapes of these structures are depicted in Figure 4.19. The 3D-FEM models are obtained by the commercial code Abaqus [252]. In particular, 20-node brick elements “C3D20” are employed for this purpose.

**Table 4.3** – Position vectors and geometric features of the laminated composite shells considered in the analyses.

a) Elliptic cone
$\mathbf{r}(\alpha_1, y) = (a \cos \alpha_1 + y \sin \alpha \sin \varphi) \mathbf{e}_1 - y \cos \alpha \mathbf{e}_2 + (b \sin \alpha_1 - y \sin \alpha \cos \varphi) \mathbf{e}_3$ $\varphi(\alpha_1) = \arctan \left( -\frac{b \cos \alpha_1}{a \sqrt{1 - \cos^2 \alpha_1}} \right), a = 3 \text{ m}, b = 2 \text{ m}, \alpha_1 \in [0, 2\pi], y \in [0, 10 \text{ m}], \alpha = \pi/9, h = 1 \text{ m}$
b) Spherical shell
$\mathbf{r}(\alpha_1, \alpha_2) = R \sin \alpha_1 \cos \alpha_2 \mathbf{e}_1 - R \sin \alpha_1 \sin \alpha_2 \mathbf{e}_2 + R \cos \alpha_1 \mathbf{e}_3$ $R = 2 \text{ m}, \alpha_1 \in [\pi/6, \pi/2], \alpha_2 \in [0, 2\pi], h = 0.1 \text{ m}, h_1 = h_2 = 0.05 \text{ m}$
c) Doubly-curved shell of translation
$\mathbf{r}(\alpha_1, \alpha_2) = \left( \frac{a^2 \tan \alpha_1}{\sqrt{b^2 + a^2 \tan^2 \alpha_1}} - d \left( 1 - \sqrt{1 - \frac{c^2 \tan^2 \alpha_2}{d^2 + c^2 \tan^2 \alpha_2}} \right) \sin \alpha_1 \right) \mathbf{e}_1 - \frac{c^2 \tan \alpha_2}{\sqrt{d^2 + c^2 \tan^2 \alpha_2}} \mathbf{e}_2 +$ $+ \left( b \left( 1 - \sqrt{1 - \frac{a^2 \tan^2 \alpha_1}{b^2 + a^2 \tan^2 \alpha_1}} \right) + d \left( 1 - \sqrt{1 - \frac{c^2 \tan^2 \alpha_2}{d^2 + c^2 \tan^2 \alpha_2}} \right) \cos \alpha_1 \right) \mathbf{e}_3$ $a = d = 10 \text{ m}, b = c = 7 \text{ m}, \alpha_1 \in [0, 2\pi], \alpha_2 \in [-5\pi/18, 5\pi/18], h = 1 \text{ m}, h_1 = h_2 = 0.5 \text{ m}$
d) Ellipsoid
$\mathbf{r}(\alpha_1, \alpha_2) = \left( \frac{a \sqrt{a^2 - b^2 \sin^2 \alpha_1 - c^2 \cos^2 \alpha_1}}{\sqrt{a^2 - c^2}} \cos \alpha_2 \right) \mathbf{e}_1 + (b \cos \alpha_1 \sin \alpha_2) \mathbf{e}_2 +$ $+ \left( -\frac{c \sqrt{a^2 \sin^2 \alpha_2 + b^2 \cos^2 \alpha_2 - c^2}}{\sqrt{a^2 - c^2}} \sin \alpha_1 \right) \mathbf{e}_3$ $\alpha_1 \in [0, \pi], \alpha_2 \in [\pi/6, 5\pi/6], a = 2 \text{ m}, b = 1.5 \text{ m}, c = 1 \text{ m}, a \geq b \geq c, h_1 = h_3 = 0.025 \text{ m}, h_2 = 0.05 \text{ m}$

**Table 4.4** – First ten natural frequencies [Hz] for a FC orthotropic elliptic cone for various higher-order shear deformation theories.

Lamination scheme: (30)

Mechanical properties:  $E_1 = 137.9$  GPa,  $E_2 = E_3 = 8.96$  GPa,  $G_{12} = G_{13} = 7.1$  GPa,  $G_{23} = 6.21$  GPa,  $\nu_{12} = \nu_{13} = 0.3$ ,  $\nu_{23} = 0.49$ ,  $\rho = 1450$  kg/m<sup>3</sup>

Discrete points:  $I_N = 61, I_M = 31$

$f$	FSDT <sub>RS</sub> <sup><math>\kappa=5/6</math></sup>	TSDT <sub>RS</sub>	ED1 <sup><math>\kappa=5/6</math></sup>	ED2 <sup><math>\kappa=5/6</math></sup>	ED3	ED4	3D-FEM
1	45.497	45.507	45.454	45.341	45.352	45.347	45.345
2	49.718	49.729	49.657	49.485	49.500	49.492	49.493
3	66.060	66.083	67.300	66.931	66.937	66.924	66.917
4	72.416	72.496	73.298	72.354	72.401	72.358	72.330
5	74.457	74.518	75.513	74.703	74.763	74.735	74.721
6	98.657	98.718	98.533	97.995	98.099	98.077	98.080
7	104.622	104.692	104.673	104.035	104.164	104.143	104.140
8	104.831	104.921	105.358	104.688	104.822	104.780	104.780
9	110.578	110.753	111.366	110.255	110.524	110.461	110.460
10	112.652	112.816	113.534	112.418	112.648	112.587	112.580

**Table 4.5** – First ten natural frequencies [Hz] for a FC laminated composite spherical shell cone for various higher-order shear deformation theories.

Lamination scheme: (30 / 45)

Mechanical properties of the two layers:  $E_1 = 137.9$  GPa,  $E_2 = E_3 = 8.96$  GPa,  $G_{12} = G_{13} = 7.1$  GPa,  $G_{23} = 6.21$  GPa,  $\nu_{12} = \nu_{13} = 0.3$ ,  $\nu_{23} = 0.49$ ,  $\rho = 1450$  kg/m<sup>3</sup>

Discrete points:  $I_N = 31, I_M = 41$

$f$	FSDT <sub>RS</sub> <sup><math>\kappa=5/6</math></sup>	TSDT <sub>RS</sub>	ED1 <sup><math>\kappa=5/6</math></sup>	ED2 <sup><math>\kappa=5/6</math></sup>	ED3	ED4
1	43.217	43.520	43.256	42.835	43.059	42.847
2	43.217	43.520	43.256	42.835	43.059	42.847
3	60.488	60.650	61.757	60.553	60.649	60.522
4	60.488	60.650	61.757	60.553	60.649	60.522
5	82.659	82.832	82.849	82.507	82.697	82.560
6	82.659	82.832	82.849	82.507	82.697	82.560
7	98.842	98.926	102.016	99.179	99.235	99.140
8	98.842	98.926	102.016	99.179	99.235	99.140
9	143.816	143.846	149.499	144.281	144.339	144.249
10	143.816	143.846	149.499	144.281	144.339	144.249

$f$	FSDTZ <sub>RS</sub> <sup><math>\kappa=5/6</math></sup>	TSDTZ <sub>RS</sub>	EDZ1 <sup><math>\kappa=5/6</math></sup>	EDZ2 <sup><math>\kappa=5/6</math></sup>	EDZ3	3D-FEM
1	43.208	43.208	42.951	42.810	42.968	42.922
2	43.208	43.208	42.951	42.810	42.968	42.922
3	60.460	60.460	60.864	60.538	60.592	60.564
4	60.460	60.460	60.864	60.538	60.592	60.564
5	82.651	82.651	82.600	82.488	82.639	82.584
6	82.651	82.651	82.600	82.488	82.639	82.584
7	98.786	98.786	99.907	99.165	99.190	99.168
8	98.786	98.786	99.907	99.165	99.190	99.168
9	143.724	143.724	145.621	144.262	144.295	144.280
10	143.724	143.724	145.621	144.262	144.295	144.280

**Table 4.6** – First ten natural frequencies [Hz] for a FC laminated composite doubly-curved shell of translation for various higher-order shear deformation theories.

Lamination scheme: (30 / 45)						
Mechanical properties of the two layers: $E_1 = 137.9$ GPa , $E_2 = E_3 = 8.96$ GPa , $G_{12} = G_{13} = 7.1$ GPa , $G_{23} = 6.21$ GPa , $\nu_{12} = \nu_{13} = 0.3$ , $\nu_{23} = 0.49$ , $\rho = 1450$ kg/m <sup>3</sup>						
Discrete points: $I_N = 31, I_M = 61$						
$f$	FSDT <sub>RS</sub> <sup><math>\kappa=5/6</math></sup>	TSDT <sub>RS</sub>	ED1 <sup><math>\kappa=5/6</math></sup>	ED2 <sup><math>\kappa=5/6</math></sup>	ED3	ED4
1	21.808	21.821	22.134	21.798	21.826	21.833
2	22.323	22.347	22.388	22.186	22.207	22.214
3	22.576	22.589	22.883	22.557	22.584	22.590
4	33.055	33.089	33.013	32.824	32.857	32.852
5	43.251	43.287	43.622	43.053	43.109	43.065
6	44.870	44.874	45.932	44.957	45.027	45.006
7	45.641	45.641	46.774	45.754	45.832	45.817
8	52.459	52.489	52.837	52.251	52.308	52.272
9	54.176	54.186	54.694	54.570	54.571	54.561
10	64.235	64.258	64.290	64.001	64.039	64.012
$f$	FSDTZ <sub>RS</sub> <sup><math>\kappa=5/6</math></sup>	TSDTZ <sub>RS</sub>	EDZ1 <sup><math>\kappa=5/6</math></sup>	EDZ2 <sup><math>\kappa=5/6</math></sup>	EDZ3	3D-FEM
1	21.795	21.806	21.886	21.797	21.827	21.811
2	22.320	22.364	22.237	22.185	22.209	22.205
3	22.563	22.580	22.642	22.556	22.585	22.566
4	33.052	33.098	32.872	32.820	32.854	32.854
5	43.244	43.318	43.189	43.045	43.090	43.085
6	44.832	44.893	45.214	44.952	45.015	44.986
7	45.595	45.636	46.024	45.749	45.822	45.783
8	52.445	52.520	52.394	52.246	52.292	52.263
9	54.173	54.187	54.602	54.567	54.567	54.561
10	64.230	64.271	64.069	63.995	64.027	64.006

**Table 4.7** – First ten natural frequencies [Hz] for a FCFC sandwich ellipsoid with an inner soft-core for various higher-order shear deformation theories.

Lamination scheme: (0 / soft-core / 90)					
Mechanical properties of the two external layers: $E_1 = 53.78$ GPa , $E_2 = E_3 = 17.93$ GPa , $G_{12} = G_{13} = 8.96$ GPa , $G_{23} = 3.45$ GPa , $\nu_{12} = \nu_{13} = 0.25$ , $\nu_{23} = 0.34$ , $\rho = 1900$ kg/m <sup>3</sup>					
Mechanical properties of the soft-core: $E = 0.232$ GPa , $\nu = 0.2$ , $\rho = 320$ kg/m <sup>3</sup>					
Discrete points: $I_N = I_M = 41$					
$f$	FSDTZ <sub>RS</sub> <sup><math>\kappa=1</math></sup>	EDZ2 <sup><math>\kappa=1</math></sup>	EDZ3	EDZ4	3D-FEM
1	118.537	117.850	117.836	117.513	117.388
2	143.202	141.851	141.836	141.412	141.253
3	146.550	145.249	145.219	144.852	144.464
4	190.693	189.694	189.663	189.190	188.798
5	218.885	217.181	217.161	216.478	216.305
6	246.935	246.334	246.311	245.978	245.851
7	250.339	250.124	250.115	249.937	249.844
8	256.981	256.322	256.288	255.655	255.512
9	263.792	262.411	262.387	261.566	261.393
10	285.312	284.283	284.247	283.221	282.904

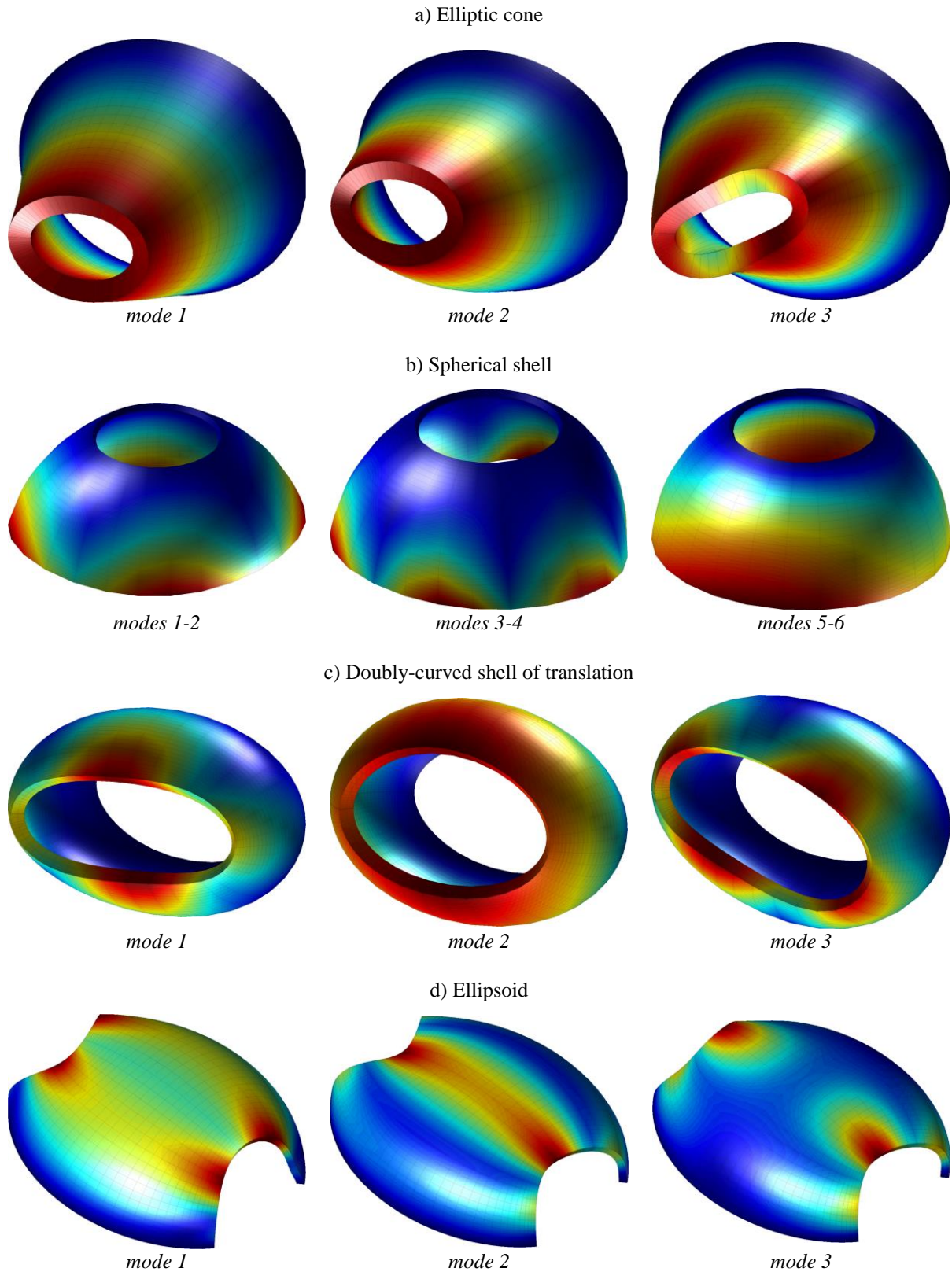


**Figure 4.19** – First three mode shapes of the laminated composite shell structures considered in the present section.

The following aspects should be mentioned for the sake of completeness:

- The Murakami's function is embedded only for laminated structures. In other words, this function is not included in the structural model when the shell is made by one single layer, since there is not any inter-laminar interface to analyze. This is the case of the elliptic cone. On the other hand, only zig-zag theories are employed to investigate the dynamic behavior of sandwich structures with an inner soft-core, as in the case of the ellipsoid.
- In general, an excellent agreement can be noted between the present solutions and the reference ones obtained through a three-dimensional FEM model for all the considered HSDTs. In particular, higher-order models provide closer results to the reference solutions especially if the structure is thicker.
- If sandwich structures with thin and stiffer external sheets are analyzed, the shear correction factor  $\kappa$  for those theories that need it could be neglected, since the difference between the effective shear stress profile and the real one is irrelevant. This aspect has been proven by the results shown in Table 4.7, where the structural theories up to the second order of kinematic expansion are used. This statement could be not true anymore if higher values of thickness characterize the external layers.
- Higher-order theories, such as the ED3, ED4, and their corresponding zig-zag models, should be employed since they are able to provide results in terms of natural frequencies that are extremely closer to the three-dimensional FEM solution. Nevertheless, it should be recalled that the computational time is greater, since the number of degrees of freedom is higher within the shell element.
- The external restraints are well-enforced, as it can be seen from the mode shapes in Figure 4.19. For this purpose, it should be specified that dark blue colors correspond to zero displacements, whereas higher displacements are denoted by reddish colors.
- Finally, the well-known First-order Shear Deformation Theory (FSDT) and Third-order Shear Deformation Theory (TSDT), as well as the corresponding zig-zag models (FSDTZ and TSDTZ), are included in Tables 4.4-4.7 for the sake of completeness.
- All the results presented in this sections are in good agreement with the ones presented in the papers [15, 237], in which the strong formulation is solved.

#### 4.2.4 ARBITRARILY SHAPED DOMAINS

In this section, the weak formulation is solved in order to compute the natural frequencies of various structures characterized by distorted domains. For the sake of conciseness, the plates and shells under consideration are all depicted in Figure 4.20, together with the corresponding mapping domains. All the data required for the isogeometric mapping (knots, weights, and control points) are listed in Figures 4.21-4.24. For brevity purposes, the position vectors and the geometric parameters for the complete description of the corresponding regular domains are listed in Table 4.8.

The numerical values are all collected in Tables 4.9-4.13 for the various structures, together with the data related to the stacking sequences, layer orientations and thicknesses, and mechanical properties. Analogously, the number of grid points is specified, too. As proven in the previous sections, some grid distributions are better than others when the Lagrange polynomials are used as basis functions. In this paragraph, the strong formulation is solved by using the Chebyshev-Gauss-Lobatto grid. As far as the weak formulations are concerned, the Legendre-Gauss-Lobatto and Chebyshev (III kind) are employed respectively for  $C^1$  and  $C^0$  continuity requirements.

**Table 4.8** – Position vectors and geometric features of the regular domains considered in the current section.

a) Rectangular plate
$\mathbf{r}(x, y) = x \mathbf{e}_1 + y \mathbf{e}_2$
b) Doubly-curved panel of translation
$\mathbf{r}(\alpha_1, \alpha_2) = (2 \tan(\alpha_1) - \sin(\alpha_2) \tan^2(\alpha_2)) \mathbf{e}_1 - 2 \tan(\alpha_2) \mathbf{e}_2 + (\tan^2(\alpha_1) \cos(\alpha_1) \tan^2(\alpha_2)) \mathbf{e}_3$ $\alpha_1 \in [-\pi/4, \pi/4], \alpha_2 \in [-\pi/4, \pi/4], h = 0.05 \text{ m}$
c) Catenoidal shell
$\mathbf{r}(\alpha_1, \vartheta) = a \cosh\left(\frac{\alpha_1}{a}\right) \cos \vartheta \mathbf{e}_1 - a \cosh\left(\frac{\alpha_1}{a}\right) \sin \vartheta \mathbf{e}_2 + a \sinh \alpha_1 \mathbf{e}_3$ $\alpha_1 \in [-\pi/3, \pi/3], \vartheta \in [-\pi/3, \pi/3], a = 1 \text{ m}, h = 0.1 \text{ m}$
d) Helicoidal shell
$\mathbf{r}(\alpha_1, \alpha_2) = -a \cos(\alpha_1 + \alpha_2) \sinh(\alpha_1 - \alpha_2) \mathbf{e}_1 - a \sin(\alpha_1 + \alpha_2) \sinh(\alpha_1 - \alpha_2) \mathbf{e}_2 + a(\alpha_1 - \alpha_2) \mathbf{e}_3$ $\alpha_1 \in [0, \pi/2], \alpha_2 \in [0, \pi/2], a = 1 \text{ m}, h = 0.5 \text{ m}$
e) Hyperbolic hyperboloid of revolution
$\mathbf{r}(\alpha_1, \vartheta) = a \cosh \alpha_1 \cos \vartheta \mathbf{e}_1 - a \cosh \alpha_1 \sin \vartheta \mathbf{e}_2 + c \sinh \alpha_1 \mathbf{e}_3$ $\alpha_1 \in [-1, 1], \vartheta \in [0, \pi/2], a = 2 \text{ m}, c = 1.5 \text{ m}, h = 0.06 \text{ m}$

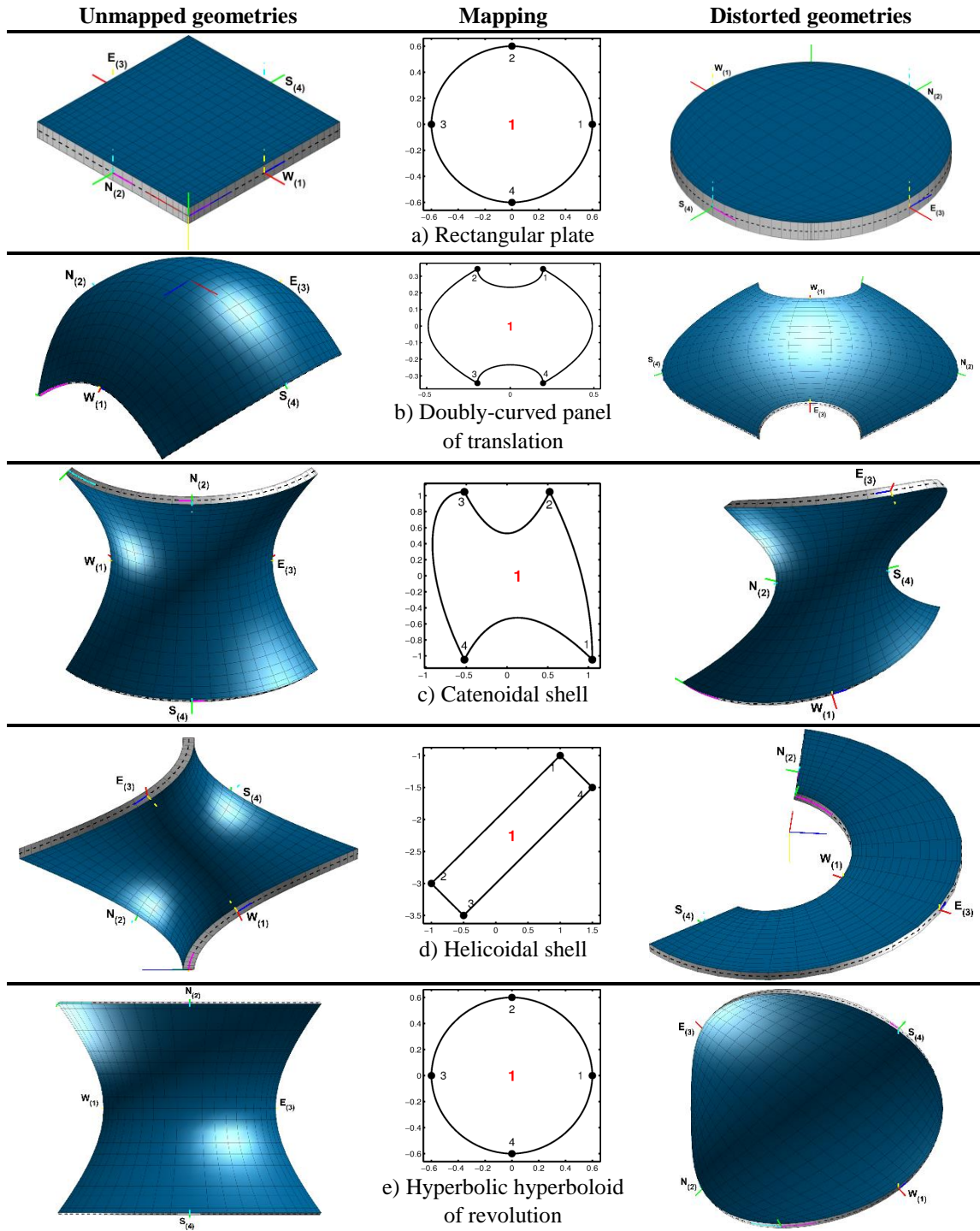
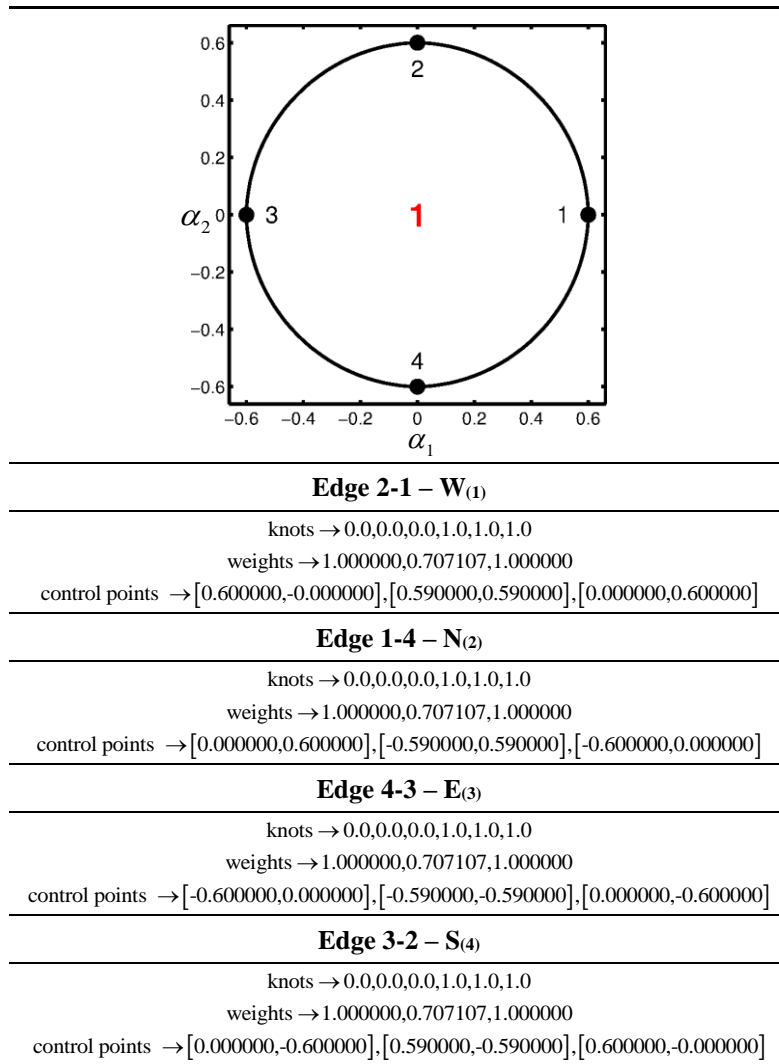


Figure 4.20 - Unmapped and distorted geometries: identification of mapping domains [62].



**Figure 4.21** - Isogeometric data (knots, weights, and control points) for the depicted mapping domain [62].

The first structure is a fully clamped isotropic circular plate of radius  $R$  and thickness  $h$ , which can be obtained by distorting a rectangular plate. A circular mapping domain is used to obtain the rounded plate at issue. It should be recalled that this circular shape is described by means of four circular arches in order to avoid that the determinant of the Jacobian matrix assumes zero values. The numerical results are compared with the ones shown in the book by Liew et al. [96]. For this purpose, the dimensionless frequencies are used

$$\lambda = 2\pi fR^2 \sqrt{\rho h/D} \quad (4.16)$$

where  $D$  is the flexural stiffness given by

$$D = \frac{Eh^3}{12(1-\nu^2)} \quad (4.17)$$

The dimensionless frequencies are presented in Table 4.9 for various ratio of  $h/R$  and several HSDT, by using the Leg-Gau-Lob grid distribution with  $I_N = I_M = 25$  and the Lagrange polynomials as basis functions, since the weak formulation is solved. In general, it can be noted that HSDTs provide results that tend to move away from the reference ones for higher value of thickness, as predictable, since the reference solution is obtained by means of a first-order theory. In this peculiar test, there is no need to label  $C^0$  and  $C^1$  boundary conditions since the fully clamped conditions affect only the generalized displacements.

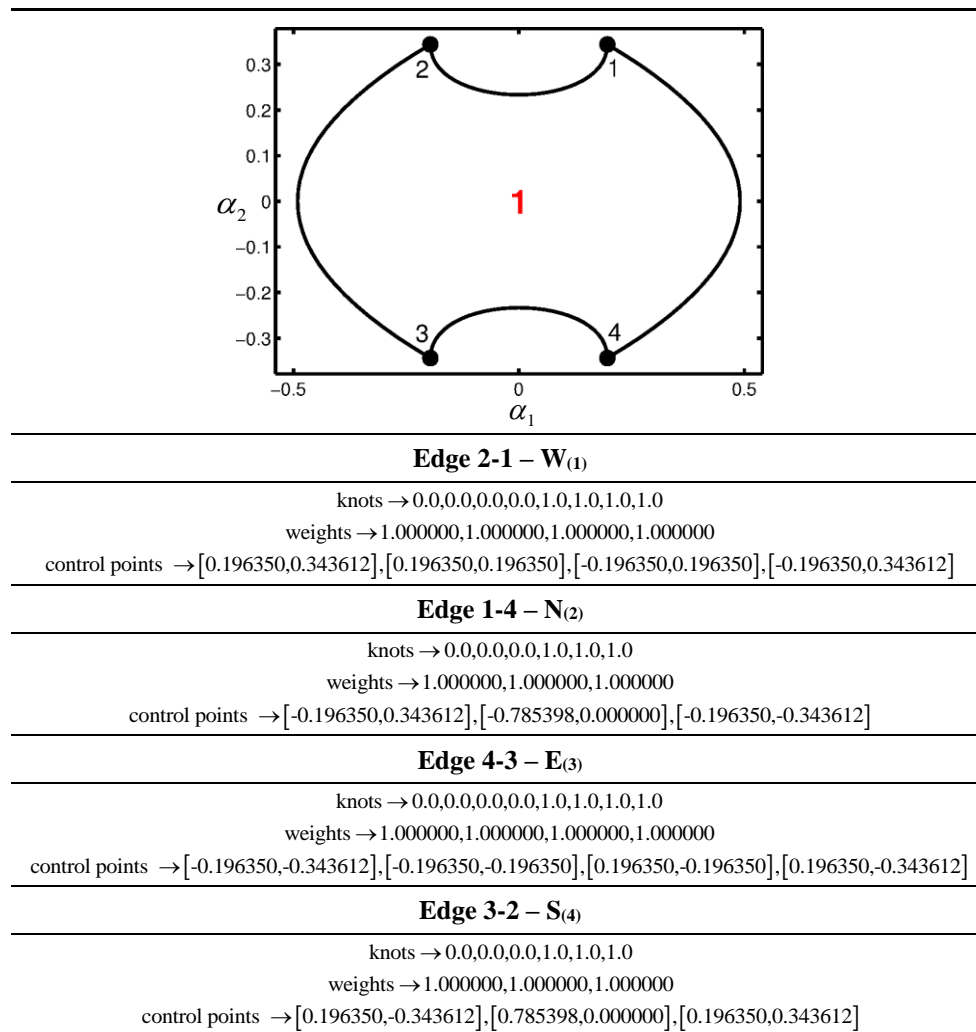
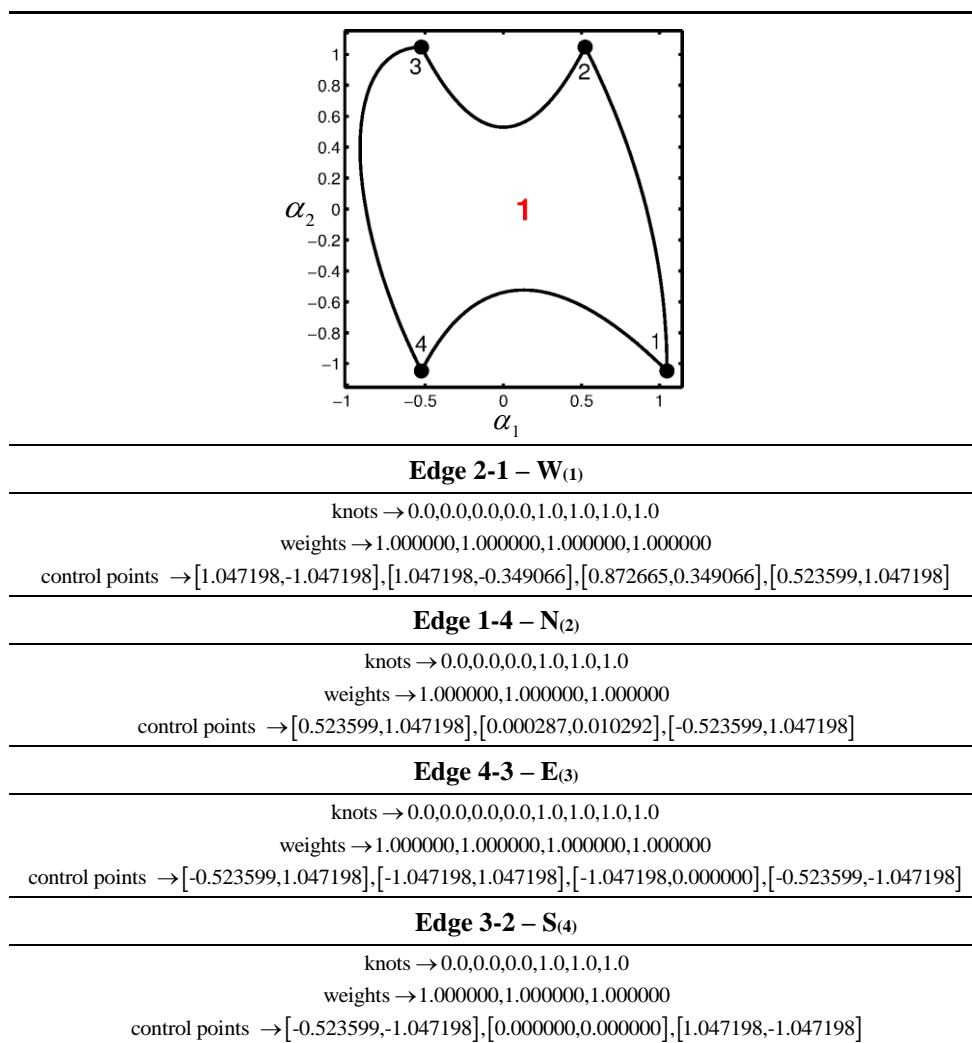


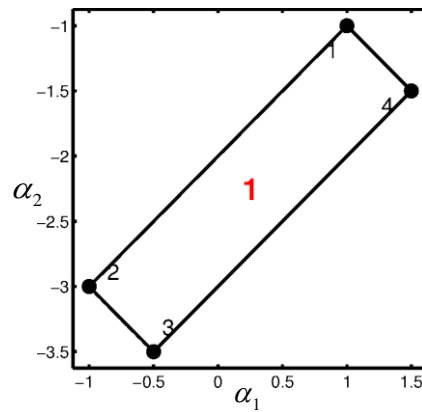
Figure 4.22 - Isogeometric data (knots, weights, and control points) for the depicted mapping domain [62].

A laminated composite CFCF doubly-curved panel of translation is the next structure. The first ten natural frequencies are presented in Table 4.10 for several HSDTs. The analyses are carried out by considering and neglecting the Murakami's function. The same considerations concerning the shear correction factor and the plane stress hypotheses in developing structural theories introduced above are still valid in this circumstance.

For these doubly-curved structure, the dynamic analysis at issue is performed also through a commercial code and the corresponding three-dimensional FEM solutions are presented in the following tables for comparison purposes.



**Figure 4.23** - Isogeometric data (knots, weights, and control points) for the depicted mapping domain [62].



**Edge 2-1 –  $W_{(1)}$**

knots  $\rightarrow$  0.0,0.0,1.0,1.0

weights  $\rightarrow$  1.000000,1.000000

control points  $\rightarrow$  [1.000000,-1.000000],[ -1.000000,-3.000000]

**Edge 1-4 –  $N_{(2)}$**

knots  $\rightarrow$  0.0,0.0,1.0,1.0

weights  $\rightarrow$  1.000000,1.000000

control points  $\rightarrow$  [-1.000000,-3.000000],[ -0.500000,-3.500000]

**Edge 4-3 –  $E_{(3)}$**

knots  $\rightarrow$  0.0,0.0,1.0,1.0

weights  $\rightarrow$  1.000000,1.000000

control points  $\rightarrow$  [-0.500000,-3.500000],[ 1.500000,-1.500000]

**Edge 3-2 –  $S_{(4)}$**

knots  $\rightarrow$  0.0,0.0,1.0,1.0

weights  $\rightarrow$  1.000000,1.000000

control points  $\rightarrow$  [1.500000,-1.500000],[ 1.000000,-1.000000]

**Figure 4.24** - Isogeometric data (knots, weights, and control points) for the depicted mapping domain [62].

Then, a laminated composite FCCF catenoidal shell is considered. The first ten natural frequencies are presented in Table 4.11 for various HSDTs, with and without the Murakami's function. Finally, the last laminated composite structures to be analyzed are a CCFC helicoidal shell and a CFCF hyperbolic hyperboloid of revolution. Their first ten natural frequencies are shown in Table 4.12 and Table 4.13, respectively. In these tables, the three-dimensional FEM solution is also presented, in order to perform the comparison between the current approach (both strong and weak formulations) and the numerical method implemented in the commercial software. Even in these circumstances, the natural frequencies are computed in the framework of several HSDTs.

Finally, the first three mode shapes of these structures characterized by distorted domains are depicted in Figure 4.25.

**Table 4.9** - Comparison of the frequency parameter  $\lambda = 2\pi fR^2\sqrt{\rho h/D}$  of a fully clamped isotropic circular plate of radius  $R$ , for different values of the ratio  $h/R$  and several HSDTs [62].

Mode	FSDT $_{RS}^{\kappa=\pi^2/12}$	ED2 $^{\kappa=\pi^2/12}$	ED3	ED4	Semi-analytical [96]
$h/R = 0.05$					
1	10.270	10.282	10.285	10.284	10.145
2	21.227	21.252	21.265	21.263	21.002
3	34.408	34.449	34.484	34.479	34.258
4	39.322	39.368	39.411	39.406	38.885
5	50.107	50.164	50.235	50.228	49.782
6	59.502	59.570	59.664	59.656	58.827
7	67.707	67.783	67.909	67.898	67.420
8	81.440	81.534	81.709	81.694	80.933
9	86.001	86.098	86.288	86.275	84.995
10	87.350	87.446	87.649	87.635	87.022
$h/R = 0.10$					
1	10.061	10.085	10.099	10.095	9.941
2	20.413	20.460	20.512	20.504	20.232
3	32.448	32.518	32.643	32.628	32.406
4	36.892	36.971	37.125	37.107	36.479
5	46.280	46.371	46.612	46.588	46.178
6	54.442	54.550	54.865	54.835	53.890
7	61.254	61.365	61.765	61.731	61.272
8	72.725	72.859	73.394	73.348	72.368
9	76.473	76.613	77.197	77.148	75.664
10	77.399	77.528	78.137	78.088	77.454
$h/R = 0.20$					
1	9.344	9.384	9.430	9.422	9.240
2	17.944	18.007	18.163	18.143	17.834
3	27.175	27.251	27.576	27.541	27.214
4	30.505	30.591	30.982	30.939	30.211
5	37.104	37.186	37.739	37.684	37.109
6	42.767	42.860	43.559	43.488	42.409
7	47.309	47.391	48.218	48.137	47.340
8	54.785	54.877	55.389	55.389	54.557
9	57.183	57.278	58.416	58.297	56.682
10	57.830	57.911	59.057	58.944	57.793
$h/R = 0.25$					
1	8.902	8.945	9.010	8.999	8.807
2	16.610	16.671	16.873	16.849	16.521
3	24.634	24.701	25.099	25.056	24.670
4	27.501	27.576	28.050	27.997	27.253
5	33.102	33.167	33.814	33.746	33.083
6	37.848	37.920	38.728	38.639	37.550
7	41.694	41.754	42.574	42.565	41.657
8	47.853	47.917	49.095	48.962	47.650
9	49.829	49.895	51.155	51.008	49.420
10	50.458	50.514	51.777	51.636	50.331

**Table 4.10** - First ten natural frequencies of a CFCF laminated doubly-curved panel of translation: comparison between strong and weak formulations [62].

Lamination scheme:  $(0/30/60/90)$ , with  $h_1 = h_2 = h_3 = h_4 = 0.0125\text{m}$   
 Mechanical properties of the four layers:  $E_1 = 137.9\text{ GPa}$ ,  $E_2 = E_3 = 8.96\text{ GPa}$ ,  $G_{12} = G_{13} = 7.1\text{ GPa}$ ,  
 $G_{23} = 6.21\text{ GPa}$ ,  $\nu_{12} = \nu_{13} = 0.3$ ,  $\nu_{23} = 0.49$ ,  $\rho = 1450\text{ kg/m}^3$   
 Discrete points:  $I_N = I_M = 25$   
 3D-FEM solution: 9248 brick elements (Hexa20)

$f$	FSDT $^{\kappa=5/6}_{RS}$	FSDTZ $^{\kappa=5/6}_{RS}$	ED2 $^{\kappa=5/6}$	EDZ2 $^{\kappa=5/6}$	ED3	EDZ3	ED4	EDZ4	3D-FEM
Strong formulation									
1	115.344	115.336	115.134	115.075	115.097	115.049	115.023	115.025	113.816
2	122.363	122.356	122.202	122.148	122.026	121.961	121.715	121.685	120.808
3	194.663	194.644	194.222	194.141	194.214	194.062	193.746	193.774	193.623
4	195.735	195.714	195.270	195.190	195.351	195.253	195.159	195.132	194.692
5	353.994	353.963	352.843	352.686	353.075	352.930	352.783	352.777	350.881
6	355.402	355.374	354.285	354.134	354.281	354.103	353.619	353.581	352.397
7	507.682	507.628	506.096	505.916	506.413	506.234	505.955	505.990	505.891
8	510.368	510.316	508.780	508.594	509.233	509.103	508.731	508.655	508.220
9	536.196	536.175	534.527	534.257	534.935	534.605	533.792	533.738	534.428
10	543.263	543.240	541.466	541.207	541.911	541.765	541.305	541.172	540.991
Weak formulation $C^1$									
1	115.916	115.899	115.302	115.237	115.213	115.173	116.115	116.212	113.816
2	122.155	122.140	121.684	121.616	121.744	121.747	122.184	122.225	120.808
3	194.165	194.136	193.449	193.364	193.425	193.373	193.516	193.448	193.623
4	196.277	196.235	195.415	195.406	195.854	195.395	195.864	195.684	194.692
5	353.920	353.857	352.402	352.277	353.407	353.282	353.648	353.575	350.881
6	355.113	355.074	353.751	353.590	354.083	353.937	354.695	354.763	352.397
7	507.457	507.382	505.614	505.426	506.269	505.939	505.544	505.498	505.891
8	509.924	509.852	508.126	508.008	509.064	508.433	507.802	507.583	508.220
9	536.163	536.133	534.208	533.960	534.567	534.140	533.520	533.532	534.428
10	542.467	542.430	540.408	540.172	540.811	540.707	541.451	541.512	540.991
Weak formulation $C^0$									
1	115.806	115.795	115.583	115.522	115.553	115.493	115.389	115.379	113.816
2	122.809	122.803	122.652	122.593	122.628	122.570	122.466	122.455	120.808
3	195.416	195.395	194.966	194.886	195.092	195.010	194.857	194.845	193.623
4	196.492	196.470	196.036	195.953	196.168	196.085	195.926	195.916	194.692
5	355.348	355.317	354.196	354.036	354.400	354.246	353.931	353.905	350.881
6	356.718	356.688	355.605	355.451	355.806	355.657	355.350	355.325	352.397
7	509.441	509.389	507.816	507.636	508.175	507.987	507.620	507.600	505.891
8	512.044	511.993	510.459	510.266	510.881	510.685	510.300	510.280	508.220
9	537.872	537.850	536.189	535.915	536.715	536.466	535.914	535.875	534.428
10	545.104	545.083	543.281	543.021	543.617	543.377	542.831	542.788	540.991

**Table 4.11** - First ten natural frequencies of a FCCF laminated catenoidal shell: comparison between strong and weak formulations [62].

Lamination scheme: (30/90/45/0/60), with $h_1 = h_2 = h_3 = h_4 = h_5 = 0.02\text{m}$									
Mechanical properties of the five layers: $E_1 = 53.78\text{ GPa}$ , $E_2 = E_3 = 17.93\text{ GPa}$ , $G_{12} = G_{13} = 8.96\text{ GPa}$ , $G_{23} = 3.45\text{ GPa}$ , $\nu_{12} = \nu_{13} = 0.25$ , $\nu_{23} = 0.34$ , $\rho = 1900\text{ kg/m}^3$									
Discrete points: $I_N = I_M = 25$									
3D-FEM solution: 11560 brick elements (Hexa20)									
$f$	FSDT $_{RS}^{\kappa=5/6}$	FSDT $_{RS}^{\kappa=5/6}$	ED2 $^{\kappa=5/6}$	EDZ2 $^{\kappa=5/6}$	ED3	EDZ3	ED4	EDZ4	3D-FEM
Strong formulation									3D-FEM
1	23.748	23.724	23.702	23.746	23.762	23.721	23.723	23.595	23.647
2	67.233	67.184	67.220	67.392	67.213	67.174	67.068	67.096	66.770
3	157.332	157.246	157.203	157.667	157.151	156.981	156.906	156.716	156.826
4	209.456	209.278	209.652	210.189	209.540	209.359	209.238	209.055	209.226
5	252.105	251.928	252.264	252.979	252.172	251.851	252.078	251.666	252.229
6	311.889	311.653	311.904	313.266	312.286	311.683	311.361	310.696	310.430
7	333.264	332.793	333.527	334.491	333.372	332.904	332.858	332.390	330.493
8	421.973	421.535	421.984	424.873	422.404	421.204	421.268	420.298	419.796
9	466.474	465.711	466.414	469.230	466.737	465.505	465.045	464.196	459.875
10	478.981	478.423	479.221	480.280	479.018	478.455	478.740	477.962	477.461
Weak formulation $C^1$									3D-FEM
1	23.536	23.455	23.187	23.277	23.558	23.419	23.255	23.297	23.647
2	67.035	66.936	67.435	67.441	66.864	67.039	66.537	66.895	66.770
3	156.778	156.676	156.101	156.133	155.873	155.905	155.620	155.936	156.826
4	208.831	208.635	208.490	208.692	208.581	208.799	207.543	208.506	209.226
5	251.346	251.126	253.226	253.000	251.935	251.838	251.104	251.110	252.229
6	310.989	310.735	310.157	309.666	309.129	308.436	309.180	308.703	310.430
7	331.965	331.394	331.847	331.342	331.649	331.369	330.360	330.386	330.493
8	420.785	420.212	420.718	420.413	421.630	420.472	419.861	419.055	419.796
9	464.318	463.481	464.332	463.560	463.992	462.901	462.090	461.633	459.875
10	478.130	477.530	478.946	478.377	477.609	477.276	477.538	477.219	477.461
Weak formulation $C^0$									3D-FEM
1	23.955	23.937	23.938	23.917	23.942	23.918	23.925	23.902	23.647
2	67.909	67.868	67.874	67.825	67.882	67.798	67.818	67.743	66.770
3	158.936	158.852	158.908	158.805	158.924	158.704	158.737	158.548	156.826
4	211.224	211.062	211.490	211.288	211.458	211.200	211.216	210.973	209.226
5	254.324	254.139	254.445	254.219	254.465	254.135	254.136	253.839	252.229
6	314.776	314.539	314.902	314.613	315.011	314.373	314.486	313.958	310.430
7	335.669	335.206	335.989	335.427	335.927	335.412	335.406	334.883	330.493
8	425.751	425.330	425.799	425.293	426.294	425.073	425.201	424.209	419.796
9	470.734	469.959	470.781	469.860	470.948	469.652	469.711	468.563	459.875
10	482.064	481.502	482.295	481.613	482.253	481.630	481.672	481.033	477.461

**Table 4.12** - First ten natural frequencies of a CCFC laminated helicoidal shell: comparison between strong and weak formulations [62].

Lamination scheme: (0/60/30/90), with $h_1 = h_2 = h_3 = h_4 = 0.125$ m									
Mechanical properties of the four layers: $E_1 = 137.9$ GPa, $E_2 = E_3 = 8.96$ GPa, $G_{12} = G_{13} = 7.1$ GPa, $G_{23} = 6.21$ GPa, $\nu_{12} = \nu_{13} = 0.3$ , $\nu_{23} = 0.49$ , $\rho = 1450$ kg/m <sup>3</sup>									
Discrete points: $I_N = I_M = 25$									
3D-FEM solution: 9600 brick elements (Hexa20)									
$f$	FSDT <sup><math>\kappa=5/6</math></sup> <sub>RS</sub>	FSDTZ <sup><math>\kappa=5/6</math></sup> <sub>RS</sub>	ED2 <sup><math>\kappa=5/6</math></sup>	EDZ2 <sup><math>\kappa=5/6</math></sup>	ED3	EDZ3	ED4	EDZ4	3D-FEM
Strong formulation									
1	13.839	13.838	13.836	13.833	13.792	13.785	13.772	13.769	13.651
2	17.514	17.513	17.504	17.499	17.491	17.485	17.471	17.469	17.358
3	21.274	21.272	21.236	21.228	21.233	21.226	21.203	21.200	21.078
4	26.970	26.967	26.877	26.865	26.865	26.855	26.818	26.814	26.683
5	35.108	35.102	34.947	34.928	34.909	34.893	34.838	34.833	34.690
6	45.444	45.434	45.201	45.174	45.120	45.097	45.020	45.013	44.853
7	52.645	52.643	52.638	52.615	52.719	52.696	52.664	52.665	52.694
8	57.670	57.655	57.335	57.298	57.195	57.162	57.058	57.048	56.876
9	61.473	61.471	61.388	61.351	61.472	61.436	61.377	61.377	61.337
10	71.357	71.337	70.906	70.857	70.681	70.637	70.499	70.485	70.287
Weak formulation C <sup>1</sup>									
1	13.624	13.624	13.611	13.605	13.575	13.559	13.532	13.518	13.651
2	17.356	17.354	17.351	17.343	17.428	17.421	17.370	17.366	17.358
3	21.113	21.109	21.091	21.080	21.290	21.291	21.206	21.211	21.078
4	26.799	26.791	26.731	26.716	27.006	27.015	26.907	26.920	26.683
5	34.923	34.910	34.788	34.769	35.099	35.114	34.988	35.006	34.690
6	45.238	45.218	45.017	44.992	45.329	45.348	45.203	45.225	44.853
7	52.418	52.417	52.420	52.404	52.230	52.220	52.290	52.288	52.694
8	57.441	57.416	57.120	57.086	57.401	57.420	57.253	57.277	56.876
9	61.226	61.225	61.139	61.107	61.002	60.976	60.996	60.996	61.337
10	71.100	71.066	70.649	70.604	70.882	70.898	70.700	70.723	70.287
Weak formulation C <sup>0</sup>									
1	13.735	13.735	13.739	13.764	13.734	13.731	13.727	13.726	13.651
2	17.488	17.487	17.484	17.530	17.482	17.477	17.469	17.468	17.358
3	21.259	21.258	21.229	21.302	21.226	21.219	21.202	21.201	21.078
4	26.978	26.975	26.893	27.009	26.878	26.866	26.835	26.832	26.683
5	35.160	35.154	35.007	35.190	34.962	34.943	34.893	34.888	34.690
6	45.559	45.549	45.324	45.610	45.232	45.205	45.132	45.123	44.853
7	52.769	52.767	52.763	53.125	52.851	52.828	52.786	52.783	52.694
8	57.871	57.857	57.542	57.976	57.389	57.352	57.251	57.239	56.876
9	61.633	61.631	61.549	62.055	61.644	61.608	61.541	61.538	61.337
10	71.660	71.640	71.213	71.847	70.972	70.921	70.786	70.768	70.287

**Table 4.13** - First ten natural frequencies of a CFCF laminated hyperbolic hyperboloid of revolution: comparison between strong and weak formulations [62].

Lamination scheme: (30/60/45), with $h_1 = h_2 = h_3 = 0.02\text{m}$									
Mechanical properties of the four layers: $E_1 = 53.78\text{ GPa}$ , $E_2 = E_3 = 17.93\text{ GPa}$ , $G_{12} = G_{13} = 8.96\text{ GPa}$ , $G_{23} = 3.45\text{ GPa}$ , $\nu_{12} = \nu_{13} = 0.25$ , $\nu_{23} = 0.34$ , $\rho = 1900\text{ kg/m}^3$									
Discrete points: $I_N = I_M = 25$									
3D-FEM solution: 9600 brick elements (Hexa20)									
$f$	FSDT $^{\kappa=5/6}_{RS}$	FSDT $^{\kappa=5/6}_{RS}$	ED2 $^{\kappa=5/6}$	EDZ2 $^{\kappa=5/6}$	ED3	EDZ3	ED4	EDZ4	3D-FEM
Strong formulation									
1	117.344	116.920	117.357	116.966	117.451	117.382	117.488	117.391	117.611
2	119.739	119.303	119.805	119.375	119.916	119.842	119.755	119.760	119.885
3	190.841	189.786	190.891	189.914	190.954	190.797	190.972	190.787	190.430
4	282.808	281.944	282.942	282.107	283.126	282.970	282.991	282.931	282.523
5	307.619	306.670	307.817	306.919	307.873	307.717	307.858	307.716	306.351
6	316.896	316.386	317.204	316.698	317.212	317.118	317.090	317.052	320.576
7	336.360	335.576	336.318	335.656	336.616	336.474	336.902	336.599	338.516
8	385.248	383.804	385.382	384.039	385.304	385.119	385.310	385.116	384.804
9	432.707	430.685	432.749	430.877	433.048	432.715	433.051	432.689	432.212
10	436.528	435.213	436.792	435.546	436.715	436.515	436.604	436.428	436.969
Weak formulation $C^1$									
1	115.432	115.041	115.384	115.722	115.554	115.508	115.660	115.553	117.611
2	118.655	118.159	118.870	119.077	118.851	118.841	118.064	118.539	119.885
3	190.213	189.137	190.141	190.667	190.318	190.159	190.589	190.184	190.430
4	281.811	281.018	281.962	282.489	282.128	282.031	282.000	282.428	282.523
5	306.475	305.543	306.698	306.985	306.719	306.574	306.508	306.757	306.351
6	316.112	315.624	316.718	316.748	316.509	316.429	315.805	316.172	320.576
7	335.728	334.854	334.839	335.940	335.689	335.553	338.096	336.550	338.516
8	384.910	383.445	384.944	385.295	384.935	384.754	385.086	384.928	384.804
9	431.797	429.817	431.711	432.971	432.214	431.894	432.526	431.922	432.212
10	436.289	434.951	436.659	436.938	436.457	436.210	436.179	435.915	436.969
Weak formulation $C^0$									
1	116.142	115.745	116.167	115.793	116.275	116.204	116.258	116.190	117.611
2	118.474	118.076	118.506	118.131	118.623	118.552	118.607	118.537	119.885
3	190.120	189.077	190.187	189.206	190.238	190.080	190.210	190.055	190.430
4	282.448	281.627	282.545	281.776	282.746	282.598	282.709	282.563	282.523
5	307.148	306.222	307.337	306.470	307.396	307.243	307.367	307.216	306.351
6	316.562	316.046	316.825	316.336	316.833	316.750	316.812	316.730	320.576
7	336.561	335.824	336.632	335.950	336.896	336.746	336.845	336.694	338.516
8	385.094	383.652	385.240	383.894	385.164	384.971	385.129	384.940	384.804
9	432.051	430.053	432.112	430.242	432.389	432.049	432.340	432.007	432.212
10	436.863	435.543	437.098	435.860	437.038	436.846	437.000	436.808	436.969

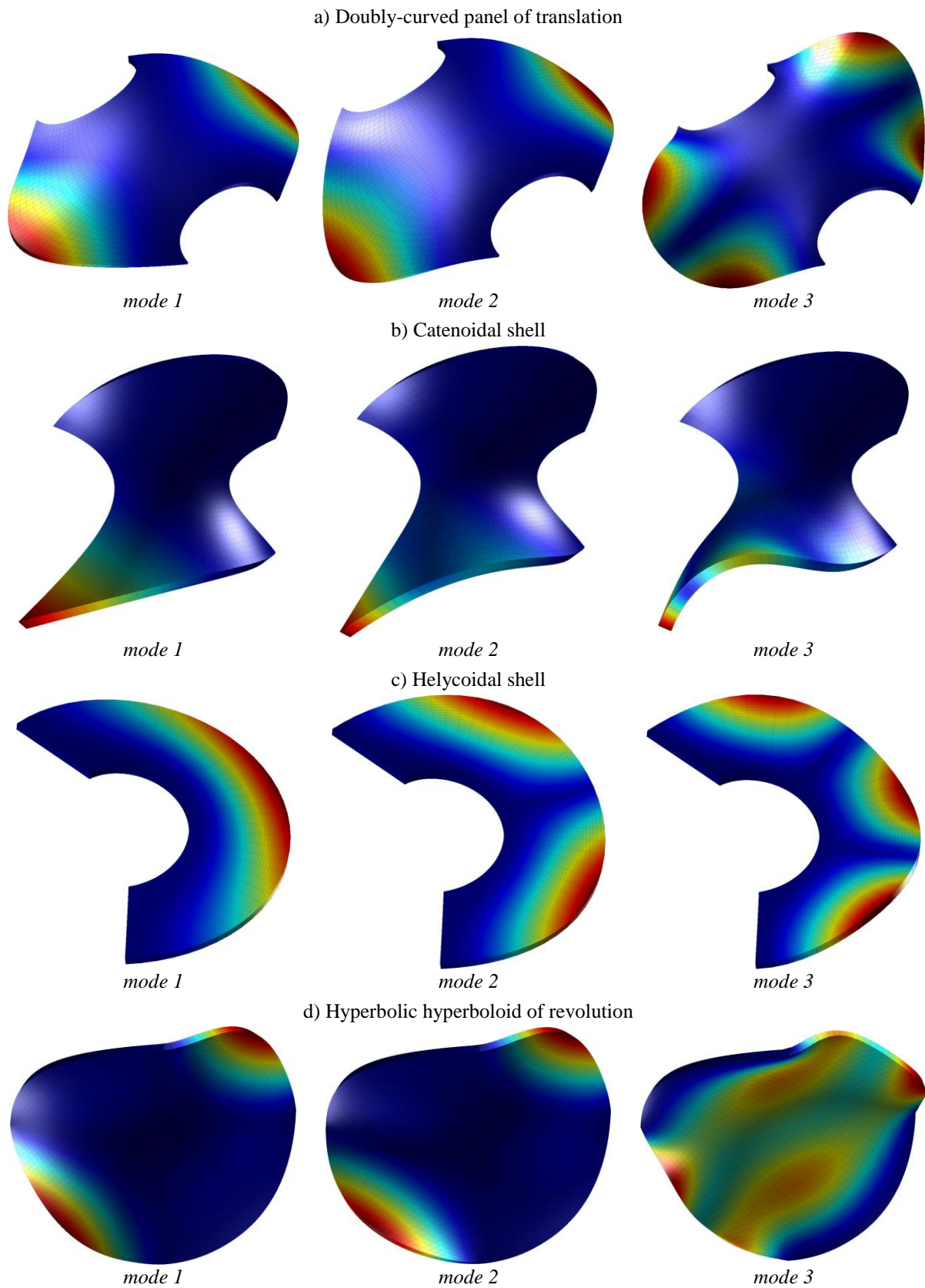


**Figure 4.25** – First three mode shapes of the laminated composite shell structures characterized by distorted domains considered in the present section.

For completeness purposes, the following comments should be mentioned and added to the ones introduced in the previous sections:

- The solutions obtained by means of higher-order models are closer to the 3D-FEM results, especially for thick and moderately thick structures, independently from the chosen formulation.
- If compared to the three-dimensional models, the present two-dimensional approaches are able to get the same results with an extremely lower number of degrees of freedom. A 20-node element model is introduced, in fact, for the 3D-FEM solutions. Thus, there is a huge advantage in terms of computational time. In fact, it should be recalled that the considered structures can be modeled by using one sole element, even if the domain is highly distorted. For the sake of completeness, it should be recalled that the 3D-FEM solutions are accomplished by means of the commercial software Strand7 [251].
- These applications prove that the mapping procedure shown in the previous chapters represents an efficient tool to deal with arbitrarily shaped geometries, for both the strong and weak formulations.
- The boundary conditions are well-enforced even for distorted domains, as it can be easily noted from the mode shapes depicted in Figure 4.25.

Finally, it can be noted that the differences between  $C^1$  and  $C^0$  formulations are negligible for the dynamic analyses performed in this section. This aspect could be different if the static response of shell structures has to be studied. In particular, the stress analysis could provide different results for the  $C^1$  and  $C^0$  formulations if the static behavior of plates or shells with sharpen or curvilinear edges is investigated, especially for thicker configurations.

#### **4.2.5 EFFECT OF CNT AGGLOMERATION**

Finally, the effect of CNT agglomeration on the natural frequencies of a composite shell is investigated. For this purpose, the same structure considered above is analyzed. For the sake of completeness, its geometry is shown in Figure 4.26a. It can be noted that this shell is given by a doubly-curved panel of translation, mapped through the relations described in Figure

4.22. Thus, the geometric features are the same presented in the previous section. In particular, the Legendre-Gauss-Lobatto grid distribution is used with  $I_N = I_M = 25$ .

In this circumstance, the structure is made of three isotropic layers, whose thickness is  $h_1 = h_3 = 0.01\text{m}$  and  $h_2 = 0.01\text{m}$ . The three plies are made of a polymer matrix ( $E^m = 2.5\text{GPa}$ ,  $\nu^m = 0.19$ ,  $\rho^m = 1190\text{kg/m}^3$ ), but only the two external skins are reinforced by CNTs. The reinforcing particles, whose density is  $\rho^r = 1400\text{kg/m}^3$ , are characterized by the following Hill's elastic moduli:  $k_r = 271\text{GPa}$ ,  $l_r = 88\text{GPa}$ ,  $m_r = 17\text{GPa}$ ,  $n_r = 1089\text{GPa}$ , and  $p_r = 442\text{GPa}$ . A five-parameter power law is used to describe the through-the-thickness distribution of CNTs in the two external layers, assuming  $a^{(1)} = a^{(3)} = 1$  and  $p^{(1)} = p^{(3)} = 0.5$ . For the sake of completeness, the distribution in hand is depicted in graphical form in Figure Figure 4.26b. Several values of the mass fraction of CNTs  $w_r$  are considered in the analysis, by assuming different combinations of the agglomeration parameters  $\mu_1, \mu_2$ .

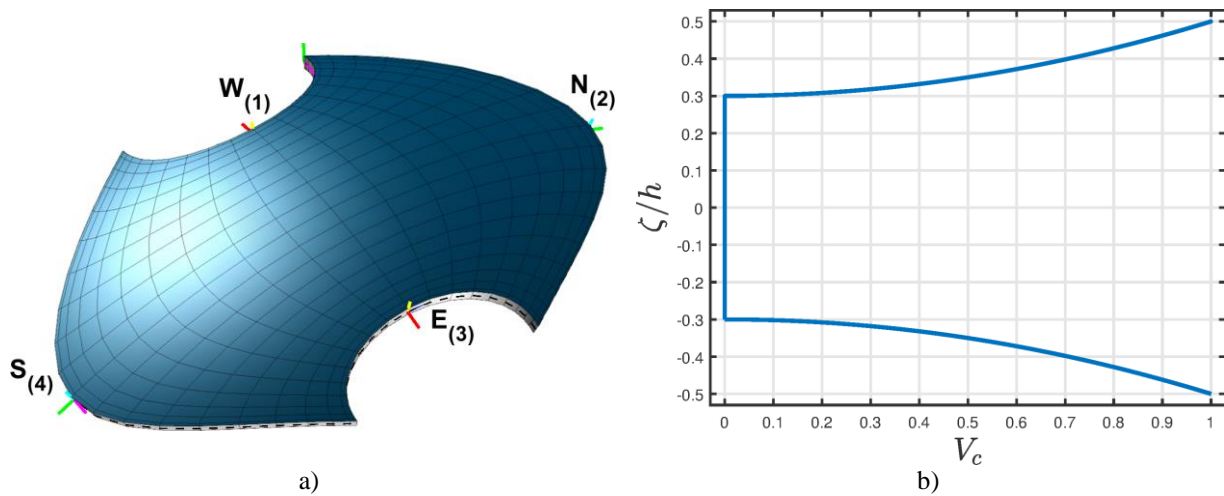


**Figure 4.26** – Shell structure reinforced by agglomerated CNTs: a) distorted domain; b) through-the-thickness distribution of the reinforcing phase.

As far as the boundary conditions are concerned, the southern and northern edges are clamped, whereas the others are free (FCFC). The structural theories used in the computation is an EDZ3, in which the Murakami's function is embedded. The weak formulation with  $C^1$  continuity conditions is solved in this circumstance.

The results are depicted in graphical form in Figures 4.27 and 4.28, whereas the numerical values are shown in Tables 4.14 and 4.15. In particular, two different parametric analyses are carried out. In the first one,  $\mu_2$  is kept constant and set equal to  $\mu_2 = 1.0$ , whereas in the second one  $\mu_1$  is kept constant and set equal to  $\mu_1 = 0.5$ .

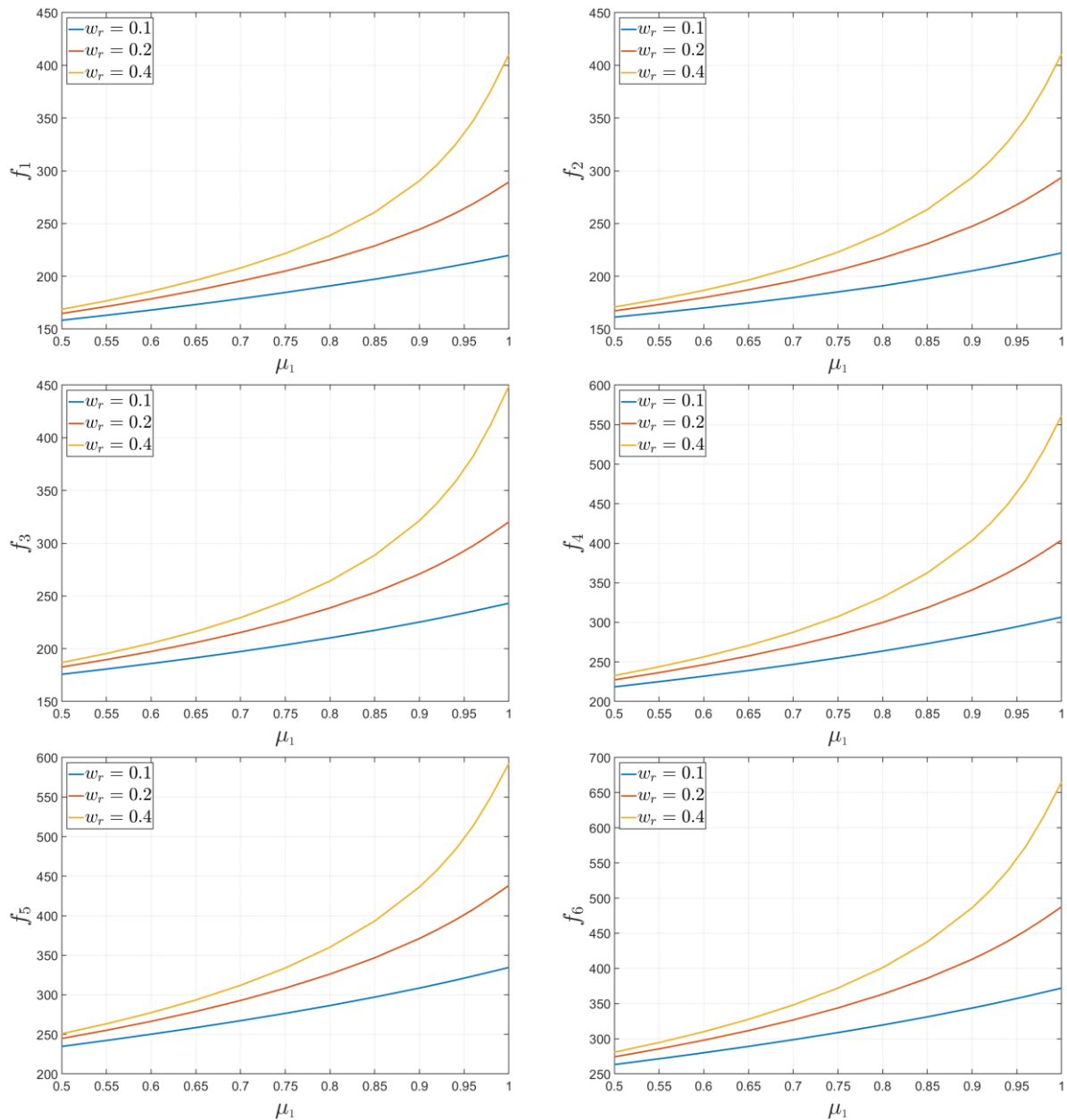


**Figure 4.27** – Variation of the first six natural frequencies for the shell structure reinforced by CNTs, as a function of the agglomeration parameter  $\mu_1$ , for several values of their mass fraction  $w_r$ . The other agglomeration parameter is set equal to  $\mu_2 = 1.0$ .

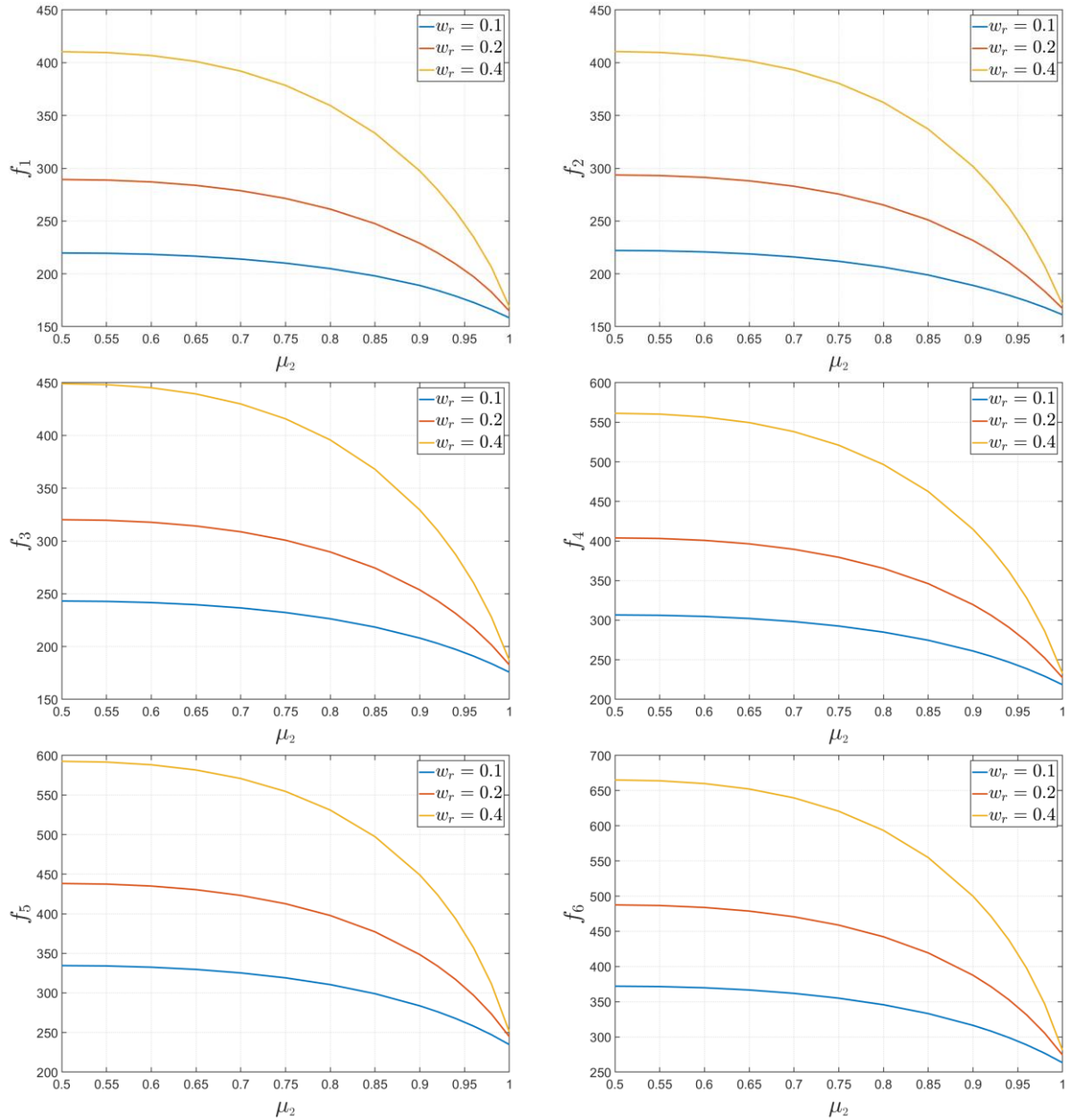


**Figure 4.28** – Variation of the first six natural frequencies for the shell structure reinforced by CNTs, as a function of the agglomeration parameter  $\mu_2$ , for several values of their mass fraction  $w_r$ . The other agglomeration parameter is set equal to  $\mu_1 = 0.5$ .

**Table 4.14** – Variation of the first ten natural frequencies for the shell structure reinforced by CNTs, as a function of the agglomeration parameter  $\mu_1$ , for several values of their mass fraction  $w_r$ . The other agglomeration parameter is set equal to  $\mu_2 = 1.0$ .

$f$	$\mu_1 = 0.5$	$\mu_1 = 0.6$	$\mu_1 = 0.7$	$\mu_1 = 0.8$	$\mu_1 = 0.9$	$\mu_1 = 1.0$
$w_r = 0.1$						
1	158.361	168.023	178.783	190.969	204.058	219.788
2	161.291	170.021	179.798	191.001	205.211	222.137
3	175.760	185.971	197.349	210.264	225.274	243.129
4	218.491	231.917	246.842	263.749	283.354	306.626
5	234.748	250.207	267.277	286.475	308.566	334.555
6	263.344	280.121	298.672	319.569	343.663	372.080
7	282.599	301.109	321.525	344.460	370.820	401.793
8	307.570	328.070	350.596	375.803	404.654	438.398
9	355.909	379.344	405.008	433.617	466.218	504.148
10	367.597	392.119	419.022	449.071	483.385	523.407
$w_r = 0.2$						
1	164.776	178.568	195.514	215.916	244.485	289.357
2	167.239	179.866	195.528	217.319	247.415	293.641
3	182.684	197.365	215.430	238.698	270.831	320.224
4	227.368	246.479	269.883	299.876	341.063	403.930
5	244.762	266.500	292.841	326.171	371.189	438.197
6	274.314	298.003	326.787	363.343	412.985	487.553
7	294.558	320.542	351.973	391.663	445.139	524.489
8	320.748	349.395	383.862	427.119	484.951	569.804
9	370.975	403.632	442.728	491.495	556.174	650.045
10	383.256	417.403	458.353	509.523	577.512	676.355
$w_r = 0.4$						
1	168.675	185.792	207.906	238.726	290.542	410.401
2	170.869	186.701	208.419	240.740	293.712	410.603
3	186.905	205.217	229.488	264.250	321.441	449.031
4	232.740	256.398	287.532	331.753	403.717	561.295
5	250.774	277.446	312.042	360.248	436.360	592.495
6	280.909	310.063	348.034	401.267	486.235	665.071
7	301.722	333.566	374.773	432.019	522.049	705.730
8	328.610	363.600	408.569	470.495	566.565	756.583
9	379.925	419.726	470.550	539.945	646.340	853.666
10	392.564	434.159	487.354	560.081	671.636	888.161

**Table 4.15** – Variation of the first ten natural frequencies for the shell structure reinforced by CNTs, as a function of the agglomeration parameter  $\mu_2$ , for several values of their mass fraction  $w_r$ . The other agglomeration parameter is set equal to  $\mu_1 = 0.5$ .

$f$	$\mu_2 = 0.5$	$\mu_2 = 0.6$	$\mu_2 = 0.7$	$\mu_2 = 0.8$	$\mu_2 = 0.9$	$\mu_2 = 1.0$
$w_r = 0.1$						
1	219.788	218.499	214.004	204.949	188.988	158.361
2	222.137	220.776	216.009	206.335	189.056	161.291
3	243.129	241.682	236.616	226.344	208.044	175.760
4	306.626	304.760	298.221	284.923	261.086	218.491
5	334.555	332.500	325.277	310.496	283.695	234.748
6	372.080	369.821	361.888	345.688	316.425	263.344
7	401.793	399.347	390.751	373.148	341.179	282.599
8	438.398	435.747	426.416	407.255	372.283	307.570
9	504.148	501.177	490.705	469.147	429.621	355.909
10	523.407	520.276	509.247	486.557	444.992	367.597
$w_r = 0.2$						
1	289.357	287.062	278.747	261.293	228.960	164.776
2	293.641	291.348	282.989	265.235	231.651	167.239
3	320.224	317.751	308.736	289.628	253.633	182.684
4	403.930	400.829	389.509	365.413	319.613	227.368
5	438.197	434.980	423.180	397.770	348.417	244.762
6	487.553	483.935	470.689	442.288	387.570	274.314
7	524.489	520.690	506.748	476.696	418.183	294.558
8	569.804	565.788	551.011	518.993	456.076	320.748
9	650.045	645.633	629.372	594.006	523.982	370.975
10	676.355	671.715	654.628	617.471	543.896	383.256
$w_r = 0.4$						
1	410.401	406.818	392.036	359.450	297.439	168.675
2	410.603	406.928	393.204	362.372	301.706	170.869
3	449.031	445.150	429.854	395.719	329.383	186.905
4	561.295	556.613	538.119	496.593	414.767	232.740
5	592.495	588.144	570.779	530.912	448.957	250.774
6	665.071	659.957	639.632	593.386	499.908	280.909
7	705.730	700.629	680.268	633.487	537.059	301.722
8	756.583	751.485	731.005	683.356	582.961	328.610
9	853.666	848.143	825.927	774.163	664.506	379.925
10	888.161	882.424	859.367	805.550	691.043	392.564

The following aspects can be observed:

- If the mass fraction of CNTs assumes higher values, the effect of agglomeration is more evident and the frequencies vary in a wider interval.
- When the value of  $\mu_2$  is closer to the unity and a noteworthy difference between the agglomeration parameters is assumed, the slope of the various graphs is higher.
- The maximum values of frequencies are obtained when  $\mu_1 = \mu_2$ . This aspect is valid for each value of mass fraction.
- The graphs presented here show the same tendency of the results proposed in terms of Young's moduli by Shi et al. in their work [200], in which the mathematical model to describe the CNT agglomeration has been proposed for the first time.

Finally, it can be stated that the natural frequencies of a generic structure can be highly affected by the agglomeration of CNTs used as reinforcing phase.

## *Conclusions*

A weak formulation (WF) has been developed for the mechanical analysis of doubly-curved shell structures made of composite materials. For this purpose, the Lagrange polynomials of high degree have been used for the interpolation of the nodal displacements. The governing equations have been obtained in the framework of Higher-order Shear Deformation Theories (HSDTs). Simultaneously, a strong formulation (SF) has been presented too, for the sake of completeness. All things considered, the following approaches have been taken into account:

- Strong formulation with  $C^1$  continuity requirement;
- Weak formulation with  $C^1$  continuity requirement;
- Weak formulation with  $C^0$  continuity requirement.

A set of comparison tests has been performed in terms of natural frequencies. The solutions have been obtained numerically by means of two different approaches, which are the Integral Quadrature (IQ) for the weak forms, and the Differential Quadrature (DQ) for the strong form. A commercial code that implements the well-known Finite Element Method (FEM) has been employed for comparison purposes.

A geometric convergence behavior characterizes the SF independently from the grid distribution, for those basis functions that allow the evaluation of the weighting coefficients through recursive formulations (Lagrange polynomials, trigonometric Lagrange polynomials). In general, an outstanding degree of accuracy is reached for a small number of discrete grid points. On the other hand, a linear convergence tendency is related to the WF with  $C^0$  continuity, whereas the WF with  $C^1$  continuity has shown a convergence trend similar to the one that characterizes the SF, if the Legendre-Gauss-Lobatto distribution is used. Thus, the accuracy that can be reached by means of the WF with  $C^0$  continuity requirement is extremely lower than the other two methodologies, if the same number of discrete points is considered. These aspects are not affected by the choice of the grid distributions, basis functions, and mechanical properties.

The SF and WF with  $C^1$  continuity conditions converge more rapidly than the FEM. Generally speaking, a huge number of degrees of freedom is required to reach a higher level

of accuracy if compared to the current approaches. In addition, a massive set of convergence analyses has proven the inadequacy of the quadrilateral plate elements provided by the commercial software to deal with laminated composite structures, especially if characterized by higher values of thickness. In some circumstances, it can be also noted that the FEM converges to completely different values.

The present approaches have been developed to investigate easily the structural behavior of shell structures made of advanced and innovative constituents. For this purpose, the effect of innovative constituents on the dynamic response of the structures has been also analyzed. The reference domains in which the governing equations can be described by arbitrary shapes described by NURBS. The accuracy and reliability of the proposed methodologies have been proven by the comparison with three-dimensional FEM models.

## References

- [1] Oden J.T., Reddy J.N., *An introduction to the mathematical theory of finite elements*, John Wiley & Sons, 1976.
- [2] Funaro D., *Polynomial Approximation of Differential Equations*, Springer-Verlag, 1992.
- [3] Tveito A., Winther R., *Introduction to Partial Differential Equations: A Computational Approach*, Springer, 1998.
- [4] Tornabene F., Fantuzzi N., Baccocchi M., Viola E., *Strutture a Guscio in Materiale Composito. Quadratura Differenziale. Elementi Finiti in Forma Forte*, Esculapio, 2015.
- [5] Tornabene F., Fantuzzi N., Baccocchi M., Viola E., *Laminated Composite Doubly-Curved Shell Structures. Differential and Integral Quadrature. Strong Formulation Finite Element Method*, Esculapio, 2016.
- [6] J.N. Reddy, *Energy Principles and Variational Methods in Applied Mechanics*, John Wiley & Sons, 2002.
- [7] Reddy J.N., *An introduction to the finite element method*, 3rd edition, McGraw-Hill, 2006.
- [8] Reddy J.N., Gartling D.K., *The Finite Element Method in Heat Transfer and Fluid Dynamics*, 3rd edition, CRC Press, 2010.
- [9] Reddy J.N., *An Introduction to Nonlinear Finite Element Analysis with applications to heat transfer, fluid mechanics, and solid mechanics*, 2nd edition, Oxford University Press, 2014.
- [10] Surana K.S., Reddy J.N., *The Finite Element Method for Boundary Value Problems: Mathematics and Computations*, CRC Press, 2016.
- [11] Tornabene F., Fantuzzi N., Baccocchi M., *The Strong Formulation Finite Element Method: Stability and Accuracy*, Fracture and Structural Integrity, 2014, 29, 251-265.
- [12] Fantuzzi N., *New Insights into the Strong Formulation Finite Element Method for Solving Elastostatic and Elastodynamic Problems*, Curved and Layered Structures, 2014, 1, 93-126.
- [13] Tornabene F., Fantuzzi N., Ubertini F., Viola E., *Strong Formulation Finite Element Method Based on Differential Quadrature: A Survey*, Applied Mechanics Reviews. 2015, 67, 020801-1-55.
- [14] Tornabene F., Fantuzzi N., Baccocchi M., *Finite Elements Based on Strong and Weak Formulations for Structural Mechanics: Stability, Accuracy and Reliability*, International Journal of Engineering & Applied Sciences, 2017, 9, 1-21.
- [15] Tornabene F., Fantuzzi N., Baccocchi M., *Strong and Weak Formulations Based on Differential and Integral Quadrature Methods for the Free Vibration Analysis of Composite Plates and Shells: Convergence and Accuracy*, Engineering Analysis with Boundary Elements, 2017. In Press.
- [16] Hrenikoff A., *Solution of problems in elasticity by the framework method*, Journal of Applied Mechanics, 1941, 8, 169-175.
- [17] McHenry D., *A lattice analogy for the solution of plane stress problems*, Journal of the Institution of Civil Engineers, 1943, 21, 59-82.

- [18] Courant R., *Variational methods for the solution of problems of equilibrium and vibrations*, Bulletin of the American Mathematical Society, 1943, 49, 1-23.
- [19] Argyris J.H., *Energy theorems and structural analysis: a generalized discourse with applications on energy principles of structural analysis including the effects of temperature and non-linear stress-strain relations part I. General theory*, Aircraft Engineering and Aerospace Technology, 1955, 27, 42-58.
- [20] Taylor A.E., *Introduction to Functional Analysis*, John Wiley, 1958.
- [21] Oden J.T., *Finite Element of Nonlinear Continua*, McGraw-Hill, 1972.
- [22] Ochoa O.O., Reddy J.N., *Finite Element Analysis of Composite Laminates*, Springer, 1992.
- [23] Zienkiewicz O.C., Taylor R.L., *The Finite Element Method for Solid and Structural Mechanics*, 6th edition, Elsevier, 2005.
- [24] Bellman R., Casti, J., *Differential quadrature and long-term integration*, Journal of Mathematical Analysis and Applications, 1971, 34, 235-238.
- [25] Bellman R., Kashef B.G., Casti J., 1972, *Differential quadrature: a technique for the rapid solution of nonlinear partial differential equations*, Journal of Computational Physics, 1972, 10, 40-52.
- [26] Bellman R., Roth R.S., *Methods in Approximation*, D. Reidel Publishing Company, 1986.
- [27] Whittaker E. T., Robinson G., *The Calculus of Observations: An Introduction to Numerical Analysis*, Dover, 1967.
- [28] Finlayson B.A., Scriven L.E., *The method of weighted residual: a review*, Applied Mechanics Reviews, 1966, 19, 735-748.
- [29] Civan F., Sliepcevich C.M., *Application of differential quadrature to transport processes*, Journal of Mathematical Analysis and Applications, 1983, 93, 206-221.
- [30] Civan F., Sliepcevich C.M., *Solution of the Poisson equation by differential quadrature*, International Journal for Numerical Methods in Engineering, 1983, 19, 711-724.
- [31] Civan F., Sliepcevich C.M., *Differential quadrature for multi-dimensional problems*, Journal of Mathematical Analysis and Applications, 1984, 101, 423-443.
- [32] Civan F., Sliepcevich C.M., *On the solution of the Thomas-Fermi equation by differential equation*, Journal of Computational Physics, 1984, 56, 343-348.
- [33] Civan F., Sliepcevich C.M., *Application of differential quadrature in solution of pool boiling in cavities*, Proceedings of the Oklahoma Academy of Science., 1985, 65, 73-78.
- [34] Quan J.R., Chang C.T., *New insights in solving distributed system equations by the quadrature method - I. Analysis*, Computers & Chemical Engineering, 1989, 13, 779-788.
- [35] Quan J.R., Chang C.T., *New insights in solving distributed system equations by the quadrature method - II. Numerical experiments*, Computers & Chemical Engineering, 1989, 13, 1017-1024.
- [36] Gottlieb D., Orszag, S.A., *Numerical Analysis of Spectral Methods: Theory and Applications*, Society for Industrial and Applied Mathematics, 1977.
- [37] Boyd J.P., *Chebyshev and Fourier Spectral Methods*, Dover Publications, 2001.

- [38] Canuto C., Hussaini M.Y., Quarteroni A., Zang T.A., *Spectral Method. Fundamentals in Single Domains*, Springer, 2006.
- [39] Quarteroni A., Valli A., *Numerical Approximation of Partial Differential Equations*, Springer, 2008.
- [40] Shen J., Tang T., Wang L.-L., *Spectral Methods. Algorithms, Analysis and Applications*, Springer, 2011
- [41] Trefethen L.N., *Spectral Methods in MATLAB*, Society for Industrial and Applied Mathematics, 2000.
- [42] Chen W.L., *A New Approach for Structural Analysis. The Quadrature Element Method*, PhD Thesis, University of Oklahoma, 1994.
- [43] Shu C., *Generalized differential-integral quadrature and application to the simulation of incompressible viscous flows including parallel computation*, PhD Thesis, University of Glasgow, UK, 1991.
- [44] Shu C., *Differential Quadrature and Its Application in Engineering*, Springer, 2000.
- [45] Shu C., Richards B.E., *Parallel simulation of incompressible viscous flows by generalized differential quadrature*, *Computing Systems in Engineering*, 1992, 3, 271-281.
- [46] Shu C., Richards B.E., *Application of generalized differential quadrature to solve two-dimensional incompressible Navier-Stokes equations*, *International Journal for Numerical Methods in Fluids*, 1992, 15, 791-798.
- [47] Bert C.W., Malik M., *Differential quadrature method in computational mechanics*, *Applied Mechanics Reviews*, 1996, 49, 1-27.
- [48] Civan F., *Solution of Transport Phenomena Type Models by the Method of Differential Quadratures as Illustrated on the LNG Vapor Dispersion Process Modeling*, PhD Thesis, University of Oklahoma, 1978.
- \* \* \*
- [49] Ambartsumyan S.A., *Theory of Anisotropic Shells*, NASA-TT-F-118, 1964.
- [50] Kraus H., *Thin Elastic Shells*, John Wiley & Sons, 1967.
- [51] Gill S.S., *The Stress Analysis of Pressure Vessel and Pressure Vessel Components*, Pergamon Press, 1970.
- [52] Calladine C.R., *Theory of Shell Structures*, Cambridge University Press, 1983.
- [53] Vinson J.R., *The Behavior of Shells Composed of Isotropic and Composite Materials*, Springer, 1993.
- [54] Ciarlet P., *Theory of Shells*, Elsevier, 2000.
- [55] Amabili M., *Nonlinear Vibrations and Stability of Shells and Plates*, Cambridge University Press, 2008.
- [56] Tornabene F., Fantuzzi N., Baccocchi M., Viola E., *Strutture a Guscio in Materiale Composito. Geometria Differenziale. Teorie di Ordine Superiore*, Esculapio, 2015.
- [57] Tornabene F., Fantuzzi N., Baccocchi M., Viola E., *Laminated Composite Doubly-Curved Shell Structures. Differential Geometry. Higher-order Structural Theories*, Esculapio, 2016.

- [58] Fantuzzi N., Tornabene F., *Strong Formulation Isogeometric Analysis (SFIGA) for Laminated Composite Arbitrarily Shaped Plates*, Composites Part B Engineering, 2016, 96, 173-203.
- [59] Tornabene F., Fantuzzi N., Bacciocchi M., *The GDQ Method for the Free Vibration Analysis of Arbitrarily Shaped Laminated Composite Shells Using a NURBS-Based Isogeometric Approach*, Composite Structures, 2016, 154, 190-218.
- [60] Dimitri R., Fantuzzi N., Tornabene F., Zavarise G., *Innovative Numerical Methods Based on SFEM and IGA for Computing Stress Concentrations in Isotropic Plates with Discontinuities*, International Journal of Mechanical Sciences, 2016, 118, 166-187.
- [61] Fantuzzi N., Della Puppa G., Tornabene F., Trautz M., *Strong Formulation Isogeometric Analysis for the Vibration of Thin Membranes of General Shape*, International Journal of Mechanical Sciences, 2017, 120, 322-340.
- [62] Tornabene F., Fantuzzi N., Bacciocchi M., *A New Doubly-Curved Shell Element for the Free Vibrations of Arbitrarily Shaped Laminated Structures Based on Weak Formulation IsoGeometric Analysis*, Composite Structures, 2017, 171, 429-461.
- [63] Pieg L., Tiller W., *The NURBS Book*, 2nd Edition, Springer, 1997.
- \* \* \*
- [64] Timoshenko S., *Vibration Problems in Engineering*, D. Van Nostrand Company, 1937.
- [65] Love A.E.H., *A Treatise on the Mathematical Theory of Elasticity*, Dover, 1944.
- [66] Timoshenko S., Goodier J.N., *Theory of Elasticity*, McGraw-Hill, 1951.
- [67] Sokolnikoff I.S., *Tensor Analysis, Theory and Applications*, John Wiley & Sons, 1951.
- [68] Sokolnikoff I.S., *Mathematical Theory of Elasticity*, McGraw-Hill, 1956.
- [69] Saada A.S., *Elasticity, Theory and Applications*, Pergamon Press, 1974.
- [70] Lekhnitskii S.G., *Theory of Elasticity of an Anisotropic Body*, Mir Publishers, 1981.
- [71] Mase G.T., Mase G.E., *Continuum Mechanics for Engineers*, CRC Press, 1999.
- [72] Cristescu N.D., Craciun E.-M., Soós E., *Mechanics of Elastic Composites*, CRC Press, 2004.
- [73] Luire A.I., *Theory of Elasticity*, Springer, 2005.
- [74] Leissa A.W., Qatu M.S., *Vibrations of Continuous Systems*, McGraw-Hill, 2011.
- [75] Love A.E.H., *On the small free vibrations and deformations of elastic shells*, Philosophical Transactions of the Royal Society of London, 1888, A 179, 491-546.
- [76] Sanders J.L., *An Improved First Approximation Theory of Thin Shells*, NASA-TR-R24, 1959.
- [77] Timoshenko S., Woinowsky-Krieger S., *Theory of Plates and Shells*, McGraw-Hill, 1959.
- [78] Flügge W., *Stresses in Shells*, Springer, 1960.
- [79] Gol'Denveizer A.L., *Theory of Elastic Thin Shells*, Pergamon Press, 1961.
- [80] Novozhilov V.V., *Thin Shell Theory*, P. Noordhoff, 1964.

- [81] Vlasov V.Z., *General Theory of Shells and Its Applications in Engineering*, NASA-TT-F-99, 1964.
- [82] Lekhnitskii S.G., Tsai S.W., Cheron T., *Anisotropic Plates*, Gordon and Breach, Science Publishers, 1968.
- [83] Leissa A.W., *Vibration of Plates*, NASA-SP-160, 1969.
- [84] Leissa A.W., *Vibration of Shells*, NASA-SP-288, 1973.
- [85] Szilard R., *Theory and Analysis of Plates*, Prentice-Hall, 1974.
- [86] Dowell E.H., *Aeroelasticity of Plates and Shells*, Noordhoff International Publishing, 1975.
- [87] Donnel L.H., *Beams, Plates and Shells*, McGraw-Hill, 1976.
- [88] Calladine C.R., *Theory of Shell Structures*, Cambridge University Press, 1983.
- [89] Niordson F.I., *Shell Theory*, North-Holland, 1985.
- [90] Markuš Š., *The Mechanics of Vibrations of Cylindrical Shells*, Elsevier, 1988.
- [91] Vorovich I.I., *Nonlinear Theory of Shallow Shells*, Springer, 1999.
- [92] Ventsel E., Krauthammer T., *Thin Plates and Shells*, Marcel Dekker, 2001.
- [93] Reissner E., *The effect of transverse shear deformation on the bending of elastic plates*, ASME Journal of Applied Mechanics, 1945, 12, 69-77.
- [94] Mindlin R.D., *Influence of rotatory inertia and shear on flexural motions of isotropic, elastic plates*, ASME Journal of Applied Mechanics, 1951, 18, 31-38, 1951.
- [95] Libai A., Simmonds J.G., *The Nonlinear Theory of Elastic Shells*, Cambridge University Press, 1998.
- [96] Liew K.M., Wang C.M., Xiang Y., Kitipornchai S., *Vibration of Mindlin Plates*, Elsevier, 1998.
- [97] Gould P.L., *Analysis of Shells and Plates*, Prentice-Hall, 1999.
- [98] Reddy J.N., *Theory and Analysis of Elastic Plates*, Taylor & Francis, 1999.
- [99] Wang C.M., Reddy J.N., Lee K.H., *Shear Deformable Beams and Plates*, Elsevier, 2000.
- [100] Soedel W., *Vibrations of Shells and Plates*, Marcel Dekker, 2004.
- [101] Wang C.M., Wang C.Y., Reddy J.N., *Exact Solutions for Buckling of Structural Members*, CRC Press, 2005.
- [102] Mindlin R.D., *An Introduction to the Mathematical Theory of Vibrations of Elastic Plates*, World Scientific Publishing, 2006.
- [103] Awrejcewicz J., Krysko V.A., Krysko A.V., *Thermo-Dynamics of Plates and Shells*, Springer, 2007.
- [104] Voyiadjis G.Z., Woelke P., *Elasto-Plastic and Damage Analysis of Plates and Shells*, Springer, 2008.
- [105] Chakraverty S., *Vibration of Plates*, CRC Press, 2009.
- [106] Viola E., Tornabene F., *Vibration Analysis of Conical Shell Structures Using GDQ Method*, Far East Journal of Applied Mathematics, 2006, 25, 23-39.
- [107] Tornabene F., Viola E., *Vibration Analysis of Spherical Structural Elements Using the GDQ Method*, Computers & Mathematics with Applications, 2007, 53, 1538-1560.

- [108] Tornabene F., Viola E., *2-D Solution for Free Vibrations of Parabolic Shells Using Generalized Differential Quadrature Method*, European Journal of Mechanics - A/Solids, 2008, 27, 1001-1025.
- [109] Tornabene F., *Free Vibrations of Laminated Composite Doubly-Curved Shells and Panels of Revolution via the GDQ Method*, Computer Methods in Applied Mechanics and Engineering, 2011, 200, 931-952.
- [110] Tornabene F., *2-D GDQ Solution for Free Vibrations of Anisotropic Doubly-Curved Shells and Panels of Revolution*, Composite Structures, 2011, 93, 1854-1876.
- [111] Tornabene F., *Free Vibrations of Anisotropic Doubly-Curved Shells and Panels of Revolution with a Free-Form Meridian Resting on Winkler-Pasternak Elastic Foundations*, Composite Structures, 2011, 94, 186-206.
- [112] Tornabene F., Liverani A., Caligiana G., *Laminated Composite Rectangular and Annular Plates: A GDQ Solution for Static Analysis with a Posteriori Shear and Normal Stress Recovery*, Composites Part B Engineering, 2012, 43, 1847-1872.
- [113] Tornabene F., Liverani A., Caligiana G., *General Anisotropic Doubly-Curved Shell Theory: a Differential Quadrature Solution for Free Vibrations of Shells and Panels of Revolution with a Free-Form Meridian*, Journal of Sound & Vibration, 2012, 331, 4848-4869.
- [114] Fantuzzi N., Tornabene F., *Strong Formulation Finite Element Method for Arbitrarily Shaped Laminated Plates - I. Theoretical Analysis*, Advances in Aircraft and Spacecraft Science, 2014, 1, 125-143.
- [115] Fantuzzi N., Tornabene F., *Strong Formulation Finite Element Method for Arbitrarily Shaped Laminated Plates - II. Numerical Analysis*, Advances in Aircraft and Spacecraft Science, 2014, 1, 145-175.
- [116] Fantuzzi N., Tornabene F., Viola E., Ferreira A.J.M., *A Strong Formulation Finite Element Method (SFEM) Based on RBF and GDQ Techniques for the Static and Dynamic Analyses of Laminated Plates of Arbitrary Shape*, Meccanica, 2014, 49, 2503-2542.
- [117] Fantuzzi N., Baccocchi M., Tornabene F., Viola E., Ferreira A.J.M., *Radial Basis Functions Based on Differential Quadrature Method for the Free Vibration of Laminated Composite Arbitrary Shaped Plates*, Composites Part B Engineering, 2015, 78, 65-78.
- [118] Tornabene F., Fantuzzi N., Baccocchi M., Viola E., *A New Approach for Treating Concentrated Loads in Doubly-Curved Composite Deep Shells with Variable Radii of Curvature*, Composite Structures, 2015, 131, 433-452.
- [119] Fantuzzi N., Tornabene F., Baccocchi M., Neves A.M.A., Ferreira A.J.M., *Stability and Accuracy of Three Fourier Expansion-Based Strong Form Finite Elements for the Free Vibration Analysis of Laminated Composite Plates*, International Journal for Numerical Methods in Engineering, 2017, 111, 354-382.
- [120] Eshelby J.D., *The determination of the elastic field of an ellipsoidal inclusion, and related problems*, Proceedings of the Royal Society of London A: Mathematical, Physical and Engineering Sciences, 1957, 241, 376-396.
- [121] Hashin Z., *The Elastic Moduli of Heterogeneous Materials*, ASME Journal of Applied Mechanics, 1962, 29, 143-150.

- 
- [122] Hashin Z., Rosen B.W., *The Elastic Moduli of Fiber-Reinforced Materials*, ASME Journal of Applied Mechanics, 1964, 31, 223-232.
- [123] Hill R., *Theory of Mechanical Properties of Fibre-Strengthened Materials: I. Elastic Behavior*, Journal of the Mechanics and Physics of Solids, 1964, 12, 199-212.
- [124] Hill R., *Theory of Mechanical Properties of Fibre-Strengthened Materials: II. Inelastic Behavior*, Journal of the Mechanics and Physics of Solids, 1964, 12, 213-218.
- [125] Tsai S.W., *Structural Behavior of Composite Materials*, NASA CR-71, 1964.
- [126] Hashin Z., *On Elastic Behaviour of Fibre Reinforced Materials of Arbitrary Transverse Phase*, Journal of the Mechanics and Physics of Solids, 1965, 13, 119-134.
- [127] Tsai S.W., *Strength Characteristics of Composite Materials*, NASA CR-224, 1965.
- [128] Tsai S.W., Adams D.F., Doner D.R., *Analyses of Composite Structures*, NASA CR-620, 1966.
- [129] Chamis C.C., Sendeckyj G.P., *Critique on Theories Predicting Thermoelastic Properties of Fibrous Composites*, Journal of Composite Materials, 1968, 2, 332-358.
- [130] Halpin J.C., *Effects of Environmental Factors on Composite Materials*, Technical Report AFML-TR-67-423, 1969.
- [131] Mori T., Tanaka K., *Average Stress in Matrix and Average Elastic Energy of Materials with Misfitting Inclusions*, Acta Metallurgica, 1973, 21, 571-574.
- [132] Hashin Z., *Analysis of Properties of Fiber Composites With Anisotropic Constituents*, ASME Journal of Applied Mechanics, 1979, 46, 543-550.
- [133] Hahn H.T., *Simplified Formulas for Elastic Moduli of Unidirectional Continuous Fiber Composites*, Journal of Composites, Technology and Research, 1980, 2, 5-7.
- [134] Hahn H.T., Tsai S.W., *Introduction to Composite Materials*, CRC Press, 1980.
- [135] Chou T.-W., *Microstructural design of fiber composites*, Cambridge University Press, 1992.
- [136] Kaw A.K., *Mechanics of Composite Materials*, CRC Press, 1997.
- [137] Kalamkarov A.L., Kolpakov A.G., *Analysis, Design and Optimization of Composite Structures*, John Wiley & Sons, 1997.
- [138] Jones R.M., *Mechanics of Composite Materials*, Taylor & Francis, 1999.
- [139] Vinson J.R., Sierakowski R.L., *The Behaviour of Structures Composed of Composite Materials*, Kluwer Academic Publishers, 2002.
- [140] Gay D., Hoa S.V., Tasi S.W., *Composite Materials, Design and Applications*, CRC Press, 2003.
- [141] Christensen R.M., *Mechanics of Composite Materials*, Dover Publications, 2005.
- [142] Chung D.C.L., *Composite Materials, Science and Applications*, Springer, 2010.
- [143] Barbero E.J., *Introduction to Composite Materials Design*, 2nd Edition, CRC Press, 2011.
- [144] Ye J., *Laminated Composite Plates and Shells. 3D Modelling*, Springer 2002.
- [145] Reddy J.N., *Mechanics of Laminated Composite Plates and Shells*, CRC Press, 2003.
- [146] Qatu M.S., *Vibration of Laminated Shells and Plates*, Elsevier, 2004.

- [147] Reddy J.N., Chin C.D., *Thermomechanical Analysis of Functionally Graded Cylinders and Plates*, Journal of thermal Stresses, 1998, 21, 593-626.
- [148] Reddy J.N., *Analysis of functionally graded plates*, International Journal for Numerical Methods in Engineering, 2000, 47, 663-684.
- [149] Tornabene F., Viola E., *Free Vibration Analysis of Functionally Graded Panels and Shells of Revolution*, Meccanica, 2009, 44, 255-281.
- [150] Viola E., Tornabene F., *Free Vibrations of Three Parameter Functionally Graded Parabolic Panels of Revolution*, Mechanics Research Communications, 2009, 36, 587-594.
- [151] Tornabene F., Viola E., *Free Vibrations of Four-Parameter Functionally Graded Parabolic Panels and Shells of Revolution*, European Journal of Mechanics - A/Solids, 2009, 28, 991-1013.
- [152] Tornabene F., *Free Vibration Analysis of Functionally Graded Conical, Cylindrical Shell and Annular Plate Structures with a Four-parameter Power-Law Distribution*, Computer Methods in Applied Mechanics and Engineering, 2009, 198, 2911-2935.
- [153] Tornabene F., Viola E., Inman D.J., *2-D Differential Quadrature Solution for Vibration Analysis of Functionally Graded Conical, Cylindrical Shell and Annular Plate Structures*, Journal of Sound & Vibration, 2009, 328, 259-290.
- [154] Reddy J.N., *Microstructure-dependent couple stress theories of functionally graded beams*, Journal of the Mechanics and Physics of Solids, 2011, 59, 2382-2399.
- [155] Reddy J.N., Kim J., *A nonlinear modified couple stress-based third-order theory of functionally graded plates*, Composite Structures, 2012, 94, 1128-1143.
- [156] Tornabene F., Viola E., *Static Analysis of Functionally Graded Doubly-Curved Shells and Panels of Revolution*, Meccanica, 2013, 48, 901-930.
- [157] Tornabene F., Reddy J.N., *FGM and Laminated Doubly-Curved and degenerate Shells resting on Nonlinear Elastic Foundation: a GDQ Solution for Static Analysis with a Posteriori Stress and strain Recovery*, Journal of Indian Institute of Science, 2013, 93, 635-688.
- [158] Tornabene F., Fantuzzi N., Bacciocchi M., *Free Vibrations of Free-Form Doubly-Curved Shells Made of Functionally Graded Materials Using Higher-Order Equivalent Single Layer Theories*, Composites Part B Engineering, 2014, 67, 490-509.
- [159] Tornabene F., Fantuzzi N., Viola E., Batra R.C., *Stress and Strain Recovery for Functionally Graded Free-Form and Doubly-Curved Sandwich Shells Using Higher-Order Equivalent Single Layer Theory*, Composite Structures, 2015, 119, 67-89.
- [160] Kim J., Reddy J.N., *A general third-order theory of functionally graded plates with modified couple stress effect and the von Kármán nonlinearity: theory and finite element analysis*, Acta Mechanica, 2015, 226, 2973-2998.
- [161] Gutierrez Rivera M., Reddy J.N., *Stress analysis of functionally graded shells using a 7-parameter shell element*, Mechanics Research Communications, 2016, 78, 60-70.
- [162] Lanc D., Turkalj G., Vo T., Brnic J., *Nonlinear buckling behaviours of thin-walled functionally graded open section beams*, Composite Structures, 2016, 152, 829-839.
- [163] Sofiyev A.H., Kuruoglu N., *Domains of dynamic instability of FGM conical shells under time dependent periodic loads*, Composite Structures, 2016, 136, 139-148.

- [164] Demir Ç., Mercan K., Civalek Ö., *Determination of critical buckling loads of isotropic, FGM and laminated truncated conical panel*, Composites Part B Engineering, 2016, 94, 1-10.
- [165] Fazzolari F.A., *Reissner's Mixed Variational Theorem and Variable Kinematics in the Modelling of Laminated Composite and FGM Doubly-Curved Shells*, Composites Part B Engineering, 2016, 89, 408-423.
- [166] Fazzolari F.A., *Stability Analysis of FGM Sandwich Plates by Using Variable-kinematics Ritz Models*, Mechanics of Advanced Materials and Structures, 2016, 23, 1104-1113.
- [167] Fantuzzi N., Tornabene F., Viola E., *Four-Parameter Functionally Graded Cracked Plates of Arbitrary Shape: a GDQFEM Solution for Free Vibrations*, Mechanics of Advanced Materials and Structures, 2016, 23, 89-107.
- [168] Tornabene F., Brischetto S., Fantuzzi N., Bacciocchi M., *Boundary Conditions in 2D Numerical and 3D Exact Models for Cylindrical Bending Analysis of Functionally Graded Structures*, Shock and Vibration, 2016, Vol. 2016, Article ID 2373862, 1-17.
- [169] Tornabene F., Fantuzzi N., Bacciocchi M., Viola E., Reddy J.N., *A Numerical Investigation on the Natural Frequencies of FGM Sandwich Shells with Variable Thickness by the Local Generalized Differential Quadrature Method*, Applied Sciences, 2017, 7, 131, 1-39.
- [170] Akgöz B., Civalek Ö., *Effects of thermal and shear deformation on vibration response of functionally graded thick composite microbeams*, Composites Part B Engineering, 2017, 129, 77-87.
- [171] Civalek Ö., *Vibration of laminated composite panels and curved plates with different types of FGM composite constituent*, Composites Part B Engineering, 2017, 122, 89-108.
- [172] Ersoy H., Mercan K., Civalek Ö., *Frequencies of FGM shells and annular plates by the methods of discrete singular convolution and differential quadrature methods*, Composite Structures, 2018, 183, 7-20.
- [173] Tzou H.S., *Piezoelectric Shells*, Kluwer Academic Publishers, 1993.
- [174] Rogacheva N.N., *The Theory of Piezoelectric Shells and Plates*, CRC Press, 1994.
- [175] Carrera E., Brischetto S., Nali P., *Plates and Shells for Smart Structures*, John Wiley & Sons, 2011.
- [176] Waldhart C., *Design of Tow-Placed, Variable-Stiffness Laminates*, Master of Science in Engineering Mechanics, Virginia Polytechnic Institute and State University, 1996.
- [177] Leissa A.W., Martin A.F., *Vibration and Buckling of Rectangular Composite Plates with Variable Fiber Spacing*, Composite Structures, 1990, 14, 339-357.
- [178] Hyer M.W., Charette R.F., *Use of Curvilinear Fiber Format in Composite Structure Design*, AIAA Journal, 1991, 29, 1011-1015.
- [179] Gürdal Z., Olmedo R., *In-Plane Response of Laminates with Spatially Varying Fiber Orientations: Variable Stiffness Concept*, AIAA Journal, 1993, 31, 751-758.
- [180] Hyer M.W., Rust R.J., Waters Jr. W.A., *Innovative design of composite structures: Design, manufacturing, and testing of plates utilizing curvilinear fiber trajectories*, NASA-CR-197045, 1994.
- [181] Tatting B.F., Gürdal Z., *Design and Manufacture of Elastically Tailored Tow Placed Plates*, NASA/CR-2002-211919, 2002.

- [182] Blom A.W., Tatting B.F., Hol J.M.A.M., Gürdal Z., *Fiber path definitions for elastically tailored conical shells*, Composites Part B Engineering, 2009, 40, 77-84.
- [183] Wu Z., Weaver P.M., Raju G., *Postbuckling optimization of variable angle tow composite plates*, Composite Structures, 2013, 103, 34-42.
- [184] Raju G., Wu Z., Weaver P.M., *Postbuckling analysis of variable angle tow plates using differential quadrature method*, Composite Structures, 2013, 106, 74-84.
- [185] Groh R.M.J., Weaver P.M., *Buckling analysis of variable angle tow, variable thickness panels with transverse shear effects*, Composite Structures, 2014, 107, 482-493.
- [186] Ribeiro P., *Non-linear modes of vibration of thin cylindrical shells in composite laminates with curvilinear fibers*, Composite Structures, 2015, 122, 184-197.
- [187] Akhavan H., Ribeiro P., *Natural modes of vibration of variable stiffness composite laminates with curvilinear fibers*, Composite Structures, 2011, 93, 3040-3047.
- [188] Yazdani S., Ribeiro P., *A layerwise p-version finite element formulation for free vibration analysis of thick composite laminates with curvilinear fibers*, Composite Structures, 2015, 120, 531-542.
- [189] Tornabene F., Fantuzzi N., Bacciocchi M., Viola E., *Higher-Order Theories for the Free Vibration of Doubly-Curved Laminated Panels with Curvilinear Reinforcing Fibers by Means of a Local Version of the GDQ Method*, Composites Part B Engineering, 2015, 81, 196-230.
- [190] Tornabene F., Fantuzzi N., Bacciocchi M., *Higher-Order Structural Theories for the Static Analysis of Doubly-Curved Laminated Composite Panels Reinforced by Curvilinear Fibers*, Thin-Walled Structures, 2016, 102, 222-245.
- [191] Tornabene F., Fantuzzi N., Bacciocchi M., *Foam Core Composite Sandwich Plates and Shells with Variable Stiffness: Effect of Curvilinear Fiber Path on the Modal Response*, Journal of Sandwich Structures and Materials, 2017. In Press.
- [192] Iijima S., *Helical Microtubules of Graphitic Carbon*, Nature, 1991, 354, 56-58.
- [193] Iijima S., Ichihashi T., *Single-shell carbon nanotubes of 1-nm diameter*, Nature, 1993, 363, 603-605.
- [194] Popov V.N., Van Doren V.E., *Elastic properties of single-walled carbon nanotubes*, Physical Review B, 2000, 61, 3078-3084.
- [195] Qian D., Wagner G.J., Liu W.K., Yu M.-F., Ruoff R.S., *Mechanics of carbon nanotubes*, Applied Mechanics Reviews, 2002, 55, 495-533.
- [196] Shen L., Li J., *Transversely isotropic elastic properties of single-walled carbon nanotubes*, Physical Review B, 2004, 69, 045414.
- [197] Liew K.M., Lei Z.X., Zhang L.W., *Mechanical analysis of functionally graded carbon nanotube reinforced composites: a review*, Composite Structures, 2015, 120, 90-97.
- [198] Odegard G.M., Gates T.S., Wise K.E., Park C., Siochi E.J., *Constitutive modeling of nanotube-reinforced polymer composites*, Composites Science and Technology, 2003, 63, 1671-1687.
- [199] Ray M.C., Batra R.C., *Effective Properties of Carbon Nanotube and Piezoelectric Fiber Reinforced Hybrid Smart Composites*, ASME Journal of Applied Mechanics, 2009, 76, 034503.

- [200] Shi D.-L., Huang Y.Y., Hwang K.-C., Gao H., *The Effect of Nanotube Waviness and Agglomeration on the Elastic Property of Carbon Nanotube-Reinforced Composites*, Journal of Engineering Materials and Technology, 2004, 126, 250-257.
- [201] Brischetto S., Tornabene F., Fantuzzi N., Baccocchi M., *Refined 2D and Exact 3D Shell Models for the Free Vibration Analysis of Single- and Double-Walled Carbon Nanotubes*, Technologies, 2015, 3, 259-284.
- [202] Tornabene F., Fantuzzi N., Baccocchi M., Viola E., *Effect of Agglomeration on the Natural Frequencies of Functionally Graded Carbon Nanotube-Reinforced Laminated Composite Doubly-Curved Shells*, Composites Part B Engineering, 2016, 89, 187-218.
- [203] Kamarian S., Salim M., Dimitri R., Tornabene F., *Free Vibration Analysis of Conical Shells Reinforced with Agglomerated Carbon Nanotubes*, International Journal of Mechanical Sciences, 2016, 108-109, 157-165.
- [204] Akgöz B., Civalek Ö., *Bending analysis of embedded carbon nanotubes resting on an elastic foundation using strain gradient theory*, Acta Astronautica, 2016, 119, 1-12.
- [205] Tornabene F., Fantuzzi N., Baccocchi M., *Linear Static Response of Nanocomposite Plates and Shells Reinforced by Agglomerated Carbon Nanotubes*, Composites Part B Engineering, 2017, 115, 449-476.
- [206] Fantuzzi N., Tornabene F., Baccocchi M., Dimitri R., *Free Vibration Analysis of Arbitrarily Shaped Functionally Graded Carbon Nanotube-Reinforced Plates*, Composites Part B Engineering, 2017, 115, 384-408.
- [207] Nejati M., Asanjarani A., Dimitri R., Tornabene F., *Static and Free Vibration Analysis of Functionally Graded Conical Shells Reinforced by Carbon Nanotubes*, International Journal of Mechanical Sciences, 2017, 130, 383-398.
- [208] Akgöz B., Civalek Ö., *A size-dependent beam model for stability of axially loaded carbon nanotubes surrounded by Pasternak elastic foundation*, Composite Structures, 2017, 176, 1028-1038.
- [209] Tornabene F., Baccocchi M., Fantuzzi N., Reddy J.N., *Multiscale Approach for Three-Phase CNT/Polymer/Fiber Laminated Nanocomposite Structures*, Polymer Composites, 2017. In Press.
- [210] Librescu L., Reddy J.N., *A few remarks concerning several refined theories of anisotropic composite laminated plates*, International Journal of Engineering Science, 1989, 27, 515-527.
- [211] Whitney J.M., Pagano N.J., *Shear Deformation in Heterogeneous Anisotropic Plates*, ASME Journal of Applied Mechanics, 1970, 37, 1031-1036.
- [212] Whitney J.M., Sun C.T., *A Higher Order Theory for Extensional Motion of Laminated Composites*, Journal of Sound and Vibration, 1973, 30, 85-97.
- [213] Reddy J.N., *A Simple Higher-Order Theory for Laminated Composite Plates*, ASME Journal of Applied Mechanics, 1984, 51, 745-752.
- [214] Reddy J.N., *A Generalization of the Two-Dimensional Theories of Laminated Composite Plates*, International Journal for Numerical Methods in Biomedical Engineering, 1987, 3, 173-180.
- [215] Reddy J.N., *On Refined Theories of Composite Laminates*, Meccanica, 1990, 25, 230-238.

- [216] Reddy J.N. Liu C.F., *A higher-order shear deformation theory for laminated elastic shells*, International Journal of Engineering Science, 1985, 23, 319-330.
- [217] Reissner E., *On transverse bending of plates, including the effect of transverse shear deformation*, International Journal of Solids and Structures, 1975, 11, 569-573.
- [218] Murthy M.V.V., *An Improved Transverse Shear Deformation Theory for Laminated Anisotropic Plates*, NASA Technical Paper 1903, 1981.
- [219] Green A.E., Naghdi P.M., *A theory of composite laminated plates*, IMA Journal of Applied Mathematics, 1982, 29, 1-23.
- [220] Bert C.W., *A Critical Evaluation of New Plate Theories Applied to Laminated Composites*, Composite Structures, 1984, 2, 329-347.
- [221] Shirakawa K., *Bending of plates based on improved theory*, Mechanics Research Communications, 1985, 10, 205-211.
- [222] Robbins D.H., Reddy J.N., *Modeling of Thick Composites Using a Layer-Wise Laminate Theory*, International Journal for Numerical Methods in Engineering, 1993, 36, 655-677.
- [223] Carrera E., *A refined multi-layered finite-element model applied to linear and non-linear analysis of sandwich plates*, Composites Science and Technology, 1998, 58, 1553-1569.
- [224] Carrera E., *Theories and Finite Elements for Multilayered, Anisotropic, Composite Plates and Shells*, Archives of Computational Methods in Engineering, 2002, 9, 87-140.
- [225] Carrera E., *Theories and Finite Elements for Multilayered Plates and Shells: A Unified Compact Formulation with Numerical Assessment and Benchmarking*, Archives of Computational Methods in Engineering, 2003, 10, 215-296.
- [226] Carrera E., *Historical review of zig-zag theories for multilayered plates and shells*, Applied Mechanics Reviews, 2003, 56, 287-308.
- [227] Carrera E., *On the use of the Murakami's zig-zag function in the modeling of layered plates and shells*, Computers & Structures, 2004, 82, 541-554.
- [228] Demasi L.,  *$\infty^3$  Hierarchy plate theories for thick and thin composite plates: The generalized unified formulation*, Composite Structures, 2008, 84, 256-270.
- [229] D'Ottavio M., *A Sublaminar Generalized Unified Formulation for the analysis of composite structures*, Composite Structures, 2016, 142, 187-199.
- [230] Viola E., Tornabene F., Fantuzzi N., *General Higher-Order Shear Deformation Theories for the Free Vibration Analysis of Completely Doubly-Curved Laminated Shells and Panels*, Composite Structures, 2013, 95, 639-666.
- [231] Viola E., Tornabene F., Fantuzzi N., *Static Analysis of Completely Doubly-Curved Laminated Shells and Panels Using General Higher-order Shear Deformation Theories*, Composite Structures, 2013, 101, 59-93.
- [232] Tornabene F., Viola E., Fantuzzi N., *General Higher-Order Equivalent Single Layer Theory for Free Vibrations of Doubly-Curved Laminated Composite Shells and Panels*, Composite Structures, 2013, 104, 94-117.
- [233] Tornabene F., Fantuzzi N., Viola E., Ferreira A.J.M., *Radial Basis Function Method Applied to Doubly-Curved Laminated Composite Shells and Panels with a General Higher-Order Equivalent Single Layer Formulation*, Composites Part B Engineering, 2013, 55, 642-659.

- [234] Tornabene F., Fantuzzi N., Viola E., Carrera E., *Static Analysis of Doubly-Curved Anisotropic Shells and Panels Using CUF Approach, Differential Geometry and Differential Quadrature Method*, Composite Structures, 2014, 107, 675-697.
- [235] Tornabene F., Fantuzzi N., Viola E., Reddy J.N., *Winkler-Pasternak Foundation Effect on the Static and Dynamic Analyses of Laminated Doubly-Curved and Degenerate Shells and Panels*, Composites Part B Engineering, 2014, 57, 269-296.
- [236] Ferreira A.J.M., Carrera E., Cinefra M., Viola E., Tornabene F., Fantuzzi N., Zenkour A.M., *Analysis of Thick Isotropic and Cross-Ply Laminated Plates by Generalized Differential Quadrature Method and a Unified Formulation*, Composites Part B Engineering, 2014, 58, 544-552.
- [237] Tornabene F., Fantuzzi N., Bacciocchi M., *The Local GDQ Method Applied to General Higher-Order Theories of Doubly-Curved Laminated Composite Shells and Panels: the Free Vibration Analysis*, Composite Structures, 2014, 116, 637-660.
- [238] Tornabene F., Fantuzzi N., Bacciocchi M., *The Local GDQ Method for the Natural Frequencies of Doubly-Curved Shells with Variable Thickness: A General Formulation*, Composites Part B Engineering, 2016, 92, 265-289.
- [239] Tornabene F., Fantuzzi N., Viola E., *Inter-Laminar Stress Recovery Procedure for Doubly-Curved, Singly-Curved, Revolution Shells with Variable Radii of Curvature and Plates Using Generalized Higher-Order Theories and the Local GDQ Method*, Mechanics of Advanced Materials and Structures, 2016, 23, 1019-1045.
- [240] Tornabene F., Fantuzzi N., Bacciocchi M., Neves A.M.A., Ferreira A.J.M., *MLSDQ Based on RBFs for the Free Vibrations of Laminated Composite Doubly-Curved Shells*, Composites Part B: Engineering, 2016, 99, 30-47.
- [241] Tornabene F., Fantuzzi N., Bacciocchi M., *On the Mechanics of Laminated Doubly-Curved Shells Subjected to Point and Line Loads*, International Journal of Engineering Science, 2016, 109, 115-164.
- [242] Bacciocchi M., Eisenberger M., Fantuzzi N., Tornabene F., Viola E., *Vibration Analysis of Variable Thickness Plates and Shells by the Generalized Differential Quadrature Method*, Composite Structures, 2016, 156, 218-237.
- [243] Tornabene F., Fantuzzi N., Bacciocchi M., Reddy J.N., *A Posteriori Stress and Strain Recovery Procedure for the Static Analysis of Laminated Shells Resting on Nonlinear Elastic Foundation*, Composites Part B Engineering, 2017, 126, 162-191.
- [244] Tornabene F., Fantuzzi N., Bacciocchi M., *Linear Static Behavior of Damaged Laminated Composite Plates and Shells*, Materials, 2017, 10, 811, 1-52.
- [245] Tornabene F., Fantuzzi N., Bacciocchi M., *Refined Shear Deformation Theories for Laminated Composite Arches and Beams with Variable Thickness: Natural Frequency Analysis*, Engineering Analysis with Boundary Elements, 2017. In Press.
- [246] Tornabene F., Fantuzzi N., Bacciocchi M., Viola E., *Accurate Inter-Laminar Recovery for Plates and Doubly-Curved Shells with Variable Radii of Curvature Using Layer-Wise Theories*, Composite Structures, 2015, 124, 368-393.
- [247] Tornabene F., Fantuzzi N., Bacciocchi M., Dimitri R., *Dynamic Analysis of Thick and Thin Elliptic Shell Structures Made of Laminated Composite Materials*, Composite Structures, 2015, 133, 278-299.

- [248] Tornabene F., Fantuzzi N., Baccocchi M., Dimitri R., *Free Vibrations of Composite Oval and Elliptic Cylinders by the Generalized Differential Quadrature Method*, *Thin-Walled Structures*, 2015, 97, 114-129.
- [249] Tornabene F., *General Higher Order Layer-Wise Theory for Free Vibrations of Doubly-Curved Laminated Composite Shells and Panels*, *Mechanics of Advanced Materials and Structures*, 2016, 23, 1046-1067.
- [250] Tornabene F., Fantuzzi N., Baccocchi M., Reddy J.N., *An Equivalent Layer-Wise Approach for the Free Vibration Analysis of Thick and Thin Laminated Sandwich Shells*, *Applied Sciences*, 2017, 7, 17, 1-34.

\* \* \*

- [251] Strand7: Strand7 Software, Release 2.4.6.
- [252] Abaqus: Abaqus/CAE 6.14, Dassault Systèmes Simulia Corp.